

Dear colleagues!

We welcome you to the International Conference on Quantum Technologies ICQT 2015 in Moscow. This is the third conference in a series of meetings dedicated to the interdisciplinary area of quantum science and technology. The conference subjects include superconductivity, quantum optics, ultra-cold atoms and molecules, plasmonics, photonics, optomechanics, cold neutrons, many-body theory and polaritons in solid state systems.

The first ICQT meeting was held in Moscow four years ago as a kick-off meeting of the Russian Quantum Center (RQC). It brought together over 120 researchers from different areas of quantum physics. The series continued with ICQT 2013, which hosted about 200 delegates. Keeping the venue and format of the meeting, we hope this third conference will keep up to the standards set by the first two.

This year, the conference program includes 34 invited talks and 95 poster presentations with the total number of participants approaching 200. The talks will be given by leading experts in the field of quantum physics and technology representing leading institutions in Europe, the USA, Australia and Japan, as well as many active groups in Russia. By tradition formed over last four years, a large fraction of conference attendees is students from all over Russia and abroad.

The financial support for the meeting is provided by our sponsors and the RQC (www.rqc.ru). RQC will celebrate its 5th anniversary in the end of 2015. By now, it has become a mature, internationally known research institution with ten groups and about 100 scientists. To date, our researchers published 150 peer-reviewed papers, many of them now reporting experiments and theoretical results based on the work physically performed at the Center.

Thanks to the generous support of our sponsors, we are able to organize this meeting at the historic Hotel Ukraina in Moscow. The registration fee paid by the participants is only a small fraction of the actual cost of the conference, the balance being covered by the RQC and other conference sponsors. As at previous meetings, a select group of students (chosen according to their research specialization and academic achievements) is given an opportunity to participate in the conference free of charge.

It is our great pleasure to welcome you to this conference.

The ICQT 2015 Program committee

Program committee



Alexey Akimov

Principal investigator at RQC;
Senior Researcher at LPI;
Member of the European Physics Society.



Vladimir Belotelov

Principal investigator at RQC;
Associate Professor at Lomonosov Moscow State University;
Alexander von Humboldt Research Fellowship (2013);
First prize in the competition of the research works
of young scientists at Lomonosov Moscow State University (2011, 2007).



Natalia Berloff

Professor of Applied Mathematics, Department of Applied Mathematics
and Theoretical Physics, University of Cambridge;
Director of Photonics and Quantum Materials Program at Skoltech.



Michael Gorodetsky

Principal investigator at RQC;
Professor at M.V. Lomonosov Moscow State University;
Visiting professor, EPFL (Switzerland).



Alexey Kavokin

Professor, Chair of Nanophysics and Photonics, University of Southampton, UK;
Scientific Director of the Mediterranean Institute of Fundamental Physics, Italy;
Principal investigator at RQC; Winner of \$5M Russian mega-grant –
Spin Optics Lab started at the St-Petersburg State University in 2011.



Nikolai Kolachevsky

Corresponding Member of the Russian Academy of Sciences;
Principal investigator at RQC;
Since 2015 – director of the Lebedev Institute RAS.



Alexander Lvovsky

Physics professor at University of Calgary, Canada;
Canada Research Chair (Level II),
member of the Canadian Institute for Advanced Research;
Principal investigator at RQC;
International Award for Quantum Communications;
Alberta Ingenuity New Faculty Award;
Deutsche Forschungsgemeinschaft Emmy Noether Award and others.



Alexey Rubtsov

Professor at M.V. Lomonosov Moscow State University;
Principal investigator at RQC.



Georgy Shlyapnikov

Director of Research, LPTMS CNRAS, Orsay (France); Professor of the University of Amsterdam (The Netherlands); Associate Editor of Advances in Physics; Co-editor of European Physics Letters; Principal investigator at RQC; Humboldt Perize (Germany, 1999); Kurchatov Prize (Russia, 2000); International Bose-Einstein Condensation Prize (2011); ERC Research Award (2013).



Alexey Ustinov

Professor of Experimental Physics at the Karlsruhe Institute of Technology, Germany; Principal investigator at RQC; established new laboratory at the National University of Science and Technology «MISiS» in Moscow (mega-grant 2011-2015); the Humboldt Fellowship, the Stefanos Pnevmatikos International Award.



Alexey Zheltikov

Professor of Moscow State University and Texas A&M University; Scientific Director at RQC; State Prize of the Russian Federation for Young Scientist; Shuvalov Prize; Willis E. Lamb Award.

Organizing committee



Alexey Akimov

Principal investigator at RQC; Senior Researcher at LPI; Member of the European Physics Society.



Alexander Lvovsky

Physics professor at University of Calgary, Canada; Canada Research Chair (Level II), member of the Canadian Institute for Advanced Research; Principal investigator at RQC; International Award for Quantum Communications; Alberta Ingenuity New Faculty Award; Deutsche Forschungsgemeinschaft Emmy Noether Award and others.



Ruslan Yunusov

Chief Executive Officer of RQC; PhD in Physics (Lomonosov Moscow State University); Economics graduate (Russian Presidential Academy of National Economy and Public Administration).

Dear participants and guests of the Conference!

I'm very glad to welcome you at our traditional forum on quantum technologies.

It's a big honour for us to greet the leading researchers from around the world. This meeting is yet another proof that Russian scientists play a significant role in the development of quantum physics internationally, and their achievements are highly appreciated by the colleagues.

The attention to the quantum physics research which is getting paid by the government authorities (particularly by the Russian Ministry of Education and Science) as well as major corporations such as Gazprombank is equally important to us.

The scientific research conducted by the RQC physicists along with other institutions over the world indicate that in the near future this scientific field will become the powerhouse, the driver of the next Technological Revolution, comparable to the mass spread of personal computers and the development of the Internet.

It is in our common interest and in our power to bring this Future.

I'd like to wish all the participants of the conference – both the prominent scientists and the students to have a fruitful work at the Conference. I hope it will become a very good start for many joint scientific projects and will lead to new scientific discoveries.

I wish you every success in the major work for every physicists that is the exploration of our Universe.

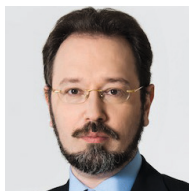
*Ruslan Yunusov,
Chief Executive Officer, RQC*

Business session committee



Dmitry Zauers

Deputy Chairman of the Management Board, Gazprombank.



Eugeny Kuznetsov

Deputy CEO, Project Office Director, Member of Management Board, Russian Venture Company.



Alexei Sitnikov

Vice-President, Institutional and Resource Development, Executive Secretary of the Board of Trustees, Skolkovo Institute of Science and Technology.



Ruslan Yunusov

Chief Executive Officer, RQC.

Organizers



The Russian Quantum Center (RQC) is a unique scientific institution in Russia, based on the principles of the most effective international research organizations and funded by both government and private sources. The main research areas of the RQC are quantum information processing, quantum optics, and quantum technologies. Scientific activities of the center are directed by its International Advisory Board, which is composed of world leading scientists in the field. RQC operation is overseen by a Board of Trustees composed of major figures in Russian and International industry. The RQC works in collaboration with leading Russian and foreign institutions and companies engaged in quantum related science and technology development. Currently, the RQC is building its laboratory complex at the Skolkovo innovation center. The RQC organizes the biannual International Conference on Quantum Technology in Moscow, drawing luminaries and young researchers from across the globe and Russia to present new results and discuss new directions in quantum science and technology. www.rqc.ru

OFFICIAL PARTNERS:



THE MINISTRY OF EDUCATION AND SCIENCE
OF THE RUSSIAN FEDERATION

The Ministry of Education and Science of Russia is a federal executive authority responsible for the state policy development and normative and legal regulation in the sphere of education, research, scientific, technological and innovation activities, nanotechnology, intellectual property, as well as in the sphere of nurturing, social support and social protection of students and pupils of educational institutions.



Fund for Infrastructure and Educational Programs (part of RUSNANO Group) – a non-profit organization that promotes the creation of infrastructure for the Russian nanotechnology industry and is part of the «innovation lift» system of Russian development institutions. The Fund is financed by the Russian federal budget.

The Fund works in seven main areas:

- 1) Development of technology infrastructure.
- 2) Building human resources for the nanoindustry.
- 3) Development of the market for innovative products.
- 4) Standardization, certification and safety assessment of nanotechnology products.
- 5) Metrological support for the nanoindustry.
- 6) Improvement of legislation in the innovation sphere.
- 7) Popularization of nanotechnologies.

www.rusnano.com

Skoltech

Skolkovo Institute of Science and Technology

The Skolkovo Institute of Science and Technology (Skoltech) is a private graduate research university in Skolkovo, Russia, a suburb of Moscow. Established in 2011 in collaboration with MIT, Skoltech educates global leaders in innovation, advances scientific knowledge, and fosters new technologies to address critical issues facing Russia and the world. Applying international research and educational models, the university integrates the best Russian scientific traditions with twenty-first century entrepreneurship and innovation.

www.skoltech.ru/en



Russian Venture Company is a government fund of funds and a development institute of the Russian Federation, one of Russia's key tools in building its own national innovation system. The mission of RVC is encourage Russia's own VC industry and boost capital of VC funds to ensure faster development of an efficient and globally competitive innovative system, engaging private venture capital, nurturing innovative entrepreneurship and technology business expertise, and mobilizing Russian human resources.

www.rusventure.ru/en

GENERAL INFORMATION PARTNER

LENTA.RU

Online Newspaper www.Lenta.ru

INFORMATION PARTNERS



Weekly business magazine «Expert» www.expert.ru

N+1

Popular science and entertainment journal «N+1» www.nplus1.ru



Web-edition «Science & Technology» in Russia www.strf.ru

ПОИСК

Russian Scientific Community's Weekly POISK www.poisknews.ru



Science News Wire «Cherdak» www.chrdk.ru



Magazine «Russian Reporter» www.rusrep.ru

Эноб.

Magazine «Snob» www.snob.ru

Monday, July 13

BUSINESS SESSION

- | | |
|-------------|--|
| 09.00-10.00 | Welcome coffee |
| 10.00-10.45 | Alexey Ustinov, RQC/KIT/MISiS
<i>Public lecture «Quantum computer: is it still a myth or reality already?»</i> |
| 10.45-11.15 | Coffee break |
| 11.15-13.15 | Plenary discussion
<i>«Advanced technologies in Russia: to catch up, overtake or..?»</i> |
| 13.15-13.45 | Informal discussions with coffee/tea |

SCIENTIFIC SESSION

- | | |
|-------------|-------|
| 13:05-14.30 | Lunch |
|-------------|-------|

CHAIRMAN OF THE SESSION **Gora Shlyapnikov**

- | | |
|-------------|---|
| 14:35-15.20 | Vladan Vuletic, MIT
<i>«Entanglement of 3000 atoms by one photon»</i> |
| 15:20-16:05 | Florian Schreck, U.of Amsterdam
<i>«New tricks with ultracold strontium: Laser cooling to BEC & Ultracold RbSr molecules»</i> |
| 16:05-16.45 | Coffee break |

CHAIRMAN OF THE SESSION **Nikolay Kolachevsky**

- | | |
|-------------|--|
| 16:50-17.35 | Francesca Ferlino, IQOQI
<i>«Superfluid-to-Mott-Insulator Transition with Ultracold Atomic Dipoles»</i> |
| 17:35-18.20 | Misha Baranov, IQOQI
<i>«Majorana fermions in atomic-molecular systems at finite temperature and in the presence of a noise»</i> |
| 18:20-19.05 | Philippe Grangier, Institute d'Optique
<i>«Quantum Optics and Quantum Communications with non-Gaussian States of Light»</i> |

Tuesday, July 14

CHAIRMAN OF THE SESSION **Michael Gorodetsky**

- 09:00-09.45 **Mikhail Lukin**, Harvard
«New interface between quantum optics and nanoscience»
- 09:45-10.30 **Olga Kocharovskaya**, Texas A&M
«Quantum Interfaces between Gamma-Photon and Nuclear Ensemble»
- 10:30-11.15 **Gerd Leuchs**, MPL
«Efficient coupling of light to a single atom in a parabolic mirror»
- 11:15-11.35 Coffee break

CHAIRMAN OF THE SESSION **Mikhail Lukin**

- 11:35-12.20 **Belotelov Vladimir**, RQC
«Active plasmonic crystals»
- 12:20-13.05 **Harald Giessen**, U. of Stuttgart
«Complex functional nanooptics and plasmonics»
- 13:05-14.30 Lunch

CHAIRMAN OF THE SESSION **Vladimir Belotelov**

- 14:35-15.20 **Maurice Skolnick**, U. of Sheffield
«Semiconductor nano-photonics nanostructures and circuits»
- 15:20-16.05 **Leonid Keldysh**, MSU
«Nonequilibrium Quantum Many Body Problems in terms of Green's Functions»
- 16:05-16.50 Coffee break
- 16:50-19:05 Poster session

Wednesday, July 15

CHAIRMAN OF THE SESSION **Alexey Akimov**

- 09:00-09.45 **Tommaso Calarco**, U. of Ulm
«Controlled quantum many-body dynamics: nonlinearity, reversibility, complexity»
- 09:45-10.30 **Tobias Kippenberg**, EPFL
«Measurement and control of a nanomechanical oscillator at the thermal decoherence rate»
- 10:30-11.15 **Michael Gorodetsky**, RQC
«Microresonator frequency combs: from chaos to solitons and platicons»
- 11:15-11.35 Coffee break

CHAIRMAN OF THE SESSION **Alexand Lvovsky**

- 11:35-12.20 **Charles Adams**, Durham U.
«Dipolar QED: an alternative paradigm for quantum optics, quantum sensors, and non-equilibrium dynamics»
- 12:20-13.05 **Eugene Polzik**, Niels Bohr Institute
«Oscillator beyond the ground state uncertainty – from one quadrature to both»
- 13:05-14.30 Lunch
- 14:35-19.00 Excursion to Kolomenskoye park
- 19:00 Conference dinner

Thursday, July 16

CHAIRMAN OF THE SESSION **Eugene Polzik**

- 09:00-09:45 **Ignacio Cirac**, MPQ
«Quantum simulations with atoms in nano-structures»
- 09:45-10:30 **Boris Altshuler**, Columbia U.
«Between Localization and Ergodicity in Quantum Systems»
- 10:30-11:15 **Eugene Demler**, Harvard
«Random-bond Heisenberg spin models and $1/f$ noise»
- 11:15-11:35 Coffee break

CHAIRMAN OF THE SESSION **Ignacio Cirac**

- 11:35-12:20 **Grigory Volovik**, Aalto U. & Landau Institute
«From Standard Model of particle physics to room-temperature superconductivity»
- 12:20-13:05 **Natalia Berloff**, Skoltech
«Engineering quantum circuits in a polariton condensate»
- 13:05-14:30 Lunch

CHAIRMAN OF THE SESSION **Alexey Zheltikov**

- 14:35-15:20 **Olga Smirnova**, Max Born Institute
«Attosecond Spectroscopy: from measuring ionization times to time-resolving chiral response»
- 15:20-16:05 **Mikhail Ivanov**, Imperial College
«High harmonic generation in strong laser fields: new questions and ideas»
- 16:05-16:50 Coffee break
- 16:50-19:05 Poster session

Friday, July 17

CHAIRMAN OF THE SESSION **Alexey Ustinov**

- 09:00-09:45 **Simon Gustavsson**, MIT
«Non-exponential energy decay and quasi-particle fluctuations in a superconducting flux qubit»
- 09:45-10:30 **Rudolf Gross**, WMI, TU Munich
«Ultrastrong Coupling in Superconducting Circuit QED»
- 10:30-11:15 **Michael Siegel**, KIT
«Superconducting Nanowire Single-Photon Detectors»
- 11:15-11:35 Coffee break

CHAIRMAN OF THE SESSION **Alexey Kavokin**

- 11:35-12:20 **Sven Hoefling**, St-Andrews, UK
«Quantum Dot Microcavity Devices for Quantum Communication and Information Applications»
- 12:20-13:05 **Pavlos Lagoudakis**, U. of Southampton
«Vortex formation in a Lattice Polariton-Condensate»
- 13:05-14:35 Lunch

CHAIRMAN OF THE SESSION **Alexey Rutsov**

- 14:35-15:20 **Alexey Kavokin**, RQC
«Weak lasing in polariton superlattices»
- 15:20-16:05 **Illia Akimov**, Dortmund
«Magnetic field induced photon echoes in semiconductor nanostructures: Storing light in the electron spin ensemble»
- 16:05-16:50 Coffee break

CHAIRMAN OF THE SESSION **Eugene Demler**

- 16:50-17:35 **Pavlos Savvidis**, U. of Crete
«Polariton lasing in hybrid organic-inorganic microcavity»
- 17:35-18:20 **Sergej O. Demokritov**, U. Münster
«Magnonic sound and its interaction with magnon Bose-Einstein condensate»
- 18.20-19.05 **Alexey Rubtsov**, RQC
«Open correlated quantum systems: what's new out of equilibrium?»

INFORMATION

TRANSPORT	14
HOTEL	17
EXCURSION	20

Aeroexpress



You are likely to arrive at the Vnukovo, Domodedovo or Sheremetyevo airport in Moscow. The best way to get to the city center is to take an Aeroexpress train, which costs about 470 rubles (~\$8). It takes about 40 minutes to get at, respectively, the Kiyevsky, Paveletsky or Belorussky railway station.

www.aeroexpress.ru/en



Metro



Metro is the main transportation system in Moscow. The network covers most of the city and provides rapid access to most of points of Interest in Moscow. Trains run every 2-3 minutes. In case you are traveling inside the city Metro is the best way to commute. Ground transportation is much less efficient and often suffers from serious traffic, so it makes sense to use it only on short distances. Taxi is often expensive and not efficient due to traffic jams.

engl.mosmetro.ru

The hotel is about one kilometer from the Kiyevsky railway station (Kiyevsky Vokzal) and the Kiyevskaya Metro station. If you are at another railway station, you will need to take the Metro. The ticket costs 50 Roubles (\$1) and can be purchased from a vending machine at any Metro station. Take the Ring Line to Kiyevskaya. You can either walk or take a cab from Kiyevskaya to the hotel. Walking scheme towards the hotel is provided below (p.14). In general you can get to the Ukraina hotel using taxi directly from airport, but due to serious traffic the use of taxi in Moscow is not recommended. If you wish to take a taxi from the airport, it will cost you about (~\$30-40).



METRO MAP

© Art. Lebedev Studio. Map version 21.2, January 2015

CARD «TROYKA»

Pledge for the card - 50 Rubles (1\$)

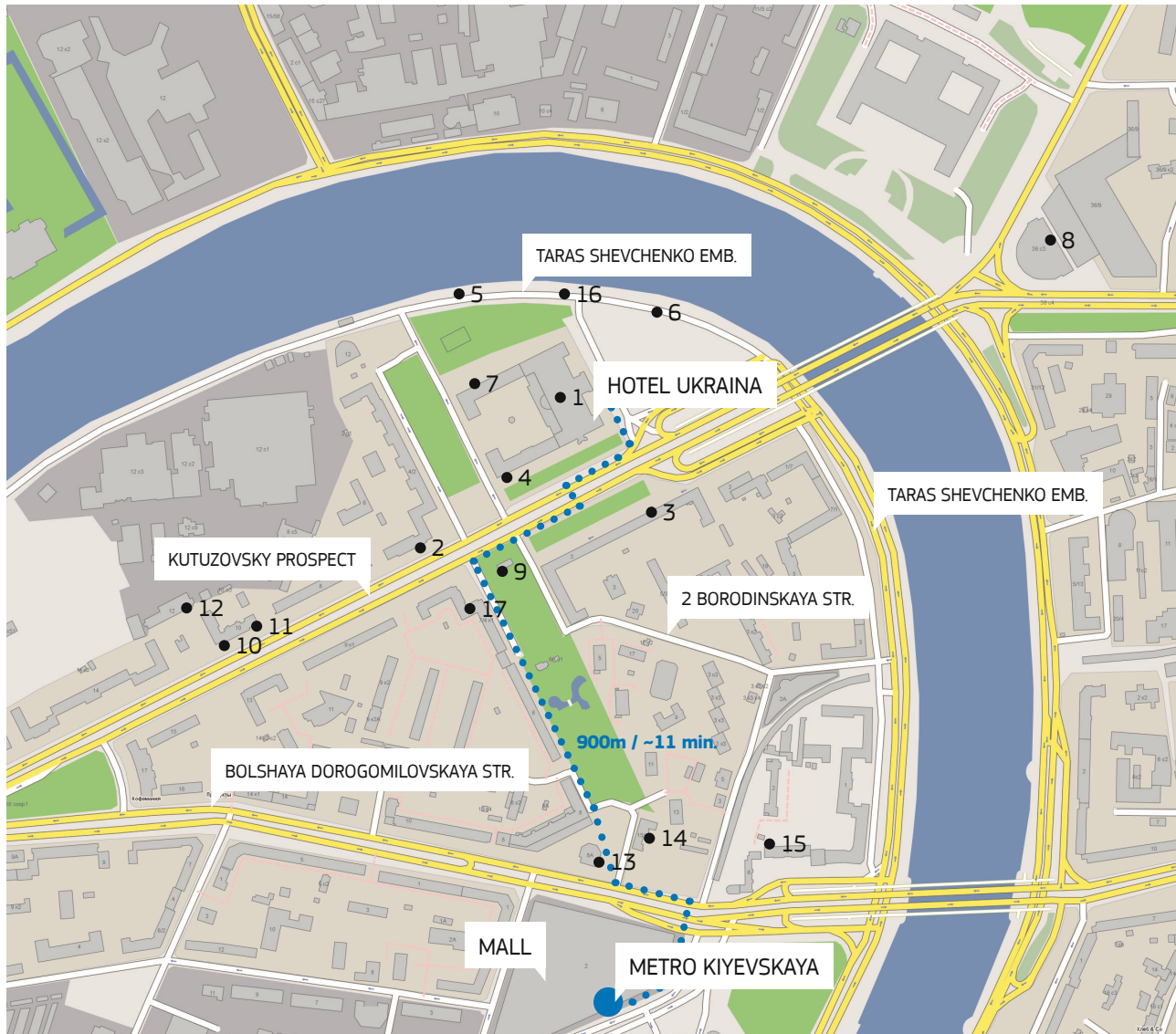
A trip on the subway and monorail	30 RUR
A trip on ground transport	29 RUR

CARD «EDINIY»

For subway, ground transport and monorail

With limited trips	
1 trip	50 RUR
5 trips	180 RUR
11 trips	360 RUR

With unlimited trips	
1 day	210 RUR
3 days	400 RUR
7 days	800 RUR



Restaurants

	TITLE	CUISINE	BILL, RUB	ADDRESS
1	Tatler Club (10:00-00:00)	European, Italian, Russian	2500-4000	Kutuzovsky prospect, 2/1, hotel Ukraina
2	Pinocchio (12:00-01:00)	Italian	1500-4000	Kutuzovsky prospect, 4/2
3	Zolotoy (12:00-23:00)	European	1500-2500	Kutuzovsky prospect, 5
4	Christian (09:00-00:00)	Italian	2500	Kutuzovsky prospect, 2/1, bld. 1a
5	La Barge (15:00-00:00)	Fusion	3000	Taras Shevchenko emb., pier hotel Ukraina
6	Soluxe club (12:00-03:00)	European, Chinese	2500	Kutuzovsky prospect, 2/1, bld. 6
7	Il Forno (11:00-00:00)	Italian	2000-3000	Kutuzovsky prospect, 2/1, bld. 6
8	White café (09:00-03:00)	European, Italian, Russian	3000	Novy Arbat street, 36
9	Take (11:00-06:00)	Japanese	1000	Kutuzovsky prospect, 5a/3
10	Peshi (10:00-23:00)	Italian	3000	Kutuzovsky prospect, 10
11	Shokoladnica (10:00-23:00)	European	500	Kutuzovsky prospect, 10
12	Uryuk (10:00-00:00)	Japanese	2500-3000	Kutuzovsky prospect, 12
13	McDonalds (06:00-00:00)	American	100-500	Bolshaya Dorogomilovskaya street, 8a
14	Beer Restaurant (12:00-00:00)	European	1500-2000	Ukrainian Blvd., 15
15	Riviere (12:00-23:00)	French	1500-2500	Bolshaya Dorogomilovskaya street, 4
16	Fish (12:00-00:00)	Italian	4000-4500	Taras Shevchenko emb., pier Radisson Royal
17	Diplomat Bar (11:00-23:00)	Italian, European	1000	Kutuzovsky prospect, 7/4



Radisson Royal Moscow Hotel (Ukraina)

Location. Hotel's location in Moscow city center places guests on the bank of the Moskva River, at the intersection of the capital's main thoroughfares – Kutuzovskiy Prospekt and Novy Arbat, and near a variety of transport options and attractions. The hotel building is one of the famous Seven Sisters, the group of skyscrapers in Moscow built from 1947 to 1953 and designed in the Stalin's Empire style. The unique feature of the hotel is the diorama located at the ground floor that shows the historical center of Moscow as it was in 1977.

ADDRESS: Moscow, Gostinichniy proezd 8 (building 1)

METRO: Kiyevskaya

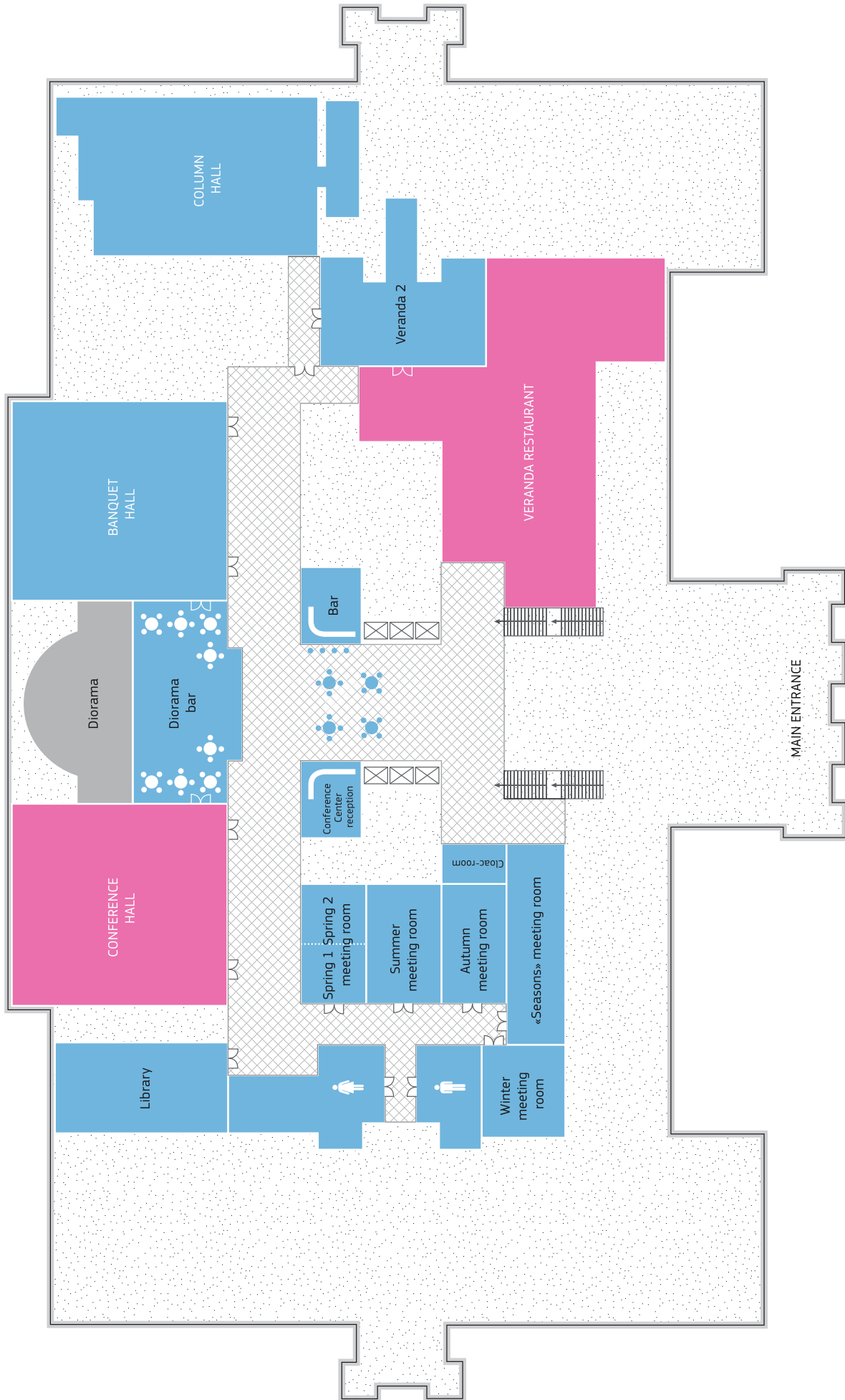
PHONE: +7 495 221 5555

FACILITIES

- 24-hour concierge service (taxi booking, theater desk, interpreting services, etc.)
- 24-hour housekeeping service
- Bank services, currency exchange
- Nine Restaurants & Bars
- Five yachts-restaurants
- Library & Business Centre
- Mono and multi-brand boutique gallery (26 boutiques)
- Cigar room
- Ballroom
- Overnight shoeshine
- Overnight laundry and drycleaning service
- Parking

www.ukraina-hotel.ru/en

HOTEL MAP



Conference center



Conference hall. The main venue of the ICQT-2015 is the Conference Room 1 located on the first floor (Russian way – 2nd floor) of the hotel. This 400 m² hall can accommodate up to 430 guests. It is fitted with up-to-date audiovisual equipment including a projector and 6x3 meters screen.



Restaurant. During the Conference breakfast and lunch will be served at classic style Veranda Restaurant located on the same floor with conference hall. Breakfast is served for those staying at hotel Ukraina or for additional price.

Sporting facilities

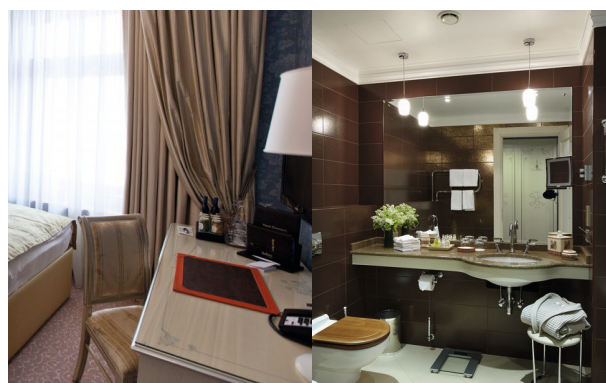


Fitness. Ideally planned, spacious rooms are ready to welcome you: gym; rooms for group, individual and martial arts trainings; comfortable changing rooms; fitness-bar; solarium. Working hours: 7:00–00:00.



Swimming & Bathing. The hotel has Olympic size swimming pool (50 m long, 6 lanes), Jacuzzi, Russian bath, sauna and hamam for guest seeking for relaxation and special treatment. Working hours: 7:00–00:00.

Accommodation





Kolomenskoye park

Kolomenskoye is a former royal estate situated in a huge natural park with its own rivers, fields and hills. It has been a summer residence of Tsar. It's famous for The Church of the Ascension that was included in the Unesco World Heritage List, a reconstruction of the Wooden Palace and the original house of Peter I, brought from the North of Russia.

We offer you a guided excursion to recently reconstructed Wooden Palace of the Tsar Alexey Mikhailovich Romanov that is often referred to as an Eighth Wonder of the World. The

building represents a huge maze of intricate corridors and 250 rooms, built without using saws, nails, or hooks. The interior décor is bright and varied: here you will find intricate wood carving, colourful wall and ceiling paintings and ornamental upholstery of furniture and walls. All this rich décor turns the whole building into a small and picturesque fairytale palace.

The excursion takes about 2 hours, and you'll have from 30 to 60 minutes of free time for walking around.

Please note that you may need photo permission, which can be bought separately in the museum's box office.

INVITED ■ TALKS

MONDAY, JULY 13.	22
TUESDAY, JULY 14.	27
WEDNESDAY, JULY 15.	34
THURSDAY, JULY 16.	39
FRIDAY, JULY 17.	46

Entanglement of 3000 atoms by one photon

Hao Zhang¹, Robert McConnell¹, Jiazhong Hu¹, Senka Ćuk^{1,2}, and V. Vuletić¹

¹ *Department of Physics and Research Laboratory of Electronics, Massachusetts Institute of Technology, Cambridge, MA 02139, USA*

² *Institute of Physics, University of Belgrade, Pregrevica 118, 11080 Belgrade, Serbia*
e-mail: vuletic@mit.edu

Quantum-mechanically correlated (entangled) states of many particles are of interest in quantum information, quantum computing and quantum metrology. Metrologically useful entangled states of large atomic ensembles (spin squeezed states) have been experimentally realized, but these states display Gaussian spin distribution functions with a non-negative Wigner quasiprobability distribution function [1-9]. Non-Gaussian entangled states have very recently been produced and characterized in atomic ensembles [10-12]. Here we generate entanglement in a large atomic ensemble via an interaction with a very weak laser pulse; remarkably, the detection of a single photon prepares several thousand atoms in an entangled state. We reconstruct a negative-valued Wigner function, and verify an entanglement depth (the minimum number of mutually entangled atoms) of 2,900(200) out of 3,100 atoms [13]. The achieved purity of the state is slightly below the threshold for entanglement-induced metrological gain, but further technical improvement should allow the generation of states that surpass this threshold, and of more complex Schrödinger cat states.

[13] R. McConnell, H. Zhang, J. Hu, S. Ćuk, and V. Vuletić, *Nature* **519**, 439-442 (2015).

- [1] M. Kitagawa, and M. Ueda, *Phys. Rev. A* **47**, 5138–5143 (1993).
- [2] J. Appel, et al., *Proc. Natl Acad. Sci. USA* **106**, 10960–10965 (2009).
- [3] T. Takano, et al., *Phys. Rev. Lett.* **104**, 013602 (2010).
- [4] M.H. Schleier-Smith, I.D. Leroux, and V. Vuletić, *Phys. Rev. Lett.* **104**, 073604 (2010).
- [5] C. Gross, T. Zibold, E. Nicklas, J. Esteve, and M.K. Oberthaler, *Nature* **464**, 1165–1169 (2010).
- [6] M.F. Riedel, et al., *Nature* **464**, 1170–1173 (2010).
- [7] C.D. Hamley, et al., *Nature Phys.* **8**, 305–308 (2012).
- [8] R.J. Sewell, et al., *Phys. Rev. Lett.* **109**, 253605 (2012).
- [9] J.G. Bohnet, et al., *Nature Photon.* **8**, 731–736(2014).
- [10] F. Haas, J. Volz, R. Gehr, J. Reichel, and J. Esteve, *Science* **344**, 180–183 (2014).
- [11] H. Strobel, et al., *Science* **345**, 424–427 (2014).
- [12] B. Luecke, et al., *Phys. Rev. Lett.* **112**, 155304 (2014).

**New tricks with ultracold strontium:
Laser cooling to BEC
&
Ultracold RbSr molecules**

F. Schreck

*University of Amsterdam, Spui 211012 WX Amsterdam Netherlands
e-mail: F.Schreck@uva.nl*

I will present two research lines that we are pursuing with ultracold strontium. In the first research line, we have cooled a gas of strontium to quantum degeneracy using laser cooling as the only cooling method. We are currently developing a setup in which we hope to exploit this technique to build a perpetual atom laser, which has many applications in precision measurement.

In the second line of research, we are working towards ultracold RbSr ground-state molecules, which are open-shell polar molecules, having a large electronic dipole moment and an unpaired electron. Compared to the already existing ultracold closed-shell polar molecules, RbSr molecules provide us with a larger parameter space for interaction control and the study of many-body physics. As first steps towards these molecules, we have created a quantum gas mixture of Rb and Sr, performed RbSr molecular spectroscopy, and established a new molecule association method.



Superfluid-to-Mott-Insulator Transition with Ultracold Atomic Dipoles

F. Ferlaino

*Institut für Experimentalphysik, Universität Innsbruck and
Institut für Quantenoptik und Quanteninformation, Österreichische Akademie der Wissenschaften, 6020
Innsbruck, Austria
e-mail: Francesca.Ferlaino@uibk.ac.at*

Strongly magnetic atoms are an ideal system to study many-body quantum phenomena with anisotropic interactions. Here, we report on the first observation of the superfluid to Mott-insulator transition in presence of the anisotropic and long-range dipole-dipole interaction [1]. We demonstrate that the dipolar interaction can favor the superfluid or the Mott phase depending on the orientation of the atomic dipoles and we observe for the first time the presence of the nearest-neighbor interaction between the particles. In a combined experimental and theoretical work, we show that the system is well described by an extended Bose-Hubbard Hamiltonian, which includes the onsite dipolar interaction, the nearest-neighbor interaction, and the density-induced tunneling.

- [1] S. Baier, M. Mark, K. Aikawa, D. Petter, L. Chomaz, Z. Cai, M. Baranov, P. Zoller, F. Ferlaino, in preparation

Majorana fermions in atomic-molecular systems at finite temperature and in the presence of a noise

M. Baranov^{1,2}, Z. Cai¹, Y. Hu¹ and P. Zoller^{1,3}

¹ *Institute for Quantum Optics and Quantum Information, Technikerstr. 21a, A-6020 Innsbruck, Austria*

² *National Research Centre “Kurchatov Institute”, Kurchatov sq. 1, Moscow 123182, Russia*

³ *Institute for Theoretical Physics, University of Innsbruck Technikerstr. 21a, A-6020 Innsbruck, Austria*

e-mail: Mikhail.Baranov@uibk.ac.at

The effects of quantum and thermal fluctuations, as well as of global and local noises, on the Majorana edge states in topological atomic-molecular wire networks are discussed. It is found that the energy of the Majorana states remains exponentially small with the length of the wire even at finite temperatures which are smaller than the bulk energy gap in the wires. The preexponential factor, on the other hand, is strongly affected by the fluctuations and increases with temperature and the length of the wire. At finite temperatures, however, initial correlations between Majorana states decay to the values which are temperature and length dependent, and vanish in the thermodynamic limit. This provides limitations on the size of the wire and on the speed of quantum manipulations with Majorana fermions. The effects of the noise are similar to those of temperature but strongly depend on the noise's frequency, amplitude, and position (for a local noise). Interesting is that, due to the Zeno effect, the life-time of correlations for a fast noise is remarkably large even when the noise causes switching between topological and non-topological phases of the wire.



Quantum Optics and Quantum Communications with non-Gaussian States of Light.

Erwan Bimbard, Rajiv Boddeda, Andrey Grankin, Imam Usmani, Valentina Parigi,
Jovica Stanojevic, Etienne Brion, Alexei Ourjountsev, Philippe Grangier

¹ *Laboratoire Charles Fabry, Institut d'Optique, CNRS, Université Paris-Sud, 91127 Palaiseau, France*
e-mail: philippe.grangier@institutoptique.fr

In recent years various quantum communication protocols have been proposed by using non-Gaussian states of the light, such as the generation of entangled “Schrödinger's cat states” [1, 2]. For applications to quantum information processing, it is interesting to use these techniques together with “giant” optical non-linear effects, that can be obtained from large interactions between Rydberg atoms, known as Rydberg blockade [3, 4].

We will present results towards the possible realization of non-linear optical effects that are large enough to induce photon-photon interactions [5, 6]. Such effects would be a significant step forward for quantum information processing and communications, including the implementation of an efficient two-photon phase gate.

[1] “Generating Optical Schrödinger Kittens for Quantum Information Processing”, A. Ourjountsev, R. Tualle-Brouri, J. Laurat, and P. Grangier, *Science* 312, 83 (2006).

[2] “Preparation of non-local superpositions of quasi-classical light states”, A. Ourjountsev, F. Ferreyrol, R. Tualle-Brouri, P. Grangier, *Nature Phys.* 5, 189 (2009).

[3] “Observation of collective excitation of two individual atoms in the Rydberg blockade regime”, A. Gaetan et al, *Nature Phys.* 5, 115 (2009)

[4] “Entanglement of Two Individual Neutral Atoms Using Rydberg Blockade”, T. Wilk et al, *Phys. Rev. Lett.* 104, 010502 (2010)

[5] “Observation of Interaction-Induced Dispersive Optical Nonlinearities in an Ensemble of Cold Rydberg Atoms”, V. Parigi et al, *Phys. Rev. Lett.* 109, 233602 (2012)

[6] “Homodyne Tomography of a Single Photon Retrieved on Demand from a Cavity-Enhanced Cold Atom Memory”, E. Bimbard et al, *Phys. Rev. Lett.* 112, 033601 (2014)

New interface between quantum optics and nanoscience**M.D. Lukin***Harvard University, 17 Oxford Str, Cambridge, MA 02138, USA**e-mail: lukin@fas.harvard.edu*

We will discuss recent developments at a new scientific interface between quantum optics, nano science, metrology and quantum information science. Specific examples include the use of quantum optical techniques for manipulation of individual atom-like impurities at a nanoscale and for realization of hybrid systems combining quantum emitters and nanophotonic devices. We will discuss how these techniques are used for realization of single photon switches, quantum networks, and for new applications such as magnetic resonance imaging with single atom resolution.



Quantum Interfaces between Gamma-Photon and Nuclear Ensembles

F. Vagizov^{1,2}, X. Zhang¹, W.-T. Liao³, R. Shakhmuratov², A. Kalachev^{2,1}, V. Antonov^{4,1},
Y. Radeonychev^{4,1}, M.O. Scully^{1,5} and O. Kocharovskaya¹

¹Department of Physics & Astronomy, Texas A & M University, College Station, TX 77843, USA

²Kazan Federal University, and Kazan Physical Technical Institute, RAS, Russian Federation

³Max-Planck-Institut für Kernphysik, Heidelberg, Germany

⁴Institute of Applied Physics, Russian Academy of Science, Nizhny Novgorod, Russia

⁵Princeton University, Princeton, New Jersey 08544, USA

e-mail: kochar@physics.tamu.edu

In the last decade interfaces between light and optically thick free space atomic ensembles have been developed as one of the basic building blocks for quantum information processing. Temporal shaping of single photon is often required for implementation of such interfaces, in particular, for preparation of time-bin qubits and for realization of quantum memories. Optical time-bin qubits are formed either by unbalanced interferometers with photons produced via parametric down conversion or by temporally modulated pumping of a single atom in a QED cavity. Optical quantum memories are implemented either by using optimally shaped coherent driving fields in Raman or EIT three-level scheme or by controlling or tailoring of the inhomogeneous broadening of the resonant two-level transition.

Gamma-photon - nuclear ensembles interfaces present an interesting alternative to optical photon - atomic ensemble interfaces and the useful platform for testing new techniques. The main advantages are: i) an existence of natural radioactive sources of heralded (due to the cascade scheme of decay) single gamma-photon sources; ii) high efficiency of the photon detectors and iii) orders of magnitude stronger coupling, leading to optical thickness on the order of one at extremely small physical thicknesses on the order of 1 μm or less. The potential advantages include also sub- λ focusing and large capacity of the information channel. At the same time the standard optical techniques of the single photon shaping, time-bin qubits formation and quantum memory are not available in the gamma-ray range.

In this talk we present a new efficient technique for temporal shaping of gamma photons, based on combination of coherent vibration of the resonant absorber with gated detection [1], a method to produce gamma-photon time-bin qubit, based on controllable phase and frequency tuning of vibrated layered absorbers [2] and a technique for implementation of gamma-photon quantum memory in the nuclear ensemble, based on the Doppler frequency comb

formed by a set of absorbing layers, moving with different velocities [3].

- [1] F. Vagizov, V. Antonov, Y.V. Radeonychev, R. N. Shakhmuratov, O. Kocharovskaya, *Nature*, **508**, 80 (2014).
- [2] R. N. Shakhmuratov, F. Vagizov, V. A. Antonov, Y.V. Radeonychev, M. O. Scully, O. Kocharovskaya, *Phys. Rev. Lett.*, submit.
- [3] X. Zhang, W.-T. Liao, A. A. Kalachev, R. N. Shakhmuratov, M.O. Scully and O. Kocharovskaya, *Nature Photonics*, submit.

Efficient coupling of light to a single atom in a parabolic mirror

G. Leuchs^{1,2,3}, M. Bader^{1,2}, M. Fischer^{1,2}, L. Alber^{1,2}, S. Heugel^{1,2}, A. Golla^{1,2}, R. Maiwald^{1,2,4}, M. Sondermann^{1,2}

¹Max Planck Institute for the Science of Light, Erlangen, Germany

²Department Physik, Universität Erlangen-Nürnberg, Erlangen, Germany

³Department of Physics, University of Ottawa, Canada

⁴Physikalisches Institut, Universität Bonn, Germany

e-mail: gerd.leuchs@mpl.mpg.de

In the electric dipole approximation an atom in free space couples to an electric dipole wave. If one wants to saturate an atomic transition with the smallest possible power, then one has to irradiate the atom with an incoming dipole wave matching the time reversed version of spontaneously emitted light pattern [1]. The smallest possible saturation power corresponds to a fraction of a photon (1/8) per lifetime of the excited atomic state [2]. The intensity of a circularly polarized dipole wave is non-zero for any solid angle, but for a linear dipole the intensity goes to zero for two angles. Hence we are aiming for a linear dipole transition because of the increased freedom in designing the optical set-up. This is important for having some space for positioning the atom in the focus of the dipole wave. As an atom we use an Ytterbium ion trapped at the focus of a parabolic mirror providing a geometry with wide-open optical access [3]. We experiment with both a singly and a doubly charged ion. The ion at the focus of the deep parabolic mirror behaves identically to an ion in free space as long as the focal length is much larger than the transition wavelength [4]. The state of the art is reviewed and the experimental progress is discussed [5]. If the interaction is efficient enough it will allow for building a few photon broadband quantum gate, with possible applications in quantum information processing such as a quantum repeater [6].

- [1] S. Quabis, R. Dorn, M. Eberler, O. Glöckl, and G. Leuchs, *Opt. Commun.* 179, 1 (2000)
- [2] P. Kochan and H. J. Carmichael, *Phys. Rev. A*, 50, 1700-1709 (1994)
- [3] R. Maiwald, D. Leibfried, J. Britton, J. C. Bergquist, G. Leuchs, and D. J. Wineland, *Nature Phys.* 5, 551 (2009)
- [4] G. Alber, J.Z. Bernád, M. Stobinska, L.L. Sánchez-Soto, and G. Leuchs, *Phys. Rev. A* 88, 023825 (2013)
- [5] M. Fischer, M. Bader, R. Maiwald, A. Golla, M. Sondermann, and G. Leuchs, *Appl. Phys. B: Lasers and Optics* 117, 797 (2014)
- [6] P. van Loock, T. D. Ladd, K. Sanaka, F. Yamaguchi, Kae Nemoto, W. J. Munro, and Y. Yamamoto, *Phys. Rev. Lett.* 96, 240501 (2006)

Active plasmonic crystals

V.I. Belotelov^{1,2}

¹Russian Quantum Center, 100 Novaya St., Skolkovo, Moscow 143025, Russia

²Lomonosov Moscow State University, Leninskie gori, Moscow 119296, Russia

e-mail: belotelov@rqc.ru

Currently, there is great research interest in the area of plasmonics, since surface plasmon-polaritons, coupled oscillations of electrons and light localized at a metal surface, are very promising as information carriers for next-generation nanophotonic devices. If such applications are anticipated, one should find different ways to control wavenumber, phase and polarization of surface plasmons. At this point, 'active plasmonics' comes to play.

There are different methods and approaches of active plasmonics. In this talk, we shall discuss how to influence on the surface plasmons by means of direct and inverse magneto-optical effects, photoexcitation of electrons in a metal, gain media, optical phonons, and acoustic waves. In all cases we consider Fano resonances in light transmitted or reflected from periodic plasmonic structures – plasmonic crystals – consisting of a metal nanograting of slits or holes and a smooth dielectric. Such type of resonances originate from excitation of surface plasmons.

Magnetic field control of light is among the most intriguing methods for modulation of light intensity and polarization on sub-nanosecond timescales. The implementation in nanostructured hybrid materials provides a remarkable increase of magneto-optical effects [1,2]. Highest figure of merit of resonances and enhancement of the magneto-optical effects are achieved for magnetic dielectrics like iron garnets.

However, not only the enhancement of already known effects has been demonstrated in plasmonic crystals. Recently, we postulate a novel magneto-optical phenomenon that originates solely from suitably designed magneto-plasmonic crystal [3]. In this material, an incident light excites coupled plasmonic oscillations and a waveguide mode. An in-plane magnetic field allows excitation of an orthogonally polarized waveguide mode that modifies optical spectrum of the magnetoplasmonic crystal and increases its transparency. The experimentally achieved light intensity modulation reaches 24%. As the effect can potentially exceed 100%, it may have great importance for applied nanophotonics. Further, the effect allows manipulating and exciting waveguide modes by a magnetic field and light of proper polarization.

Magnetization of the magnetoplasmonic crystal can be modified by either an external magnetic field or by laser pulse of circular polarization [4]. In the later

case, inverse Faraday effect is involved thus allowing to switch magnetization on picosecond time scales.

Alternatively, optical properties of the plasmonic crystals can be tuned by femtosecond laser pulses. As a result, surface plasmons propagation through the plasmonic crystal are modified and corresponding differential transmittance and reflectance changes of the order of 5% are observed [5]. The response time of plasmonic crystals can be varied widely from 200 to 800 fs by tuning the relative spectral positions of the probe and the SPP resonance.

Another approach of the active plasmonics uses coherent sub-THz phonons incident on a gold grating that is deposited on a dielectric substrate. They undergo diffraction and thereby induce an alteration of the surface plasmon-polariton resonance. This results in efficient high-frequency modulation (up to 110 GHz) of the structure's reflectivity for visible light in the vicinity of the plasmon-polariton resonance [6]. High modulation efficiency is achieved by designing a periodic nanostructure which provides both plasmon-polariton and phonon resonances. Our theoretical analysis shows that the dynamical alteration of the plasmon-polariton resonance is governed by modulation of the slit widths within the grating at the frequencies of higher-order phonon resonances.

- [1] V.I. Belotelov, I.A. Akimov, A.K. Zvezdin et. al, *Nature Nanotech.* **6**, 370 (2011).
- [2] V.I. Belotelov, L.L. Doskolovich, A.K. Zvezdin: *Phys. Rev. Lett.*, **98**, 77401 (2007).
- [3] V.I. Belotelov, L.E. Kreilkamp, I.A. Akimov, et al. *Nature Comm.* **4**, 2128 (2013).
- [4] V.I. Belotelov and A.K. Zvezdin, *Phys. Rev. B* **86**, 155133 (2012).
- [5] M. Pohl, V.I. Belotelov, I.A. Akimov, S. Kasture, A.S. Vengurlekar, A.V. Gopal, A.K. Zvezdin, M. Bayer, *Phys. Rev. B* **85**, 081401(R) (2012).
- [6] C. Brüggemann, A.V. Akimov, V.I. Belotelov, et. al, *Phys. Rev. B* **86**, 121401(R) (5) (2012).

Complex functional nanooptics and plasmonics

Harald Giessen

4th Physics Institute and Research Center SCoPE, University of Stuttgart, Germany
e-mail: h.giessen@pi4.uni-stuttgart.de

Nanooptics has experienced tremendous growth over the last few years. The possibility to tailor materials and their dielectric and optical properties from the bottom up on the subwavelength level has opened the door to ultimate control of light-matter interaction. This holds true for the linear optical properties, as well as for optical nonlinearities.

Particularly, plasmonics which involves resonant electron oscillations in metallic nanostructures, allowed for large electric field confinement and enhancement on the sub-100 nm length scale.

Specifically, the combination of a variety of geometrical shapes and structures has enabled optical resonance tailoring, for example by utilizing narrow Fano resonances. Novel functionalities such as plasmonic chirality, leading to giant optical activity, can be attained through geometrical arrangement of simpler plasmonic building blocks. Hybrid plasmonic structures, which involve additional elements such as active phase-change, nonlinear, or magneto-optical materials, give control over the dynamical behavior of nanoscopic light-matter interaction.

In this contribution, I am going to review some of the key fundamentals for building more complex plasmonic and nano-optical systems, and first applications for sensing as well as dynamic changes of their functionality will be presented.



Semiconductor nano-photonic quantum structures and circuits

M S Skolnick

Department of Physics and Astronomy, University of Sheffield, Sheffield S3 7RH
 e-mail: *m.skolnick@sheffield.ac.uk*

This talk will begin with a general overview of the favorable properties of III-V semiconductor quantum dots grown by self assembly crystal growth techniques. It will then focus on some of the key properties and demonstrators for quantum science and applications. These will include chiral properties for spin readout by integration into nano-photonic structures (Fig 1), enhancement of coherence times by resonance fluorescence, 50:50 on-chip beam splitting (Fig 2) and single photon routing. Deterministic registration to achieve desired properties, including spin readout will also be shown.

INVITED TALKS

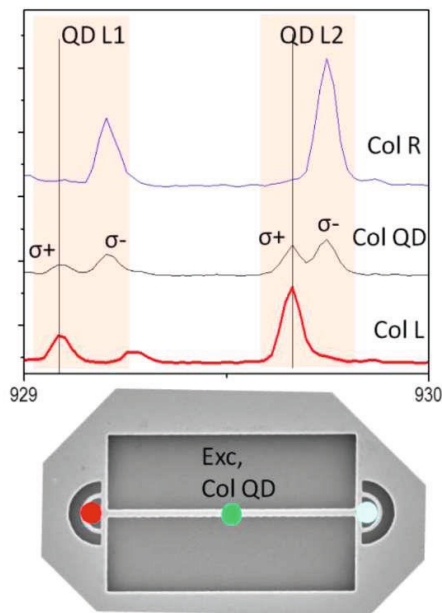


Fig 1 Spin to path conversion

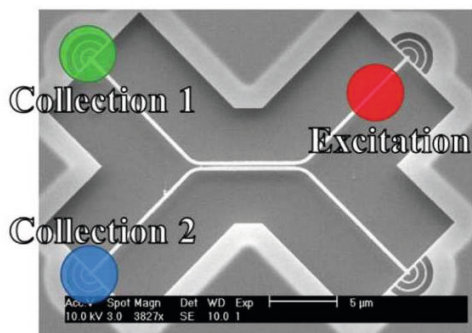


Fig 2 On-chip beam splitter

TUESDAY, JULY 14

LEONID KELDYSH 15:20-16:05

Nonequilibrium Quantum Many Body Problems in terms of Green's Functions

L. Keldysh

Lomonosov Moscow State University, Leninskie Gory, Moscow, 119991, Russia
e-mail: *keldysh@td.lpi.ru*

The Nonequilibrium Real Time Green's functions formalism will be presented including some general properties and the physical meaning of different components of 2×2 Green's function matrices and corresponding self-energy matrices, and also that's connection to the quantum generalization of Boltzmann Equation accounting for the close interrelation of quantum kinetics and dynamics

INVITED TALKS



Controlled quantum many-body dynamics: nonlinearity, reversibility, complexity

T. Calarco

Institute of Complex Quantum Systems, University of Ulm, Albert-Einstein-Allee 11, 89069 Ulm, Germany
e-mail: *tommaso.calarco@uni-ulm.de*

The control of quantum states is an important building block for fundamental investigations and technological applications of quantum physics. However, quantum many-body systems exhibit complex behaviors that make them difficult to manipulate, in particular in the presence of intrinsic dephasing, decoherence or decay. One strategy to control such quantum states is to implement operations faster than the characteristic timescales of the prejudicial processes, using for example optimal control theory (OCT). The speedup can be exploited to experimentally realize elaborate manipulations, for instance precisely controlled ultra-fast single electron spin gates using specially designed microwave fields [1] or a sequence of state transfer pulses for interferometry [2].

The maximum achievable speedup is influenced non-trivially by inter-particle interactions, but their effect can be compensated for if many-body nonlinearity is properly taken into account (see Fig. 1).

Reversibility of quantum dynamics can also be attained experimentally via optimal control [4]. The bandwidth of the corresponding control pulses allows for a characterization of quantum many-body processes [5], and for dynamical discrimination between different level of complexity in quantum many-body systems.

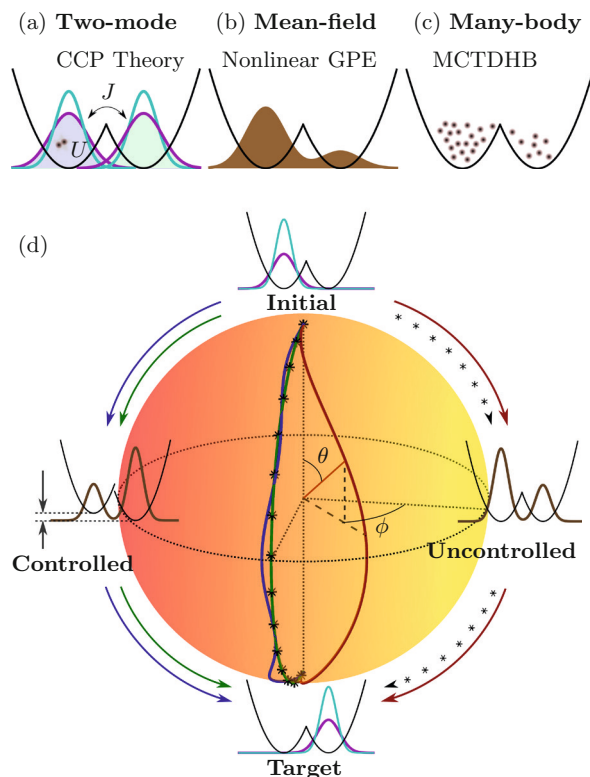


Figure 1: Effect of nonlinearity on the optimal dynamics of a Bosonic Josephson Junction [3].

- [1] J. Scheuer, X. Kong, R. Said, J. Chen, A. Kurz, L. Marseglia, J. Du, P. Hemmer, S. Montangero, T. Calarco, B. Naydenov, F. Jelezko, *New J. Phys.* 16, 093022 (2014).
- [2] S. van Frank, A. Negretti, T. Berrada, T. Bücke, S. Montangero, J.-F. Schaff, T. Schumm, T. Calarco, J. Schmiedmayer, *Nature Communications* 5, 4009 (2014).
- [3] I. Brouzos, A. Streltsov, A. Negretti, R. Said, T. Caneva, S. Montangero, T. Calarco, arXiv:1504.02858.
- [4] C. Lovecchio, F. Schäfer, S. Cherukattil, A. K. Murtaza, I. Herrera, F. Cataliotti, T. Calarco, S. Montangero, F. Caruso, arXiv:1405.6918; in preparation.
- [5] T. Caneva, A. Silva, R. Fazio, S. Lloyd, T. Calarco, S. Montangero, *Phys. Rev. A* 89, 042322 (2014); S. Lloyd and S. Montangero, *Phys. Rev. Lett.* 113, 010502 (2014).

Measurement and control of a nanomechanical oscillator at the thermal decoherence rate

Tobias J. Kippenberg (PhD)

Institute of Condensed Matter Physics, EPFL, Switzerland

e-mail: tobias.kippenberg@epfl.ch

In real-time quantum feedback protocols (1), the record of a continuous measurement is used to stabilize a desired quantum state. Recent years have seen spectacular advances in a variety of well-isolated micro-systems, including microwave photons(2) and superconducting qubits(3). By contrast, the ability to stabilize the quantum state of a tangibly massive object, such as a nano-mechanical oscillator, remains a difficult challenge. The main obstacle is environmental decoherence, which places stringent requirements on the timescale in which the state must be measured. Using cavity optomechanical coupling we report on a position sensor that is capable of resolving the zero-point motion of a solid-state, 4.3 MHz frequency nanomechanical oscillator in the timescale of its thermal decoherence(4), a basic requirement for preparing its ground-state using feedback as well as (Markovian) quantum feedback. The sensor is based on evanescent coupling to a high-Q optical microcavity(5), and achieves an imprecision 40 dB below that at the standard quantum limit for a weak continuous position measurement(6), a 100-fold improvement over previous reports, while maintaining an imprecision-back-action product within a factor of 5 of the Heisenberg uncertainty limit. As a demonstration of its utility, we use the measurement as an error signal with which to feedback cool the oscillator. Using radiation pressure as an actuator, the oscillator is cold-damped(7) with unprecedented efficiency: from a cryogenic bath temperature of 4.4 K to an effective value of 1.1mK, corresponding to a mean phonon number of 5.3 (i.e., a ground state probability of 16%). Our results set a new benchmark for the performance of a linear position sensor, and signal the emergence of mechanical oscillators as practical subjects for measurement-based quantum control.

- [1] H. Wiseman, Quantum theory of continuous feedback. *Physical Review A* **49**, 2133 (1994).
- [2] C. Sayrin *et al.*, Real-time quantum feedback prepares and stabilizes photon number states. *Nature* **477**, 73 (Sep 1, 2011).
- [3] R. Vijay *et al.*, Stabilizing Rabi oscillations in a superconducting qubit using quantum feedback. *Nature* **490**, 77 (Oct 4, 2012).
- [4] D. J. Wilson *et al.*, Measurement and control of a mechanical oscillator at its thermal decoherence rate. *arXiv:1410.6191 (Nature, in press)*, .

- [5] E. Gavartin, P. Verlot, T. J. Kippenberg, A hybrid on-chip optomechanical transducer for ultrasensitive force measurements. *Nature nanotechnology* **7**, 509 (Aug, 2012).
- [6] A. A. Clerk, M. H. Devoret, S. M. Girvin, F. Marquardt, R. J. Schoelkopf, Introduction to quantum noise, measurement, and amplification. *Reviews of Modern Physics* **82**, 1155 (2010).
- [7] M. Pinard, P. Cohadon, T. Briant, A. Heidmann, Full mechanical characterization of a cold damped mirror. *Physical Review A* **63**, (2000).

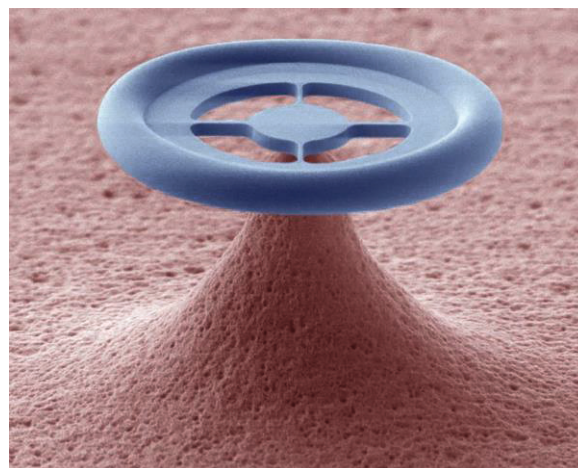


Figure 1: SEM image of a toroid resonator

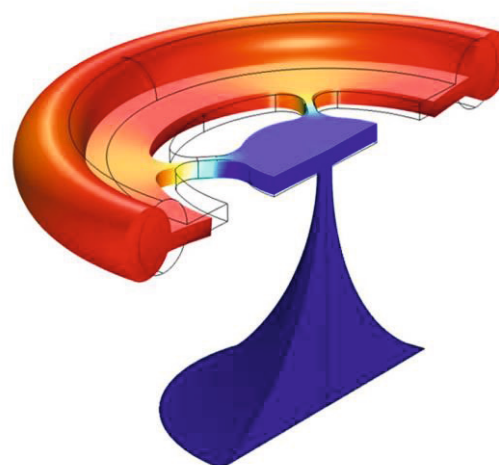


Figure 2: the optomechanical coupling between the optical and mechanical degree of freedom mediated by radiation pressure.

Microresonator frequency combs: from chaos to solitons and platicons

M. L. Gorodetsky^{1,2}

¹Russian Quantum Center, 100 Novaya St., Skolkovo, Moscow 143025, Russia

²Faculty of Physics, M. V. Lomonosov Moscow State University, Moscow 119991, Russia

e-mail: mg@rqc.ru

Optical frequency combs [1], which got their name due to characteristic spectra consisting from plurality of narrow equidistant lines, produced a revolution in metrology and high-precision measurements in the last decade. These combs are obtained traditionally with femtosecond mode-locked lasers. However in 2007 a new phenomenon was discovered in nonlinear optics - spontaneous formation of similar Kerr combs in passive dielectric microresonators under continuous wave pump [2]. These microresonator based combs which can be as broad as one octave [3] are formed as a result of multiple and cascaded four-wave-mixing hyper-parametric processes. The report presents the results of recent theoretical and experimental studies demonstrating the possibility to generate broadband coherent combs. Microresonator based Kerr combs open the route to novel compact and efficient photonic devices, namely portable comb sources, ultrastable microwave photonic oscillators and femtosecond pulse generators. This promise is supported by predicted and recently experimentally demonstrated controlled transition from chaotic to phase locked stable combs associated with circulating bright temporal solitons in whispering gallery mode crystalline [4] and integrated ring resonators [5] with anomalous group velocity dispersion. Experimental results are in excellent agreement with theoretical analysis and numerical simulations. Coherent optical frequency combs are also possible in normal dispersion regime with the formation of dark solitons and flat-topped stationary solitonic structures – platicons [6]. These platicons allow more efficient conversion of the of c.w. pump to the comb power than bright solitons. Soft excitation of platicons is possible with dispersion engineering, laser injection locking and amplitude modulation of the pump at a frequency corresponding to free spectral range of the microresonator.

- [1] Th. Udem, R Holzwarth, and T W Hänsch. Optical frequency metrology. *Nature*, 416:233–237, 2002.
- [2] P Del’Haye, A Schliesser, O Arcizet, T Wilken, R Holzwarth, and T Kippenberg. Optical frequency comb generation from a monolithic microresonator. *Nature*, 450:1214–1217, 2007.
- [3] P Del’Haye, T Herr, E Gavartin, M L Gorodetsky, R Holzwarth, and T J Kippenberg. Octave spanning tunable frequency comb from a microresonator. *Physical Review Letters*, 107(6):063901, 2011.
- [4] T. Herr, V. Brasch, J. D. Jost, C. Y. Wang, N. M. Kondratiev, M. L. Gorodetsky, and T. J. Kippenberg. Temporal solitons in optical microresonators. *Nature Photonics*, 8(2):145–152, 2013.
- [5] V. Brasch, T. Herr, M. Geiselmann, G. Lihachev, M. H. P. Pfeiffer, M. L. Gorodetsky, and T. J. Kippenberg. Photonic chip based optical frequency comb using soliton induced cherenkov radiation. *arXiv*, 1410.8598, 2014.
- [6] V. E. Lobanov, G. Lihachev, T. J. Kippenberg, and M. L. Gorodetsky. Frequency combs and platicons in optical microresonators with normal GVD. *Opt. Express*, 23, 7713, 2015.

Dipolar QED: an alternative paradigm for quantum optics, quantum sensors, and non-equilibrium dynamics

C. S. Adams¹

¹Joint Quantum Centre (JQC) Durham-Newcastle, Department of Physics, Durham University, Durham DH1 3LE, UK

e-mail: c.s.adams@dur.ac.uk

In dipolar QED (dQED) the effect of neighbouring dipoles dominate the interaction between an emitter and the electromagnetic field (similar to the effect of a cavity in cavity QED). The strong coupling regime of dQED is characterised by the hopping of excitations (photons) between dipoles and for regular arrays maps onto a XY spin model [1]. The hopping of virtual photons can also be detected via a change in the optical transmission [2] as illustrated in Fig. 1, or as a level shift which for an ensemble is referred to as the N -atom ‘Lamb’ shift [3]. In terms of applications, by mixing optical and microwave dipoles in the dQED regime it is possible to realise large single photon non-linearities [4] and detect weak fields by inducing optical bistability [5].

- [1] D. Barredo *et al.*, Phys. Rev. Lett. **114**, 113002 (2015).
- [2] R. J. Bettles, S. A. Gardiner, and C. S. Adams, in preparation, see also arxiv:1410.4776
- [3] J. Keaveney *et al.*, Phys. Rev. Lett. **108**, 173601 (2012).
- [4] D. Maxwell *et al.*, Phys. Rev. Lett. **110**, 103001 (2013).
- [5] C. Carr *et al.*, Phys. Rev. Lett. **111**, 113901 (2013).

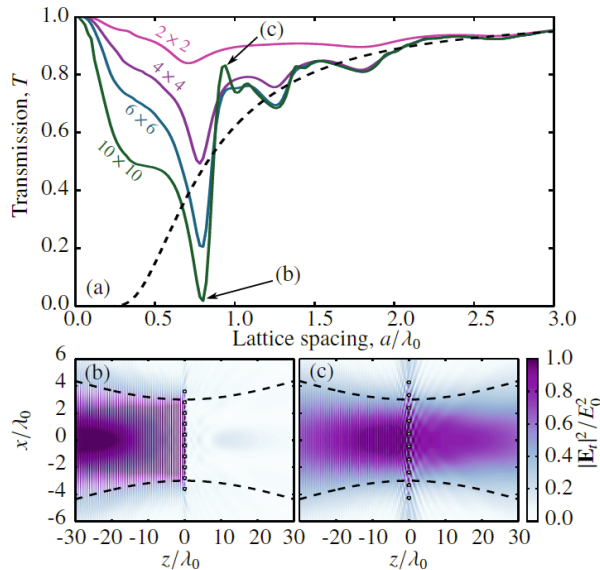


Figure 1: (a) Optical transmission on resonance through a 2D $N \times N$ square array of dipoles as a function of their spacing. Interaction between the dipoles may either suppress (b) or enhance (c) the transmission.

Oscillator beyond the ground state uncertainty – from one quadrature to both

Eugene S. Polzik

Niels Bohr Institute, Copenhagen University, Blegdamsvej 17, 2100 København, Denmark
e-mail: polzik@nbi.ku.dk

Measurements of one quadrature of an oscillator with precision beyond its vacuum state uncertainty have occupied a central place in quantum physics for decades. A squeezed state of one of the quadratures is a prominent example of a state which provides such precision. One of the first proposals for generation of such a state [1] involves a quantum nondemolition measurement at twice the frequency of the oscillator. We have recently reported the first experimental implementation of this proposal [2] with a magnetic oscillator. It has been widely assumed that sensing with the precision beyond the vacuum state uncertainty in *both* quadratures is prohibited by the uncertainty principle. We have demonstrated that this limitation can be overcome by entangling of an oscillator with a quantum reference frame with an effective negative mass [3,4]. In a more general sense, this approach leads to trajectories without quantum uncertainties [5] and to achieving new fundamental bounds on the measurement precision [6]. Progress towards such a measurement on a mechanical oscillator will be reported.

- [1] Braginsky, V. B., Vorontsov, Y. I. & Thorne, K. S. Quantum nondemolition measurements. *Science* 209, 547–557 (1980).
- [2] Generation of a squeezed state of an oscillator by stroboscopic back-action-evading measurement. G. Vasilakis, H. Shen, K. Jensen, M. Balabas, D. Salart, B. Chen, and E. S. Polzik. *NaturePhysics*, (2015) doi:10.1038/nphys3280
- [3] Experimental long-lived entanglement of two macroscopic objects. B. Julsgaard, A. Kozhekin, and E. S. Polzik, *Nature*, 413, 400 (2001).
- [4] Establishing Einstein-Podolsky-Rosen channels between nanomechanics and atomic ensembles. K. Hammerer, M. Aspelmeyer, E.S. Polzik, P. Zoller. *Phys. Rev. Lett.* 102, 020501 (2009).
- [5] Trajectories without quantum uncertainties. E.S. Polzik and K.Hammerer. *Annalen der Physik*. 527, No. 1–2, A15–A20 (2015).
- [6] M. Tsang and C. Caves, *Phys. Rev. Lett.* 105(12), (2010).

Quantum simulations with atoms in nano-structures

Ignacio Cirac

Max-Planck-Institut für Quantenoptik Hans-Kopfermann-Str. 1 85748 Garching, Germany
e-mail: ignacio.cirac@mpq.mpg.de

Many-body quantum systems are very hard to simulate with classical computers, as the running time increases exponentially with the size of the system. Quantum simulation offers a way to circumvent this problem. A quantum simulator is a system where interactions can be engineered, such that its dynamics correspond to the ones of the system one wants to emulate. Ultra-cold atoms in optical lattices can be used for that purpose; in particular, to simulate many-body problems that appear in strongly-correlated systems. In this talk I will show how photonic crystal structures can be used to design subwavelength optical lattices in two dimensions for ultracold atoms, achieving a better performance than current experimental set-ups. Furthermore, guided modes can be used for photon-induced large and strongly long-range interactions between trapped atoms, giving rise to quantum simulations which cannot be performed with other systems. (in collaboration with A. Gonzalez-Tudela, C.-L. Hung, D. Chang, and J. Kimble)



Between Localization and Ergodicity in Quantum Systems

Boris Altshuler

Columbia University, 116th Street and Broadway, New York, NY 10027, USA

e-mail: bla@phys.columbia.edu

Strictly speaking the laws of the conventional Statistical Physics, in particular the Equipartition Postulate, apply only in the presence of a thermostat. For a long time this restriction did not look crucial for most of the interesting systems - arbitrary weak coupling with the reservoir was believed to be sufficient. Recently there appeared two classes of quantum many-body systems with the coupling to the outside world that is (or is hoped to be) negligible: (1) cold quantum gases and (2) systems of qubits, which enjoy a continuous progress in their disentanglement from the environment. To describe such systems properly one should revisit the very foundations of the Statistical Mechanics. The first step in this direction was the development of the concept of Many-Body Localization (MBL) [1]: under certain conditions the states of a many-body system are localized in the Hilbert space resembling the celebrated Anderson Localization of single particle states in a random potential. There are reasons to believe that one-particle localization of the eigenfunctions of the Anderson tight-binding model with on-site disorder on regular random graphs (RRG) in many aspects is similar to a generic MBL.

MBL implies that the state of the system decoupled from the thermostat depends on the initial conditions: the time averaging does not result in equipartition distribution, the entropy never reaches its thermodynamic value, and i.e. the ergodicity is violated. Variations of e.g. temperature can delocalize many body states. However, the recovery of the equipartition is not likely to follow the delocalization immediately: numerical analysis of the RRG problem suggests that the extended states are multi-fractal at any finite disorder [2]. Moreover, regular (no disorder!) Josephson junction arrays (JJA) under the conditions that are feasible to implement and control experimentally demonstrate both MBL and non-ergodic behavior [3].

- [1] D. Basko, I. Aleiner, and B. Altshuler, *Ann. Phys.* 321, 1126 (2006).
- [2] A. De Luca, B.L. Altshuler, V.E. Kravtsov, and A. Scardicchio, *Phys. Rev. Lett.* 113, 046806, (2014)
- [3] M. Pino, B.L. Altshuler and L.B. Ioffe, arXiv:1501.03853

Random-bond Heisenberg spin models and 1/f noise

K. Agarwal¹, E. Demler¹, and I. Martin¹

¹ *Physics Department, Harvard University, Cambridge, Massachusetts 02138, USA*

² *Material Science Division, Argonne National Laboratory, Argonne, Illinois 60439 USA*

e-mail: demler@physics.harvard.edu

We use a real-space renormalization group procedure to determine the 'flux noise' spectrum of random-bond Heisenberg spin models in 1d and quasi-1d geometries. Our approach accounts for both the renormalization of the system Hamiltonian and a generic probe that measures this noise. We demonstrate that the structure factor, at both high and low temperatures, exhibits a piece-wise high- and low-frequency power-law behavior. We discuss implications of our results for the explanation of 1/f flux noise in SQUIDs.



From Standard Model of particle physics to room-temperature superconductivity

G.E. Volovik^{1,2}

¹Low Temperature Laboratory, Aalto University, P.O. Box 15100, FI-00076 Aalto, Finland

²Landau Institute for Theoretical Physics, acad. Semyonov av., 1a, 142432, Chernogolovka, Russia

e-mail: volovik@boojum.hut.fi

Topological media are gapped or gapless fermionic systems, whose properties are protected by topology, and thus are robust to deformations of the parameters of the system and generic [1]. We discuss the classes of gapless topological media, which contain the quantum vacuum of Standard Model in its symmetric phase, and also the condensed matter systems with zeroes in the fermionic energy spectrum, which form Fermi surfaces, Weyl and Dirac points, Dirac lines, flat bands, etc. Some zeroes are topologically protected, being characterized by topological invariants, expressed in terms of Green's function. For the stability of the others the \mathbf{p} -space topology must be accompanied by symmetry.

Vacua with Weyl points serve as a source of effective relativistic quantum fields emerging at low energy: chiral fermions, effective gauge fields and tetrad gravity emerge together in the vicinity of a Weyl point. The accompanying effects, such as chiral anomaly, electroweak baryo-production and chiral vortical effect, are expressed via the symmetry protected \mathbf{p} -space invariants.

The gapless topological media exhibit the bulk-surface and bulk-vortex correspondence: which in particular may lead to the dispersionless spectrum (flat band) on the surface of the system or in the core of topological defects. The materials with flat band in bulk, on the surface or within the dislocations have singular density of states, which crucially influences the critical temperature of the superconducting transition in such media. While in all the known superconductors the transition temperature is exponentially suppressed as a function of the pairing interaction, in the flat band the transition temperature is proportional to the pairing interaction, and thus can be essentially higher. So the \mathbf{p} -space topology may give us the recipe for the search or artificial fabrication of the room-temperature superconductors.

There are several ways of how to find or construct the flat band materials.

If the interaction between the electrons is strong enough, the Khodel-Shaginyan flat band is formed in the bulk material due to the effect of merging of the energy levels [2, 3] (see also review [4]). Both the phenomenological Landau type theory [5] and the Hubbard model calculations [6] indicate, that the flat band supported by interaction should be searched for in materials, where the Fermi surface is in the vicinity

of the saddle point of the energy spectrum.

Another route is the search for the topologically protected flat bands. Such flat bands for example emerge on the boundary of semimetals with nodal Dirac lines, or at the interface between materials with different topological properties. Examples are provided by graphite materials.

The rhombohedral graphite (ABCABC... stacking) contains topologically stable spiral Dirac lines, which generate the flat band on the boundary [8]. Based on this theory, the flattening of the spectrum has been recently observed in epitaxial rhombohedral multilayer graphene [9].

For the Bernal graphite (ABAB... stacking), there is an experimental evidence of the flat band and superconductivity with enhanced temperature at the interfaces of the highly oriented pyrolytic graphite [10] (see also review paper [11]). The flat band originates from the misfit dislocation array, which is formed at the interface due to the lattice mismatch. Similar mechanism of the interface superconductivity in other materials is reported in Ref. [12].

- [1] G.E. Volovik, *The Universe in a Helium Droplet*, Clarendon Press, Oxford (2003).
- [2] V.A. Khodel and V.R. Shaginyan, *JETP Lett.* **51**, 553 (1990).
- [3] A.A. Shashkin, V.T. Dolgoplov, *et al.*, *Phys. Rev. Lett.* **112**, 186402 (2014).
- [4] G.E. Volovik, arXiv:1409.3944.
- [5] G.E. Volovik, *JETP Lett.* **59**, 830 (1994).
- [6] D. Yudin, *et al.*, *Phys. Rev. Lett.* **112**, 070403 (2014).
- [7] G.E. Volovik, *Lecture Notes in Physics*, **870**, 343 (2013).
- [8] T.T. Heikkilä, N.B. Kopnin and G.E. Volovik, *JETP Lett.* **94**, 233 (2011).
- [9] D. Pierucci, *et al.*, 10.1021/acsnano.5b01239.
- [10] P. Esquinazi, *et al.*, *JETP Lett.* **100**, 336 (2014).
- [11] T.T. Heikkilä and G.E. Volovik, arXiv:1504.05824.
- [12] E. Tang and L. Fu, *Nature Phys.* **10**, 964 (2014).

Engineering quantum circuits in a polariton condensate

Natalia Berloff^{1,2}

¹Skolkovo Institute of Science and Technology, 100 Novaya St., Skolkovo, Moscow 143025, Russia

²DAMTP, University of Cambridge, Wilberforce Road, Cambridge, CB30WA, United Kingdom e-mail: N.Berloff@skoltech.ru, N.G.Berloff@damtp.cam.ac.uk

Microcavity exciton-polaritons are quasiparticles that result from the hybridisation of excitons (bound electron hole pairs) and light confined inside semiconductor microcavities. At low enough densities, they behave as bosons according to Bose-Einstein statistics, but they have finite lifetimes and have to be continuously re-populated. Recent experiments investigated polariton condensation and the phenomena associated with it, such as pattern formation, quantised vortices and solitons, increased coherence and cross-over to regular lasing.

Polariton condensates have a number of features that put them aside from other condensates: (1) they are nonequilibrium systems capable of pattern forming; (2) polaritons condense at relatively high (even room) temperatures due to very small effective masses; (3) polaritons leak out of the cavity in the form of photon emission carrying all information related to their density, frequency, phase, spacial and temporal coherence, so completely characterising the condensate inside the cavity (4) polaritons have polarisation degree of freedom that are affected and, therefore, can be manipulated by magnetic fields; (5) one can easily engineer any external landscape and vary pumping in space and time; (6) polariton condensates form quantized vortices in response to slight changes in the environment: when flow exceeds critical velocities, when fluxes interact, when trapped in harmonic potentials, when pumping powers exceed a threshold for pattern forming instabilities, when magnetic field exceeds a threshold etc. In my talk I discuss mathematical modelling of the dynamical behaviour of polariton condensates and recent experimental findings on condensates pumped in localised space positions to generate new type of quantum circuits.

When polaritons condense they flow away from the pumping spot due to polariton-polariton interactions and repulsive interactions with hot reservoir excitons. The outflow of polaritons interact with polaritons created by other pumping positions resulting in phase difference locking between condensates as shown on Figure 1 or to a relative dynamical motion between the spots [1, 2]. By controlling the geometry of pumping spots and the parameters of the pump it is possible to create and control the quantum circuits consisting of many condensates [3, 4].

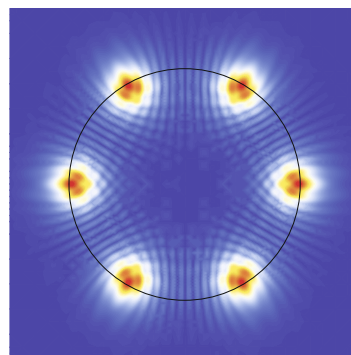


Figure 1: The density contourplot of six equidistant condensates locked into π phase difference between the adjacent condensates.

References

- [1] G. Tosi, et al Nature Phys, **8**, 190 (2012)
- [2] G.Tosi, et al Nature Comm., **3**, 1243, (2012).
- [3] H. Ohadi et al, arXiv:1406.6377 (2014).
- [4] A. Askitopoulos et al arXiv:1411.4579 (2014).

Attosecond Spectroscopy: from measuring ionization times to time-resolving chiral response

Olga Smirnova

Max Born Max-Born-Institute, Max-Born-Str. 2A, 12489 Berlin, Germany

e-mail: Olga.Smirnova@mbi-berlin.de

Ionization of atoms and molecules in strong infrared laser fields is a fundamental process that plays key role in many research fields, from attosecond physics to laser modification of transparent materials. I will describe new results related to this process.

I will first introduce protocols that can be used to define and measure time delay associated with strong-field ionization, and will discuss how this time depends on the number of photons required to overcome the ionization potential. Since strong field ionization is often viewed as electron tunnelling through the barrier created by the superposition of the atomic binding potential and the laser field, this question touches upon the famous problem of time delays in tunnelling. Using the combination of analytical theory and ab-initio numerical simulations, I will show that optical tunnelling is instantaneous [1], at least within the framework of non-relativistic quantum mechanics.

I will then show that optical tunnelling in polyatomic molecules populates different hole states, inducing correlated electron-hole dynamics. Importantly, in chiral molecules the hole dynamics becomes chiral, sensitive to the helicity of the driving laser field and the chirality of the molecule. The infrared laser field that removes the electron from the molecule can also bring this electron back to the parent ion, where it can recombine with the hole left behind. Light emitted during recombination takes the snapshot of the recombining system, recording the electron-hole dynamics with attosecond temporal resolution. I will show that in chiral systems the emitted light distinguishes left-handed and right-handed molecules with extreme sensitivity and records the chiral dynamics of the hole with about 0.1 fsec temporal resolution [2].

- [1] L. Torlina, F. Morales, J. Kaushal, I. Ivanov, A. Kheifets, A. Zielinski, A. Scrinzi, H. G. Muller, S. Sukiasyan, M. Ivanov and O. Smirnova, Interpreting attoclock measurements of tunnelling times, *Nature physics*, 2015
- [2] R. Cireasa, A. E. Boguslavskiy, B. Pons, M. C. H. Wong, D. Descamps, S. Petit, H. Ruf, N. Thire, A. Ferre, J. Suarez, J. Higuette, B. E. Schmidt, A. F. Alharbi, F. Legare, V. Blanchet, B. Fabre, S. Patchkovskii, O. Smirnova, Y. Mairesse, V. R. Bhardwaj, Probing molecular chirality on sub-femtosecond time-scale, *Nature physics*, 2015

High harmonic generation in strong laser fields: new questions and ideas

Misha Ivanov^{1,2,3}

¹Max Born Institute for Nonlinear Optics, Berlin, Germany

²Department of Physics, Humboldt University, Berlin Germany

³Department of Physics, Imperial College, London, UK

e-mail: m.ivanov@imperial.ac.uk

This talk is about one aspect of highly nonlinear response of matter to intense infrared light: the generation of very high harmonics of the incident light by the irradiated medium. High harmonics have now become an important table-top source of bright, coherent emission in the extreme UV and soft X-ray region, including the generation of sub-femtosecond (attosecond) light pulses. A lot of work goes into improving this source: making it brighter, extending it to shorter wavelengths, controlling its polarization. The first part of the talk will discuss two ideas that go in this direction: one realistic, one a bit on the crazy side.

The first idea deals with controlling polarization of attosecond pulses. All attosecond pulses produced so far have been linearly, or nearly linearly, polarized. Making them circular later, after they have already been generated, is not a good option: too much already precious energy is lost. I will describe what we think is a realistic way of generating nearly circular attosecond pulses from the start. Highly elliptic pulses of sub-femtosecond duration will open many doors, such as time-resolving chiral response at the electronic time scale.

The second idea addresses another challenge: increasing the intensity of high harmonic radiation. I will describe a series of results that show how intense infrared field can be used to amplify weak high-frequency signal, by controlling the nonlinear response of the medium. The main challenge here is in amplifying high-frequency radiation which is very well absorbed by the medium. Fighting and defeating linear absorption with the help of highly nonlinear absorption seems like a crazy strategy, but it might be paying off, at least in theory.

If time permits, I will also speak about using high harmonic emission to time-resolve highly nonlinear dynamics induced in the generating medium. It is not surprising that harmonic light encodes information about ultrafast electronic dynamics that is responsible for harmonic emission. I will explore the application of this idea to studying effective band structure of a dielectric driven by intense mid-infrared light. I will show how, under certain conditions, strong IR laser field can start erasing the edges of the Brillouin zones, suppress the Bragg scattering and Bloch oscillations,

and how changes in the harmonic radiation emitted by this dielectric can help us spot this dramatic modification.



Non-exponential energy decay and quasi-particle fluctuations in a superconducting flux qubit

S. Gustavsson¹, F. Yan¹, A. Kamal¹, J. Birenbaum², A. Sears³, D. Hover³, T. Gudmundsen³, J. Yoder³,
G. Catelani⁴, T.P.Orlando¹, John Clarke², A.J. Kerman³, and W.D. Oliver^{1,3}

¹ Research Laboratory for Electronics, Massachusetts Institute of Technology, Cambridge, MA 02139;

² Department of Physics, University of California, Berkeley, CA 94720-7300;

³ MIT Lincoln Laboratory, 244 Wood Street, Lexington, MA 02420;

⁴ Forschungszentrum Julich, Germany

e-mail: simongus@mit.edu

The scalable application of quantum information science begins with reproducible and controllable high-coherence qubits. In this work, we present an improved superconducting qubit, leveraging design elements from both charge- and flux-based qubits to achieve a device with large frequency tunability, large anharmonicity, and energy relaxation and dephasing times in excess of 40 μ s. We show that the qubit relaxation times are limited by a combination of Ohmic charge noise and $1/f$ -type flux noise, a noise source that previously has been considered mainly in the context of dephasing. Furthermore, by mapping out the noise power spectral density seen by the qubit, we uniquely identify thermal shot noise of residual photons in the readout resonator as the dominant source of dephasing in our system, a result that applies to any qubit modality where the read out is implemented by a transverse dispersive coupling of the qubit to a resonator. By implementing the CPMG dynamical-decoupling protocol, we are able mitigate to the adverse influence of the photon shot noise, and improve $T_2^{\text{Echo}} \sim 40$ μ s to reach $T_2^{\text{CPMG}} \sim 80$ μ s $\sim 2 \cdot T_1$.

In a separate experiment, we measure pronounced non-exponential energy relaxation in a superconducting flux qubit, observing a decay function that exhibits a fast initial decay followed by a much slower decay for long times. When applying a sequence of pi pulses to the qubit and measuring the decay after the last pi pulse, we observe strong modifications to the decay function, including a slow-down of the fast initial decay and a three-fold increase of the $1/e$ -time. If we attribute the non-exponential decay to quasiparticle number fluctuations, we speculate that the improvements in T_1 are due to a qubit-mediated shuffling of quasiparticles between the metallic islands of the device, which will eventually pump them away from the Josephson junctions to a larger ground plane where their contribution to qubit energy relaxation become negligible.

Ultrastrong Coupling in Superconducting Circuit QED

Rudolf Gross

¹*Walther-Meißner-Institut, Bayerische Akademie der Wissenschaften, D-85748 Garching, Germany*

²*Physik-Department, Technische Universität München, D-85748 Garching, Germany*

³*Nanosystems Initiative Munich (NIM), Schellingstraße 4, 80799 München, Germany*

e-mail: Rudolf.Gross@wmi.badw.de

Circuit quantum electrodynamics (cQED) has not only become a versatile toolbox for quantum information processing and quantum simulation but is also a powerful platform for the study of light-matter interaction and fundamental aspects of quantum mechanics. In cQED setups, the coupling strength between an artificial solid state atom and the quantized resonator modes can not only exceed the dissipation rates (strong coupling regime) but can even reach a significant fraction of the system energy. In this ultrastrong coupling regime the Jaynes-Cummings approximation breaks down [1,2]. The interaction between light and matter can only be described correctly by the quantum Rabi model which also takes into account the counter-rotating terms.

We report on ultrastrong coupling between a superconducting flux qubit and the resonant modes of a system comprised of two superconducting coplanar stripline resonators coupled galvanically to the qubit. With a coupling strength as high as 17% of the mode frequency, we observe a pronounced Bloch-Siegert shift. The spectroscopic response of our multimode system reveals a clear breakdown of the Jaynes-Cummings model, demonstrating the presence of ultrastrong coupling. This paves the way for various applications and the study of interesting phenomena. For instance, it allows for the realization of ultrafast gates and provides deeper insight into Zeno physics or photon transfer through cavity arrays.

The system comprised of two superconducting coplanar stripline resonators coupled via a superconducting flux qubit is used to realize a device allowing for tunable and switchable coupling between two frequency-degenerate superconducting resonators [2-4]. We show tunable and switchable coupling in the frequency and time domain and demonstrate that the coupling between the relevant modes can be varied in a controlled way. Specifically, the coupling can be tuned by adjusting the magnetic flux through the qubit loop or by controlling the qubit population via a microwave drive.

We also studied a system consisting of a superconducting flux qubits ultrastrongly coupled to an open microwave transmission line. The coupling within the transmission line depends on the available density of electromagnetic modes. The latter can be

tuned by introducing circuit elements into the line which result in a finite impedance matching, thereby modifying the spectral density of the electromagnetic modes and, in turn, the qubit coupling. We present experimental data on a superconducting flux qubits ultrastrongly coupled to such a shaped electromagnetic environment. By further increasing the coupling strength to the deep ultrastrong coupling regime, a phase transition from resonance fluorescence physics to a regime resembling Kondo physics is expected.

This work is supported by the German Research Foundation through SFB 631 and the German Excellence Initiative through the Nanosystems Initiative Munich (NIM).

- [1] T. Niemczyk, F. Deppe, H. Huebl, E. P. Menzel, F. Hocke, M. J. Schwarz, J. J. Garcia-Ripoll, D. Zueco, T. Hümmer, E. Solano, A. Marx, R. Gross, *Nature Physics* **6**, 772 (2010).
- [2] A. Baust, E. Hoffmann, M. Haeberlein, M. J. Schwarz, P. Eder, J. Goetz, F. Wulschner, E. Xie, L. Zhong, F. Quijandria, D. Zueco, J.-J. Garcia Ripoll, L. Garcia-Alvarez, G. Romero, E. Solano, K. G. Fedorov, E. P. Menzel, F. Deppe, A. Marx, R. Gross, arXiv:1412.7372.
- [3] A. Baust, E. Hoffmann, M. Haeberlein, M. J. Schwarz, P. Eder, E. P. Menzel, K. Fedorov, J. Goetz, F. Wulschner, E. Xie, L. Zhong, F. Quijandria, B. Peropadre, D. Zueco, J.-J. Garcia Ripoll, E. Solano, F. Deppe, A. Marx, R. Gross, *Phys. Rev. B* **91**, 014515 (2015).
- [4] M. Mariani, F. Deppe, A. Marx, F.K. Wilhelm, R. Gross, E. Solano, *Phys. Rev. B* **78**, 104508 (2008)

Superconducting Nanowire Single-Photon Detectors

Michael Siegel

*Institute of Micro- and Nanoelectronic Systems (IMS), Karlsruhe Institute of Technology (KIT),
Hertzstr. 16, 76187 Karlsruhe, Germany
e-mail: Michael.siegel@kit.edu*

Superconducting nanowire single-photon detectors (SNSPD) offer a high sensitivity up to the single-photon level over a wide spectral range with high counting rates and high detection efficiencies. Innovative applications require multi-pixel systems to cover the essential advantages of SNSPDs with the advantages of common imaging systems based on standard CMOS/CCD techniques.

Considerable effort has been made in methods of generating, manipulating and detecting single photons. An ultimate goal is a compact device capable of scalable quantum information processing. The approach using semiconductor quantum dots as single and entangled photon sources, GaAs waveguides for light guiding, waveguide couplers, electro-optic modulators and superconductors as single-photon detectors seem to be very promising for a full integration on a photonic chip. So far, group III-V semiconductor approaches have mostly been performed on a GaAs substrate demonstrating individual components or preliminary stages of an optical quantum circuit. The conversion from light information to electronic information suitable for further acquisition and analysis is an important requirement for photonic quantum circuits. On-chip single-photon detection requires detectors that are compatible with quantum-dot fabrication schemes and that have a fast response and high detection efficiency.

Aluminum nitride (AlN) has recently emerged as a promising material for integrated photonics due to a large bandgap and attractive optical properties. Exploiting the wideband transparency, we demonstrate waveguiding in AlN-on-Insulator circuits from near-infrared to ultraviolet wavelengths using nanophotonic components with dimensions down to 40 nm. By measuring the propagation loss over a wide spectral range, we conclude that both scattering and absorption of AlN-intrinsic defects contribute to strong attenuation at short wavelengths, thus providing guidelines for future improvements in thin-film deposition and circuit fabrication.

For some time, Superconducting Nanowire Single-Photon Detectors (SNSPD) based on superconducting ultra-thin films have been investigated by the scientific community, leading to various new insights into their optical, electrical and physical properties. The spectral bandwidth of a SNSPD is limited by a cut-off wavelength determined by parameters of the superconducting film used for the detector and its

particular geometry. The SNSPD detection efficiency is determined by material parameters like energy gap, density of electron states, electron diffusivity etc. and by a ratio of j_c to the depairing current density. Today, there are various applications where SNSPDs, implemented in cryogenic systems, enable experiments in the area of quantum cryptography, quantum-dot radiation or in spectroscopy. The reason behind the complex utilization of SNSPDs for such tasks can be explained by taking their other favourable properties into account, namely the low dark count rate, the fast detection speed and the high timing accuracy in the picosecond range. To this end, superconducting nanowire single-photon detectors (SNSPDs) with 100 % intrinsic detection efficiency, low dark counts < 100 cps and jitter down to 20 ps are the most promising candidates, not only for optical circuits based on quantum dots, but also for other quantum light sources.

Nowadays SNSPD detection systems are based mainly on a single-pixel detector. Multi-pixel systems would extend a possible field of applications. Therefore, new concepts are required for effective readout of multi-pixel SNSPDs. We give an overview of possible concepts, the conditions of operation and the dedicated effort optimized to the requirements of different applications, which operate in the single-photon regime.

Quantum Dot Microcavity Devices for Quantum Communication and Information Applications

S. Höfling^{1,2,3}, C. Schneider¹, Y.-M. He^{1,3}, Y. He², C.-Y. Lu³, J.-W. Pan³,

K. De Greve⁴, P. McMahon⁴, L. Yu⁴, Y. Yamamoto⁴, M. Kamp¹

¹Technische Physik, Physikalisches Institut and Wilhelm Conrad Röntgen-Research Center for Complex Material Systems, Universität Würzburg, Am Hubland, D-97074, Würzburg, Germany

²SUPA, School of Physics and Astronomy, University of St Andrews, St Andrews, KY16 9SS, United Kingdom

³Hefei National Laboratory for Physical Sciences at Microscale and Department of Modern Physics, University of Science and Technology of China, Hefei, Anhui 230026, China

⁴E. L. Ginzton Laboratory, Stanford University, Stanford, California 94305, USA

e-mail: sven.hoefling@physik.uni-wuerzburg.de

Single semiconductor quantum dots (see fig.1) are regarded as artificial atoms hosted in a solid-state platform. They enable one to confine charges, excitons and spins at the single quantum level and to generate on-demand single photons, entangled photon-pairs and establish spin-photon interfaces. While accomplishing all this in a solid-state platform is a major advantage for applications in quantum information processing and quantum sensing, the solid-state environment poses particular challenges in overcoming decoherence phenomena compared to single well isolated atoms. In this presentation, single quantum dots and their general coherence properties will be described. The emphasis is two-fold, on the generation of coherent single photons with high degrees of indistinguishability [1-4] and on spin-photon interfaces with spins as quantum memories in quantum dots [5-8]. Enhanced light-matter interaction in microcavities will be discussed and its impact on improved characteristics will be detailed.

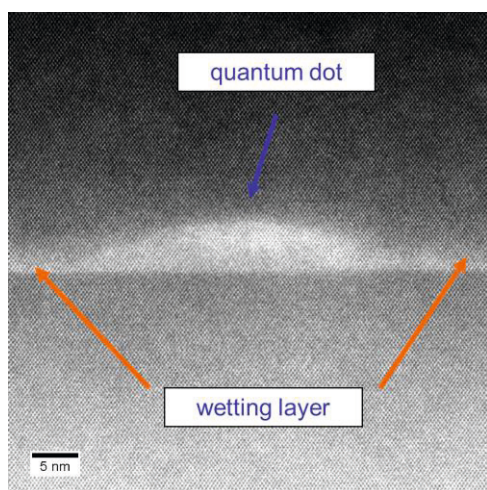


Figure 1: Scanning tunneling electron microscopy image of an InGaAs/GaAs quantum dot.

- [1] Y.-M. He, Y. He, Y.-J. Wei, D. Wu, M. Atatüre, C. Schneider, S. Höfling, M. Kamp, C.-Y. Lu, J.-W. Pan, *Nature Nanotechnol.* **8**, 213 (2013).
- [2] Y. He, Y.-M. He, Y.-J. Wei, X. Jiang, M.-C. Chen, F.-L. Xiong, Y. Zhao, C. Schneider, M. Kamp, S. Höfling, C.-Y. Lu, J.-W. Pan, *Phys. Rev. Lett.* **111**, 237403 (2013).
- [3] Y.-J. Wei, Y. He, Y.-M. He, C.-Y. Lu, J.-W. Pan, C. Schneider, M. Kamp, S. Höfling, D. P. S. McCutcheon, A. Nazir, *Phys. Rev. Lett.* **113**, 097401 (2014).
- [4] Y.-J. Wei, Y.-M. He, M.-C. Chen, Y.-N. Hu, Y. He, D. Wu, C. Schneider, M. Kamp, S. Höfling, C.-Y. Lu, J.-W. Pan, *Nano Letters* **14**, 4615 (2014).
- [5] Press, K. De Greve, P.L. McMahon, T.D. Ladd, B. Friess, C. Schneider, M. Kamp, S. Höfling, A. Forchel, Y. Yamamoto *Nature Phot.* **4**, 367 (2010).
- [6] K. De Greve, P. L. McMahon, D. Press, T. D. Ladd, D. Bisping, C. Schneider, M. Kamp, L. Worschech, S. Höfling, A. Forchel, Y. Yamamoto *Nature Phys.* **7**, 872 (2011).
- [7] K. De Greve, L. Yu, P. L. McMahon, J. S. Pelc, C. M. Natarajan, N. Y. Kim, E. Abe, S. Maier, C. Schneider, M. Kamp, S. Höfling, R. H. Hadfield, A. Forchel, M. M. Fejer, Y. Yamamoto, *Nature* **491**, 421 (2012).
- [8] K. De Greve, P. L. McMahon, L. Yu, J. S. Pelc, C. Jones, C. M. Natarajan, N. Y. Kim, E. Abe, S. Maier, C. Schneider, M. Kamp, S. Höfling, R. H. Hadfield, A. Forchel, M. M. Fejer, Y. Yamamoto, *Nature Comm.* **4**, 2228 (2013).

Vortex formation in a Lattice Polariton-Condensate ICQT abstract template

Pavlos Lagoudakis

Department of Physics & Astronomy, University of Southampton, UK

e-mail: lagous@soton.ac.uk

Spontaneous vortices are topological defects resulting from a symmetry breaking process in a system when it undergoes a phase transition. Recently, there has been a great deal of interest in the experimental observation of topological objects in Bose-Einstein condensates of exciton-polaritons [1],[2],[3]. Self-organization in bosonic condensates attracts a great interest as it sheds light on the mechanisms of spontaneous processes in nature. Curiously, the vorticity observed in these and the following works the vortices appeared to be pinned to structure imperfections and their winding numbers being defined by the excitation conditions. Here I will present evidence of vortices in the phase relation between neighboring sites of a polariton lattice condensate. It will be shown that such mesoscopic vortices are formed in the process of condensation in an interacting lattice and are independent of structural imperfections.

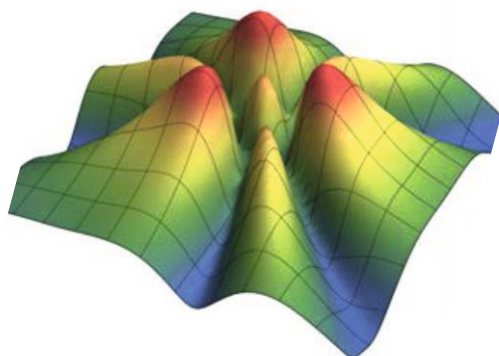


Figure 1 The trivial case for phase locking of three condensates where all of them are in phase is shown. The system is rotationally symmetric and there is a constructive interference at the center of the lattice (marked by a black arrow).

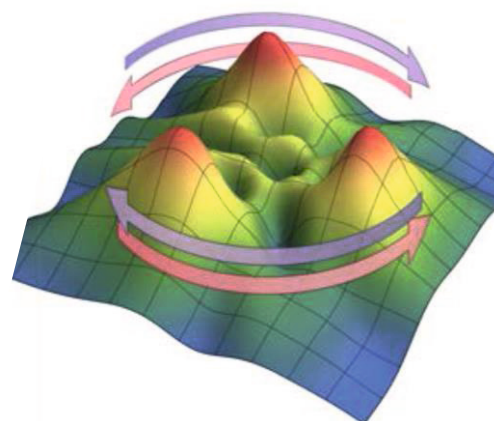


Figure 2 The three condensates could spontaneously break the rotational symmetry and phase lock with a $\pm 2\pi/3$ phase difference between adjacent neighbors, which correspond to clockwise or anticlockwise vortices with winding numbers of ± 1 .

The simplest spatial configuration where such vortices can occur is that of a triangle. In the case of an equilateral triangle in real space and under pulsed excitation the phases of the individual polariton at some stage lock. If they lock in phase, no vortices appear, while if they lock with specific phase-shifts vortices with winding numbers of $+1$ or -1 are formed stochastically (see Fig. 1,2). Analysis of the dynamics of the vortex formation reveals that the coupling mechanism is dissipative similar to the one in the classical Huygens's clocks.

- [1] Nature Physics 4, 706 (2008)
- [2] Science 326, 974 (2009)
- [3] Science 332, 1167 (2011)

Weak Lasing in Polariton Superlattices

Long Zhang¹, Wei Xie¹, Jian Wang¹, Alexander Poddubny², Jian Lu¹, Yinglei Wang¹, Jie Gu¹, Wenhui Liu¹, Dan Xu¹, Xuechu Shen¹, Yuriy Rubo³, Boris Altshuler⁴, Alexey Kavokin^{5*} and Zhanghai Chen^{1A}.

¹State Key Laboratory of Surface Physics, Key Laboratory of Micro and Nano Photonic Structure (Ministry of Education), Department of Physics, Fudan University, Shanghai 200433, China

²Ioffe Physical-Technical Institute of the Russian Academy of Sciences, St-Petersburg 194021, Russia

³Instituto de Energías Renovables, Universidad Nacional Autónoma de México, Temixco, Morelos 62580, Mexico

⁴Physics Department, Columbia University, New York, New York 10027, USA

⁵Spin Optics Laboratory, St-Petersburg State University, 1, Ulianovskaya, St-Petersburg, Russia and Physics and Astronomy School, University of Southampton, Highfield, Southampton, SO171BJ, UK
e-mail: A.Kavokin@soton.ac.uk

Bosons with finite life-time exhibit condensation and lasing when their influx exceeds the lasing threshold determined by the dissipative losses. In general, different one-particle states decay differently, and the bosons are usually assumed to condense in the state with the longest life-time. Interaction between the bosons partially neglected by such an assumption can smear the lasing threshold into a threshold domain – a stable lasing many-body state exists within certain intervals of the bosonic influxes. This recently described *weak lasing*¹ regime is formed by the spontaneously symmetry breaking and phase-locking self-organization of bosonic modes, which results in an essentially many-body state with a stable balance between gains and losses. Here we report the first observation of the weak lasing phase in a one-dimensional condensate of exciton-polaritons² subject to a periodic potential. Real and reciprocal space photoluminescence images demonstrate that the spatial period of the condensate is twice as large as the period of the underlying periodic potential. These experiments are realized at room temperature in a ZnO microwire deposited on a silicon grating. The period doubling takes place at a critical pumping power, while at a lower power polariton emission images have the same periodicity as the grating.

- [1] I. L. Aleiner, B. L. Altshuler, Y. G. Rubo, Radiative coupling and weak lasing of exciton-polariton condensates, Phys. Rev. B 85, 121301 (2012).
- [2] L. Zhang, et al, Weak lasing in one-dimensional polariton superlattices, Proceedings of the National Academy of Sciences, 112, 1516 (2015).



Magnetic field induced photon echoes in semiconductor nanostructures: Storing light in the electron spin ensemble

Ilya Akimov¹

¹ *Experimentelle Physik 2, Technische Universität Dortmund, D-44221 Dortmund, Germany*
e-mail: ilja.akimov@tu-dortmund.de

The possibility to store optical information is important for classical and quantum communication. Atoms or ions as well as color centers in crystals offer suitable two-level systems for absorbing incoming photons and releasing them later on again. To obtain a reliable coherent transfer, strong enough light-matter interaction is required, which may enforce use of ensembles of absorbers, but has the disadvantage of unavoidable inhomogeneities leading to fast dephasing. This obstacle can be overcome by echo techniques that allow recovery of the information as long as the coherent state is preserved.

From first sight also semiconductor quantum structures appear appealing for information storage due to the large oscillator strength of the involved optical transitions. Furthermore, semiconductors form the backbone of current information technology, so that interfaces between established and novel information processing tools may be more easily obtained than with different hardware platforms. However, the inhomogeneity typically is even more pronounced for semiconductors and most importantly the optical coherence time is limited to nanoseconds or shorter.

The fundamental optical excitations in semiconductors, the excitons, possess large oscillator strength so that resonant absorption may be achieved with close to unity efficiency even for structure thicknesses smaller than the light wavelength. The large oscillator strength also enables ultrafast information processing. Ultrafast coherent spectroscopy of excitons employing laser pulses is well established for semiconductor nanostructures [1]. However, for storage applications excitons have been scarcely considered because of their limited optical coherence time T_2 due to complex many body interactions and their short radiative lifetime ($T_1 \leq 1$ ns) being the downside of the large oscillator strength. In nanostructures such as quantum dots the optical decoherence is weak but still limited by radiative decay. Therefore approaches to involve the long-lasting coherence of electron spins have been pursued recently.

Here, we demonstrate for a semiconductor that the ultrashort picosecond optical pulses tuned in resonance with charged exciton transition (trion) and the weak transverse magnetic field applied in our experimental protocol can lead to the transfer of a short-lived optical

excitation into a long-lived electron spin state [2]. This allows stimulated photon echoes to be induced with high bandwidth on submicrosecond timescales, exceeding the radiative lifetime of the optical excitations by more than three orders of magnitude [3].

Essential for the present experiments is the selection of a well-defined spin level system, optically excitable according to clean selection rules. Accordingly, we did not select the neutral exciton, but instead chose the charged exciton consisting of two electrons and a hole, which requires a resident electron population. We used quantum well structures for demonstration, because exciton and trion transitions are well isolated spectrally. Application of an external magnetic field leads to Larmor precession of the electron spin in the ground state. In this way, the transfer of an optical excitation into a long-lived electron spin state can be achieved, and a dramatic increase in the photon echo decay time by several orders of magnitude may be accomplished. The whole process comprises three steps: (1) pulse 1 creates the optical excitation (initialization—conversion of the optical field into a material excitation), (2) pulse 2 performs a transformation of the optical excitation into the spin system (storage), and (3) pulse 3 induces the photon echo (readout). We reveal two mechanisms contributing to the magnetic-field-induced signal - coherent transfer and spin fringes - and show that, depending on the magnetic field strength and the polarization configuration of the three involved laser pulses, we are able to shuffle the optical field into a spin component that is directed either along or perpendicular to the magnetic field.

- [1] G. Moody, I. A. Akimov, H. Li, R. Singh, D. R. Yakovlev, G. Karczewski, M. Wiater, T. Wojtowicz, M. Bayer, S. T. Cundiff, *Phys. Rev. Lett.* **112**, 097401 (2014).
- [2] L. Langer, S. V. Poltavtsev, I. A. Yugova, D. R. Yakovlev, G. Karczewski, T. Wojtowicz, J. Kossut, I. A. Akimov, and M. Bayer, *Phys. Rev. Lett.* **109**, 157403 (2012).
- [3] L. Langer, S. V. Poltavtsev, I. A. Yugova, M. Salewski, D. R. Yakovlev, G. Karczewski, T. Wojtowicz, I. A. Akimov, and M. Bayer *Nature Photonics* **8**, 851–857 (2014).

Polariton lasing in hybrid organic-inorganic microcavity

G. Paschos⁵, N. Somaschi^{1,2}, G. Christmann¹, D. Coles³, D. G. Lidzey³, Z. Hatzopoulos^{1,4}, P. G. Lagoudakis²

S. I. Tsintzos¹, P. G. Savvidis^{1,5}

¹Institute of Electronic Structure & Laser-FORTH, PO Box 1527, 71110 Heraklion, Greece

²Department of Physics and Astronomy, University of Southampton, Southampton SO17 1BJ, UK

³Department of Physics and Astronomy, University of Sheffield, Sheffield S37RH, UK

⁴Department of Physics, University of Crete, 71300 Heraklion, Greece

⁵Department of Materials Science and Technology, University of Crete, 71300 Heraklion, Greece

e-mail: psav@materials.uoc.gr

Cavity polaritons are formed when a confined optical mode within a high Q cavity strongly couples with exciton within the same cavity. A reversible exchange of energy between excitons and photons results in new allowed energy eigenstates of the system manifesting as a mixture of the uncoupled photon and exciton energies while exhibiting an anticrossing at the point of exciton-photon resonance. Strong coupling regime has been observed in microcavity structures incorporating both inorganic quantum wells (QWs) as well as organic materials such as J-aggregates, molecular crystals and polymers[1].

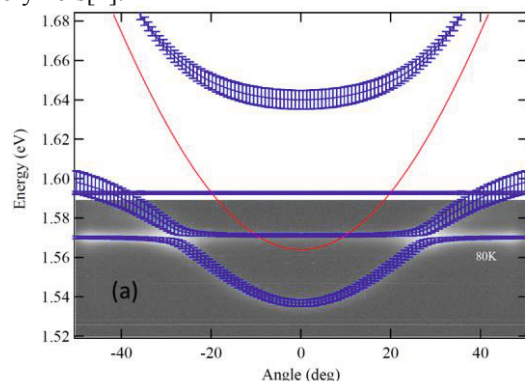


Figure 1: PL images recorded with Fourier plane projection technique. In left figure, 1(a), clear polariton dispersion is revealed at 80K while in the right hand figure

In this work we study hybrid exciton-polaritons that arise from mixing of two different organic-inorganic excitonic species with the resonant photon mode[2]. A planar microcavity structure consists of GaAs QWs and Jaggregate molecular dye assembled together in a multi-layered stack to form the active region. Angle-resolved photoluminescence at 80K, when the system is excited almost-resonantly by a low repetition laser pulse at 780nm reveals clear anticrossing. The complete structure containing both species exhibits large Rabi splitting of ~68meV shown in Figure 1, consistent with the presence of large oscillator strength J-aggregate Frenkel excitons. The

measured polariton dispersion relations can be fitted well using coupled harmonic oscillator model in which both Wannier-Mott and Frenkel excitons couple to cavity photon. Furthermore, through power dependent measurements we demonstrate for the first time strong nonlinear emission and onset of hybrid polariton lasing regime with simultaneous line narrowing and interaction induced energy blueshift shown in Figure 2.

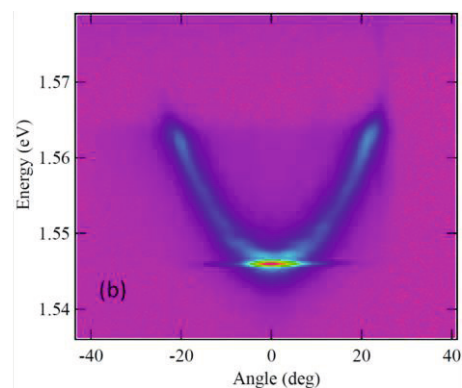


Figure 2: Clear polariton lasing obtained in similar detuning at 20K.

Such hybrid excitonic system presents an ideal playground for engineering nonlinear interactions and at the same time offers concrete possibilities for optoelectronics application. For example, laser diode designs combining high electrical conductivity of inorganic semiconductors with exciton robustness of organic compounds to maintain strong coupling regime at room temperature could provide efficient means to achieve electrically pumped organic polariton lasers.

[1] D. G. Lidzey, et al., Strong exciton-photon coupling in an organic semiconductor microcavity, *Nature* 395, 53 (1998).

[2] V.M. Agranovich, H. Benisty, C. Weisbuch "Organic and inorganic quantum wells in a microcavity: Frenkel-Wannier-Mott excitons hybridization and energy transformation" *Solid State Communications* 102, 631-636 (1997).

Magnonic sound and its interaction with magnon Bose-Einstein condensate

S. O. Demokritov^{1,2}, P. Nowik-Boltyk¹, V. E. Demidov¹, V. Tiberkevich³, and A.N. Slavin³

¹*Department of Physics and Center for Nonlinear Science, University of Muenster, Corrensstrasse 2-4, 48149 Muenster, Germany*

²*Institute of Metal Physics, Ural Division of RAS, Yekaterinburg 620041, Russia*

³*Department of Physics, Oakland University, Rochester, MI, USA*
e-mail: demokrit@uni-muenster.de

Investigation of the sound-like excitations in systems demonstrating macroscopic quantum effects (second sound in superfluid helium, zero-sound in Fermi liquids, and first sound in atomic Bose-Einstein condensation (BEC)) proved to be a reliable way to probe internal properties of these quantum systems. Up to now quasi-equilibrium gas of parametrically pumped bosonic quasiparticles - magnons - is the only known system demonstrating BEC at room temperature. Here we report the experimental observation and theoretical interpretation of dissipative sound-like waves propagating in a gas of parametrically pumped magnons undergoing BEC. The discovered "magnonic sound" shows a linear dispersion at low wavenumbers with sound velocity that is independent of the magnon density, while at larger wavenumbers the dispersion becomes almost quadratic. The magnonic sound is dissipative in a sense that the real and imaginary parts of its wavenumber are comparable. The observed waves find an explanation within a classical Boltzmann theory modified for the case of a quasi-equilibrium gas of quasiparticles. The discovered phenomenon can be used for the experimental characterization of the magnon-magnon interactions in this room-temperature BEC-system, as the rate of magnon energy relaxation, obtained from the sound dispersion, goes through a pronounced maximum at the BEC transition point.

Open correlated quantum systems: what's new out of equilibrium?

A. Shakirov^{1,2}, D. Chichinadze^{1,2}, P. Ribeiro¹, Y. Shchadilova¹, A. Rubtsov^{1,2}

¹Russian Quantum Center, 100 Novaya St., Skolkovo, Moscow 143025, Russia

²Physics Dept. of M.V. Lomonosov University, Moscow 119991, Russia

e-mail: ar@rqc.ru

Modern experimental techniques allow to construct and study a variety of correlated quantum systems, in particular those based on ultracold atoms in optical traps and artificial structures constructed by scanning microscopy techniques. An important advance over the experiments with conventional solid-state systems is that contemporary set-ups allow to monitor the quantum dynamics, e.g. quenching to the system. This gives rise to fundamental questions about the transient dynamics of a system quenched through the phase transition line, thermalization of open quantum systems, new phases arising due to the current effects etc. We will discuss how the non-equilibrium correlated system can be simulated. As well, we highlight some of our recent results in the field, which are also presented in the posters in more details.

We emphasize the difference between the simulation of quantum dynamics and of the equilibrium state of correlated systems. Quantum Monte Carlo (QMC) methods, being an established tool for equilibrium calculations within so-called DMFT framework, suffer from a very strong sign problem in its time-dependent version. The variance of the numerical result grows exponentially in time of evolution, thus limiting the QMC calculation by a very short timescale. A calculation of the most interesting slow dynamics related to collective quantum motion requires different approaches. In fact, the almost only option is to use the exact diagonalization of the Hamiltonian of a relatively small cluster, and to take the effect of the bath into account in a simplified form: the self-consistent mean-field, Lindblad operator etc. This complicates an account of many important phenomena: for example, the effect of hybridization of local levels by the bath, being exactly accounted in the DMFT, is missed in the mean-field picture. On the other hand, we observed that non-equilibrium time evolution makes some quantum effects more pronounced and easier to describe. In particular, we discuss how an increase of quantum fluctuations in Bose-Anderson impurity model is seen from the time dependent mean-field data (see Figure).

Finally, we report a formation of so-called quantum emissive ensemble, related to a dynamics of particle loss by a correlated quantum system. It is well known that the steady state of subsystems, weakly interacting with their environment, is described by the

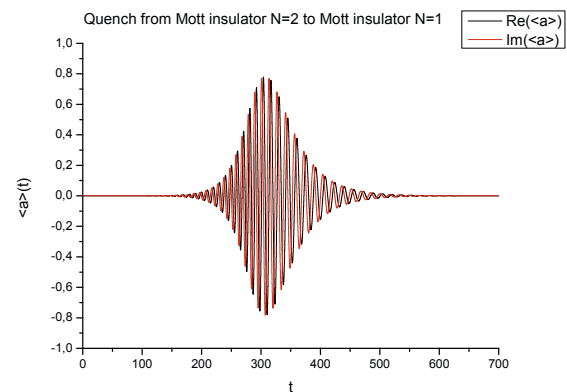


Figure 1: The time-dependence of anomalous average $\langle a \rangle$ after the quench of Bose-Anderson impurity model between the two different Mott phases. In the Mott phase $\langle a \rangle$ is vanished. Starting with exactly $\langle a \rangle = 0$, the approximation (wrongly) predicts no transition after the quench. However, after a small seed noise is introduced, the initial phase appears to be unstable. The transition occurs via an increase of the $\langle a \rangle$, with a subsequent fall it down to zero. For the exact theory without a seed noise, the symmetry remains unbroken. However, we interpret our result as a signature of an increase in quantum fluctuations $\langle |a|^2 \rangle$ during the quench.

canonical ensemble, as it follows from the detailed balance with the environment. We considered the contrasting case, the relaxation of an open correlated quantum system brought into contact with a reservoir in a vacuum state. The steady state of the system is a statistical mixture of stable eigenstates from which particles cannot escape due to the finite binding energy. We have found that, despite the absence of the detailed balance, the stationary probability distribution over these eigenstates is of the Boltzmann form in each N -particle sector. A quantum statistical ensemble corresponding to the steady state is characterized by different temperatures in different sectors, which is in contrast to the Gibbs ensemble. We argue that the emergence of the Boltzmann distribution in each N -particle sector is rooted in a regular dependence of transition rates between eigenstates of the system on the transition energy.

POSTER ■ TALKS

TUESDAY, JULY 14. P1-P50	62
THURSDAY, JULY 16. P51-P97	112

CONTENT

P1	Farid Ablayev	Quantum Hashing via ϵ -Universal Hashing Constructions	62
P2	Serhan Aksu	Mechanically Controlled Quantum Switch Defined on a Curved 2DEG.	63
P3	Murtaza Ali Khan	Nanometric surface probing with ultra-cold atoms	64
P4	Alexander Alodjants	Quantum hyperbolic metamaterials with exciton-polaritons in semiconductor Bragg mirrors	65
P5	Rostislav Arkhipov	Self-Induced Transparency Coherent Mode-Locking: Theory and Experiment.	66
P6	Silvia Arroyo Camejo	Room temperature high-fidelity holonomic single-qubit gate on an NV center in diamond	67
P7	Maksim Basalaev	Slowing-down of the light phase pulses in resonant atomic Λ -type medium	68
P8	Axel Beyer	Precision spectroscopy of the 2S-4P transition in atomic hydrogen	69
P9	Alexander Bilmes	Probing the Interaction of Microscopic Material Defects with Quasiparticles using a Superconducting Qubit	70
P10	Olga Borovkova	Transverse magneto-optical Kerr effect in active bismuth iron garnet films	71
P11	Jochen Braumüller	Quantum simulation of the spin boson model using a superconducting circuit.	72
P12	Denis Brazhnikov	Magneto-optical switch based on the high-contrast electromagnetically-induced-absorption resonance	73
P13	Denis Brazhnikov	Quantum treatment of two-stage laser cooling of ^{24}Mg atoms .	74
P14	Mikhail Bukharin	Ultra short pulse writing of waveguides for advanced 3D integrated optical circuits in fused silica	75
P15	David Colas	Dynamics of Polariton Wavepackets.	76
P16	Shuang Cong	Ultrafast manipulation of a double quantum-dot system based on Lyapunov technology	77
P17	Elena del Valle	Spontaneous, collective coherence in driven, dissipative cavity arrays	78
P18	Dmitry Efimkin	Analytical theory of moving solitons in a fermionic superfluid. .	79
P19	Mikhail Elezov	Limitations for Quantum hacking Superconducting Single-Photon Detector.	80
P20	Matteo Fadel	Measurements of non-locality and phase coherence in Bose-Einstein condensates	81
P21	Yury Kurochkin	Quantum key distribution protocol with floating bases and decoy states	82
P22	Aleksey Fedorov	Roton-maxon spectrum and local density waves in two-dimensional Bose gas of dipoles.	83
P23	Mikhail Fistul	Quantum synchronization in superconducting metamaterials. .	84

P24	Aurél Gábris	Discrete time quantum walks on dynamically changing graphs.	85
P25	Leonid Gerasimov	Raman amplification and trapping of radiation in an inhomogeneous and disordered system of cold atoms	86
P26	Semen Germanskiy	Prospects of observing the non-classicality with optical-terahertz biphoton pairs	87
P27	Lyudmila Golobokova	Si vertical nanowires for photonics applications	88
P28	Artem Golovizin	First investigation of the potentially clock transition in ultracold thulium atoms	89
P29	Elena Kalganova	Laser cooling on the weak transition and optical trapping of thulium atoms	90
P30	Kirill Kalinin	Polarisation reversal in spin-dependent polariton condensates	91
P31	Alia Khamidullina	Three-photon spontaneous parametric down-conversion in optical nanofiber resonators.	92
P32	Emiliya Khan	Multi-element superconducting single-photon detector	93
P33	Oleg Kibis	Aharonov-Bohm effect induced by circularly polarized photons	94
P34	Evgeniy Kiktenko	Operating with five-level superconducting circuit as a two-qubit system	95
P35	Balint Kollar	Quantum walks with strong trapping	96
P36	Vadim Kovalyuk	Waveguide integrated superconducting nanowire single-photon detector for quantum application	97
P37	Nadezhda Kukharchyk	Ion-Beam Implanted Erbium Spin-Ensemble in YSO.	98
P38	Dmitriy Kupriyanov	On a theory of light scattering from a Bose-Einstein condensate.	99
P39	Elena Kuznetsova	Control of polar molecules by Rydberg atoms	100
P40	Jie Li	Generation and detection of robust entanglement between two different mechanical resonators in cavity optomechanics	101
P41	Juan López Carreño	A new spectroscopic technique with quantum light	102
P42	Anna Lyamkina	Exciton-plasmon interaction in hybrid metal-semiconductor structures with proximal InAs/AlGaAs QDs and bowtie antennas	103
P43	Oleg Lychkovskiy	Large spatial superpositions of nanoparticles immersed in superfluid helium.	104
P44	Alexey Melnikov	Coherent controlization using superconducting qubits	105
P45	Daria Mokrousova	Polarization orientation influence on filamentation in non-axis-symmetrical focusing	106
P46	Andreas Neuzner	Radiative dynamics in spatially resolved two-atom cavity QED	107
P47	Henni Ouerdane	Enhanced thermoelectric coupling near electronic phase transition: The role of fluctuation Cooper pairs	108
P48	Evgeny Polyakov	Quasiprobability distributions in the stochastic wavefunction methods	109
P49	Sergey Pyatchenkov	Thulium as new atom for quantum simulators.	110
P50	Carlos Sánchez Muñoz	Photon bundles: a new type of light	111



CONTENT

P51	Albert Schliesser	Nanomechanical membranes as transducers for classical and quantum signals	112
P52	Alexandra Sheremet	Stochastic conversion processes in bosonic condensate of exciton-polaritons	113
P53	Timofey Shpakovskiy	Raman sideband cooling of Mg^+ ions	114
P54	Andrei Sidorov	False vacuum decay in ultracold atoms	115
P55	Maria Sidorova	Ultra-high time resolution SSPD coupled to single-mode fiber	116
P56	Blanca Silva	Measuring photon correlations in time and frequency	117
P57	Sebastian Skacel	Coherent Quantum Phase Slips in AlOx Nanowires	118
P58	Yuuki Tokunaga	High-fidelity cluster state generation using orbital degrees of freedom of ultracold atoms in an optical lattice	119
P59	Dmitry Tregubov	Measurement of the 5D Level Polarizability in Laser Cooled Rb Atoms	120
P60	Anton Vetlugin	Parallel quantum memory applications in quantum information	121
P61	Nina Voronova	Nonlinear exciton-photon oscillations in a polariton condensate	122
P62	Matthew Woolley	Photon-assisted tunnelling with nonclassical microwaves in hybrid circuit QED systems	123
P63	Elena Yakshina	Controlling the interactions of a few cold Rb Rydberg atoms by radio-frequency-assisted Förster resonances	124
P64	Cem Yuce	Rogue Waves in Optical Lattices	125
P65	Boris Zelener	Identifications of S and D Rydberg states in ultracold lithium-7 atoms	126
P66	Yi-Chen Zhang	Practical Squeezed-State Measurement-Device-Independent Quantum Cryptography	127
P67	Philipp Zolotov	Capability investigation of superconductive single-photon detectors optimized for 800–1200 nm spectrum range	128
P68	Ilya Fedorov	Quantum Vampire: a new type of action at a distance	129
P69	Dmitry Chichinadze	Symmetry breaking in quantum dot coupled to ultracold bosons	130
P70	Joseph Cotter	Coherence, absorption and heating in a molecule interferometer	131
P71	David Eger	Optical Coherence in Closed-Loop Double-V Configuration	132
P72	Adel Garifullin	Defining the properties of the electromagnetic field in photonic crystals by method of plane waves expansion	133
P73	Una Karahasanovic	Manifestation of nematic degrees of freedom in the Raman response function of iron pnictides	134
P74	Anna Kardakova	Electron-phonon interaction time in disordered TiN films	135
P75	Anton Kharitonov	Probing radially- and azimuthally polarized light with photo-induced azobenzene polymers	136
P76	Yury Kurochkin	Complete characterization of multimode quantum process	137
P77	Grigoriy Lihachev	Frequency combs and platons in optical microresonators with normal GVD	138

P78	Alexander Lukin	A scalable method for measuring entanglement entropy of quantum many-body systems	139
P79	Nikita Kondratyev	One-dimensional model of chirped slab photonic crystal	140
P80	Oxana Mishina	Squeezing of a collective atomic motion	141
P81	Andrey Pankratov	Josephson vortex interferometer as an advanced ballistic single-shot detector for qubit readout.	142
P82	Evgeniya Pankratova	Spectral linewidth and coherent dynamics in parallel chains of inductively coupled Josephson junctions.	143
P83	Alexander Pechen	Emergence of traps for fast control of a qubit	144
P84	Mihail Petrov	From plasmonic to cold-atomic disordered chains	145
P85	Pedro Ribeiro	Pattern formation in non-equilibrium correlated electronic systems	146
P86	Vladimir Sautenkov	Self-focusing and wave-guiding of optical beam in rubidium atomic vapor.	147
P87	Revin Sergeevich	Underdamped Josephson junction as a switching current detector.	148
P88	Alexey Shakirov	Quantum statistical ensemble for emissive correlated systems	149
P89	Yulia Shchadilova	Quantum dynamics of an impurity in ultracold Bose gas	150
P90	Renat Sibatov	Fractional stable statistics for cold atoms in optical lattices	151
P91	Ivan Solovev	Partial suppression of the bleaching effect in AlGaAs/GaAs quantum well by lowering Al concentration in barriers.	152
P92	Evgeny Stepanov	Plasmon effect on single-electron spectrum near Mott transition	153
P93	Anton Trushechkin	Measurement-assisted Landau-Zener transitions	154
P94	Alexander Ulanov	Distillation of Continuous Variable Entanglement via Quantum Catalysis	155
P95	Leonid Beliaev	Temperature behavior of the reflection and diffraction spectra of resonant grating based on the InGaAs/GaAs quantum wells	156
P96	Jean-Loup Smirr	Sideband transitions in circuit QED based on ux qubits.	157
P97	Philipp Preiss	Strongly Correlated Quantum Walks in Optical Lattices	158

Quantum Hashing via ε -Universal Hashing Constructions

Farid Ablayev¹, Marat Ablayev¹, and Alexander Vasiliev¹

¹Kazan Federal University, 18 Kremlyovskaya St., Kazan 420008, Russian Federation
e-mail: fablayev@gmail.com

Quantum computing is inherently a very mathematical subject, and discussions of how quantum computers can be more efficient than classical computers in breaking encryption algorithms have started since Peter Shor invented his famous quantum algorithm. The reaction of a cryptography community was a “Post-quantum cryptography”, which refers to the research of problems (usually public-key cryptosystems) that are not efficiently breakable using quantum computers. Currently post-quantum cryptography includes different approaches, in particular, hash-based signature schemes such as Lamport signature and Merkle signature scheme. Hashing itself is an important basic concept of computer science. The concept known as “universal hashing” was invented by Carter and Wegman in 1979.

In our research we define quantum hashing as a quantum generalization of the classical hashing. We define the concept of a quantum hash generator and offer design, which allows one to build a large number of different quantum hash functions. The construction is based on composition of a classical ε -universal hash family and a given family of functions – quantum hash generator.

The relationship between ε -universal hash families and error-correcting codes give possibilities to build a large amount of different quantum hash functions. In particular, we present quantum hash function based on Reed-Solomon code, and we prove, that this construction is optimal in the number of qubits needed.

Using the relationship between ε -universal hash families and Freivalds’ fingerprinting schemas we present an explicit quantum hash function and prove that this construction is optimal with respect to the number of qubits.

The work is performed according to the Russian Government Program of Competitive Growth of Kazan Federal University. Work was in part supported by the Russian Foundation for Basic Research (under the grant 14-07-00878).

- [1] F. Ablayev, A. Vasiliev : Cryptographic quantum hashing, Laser Physics Letters Volume 11 Number 2, 2014.
- [2] F. Ablayev, M. Ablayev : Quantum Hashing via Classical epsilon-universal Hashing Constructions, 2014 arXiv:1404.1503 [quant-ph] (2014).

Mechanically Controlled Quantum Switch Defined on a Curved 2DEG

S. S. Aksu¹, O. Kasıkcı¹ and A. Siddiki¹

¹Physics Department, Faculty of Science and Letters, Mimar Sinan Fine Arts University, 34380 Sisli, Istanbul, Turkey
e-mail: seyyareaksu@gmail.com

To investigate quantum nature of two dimensional electrons subject to high perpendicular magnetic fields, usually a planar electronic Fabry-Pérot interferometer is utilized. In this work, we investigate an interferometer defined on a curved hetero-structure. In the presence of a magnetic field perpendicular to the cylindrical axis, the location and the properties of the edge channels depend on the radial component of the magnetic field. Considering a curved structure, we perform numerical and semi-analytical calculations to determine widths of the incompressible edge states. We observe that the edge states form a closed loop for certain magnetic field strengths yielding observation of conductance oscillations, which can be manipulated by changing the Azimuthal angle mechanically. In addition, we investigate the effect of spin polarization on the edge state distribution considering Zeeman splitting and obtained odd integer edge states. The proposed experiment would yield a novel method to clarify the ongoing debate on the origin of conductance oscillations, namely whether they stem from Aharonov-Bohm phase or charging effects.

A non-planar 2DEG can be created at self-rolled hetero-structures [1]. The Aharonov-Bohm phase [2] is measured when an electron travels along a closed path, where a magnetic field penetrates the loop. In the presence of an external B field directed along the z axis, the spinless electrons experience a spatially varying field, since Landau quantization depends only on the perpendicular field component B_z . Hence, on a curved 2DEG (C2DEG) the widths of the incompressible strips will vary depending on the location along the current direction and is modified as,

$$a_k = \sqrt{\frac{16a_B l_d k}{\pi}} \frac{v_0}{v_0^2 - k^2} \quad (1)$$

where a_B is effective Bohr Radius and v_0 is the filling factor. In this work, we numerically define QPCs on curved 2DES by imposing position dependent depletion length assuming a Gaussian form as

$$I_d = V_g \left(\exp\left(\frac{(\theta - \theta_L)^2}{2a^2}\right) + \exp\left(-\frac{(\theta - \theta_R)^2}{2a^2}\right) \right) \quad (2)$$

where V_g is the normalized gate voltage, a determines the width of the QPC and θ_L, θ_R fix the location of the centers of the QPCs, at left and right sides of the quantum dot, respectively.

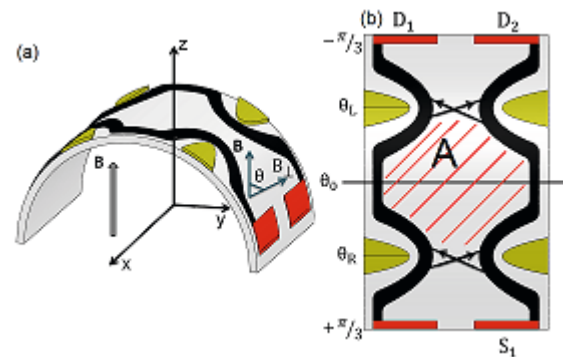


Figure 1: Three dimensional illustration of the curved interferometer. (b) The surface projection of the dot.

We show the spatial distributions of $\nu=2$ incompressible strips calculated at characteristic field strengths.

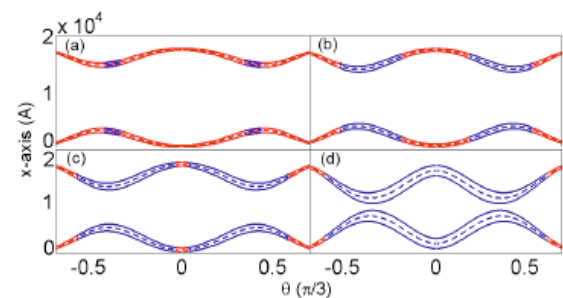


Figure 2: The width of the incompressible edge states are calculated at (a) 1.7T, (b) 1.8T, (c) 1.9T, (d) 2T.

The blue line represents the real incompressible strip while the red line represents the evanescent incompressible strip [3]. We see that the observation of the interference pattern can only be possible in the close vicinity of $B=2T$.

- [1] K.-J. Friedland *et al.*, Physica E, **40**, 1087-1088 (2008).
[2] Y. Aharonov *et al.*, The Physical Review, **115**, 485-491 (1959).
[3] A. Siddiki *et al.*, Europhysics Letters, **92**, 67010 (2010).

Nanometric surface probing with ultra-cold atoms

Murtaza Ali Khan^{1,2}, Florian Schaefer¹, Wolfram H. P. Pernice², Francesco S. Cataliotti¹

¹*European Laboratory for Non-Linear Spectroscopy (LENS), via Nello Carrara 1, 50019 Sesto F.no, Italy*

²*Karlsruhe School of Optics (KSOP), Schlossplatz 19, 76131 Karlsruhe, Germany*

e-mail: alikhan@lens.unifi.it

We intend explore the possibilities offered by Ultra-cold atoms as nano metric surface probes. The interaction between a neutral atom and the surface of a dielectric or a conductor is a subject of research around which are concentrated many experimental and theoretical efforts in recent years. The reasons are varied. On the one hand it is a fundamental problem of QED, which has open conceptual and experimental aspects, such as e.g. the role of thermal fluctuations of the electromagnetic field produced by the surface. On the other hand, the interest is also motivated by the possibility of technological applications for advanced sensors. Finally, the systematic study of these forces is a crucial step for the derivation of new limits on hypothetical forces in non-Newtonian short distance.

The experimental project at LENS is concerned with the realization of an apparatus for laser cooling of atoms and their manipulation at sub-micrometric distances from a nano-structured surface that allows for rapid replacement of the test surfaces.

Quantum hyperbolic metamaterials with exciton-polaritons in semiconductor Bragg mirrors

A. P. Alodjants^{1,2}, E. S. Sedov¹, I. V. Iorsh³, M. Charukhchyan¹ and, A.V. Kavokin^{2,4,5}

¹Vladimir State University named after A. G. and N. G. Stoletovs, Gorky str, 87, Vladimir 600000, Russia

²Russian Quantum Center 100 Novaya St., Skolkovo, Moscow 143025, Russia

³University of ITMO, St. Petersburg 197101, Russia

⁴Spin Optics Laboratory, St. Petersburg State University, Peterhof, St. Petersburg, 198504, Russia

⁵School of Physics and Astronomy, University of Southampton, SO17 1NJ Southampton, United Kingdom
email: alodjants@vlsu.ru

One of the intriguing fundamental problems of modern quantum physics, condensed matter physics, classical general relativity, and quantum field theory is how far the analogy goes between on-table (toy) optical, atomic, solid-state systems and fundamental models existing in astrophysics and cosmology aimed at describing fundamental features of our Universe [1].

We propose a novel approach for emulating quantum effects in curved space-time using resonant semiconductor Bragg mirrors. The discussed structure is schematically shown in Fig. 1. It consists of the periodic array of alternating dielectric layers with QWs placed in the centres of the layers of one type. We show that planar periodic semiconductor Bragg mirror structures allow for controlling the signs of effective masses of mixed light-matter quasiparticles known as Bragg exciton-polaritons in order to create hyperbolic metamaterials (HMMs) [2].

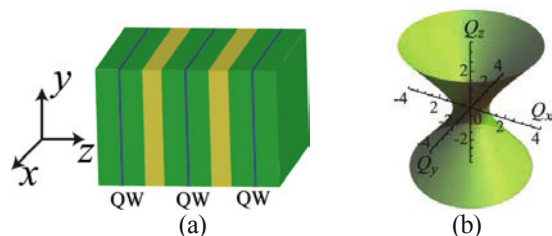


Figure 1. (a) - Schematic picture of spatially periodical structure ("Bragg mirror"), (b) – isofrequency surface for Bragg exciton-polaritons in the linear dissipationless regime.

In particular, important peculiarity of our system is the negative transverse component of the polaritonic effective mass. We demonstrate mapping of the Gross-Pitaevskii equation described LB polaritons onto a nonlinear Ginzburg-Landau-Higgs equation, which exhibits physically non-trivial features. In the linear case, i.e. for non-interacting low branch polaritons we obtain a polariton X-wave solution that is reminiscent of a non-diffractive (spatially localized) matter wave packet. Second, we predict formation of kink-shaped states for weakly interacting polaritons. Small amplitude

oscillations (oscillons) are studied and discussed in details in a perturbed polariton Higgs field.

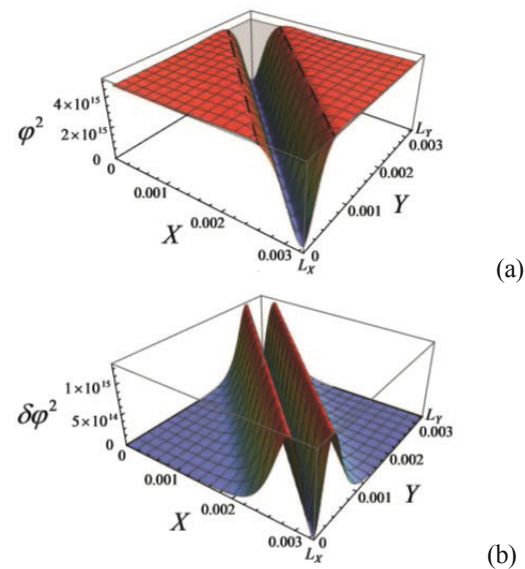


Figure 2. (a) – Probability density φ^2 and (b) – perturbation $\delta\varphi^2$ versus dimensionless spatial coordinates X and Y for Higgs field. Upper shadow plane in (a) indicates vacuum state solution.

Going beyond the mean field theory we examine a Schrodinger cat state formation as a macroscopic superposition of two vacuum states. Polaritonic nonlinear HMMs have a high potentiality for simulation of fundamental cosmological processes.

[1] M. V. Charukhchyan, E. S. Sedov, S. M. Arakelian, and A. P. Alodjants, *Phys. Rev. A*, **89**, 063624 (2014).

[2] E. S. Sedov, I. V. Iorsh, S. M. Arakelian, A. P. Alodjants, A.V. Kavokin, arXiv:cond-mat/1409.3009v2, *Phys. Rev. Letts* (2015), in press.

Self-Induced Transparency Coherent Mode-Locking: Theory and Experiment

R. Arkhipov^{1,2,3}, M. Arkhipov³, A. Shimko³, I. Babushkin⁴

¹Weierstrass Institute, Mohrenstr. 39, 10117, Berlin, Germany

²Humboldt-Universität zu Berlin, Mathematisch-Naturwissenschaftliche Fakultät, 12489 Berlin, Germany

³Faculty of Physics, St. Petersburg State University, 198504 St. Petersburg, Russia

⁴Institute of Quantum Optics, Leibniz University Hannover, 30167 Hannover, Germany

e-mail: arkipovrostislav@gmail.com

Development of compact ultrashort laser pulse sources with high repetition rates is an area of principal interest in optics. Passive mode-locking (PML) is a well-known method for generating of ultrashort optical pulses [1]. In order to achieve PML, a nonlinear saturable absorber is placed into the laser cavity. In such passively mode-locked lasers generation of ultrashort pulses arises due to the absorption/gain saturation in the gain and absorber sections. In this case, the ultimate limit on the output pulse duration is set by the inverse bandwidth of the gain medium. To overcome this limit it was proposed to use coherent light-matter interactions which lead to arising of self-induced transparency in absorber and π pulse formation in the gain medium [2-4]. Such a coherent mode-locking (CML) technique allows to generate optical pulses with a duration much shorter than the medium polarization relaxation time T_2 . All previous theoretical studies of CML were performed for a laser with an amplifier and absorber implemented within the same sample. However, such situation is difficult to realize experimentally.

In the present work, we study CML theoretically and experimentally when the amplified and absorber media are spatially separated [5-6]. Our numerical simulations show that the CML can be achieved via self-starting without any need for a seed pulse, in contrast to previous considerations [2-4]. The dynamics and attractors of such system can be analyzed using a new diagram technique based on the McCall and Hahn area theorem.

Despite of the great promise, there was no experimental demonstration of CML up to now. In this work we make an important step towards this direction by presenting a first experimental demonstration of PML where the absorber works clearly in the coherent regime. The experiment was made using a narrowband dye laser with a coherent iodine I_2 absorber cell [6]. Various mode-locking regimes were observed when a laser frequency was tuned to different absorption lines of I_2 . Example of the oscillogram of the output laser intensity is presented in Fig. 1.

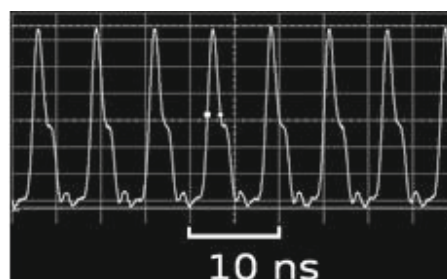


Figure 1: Example of experimentally observed output intensity mode-locked time trace in a laser with a coherent absorber cell at wavelength near 585.181 nm, time base 5 ns/div. Pulse repetition period $T=6.4$ ns [6].

We observed output pulse trains with repetition rates equal or multiple of laser cavity repetition frequency. Laser pulse durations were order of ns which is at least an order of magnitude smaller than relaxation time T_2 of I_2 (tens to hundreds of ns), which would be impossible for a saturable absorber. Experiments were performed at the Center for Optical and Laser Materials Research of Research park of St. Petersburg State University. R. Arkhipov would like to acknowledge the support of EU FP7 ITN PROPHET, Grant No. 264687.

- [1] U. Keller, Appl. Phys. B, **100**, 15 (2010).
- [2] V. V. Kozlov, Phys. Rev. A **56**, 1607 (1997).
- [3] M. A. Talukder, C. R. Menyuk, Phys. Rev. A **79**, 063841 (2009).
- [4] V. V. Kozlov, N. N. Rosanov, Phys. Rev. A **87**, 043836 (2013).
- [5] R. M. Arkhipov, M. V. Arkhipov, I. Babushkin, JETP Letters **101(3)**, 164 (2015).
- [6] M. V. Arkhipov, R. M. Arkhipov, A.A. Shimko, I. Babushkin, JETP Letters **101(4)**, 250 (2015).

Room temperature high-fidelity holonomic single-qubit gate on an NV center in diamond

Silvia Arroyo-Camejo¹, Andrii Lazariev², Stefan W. Hell¹ and Gopalakrishnan Balasubramanian²

¹Department of NanoBiophotonics, Max Planck Institute for Biophysical Chemistry, Göttingen 37077, Germany

²Max Planck Research Group Nanoscale Spin Imaging, Max Planck Institute for Biophysical Chemistry, Göttingen 37077, Germany
e-mail: sarroyo@mpibpc.mpg.de

A quantum computer would be able to solve important problems that are intractable for a classical computer [1]. On the way to the realization of a quantum computer experimental imperfections and decoherence are the major hurdles. Quantum error correction codes enable the construction of quantum computers from a universal set of realistic, imperfect quantum gates [2]. However, quantum error correction codes only become efficacious, if the fundamental quantum gate reaches a certain fidelity. Depending on the correction code this error threshold per gate lies between 10^{-6} to 10^{-2} [3]. On the search for realistic quantum computing architectures, therefore, one needs to rely on fault-tolerant hardware. To this end, quantum gates based on geometric [4, 5] instead of dynamic phase shifts may provide intrinsic fault-tolerance, as geometrical phases show remarkable robustness with respect to certain types of experimental errors.

Here we present an experimental realization of an all-geometric single-qubit quantum gate on a single spin at room temperature. This quantum gate is based on a recent proposal [6] for holonomic quantum computing featuring both fast (non-adiabatic) and universal (non-Abelian) quantum gate performance. In resorting to a single nitrogen-vacancy color center in diamond we achieve close to perfect quantum gate fidelities for the Pauli-X, Pauli-Y, Pauli-Z gate and the Hadamard gate exceeding $F = 0.98$ [7] (see quantum gate process matrices in Figure 1).

This quantum gate realization is based on integrable and scalable hardware exhibiting strong analogy to current silicon technology. Thus, it is a promising step towards viable, fault-tolerant quantum computing under ambient conditions.

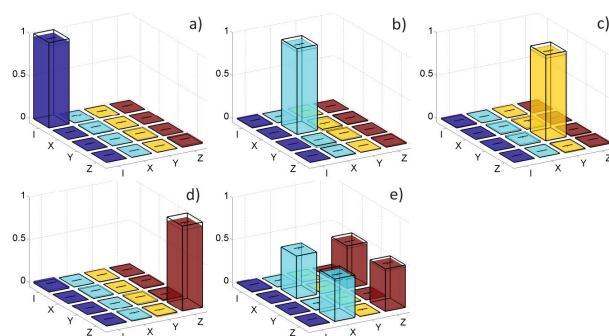


Figure 1: Representations of the experimentally accomplished quantum processes: a) Process matrix of the identity operation, b) the Pauli-X, c) the Pauli-Y, d) the Pauli-Z and e) the Hadamard gate (colored bars: experimental data and error bars, transparent boxes: ideal quantum gates).

- [5] P. Zanardi and M. Rasetti, Phys. Lett. A **264**, 9499 (1999).
- [6] E. Sjöqvist et al., New. J. Phys. **14**, 103035 (2012).
- [7] S. Arroyo-Camejo, A. Lazariev, S. W. Hell and G. Balasubramanian, Nat. Commun. **5**, 4870 (2014).

[1] M. A. Nielsen and I. L. Chuang, Cambridge University Press (2000)

[2] P. W. Shor, Phys. Rev. A **52**, R2493(R) (1995)

[3] E. Knill, Nature **434**,3944 (2005).

[4] M. V. Berry, Proc. R. Soc. Lond. A **392**, 4557 (1984).

Slowing-down of the light phase pulses in resonant atomic Λ -type medium

M. Basalaev¹⁻³, D. Brazhnikov^{1,2}, A. Taichenachev^{1,2} and V. Yudin¹⁻³

¹Novosibirsk State University, ul. Pirogova 2, Novosibirsk 630090, Russia

²Institute of Laser Physics SB RAS, pr. Akademika Lavrent'eva 13/3, Novosibirsk 630090, Russia

³Novosibirsk State Technical University, pr. Karla Marksa 20, Novosibirsk 630073, Russia
e-mail: mbasalaev@gmail.com

A great number of theoretical and experimental works have been devoted to problem of optical pulse propagation in electromagnetically induced transparency (EIT) media. At the same time in the overwhelming majority of these studies the amplitude modulation of light (i.e. the intensity pulses) was considered. It was shown that the group velocity of amplitude pulses propagating in resonant media can be controlled and can take value much smaller than the speed of light in free space c ("slow light"). However, along with the amplitude the inherent parameter of electromagnetic wave is its phase, which similarly to the amplitude can be modulated in a pulse form. Therefore naturally the question arises, which is important for both fundamental and applied nonlinear optics: whether have place the effects of deceleration for the phase pulses?

On the example of Λ system (see Fig. 1) we investigate the space-time evolution of the phase pulses propagating under the EIT conditions. We establish that the medium has a strong influence on the dynamics of the phase pulses. We show that the pulse modulation of the field phase is divided in medium into two fractions, one of which travels at the speed of light in vacuum (in the absence of decoherence between states $|1\rangle$ and $|2\rangle$), and the other is experienced significant slowing-down.

Let us introduce a parametrization of the slowly varying complex amplitudes $\tilde{E}_{1,2}$ in terms of real amplitudes $A_{1,2}$ and phases $\alpha_{1,2}$:

$$\tilde{E}_1 = A_1 e^{i\alpha_1}, \quad \tilde{E}_2 = A_2 e^{i\alpha_2}. \quad (1)$$

The expressions for phase of each field component have the following form

$$\alpha_1(t, z) = \tilde{\alpha}(t - z/c) - \sin(2\varepsilon)\tilde{\phi}(t - z/c) + (\sin(2\varepsilon) - 1)\tilde{\phi}(t - z/v_g), \quad (2)$$

$$\alpha_2(t, z) = \tilde{\alpha}(t - z/c) - \sin(2\varepsilon)\tilde{\phi}(t - z/c) + (\sin(2\varepsilon) + 1)\tilde{\phi}(t - z/v_g), \quad (3)$$

where the functions $\tilde{\alpha}(t)$ and $\tilde{\phi}(t)$ are given by the boundary conditions

$$\tilde{\alpha}(t) = \frac{1}{2}[\alpha_1(t, z=0) + \alpha_2(t, z=0)], \quad (4)$$

$$\tilde{\phi}(t) = \frac{1}{2}[\alpha_2(t, z=0) - \alpha_1(t, z=0)]. \quad (5)$$

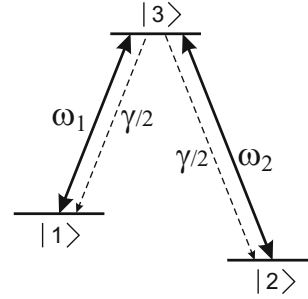


Figure 1: Energy level diagram of a three-level Λ atom. The field component at frequency ω_1 excites the dipole transition $1 \leftrightarrow 3$, and the field at frequency ω_2 is resonant to the transition $2 \leftrightarrow 3$. We assume that $\omega_1 \approx \omega_2 = \omega$. The transition $1 \leftrightarrow 2$ is forbidden.

The group velocity of slow phase pulse is

$$v_g = \frac{c}{1 + s(A^2, \varepsilon)}, \quad (6)$$

where slowing factor $s(A^2, \varepsilon)$ have the form

$$s(A^2, \varepsilon) = \frac{2\pi N_a \hbar \omega |d_{31}|^2 |d_{32}|^2}{A^2} \times \left(\frac{|d_{31}|^2 + |d_{32}|^2}{2} + \frac{|d_{31}|^2 - |d_{32}|^2}{2} \sin 2\varepsilon \right)^{-2}, \quad (7)$$

$$A^2 = A_1^2 + A_2^2, \quad \varepsilon = \frac{\pi}{4} - \arctan \frac{A_2}{A_1}.$$

From the solutions (2) and (3) it is seen that ultra-slow pulses can be observed not only for amplitude modulation, but also in the case of phase modulation. The group velocity of these pulses is determined by amplitudes of the resonance fields. We have shown that in Λ system under the EIT conditions the phase self- and cross-modulation take place.

The work was supported by the Ministry of Education and Science of the Russian Federation (state assignment No. 2014/139 project No. 825), by the Russian Foundation for Basic Research (grants No. 14-02-00712, No. 14-02-00939, No. 15-02-08377, No. 15-32-20330). M. Basalaev and D. Brazhnikov were supported by the Presidential Grant (MK-4680.2014.2). M. Basalaev was also supported by the non-profit Dynasty Foundation.

Precision spectroscopy of the 2S-4P transition in atomic hydrogen

A. Beyer¹, L. Maisenbacher¹, A. Matveev¹, K. Khabarova^{2,3}, R. Pohl¹, Th. Udem¹,
T. W. Hänsch^{1,4} and N. Kolachevsky^{2,3}

¹Max-Planck-Institut für Quantenoptik, 85748 Garching, Germany

²P.N. Lebedev Physical Institute, Moscow 119991, Russia

³Russian Quantum Center, 100 Novaya St., Skolkovo, Moscow 143025, Russia

⁴Ludwig-Maximilians-Universität, München, Germany

e-mail: Axel.Beyer@mpq.mpg.de

Precision spectroscopy of atomic hydrogen, the simplest atomic system, has been one of the major benchmarks for fundamental theories ever since the dawn of modern physics. For more than one decade now, the comparison between theoretical and experimental values of transition frequencies in hydrogen has been limited by insufficient knowledge of the proton r.m.s. charge radius. Laser spectroscopy of muonic hydrogen provided values for the proton size in 2010 and 2013, which are ten times more accurate than any other determination [1, 2]. However, there is a seven combined standard deviations discrepancy between the values for the charge radius extracted from electronic hydrogen spectroscopy and electron-proton scattering on the one hand and muonic hydrogen on the other hand. With this 'proton size puzzle' unresolved, theoretical predictions could not yet benefit from the outstanding accuracy of the latter results [3].

For the existing electronic hydrogen data set (see references in [4]), the longest lever arm on this puzzle is found in improving measurements of transition frequencies starting from the metastable 2S state to higher lying nL states. We will report on our current measurement of the one photon 2S-4P transition which is aiming shed new light to the hydrogen part of the puzzle.

Our experiment is the first probing a 2S- nL transition in atomic hydrogen utilizing a cryogenic beam of atoms in the 2S state [5]. We perform optical excitation to the 2S state instead of electron-impact excitation commonly used in previous experiments. This approach exclusively populates the 2S($F = 1$) hyperfine state, leading to a significant simplification of the dynamics in the subsequent 2S-4P spectroscopy. In addition, optical excitation preserves the low thermal velocity of our sample atoms originating from a cryogenic source at 5.8 K. Accordingly, their mean velocity is more than one order of magnitude smaller than in previous experiments (see e.g. [6]). However, the first order Doppler effect (FOD) still needs to be suppressed by six orders of magnitude to achieve the desired experimental accuracy in the low kHz range. We will discuss a new method to characterize and on-line monitor the FOD suppression in

our system based on an active stabilization scheme and time-of-flight resolved detection.

The effects of quantum interference due to neighboring resonances have recently come to the attention of the precision spectroscopy community. They have been calculated to cause significant geometry dependent shifts even if the next neighboring resonances are separated by as much as 10,000 line widths [7, 8]. Experimental evidence for these shifts only existed for the partially unresolved hyperfine components in Li^{6,7} up to now [9, 10]. We will present a dedicated measurement demonstrating the significance of these shifts for the case of neighboring resonances being separated by 100 line widths. Shifts up to multiple tens of kHz can be observed in the experiment and brought under control by proper modeling, paving the way towards an improved measurement of the 2S-4P transition frequency.

- [1] R. Pohl *et al.*, Nature **466**, (2010).
- [2] A. Antognini *et al.*, Science **339**, (2013).
- [3] R. Pohl, R. Gilman, G.A. Miller and K. Pachucki, Annu. Rev. Nucl. Part. Sci. **63**, 175–204 (2013).
- [4] P.J. Mohr, B.N. Taylor, D.B. Newell, Rev. Mod. Phys. **84**, 1527 (2012).
- [5] A. Beyer *et al.*, Ann. d. Phys. (Berlin) **525**, 671 (2013).
- [6] D.J. Berkeland, E.A. Hinds, M.G. Boshier, Phys. Rev. Lett. **75**, 2470–2473 (1995).
- [7] M. Horbatsch and E.A. Hessels, Phys. Rev. A **84**, 032508 (2011).
- [8] A. Marsmann, M. Horbatsch and E.A. Hessels, Phys. Rev. A **86**, 012510 (2012).
- [9] C.J. Sansonetti *et al.*, Phys. Rev. Lett. **107**, 023001 (2013).
- [10] R.C. Brown *et al.*, Phys. Rev. A **87**, 032504 (2013).

Probing the Interaction of Microscopic Material Defects with Quasiparticles using a Superconducting Qubit

A. Bilmes¹, J. Lisenfeld¹, A. Heimes², S. Zanker², G. Schön², G. Weiß¹, A. V. Ustinov^{1,3}

¹Physikalisches Institut, Karlsruhe Institute of Technology, Wolfgang-Gaede-Str. 1, 76131 Karlsruhe, Germany

²Institut für theoretische Festkörperphysik, Karlsruhe Institute of Technology, Wolfgang-Gaede-Str. 1, 76131 Karlsruhe, Germany

³Russian Quantum Center, 100 Novaya St., Skolkovo, Moscow 134025, Russia
e-mail: alexander.bilmes@kit.edu

The functionality of various superconducting nanoscale devices such as SQUIDS, photon detectors, resonators or quantum circuits (qubits) suffers from structural material defects, which reside in dielectric layers, surface oxides or film interfaces. A well-known model by Phillips and Anderson assumes that in highly disordered solids defects emerge from small groups of atoms which can slightly rearrange by reversible tunneling processes. This forms a so-called two-level tunneling system (TLS) which can be regarded as one effective atom capable to tunnel between two almost equivalent sites of the lattice (Fig. 1a). TLS' dynamics is described by tunneling in a double-well potential (Fig. 1b) with transition frequencies widely distributed up to about 20 GHz or $1\text{ K}\cdot k_B/\hbar$. Since the displacement of an atom involves local charge redistribution and local strain changes, TLS possess both electric and elastic dipole moments by which they can couple to their environment.

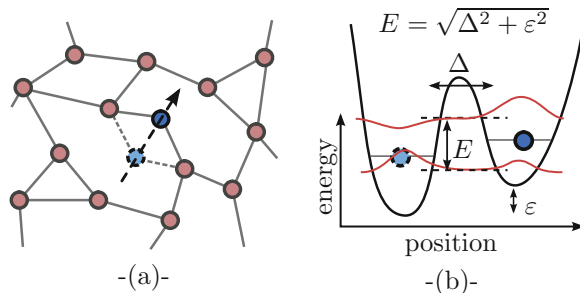


Figure 1: (a) TLS modeled by a single tunneling atom. (b) Double-well potential for a TLS. Similar to a flux qubit tunneling energy Δ and asymmetry energy ϵ determine the TLS transition frequency E/\hbar .

Superconducting qubits are very promising candidates to build the universal quantum computer. They are easy to fabricate using standard lithography techniques and simply to manipulate using microwave pulses. Their quality is affected by parasitic TLS in different manners. The qubit coherence time shows frequency dependent drops due to weakly coupling surface TLS' [1], which limit the maximal number of single- and two-qubit quantum gates. Coherent individual TLS hosted within the

tunnel barrier of the qubit's Josephson junction lead to avoided level crossings [2] in the qubit spectrum which makes the bandwidth discontinuous and limits the qubit scalability. The TLS microscopic nature is still under debate, therefore we perform fundamental research on TLS in superconducting qubits which for example is helpful to better understand how to control the TLS density during sample fabrication.

We use a superconducting phase qubit to detect *coherent* TLS contained within the qubit's Josephson junction. Quantum operations on *individual* TLS are performed by resonant microwave pulses and readout of TLS state is possible due to their strong coupling to the qubit ($< 50\text{ MHz}$). Our previous measurements of TLS coherence in dependence of the temperature indicate that thermal quasiparticles may dominate the TLS energy loss and dephasing above 150 mK [3]. We believe that quasiparticles interact with TLS during tunneling through the Josephson barrier: they induce an electric field and change the local lattice strain which varies the TLS asymmetry energy. We probe the TLS-quasiparticle interaction using a reliable method of *in-situ* quasiparticle injection via an on-chip dc-SQUID that is pulse-biased beyond its critical current. The injected quasiparticles then diffuse over a distance of about 1 μm through the superconducting ground plane towards the Josephson junction hosting TLS. The quasiparticle density is calibrated by measuring associated characteristic changes to the qubit's resonance frequency and energy relaxation rate [4]. We will present experimental data that clearly show the influence of injected quasiparticles on TLS coherence.

- [1] R. Barends et al., Phys. Rev. Lett. **111**, 080502 (2013).
- [2] R. W. Simmonds et al., Phys. Rev. Lett. **93**, 077003 (2014).
- [3] J. Lisenfeld et al., Phys. Rev. Lett. **105**, 230104 (2010).
- [4] M. Lenander et al., Phys. Rev. B **84**, 024501 (2011).

Transverse magneto-optical Kerr effect in active bismuth iron garnet films

O. Borovkova¹, N. Khokhlov^{1,2}, A. Kalish^{1,2}, V. Belotelov^{1,2}, and P. Vetoshko¹

¹Russian Quantum Center, 100 Novaya St., Skolkovo, Moscow 143025, Russia

²Lomonosov Moscow State University, Leninskie Gori, 1, bld.2, Moscow 119991, Russia

e-mail: o.borovkova@rqc.ru

Up-to-date data storage technologies employ magnetic effects in ferromagnetic layers separated by thin layer of nonmagnetic dielectric. Information is encoded by the magnetization direction inside domains of these ferromagnetic layers. Improvement of magnetization control and enhancement of magnetic effects are required for the further development of technology. An employment of magneto-optical (MO) effects seems to be a very promising approach. MO effects mean that the magnetization of material essentially depends on the intensity and polarization of the light passing through the material. We are focused on the intensity MO effects like transverse magneto-optical Kerr effect (TMOKE). Such effects can be significantly enhanced by the excitation of surface plasmon-polaritons (SPPs) at the surface of ferromagnetic dielectric. In Ref. [1] it was investigated the influence of SPPs propagating along the interface of ferromagnetic dielectric film and the nanoscaled grating of noble metal on the TMOKE. SPPs increase the interaction area of light beam and magnetic material, and therefore enhance the MO effect in both reflected and transmitted light.

However, it is well-known that SPPs dissipate their energy through the interaction with metal that limits their propagation length. Moreover, the ferromagnetic material containing iron ions contributes additional losses. Thus, the problem of loss compensation and amplification of SPPs is crucial for the further enhancement of the MO effect.

Loss compensation and amplification of surface plasmon-polaritons have been investigated deeply in active nonmagnetic materials, like dye solution, or PMMA doped by quantum dots, etc. (see review [2]). Amplified spontaneous emission of surface plasmon polaritons can be observed at the interface with a resonant amplifying medium. In our work we consider a ferromagnetic film doped by active ions. These ions can be pumped at the wavelengths where bismuth iron garnet has good transmission. We address a magnetoplasmonic crystal of one dimensional gold grating deposited on the doped iron garnet grown on top of the non-magnetic gadolinium gallium garnet substrate. Choosing the incident parameters of the probe beam we excite SPP at the emission wavelength of dopant ions, thus, luminescence of dopants

enhances surface plasmon-polariton wave at the interface of ferromagnetic material and gold grating.

We analysed different types of dopants, their absorption and emission spectra and revealed that ions of Cr are the most suitable dopants. Chromium has peaks of absorption at 470 nm and 630 nm and peak of emission at 697 nm and 730 nm. For bismuth iron garnet the magneto-optical activity is significant in the wavelength range of 550-900 nm. Emission of Cr ions enhance the surface plasmon wave at these wavelengths, and increase their propagation length. In their turn, surface plasmon waves amplify the interaction area of the incidence beam and the ferromagnetic material.

We show that emission of dopants adjusted with SPP wavelength increase the intensity of transmitted light by 50%. At the same time, the intensity of the transverse magneto-optical Kerr effect also increases by 50%. Dependences of transmittance intensity and TMOKE effect on the value of the gain parameter and on the geometrical parameters of the magnetoplasmonic crystal are investigated.

The work is supported by the Russian Foundation for Basic Research (projects № 13-02-01122, 14-02-01012).

[1] V.I. Belotelov and et al, Nature Nanotech. **6**, 370 (2011).

[2] P. Berini, and I. De Leon, Nature Photon. **6**, 18 (2012).

Quantum simulation of the spin boson model using a superconducting circuit

J. Braumüller¹, M. Weides^{1,2}, M. Marthaler³, H. Rotzinger¹, and A. V. Ustinov^{1,4}

¹Physikalisches Institut, Karlsruhe Institute of Technology, Wolfgang-Gaede-Str. 1, 76131 Karlsruhe, Germany

²Physikalisches Institut, Johannes Gutenberg University Mainz, Staudinger Weg 9, 55128 Mainz, Germany

³Institut für Theoretische Festkörperphysik, Karlsruhe Institute of Technology, Wolfgang-Gaede-Str. 1, 76131 Karlsruhe, Germany

⁴Russian Quantum Center, 100 Novaya Str., Skolkovo, Moscow 143025, Russia
e-mail: jochen.braumueller@kit.edu

Finding the solution for a quantum mechanical problem is known to be often a very difficult and challenging task. The reason for that is the exponentially large number of degrees of freedom in a quantum system, requiring an incredible amount of memory and computational power that is not available from present computers. A promising idea to approach this problem is to implement a physical device comprising computational elements that themselves obey the laws of quantum mechanics [1]. Measuring the time evolution of an artificially built superconducting quantum circuit, a quantum system of interest is mapped onto, allows to infer the time evolution of the underlying quantum system. This corresponds to finding an exact solution of the quantum problem on-chip and is referred to as analog quantum simulation [2, 3].

Here we report on the implementation of an analog quantum simulator of the spin-boson model. While being a quantum mechanical model of major relevance in nature, it is very hard to approach theoretically and numerical solutions are scarce. Its Hamiltonian reads

$$\begin{aligned}\hat{H} &= \hat{H}_q + \hat{H}_b + \hat{H}_i \\ &= \hbar \frac{\omega_q}{2} \hat{\sigma}_z + \hbar \sum_i \omega_i \hat{b}_i^\dagger \hat{b}_i + \hbar \hat{\sigma}_x \sum_i t_i (\hat{b}_i^\dagger + \hat{b}_i).\end{aligned}$$

\hat{H}_q denotes the atomic Hamiltonian with transition frequency ω_q , \hat{H}_b is the Hamiltonian of the bosonic bath with harmonic modes of frequencies ω_i and creation (annihilation) operators \hat{b}_i^\dagger (\hat{b}_i). \hat{H}_i denotes the interaction of atom and bosonic bath and $\hat{\sigma}_i$ are the Pauli spin matrices.

We map the spin of an atom to a quantum bit (qubit), which is a fast tunable superconducting transmon qubit coupled to a dispersive readout resonator. The bosonic bath is constituted by a set of harmonic resonators. It is engineered to have a continuous spectral mode density which is formed by an overlapping frequency response of resonators equipped with resistive elements. Tuning the spectral mode density allows to access a large class of possible parameter regimes within the spin-boson model. Our sample furthermore features a connection line

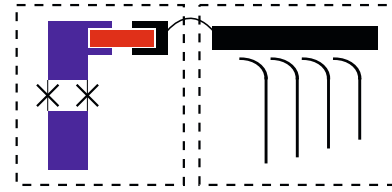


Figure 1: Schematic sample design emulating the spin boson model. A tunable transmon qubit (left) couples via a bandpass filter to a set of harmonic resonators, connected to a common transmission line. They form a continuous band of modes with an artificially tailored spectral mode density. The bosonic bath is implemented on a separate chip, allowing for a fast switching between different bath environments in experiment.

to the bosonic bath via a designated band-pass filter to prevent the qubit to be coherence limited by the Purcell effect. The sample design is schematically depicted in Fig. 1. We will present the design, simulation and a first experimental characterization of engineered bosonic bath samples.

Interesting effects, like a quantum phase transition [4] for instance, can occur when reaching the ultra-strong coupling regime between atom and bosonic bath. While a geometric coupling this large would make it impossible to operate the qubit, we achieve a switchable effective ultra-strong coupling by applying a microwave tone close to resonance when the atom is tuned into the band of bosonic modes. We present numerical simulations of our quantum circuit in the ultra-strong coupling regime as well as preliminary measurement results.

Another interesting aspect of the work is the study of an open quantum system, which is of particular importance for the scaling of quantum systems.

- [1] R. Feynman, Int. J. Theor. Phys. **21**, 467 (1982).
- [2] I. M. Georgescu, S. Ashhab, and F. Nori, Rev. Mod. Phys. **86**, 1 (2014).
- [3] A. A. Houck, H. E. Türeci, and J. Koch, Nat. Phys. **8**, 292 (2012).
- [4] S. Florens, D. Venturelli, and R. Narayanan, arXiv:1106.2654 (2011).

Magneto-optical switch based on the high-contrast electromagnetically-induced-absorption resonance

D.V. Brazhnikov^{1,2}, A.V. Taichenachev^{1,2}, A.M. Tumaikin¹ and V.I. Yudin^{1,4}

¹*Institute of Laser Physics SB RAS, pr. Lavrent'eva 13/3, Novosibirsk 630090, Russia*

²*Novosibirsk State University, ul. Pirogova 2, Novosibirsk 630090, Russia*

³*Novosibirsk State Technical University, pr. Karla Marksa 20, Novosibirsk 630073, Russia*

⁴*Russian Quantum Center, 100 Novaya St., Skolkovo, Moscow 143025, Russia*

e-mail: brazhnikov@laser.nsc.ru

Phenomenon of coherent population trapping (CPT), discovered in the late 70s of the last century, underlies many interesting nonlinear effects in atom physics. One of them is electromagnetically induced transparency (EIT), which has found several applications in laser physics and laser spectroscopy, optical communications and quantum metrology (miniature atomic clocks and magnetometers). The width of EIT resonance can be much less than the natural linewidth, therefore such the resonances are often called subnatural-width ones.

In 1997 subnatural-width resonance with opposite sign was discovered – electromagnetically induced absorption (EIA) [1]. Firstly that resonance was observed under a bichromatic laser field composed of co-directional beams with opposite circular polarizations. Then the effect was also studied under a single-frequency light wave accompanied with a static magnetic field applied along the wave vector (magneto-optical or, so-called, Hanle configuration) [2]. Since its discovery the scope of EIA applications happened to be rather small in comparison with EIT resonances due to some difficulties. The fact is that the most effective methods for getting the resonance width narrower based on the usage of buffer gas or a cell with antirelaxation coating of walls. These methods, demonstrating perfect results for EIT signals, happened to be useless for EIA ones in the standard schemes of observation [1,2]. It is due to the fact that EIA in those schemes is resulted from formation of anisotropy on an atomic excited state and its spontaneous transfer to ground one [3]. Collisional process between atoms and buffer gas or cell walls rapidly destroys the excited state anisotropy, what leads to damping of EIA signal. At present EIT signals can have simultaneously 40-90% contrast and kHz or sub-kHz widths. Unfortunately, the known results for EIA signals cannot provide the same.

In the series of papers [4-6] we have proposed and studied in details some “unconventional” scheme for observing EIA signals in the Hanle configuration under counterpropagating light waves (“probe” and “pump”). Here we suggest an idea of magneto-optical switch, basing on that new scheme. Operation of the device is as follows. A vapour cell filled with alkali

work atoms and buffer gas is irradiated by two counterpropagating laser beams of equal frequency and orthogonal linear polarizations. Absorption of one of them (probe beam) is monitored as the function of static magnetic field B , applied along the wave vectors. At some conditions, in vicinity of $B=0$ the probe transmittance almost equals to zero (see fig.1). Otherwise, when $B \neq 0$, the probe transmittance is very close to 100%. At that, the magnetic field B can be as low as just several mG for effective controlling over probe transmittance. In other words, compact, low consumption, high-sensitive and easy to control magneto-optical switch can be constructed for governing laser beam intensity.

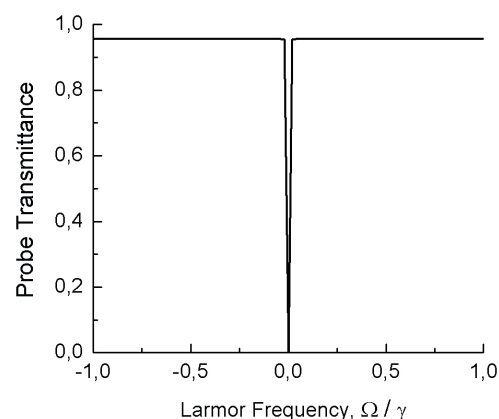


Figure 1: Normalized probe beam power transmitted through a cell. Larmor frequency Ω is linearly proportional to the magnetic field amplitude B , γ is the spontaneous relaxation rate of the excited atomic state.

This work was partially supported by RFBR (15-02-08377, 15-32-20330, 14-02-00806, 14-02-00712, 14-02-00939), Ministry of Education and Science of Russian Federation, Russian Academy of Sciences and by Russian Presidential Grant (MK-4680.2014.2).

- [1] A.M. Akulshin et al., *Phys. Rev. A* **57**, 2996 (1998).
- [2] Y. Dancheva et al., *Opt. Commun.* **178**, 103 (2000).
- [3] A.V. Taichenachev et al., *JETP Lett.* **69**, 819 (1999).
- [4] D.V. Brazhnikov et al., *JETP Lett.* **91**, 625 (2010).
- [5] D.V. Brazhnikov et al., *Eur. Phys. J. D* **63**, 315 (2011).
- [6] D.V. Brazhnikov et al., *Laser Phys. Lett.* **11**, 125702 (2014).

Quantum treatment of two-stage laser cooling of ^{24}Mg atoms

O.N. Prudnikov¹, D.V. Brazhnikov^{1,2}, A.E. Bonert¹, A.N. Goncharov^{1,3}, R.Ya. Ilenkov¹,
A.V. Taichenachev^{1,2} and V.I. Yudin^{1,4}

¹Novosibirsk State University, ul. Pirogova 2, Novosibirsk 630090, Russia

²Institute of Laser Physics SB RAS, pr. Lavrent'eva 13/3, Novosibirsk 630090, Russia

³Novosibirsk State Technical University, pr. Karla Marksa 20, Novosibirsk 630073, Russia

⁴Russian Quantum Center, 100 Novaya St., Skolkovo, Moscow 143025, Russia

e-mail: brazhnikov@laser.nsc.ru

Deep laser cooling of magnesium atoms has special importance for quantum metrology: new-generation frequency standards based on large number of neutral atoms confined in an optical lattice. In contrast to the other main atom-candidates for the standard (Yb, Sr, Hg, Ca), deep laser cooling of ^{24}Mg atoms close to the recoil energy limit is an intricate problem ($T_{\text{rec}} \approx 3\text{--}10\ \mu\text{K}$, depending on the cooling transition). In the recent experiments [1,2] researchers have managed to cool magnesium atoms down to 1.3 μK and confine them in a lattice, but effective evaporative cooling technique was applied after a magneto-optical trap (MOT), what led to great loss in number of atoms ($N_{\text{final}} \sim N_{\text{initial}}/10^4$). At the same time, temperature of the cloud in MOT did not exceed 1 mK, what is rather far from the desirable range of temperatures and the problem of deep cooling of ^{24}Mg atoms by means of laser fields is still relevant.

Here we theoretically examine $3^3P_2 \rightarrow 3^3D_3$ dipole transition ($T_{\text{rec}} \approx 5\ \mu\text{K}$) and propose the way for overcoming current difficulties in deep laser cooling of ^{24}Mg atoms by analyzing a magneto-optical trap and an optical molasses on the basis of quantum treatment with full account for the recoil effect.

Quantum treatment of the problem for the case of 1D MOT has revealed that sub-Doppler temperatures are not achievable in contrast to the results provided by the semi-classical approach [3]. With increasing the frequency detuning the lowest atomic energy that can be obtained in MOT is about $110 \times E_{\text{rec}}$ (at $\delta \approx -5\gamma$). Roughly speaking it corresponds to $T_{\text{eff}} \sim 600\ \mu\text{K}$, while the Doppler limit is $83 \times E_{\text{rec}}$.

To achieve much less temperatures of the cloud we propose using optical molasses with $lin \perp lin$ configuration as the second stage. Fig.1 shows that the lowest energy can be as low as $17 \times E_{\text{rec}}$ ($T_{\text{eff}} \sim 90\ \mu\text{K}$). After the second cooling stage the selection of an ultracold atomic fraction can be undertaken by the evaporation technique to reach μK s range. At that, there are the special conditions, when the ultracold fraction is maximized (see Fig.2). These conditions are not immediately the same as for profiles at Fig.1 to reach the minimum of $E(I)$. The relative number $N \approx 60\%$ at Fig.2 means that more than a half of all atoms

in the molasses account for the ultracold fraction with T_{eff} equals to several μK s.

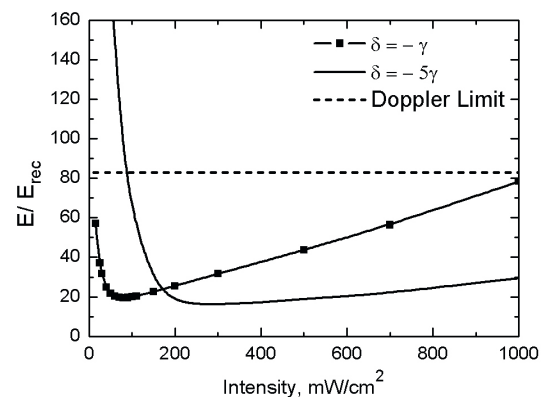


Figure 1: Average kinetic energy of an atom in an optical molasses.

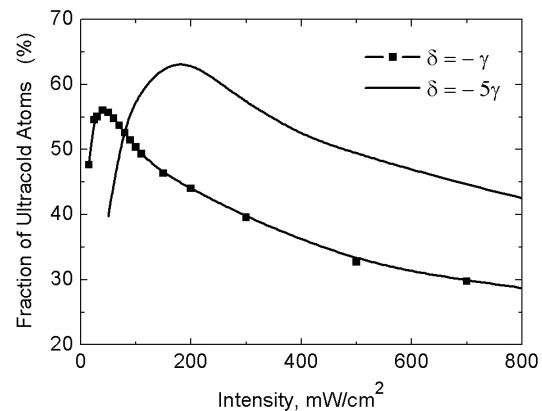


Figure 2: The fraction of atoms in a cloud under optical molasses, whose linear momentum less than $3 \times \hbar k$.

This work was partially supported by RFBR (15-02-06087, 15-32-20330, 14-02-00806, 14-02-00712, 14-02-00939), Ministry of Education and Science of Russian Federation, Russian Academy of Sciences and by Russian Presidential Grant (MK-4680.2014.2).

E.M. Rasel et al., Book of Abstracts of the 28th International Frequency and Time Forum (EFTF-2014), 23-26 July 2014, Neuchatel, Switzerland. Page 138.

M. Riedmann et al., Phys. Rev. A **86**, 043416 (2012).

D.V. Brazhnikov et al., Laser Phys. **24**, 074011 (2014).

Ultra short pulse writing of waveguides for advanced 3D integrated optical circuits in fused silica

M.A. Bukharin^{1,2}, and D.V. Khudyakov²

¹Moscow Institute of Physics and Technology, 9 Institutskiy per.,
Dolgoprudny, Moscow Region, 141700, Russia

²Optosystems Ltd., Troitsk, Moscow, 142190, Russia
e-mail: mikhail.bukharin@phystech.edu

Three-dimensional integrated optical circuits can be fabricated inside glasses and crystals by focusing of femtosecond laser pulses [1-3]. One can distinguish two different geometries of waveguides: core written (in materials with increasing refracted index) and depressed cladding waveguides (primarily in crystals and active glasses). The second geometry offers a number of advantages over the core written waveguides. Unfortunately, in one of the most favourable material, in fused silica, refractive index increases in the focal region under usual conditions of femtosecond writing, thus one can inscribe in the material only core written waveguides.

In this paper we proposed to write waveguides into fused silica in cumulative regime. It realizes only at high pulses repetition rate (> 3 MHz for fused silica), when each subsequent laser pulse comes to the focus before the heat, evolved from the previous pulse, dissipates away the focal region. The profile, induced in cumulative regime, possesses side region with reduced refracted index (see Fig. 1), while in the focal region it increases as usual.

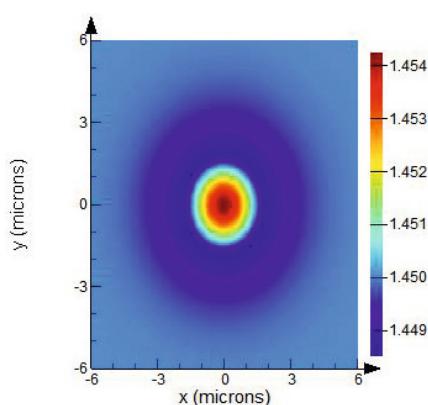


Figure 1: Spatial profile of refracted index, induced in cumulative regime into fused silica.

We proposed, for what is believed to be the first time, to use side regions of several closely spaced tracks to form depressed cladding waveguide in fused silica according to the geometry, represented in Fig.2. Such new geometry allows taking advantages of depressed cladding waveguides even in materials with increasing refracted index.

For the purposes of 3D integrated optical circuits

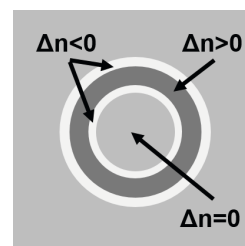


Figure 2: Cross section of depressed cladding waveguide in fused silica.

development, the proposed geometry provides following advantages:

- writing directly at wavelength of $1 \mu\text{m}$ without second harmonic generation [4] or correction optical schemes [5] thanks to spherically symmetric region, induced in cumulative regime, and writing of cladding;
- writing of advanced 3D circuits within depth range more than $500 \mu\text{m}$ in contrast to $100 \mu\text{m}$ range for usual core written geometry [2] thanks to reduced impact of spherical aberration and self-focusing [4];
- reduced influence of color centers and change of Raman spectrum on propagated light thanks to low intensity in the treated regions [2].

Based on the obtained profile and to verify our hypothesis by experiment, we fabricated depressed cladding waveguide inside fused silica. Guiding of light was supported with side regions of decreased refractive index $-1.5 \cdot 10^{-3}$. The waveguide supported propagation of both polarizations with typical propagation losses less than 0.2 dB/cm at $\lambda = 633 \text{ nm}$.

- [1] Xiao-Song Ma, Nature Photonics, **8**, 749 (2014).
- [2] C. Miese, S. Gross, M.J. Withford, and A. Fuerbach, Opt.Mat.Exp., **5**, 2, 323 (2015)
- [3] G.D. Marshall, *et.al.*, Opt. Exp., **17**, 15, 12546 (2009).
- [4] S.M. Eaton, Mi Li Ng, R. Osellame, and P.R. Herman, Journal of Non-Crystalline Solids **357**, 2387 (2011).
- [5] G. Cerullo, *et.al.*, Opt. Lett., **27**, 21, 1938 (2002)

Dynamics of Polariton Wavepackets

D. Colas¹, L. Dominici^{2,3}, J.P. Restrepo Cuartas¹, A.V Kavokin⁴, D. Sanvitto^{2,3} and F.P Laussy^{1,4}

¹Departamento de Física Teórica de la Materia Condensada and Condensed Matter Physics Center (IFIMAC), Universidad Autónoma de Madrid, E-28049, Spain

²NNL, Istituto Nanoscienze-CNR, Via Arnesano, 73100 Lecce, Italy

³Istituto Italiano di Tecnologia, IIT-Lecce, Via Barsanti, 73010 Lecce, Italy

⁴Russian Quantum Center, Novaya 100, 143025 Skolkovo, Moscow Region, Russia

e-mail: david.colas@uam.es

Polaritons arise from the strong light-matter coupling between a cavity photon and a semiconductor exciton [1]. They have been the object of many attention in the last decades for their quantum properties at the macroscopic level, such as Bose-Einstein Condensation or superfluidity. While interactions have been at the forefront of the theoretical interest, particularly as solitonic properties have been recently of very high interest, we take here an interest in fundamental aspects of their *linear regime*.

As two-coupled fields of greatly differing masses, the polariton dynamics poses many interesting questions. For instance, what happens when they reach relativistic speed? This is a topical question since such a report has been recently made with organic polaritons [2]. On the other hand, it is known that superpositions of different masses is a vexing problem for the Schrödinger equation, that rules the polariton dynamics in absence of interactions [3].

Even the textbook Rabi oscillations—the energy transfer between the two fields—leaves room for being revisited. Recently, we have demonstrated an ultrafast control of such Rabi oscillations for coherent states of polaritons [4] and discussed their interpretation as “cebits” (not yet as qubits [5]). We also showed how, with the added polarization degree of freedom, this allows to generate a new type of polarization shaping: Full Poincaré beams in time [6]. An experimental result for an half-spanning of the sphere is shown on Fig. 1(a-b). This promises applications in photon ionization, sub-wavelength localization or more mundane industrial concerns such as hole drilling, laser micro-processing or the machining of medical stent devices.

Regarding the dynamics of the polariton wavepacket itself, we introduce a new concept of wave propagation: the “*Self-Interfering Packet*” (SIP), that, still in the linear regime, brings about several sub-packets exhibiting solitonic properties: shape preserving and self-healing (without being solitons). This is thanks to the peculiar polariton dispersion that allows, around the saddle point, to superimpose propagation with an effective mass that can be positive or negative for various parts of the packet. This results in a diffusion of the wavepacket constrained in a well defined spacetime

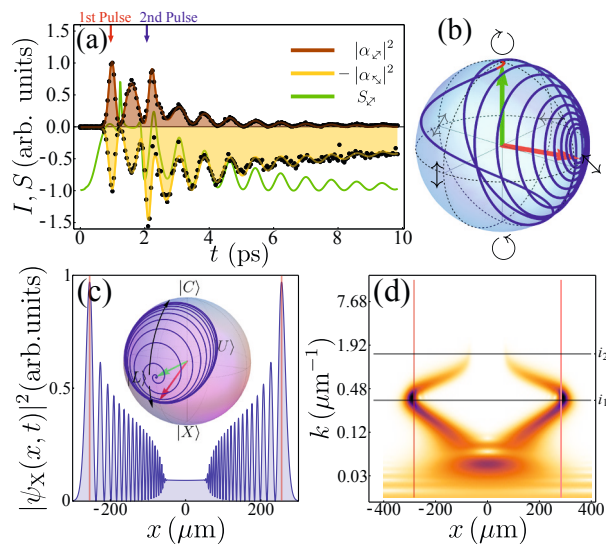


Figure 1: (a-b) Polarized Rabi oscillations. The experimental data (black dots) is fitted with the theoretical model (solid lines), providing the amplitudes $|\alpha_{\sigma, \sigma'}|^2$ and the degree of polarization S_z . The polarization dynamics is displayed on the Poincaré sphere. (c-d) Self-Interfering polariton wavepacket (SIP). (c) Probability amplitude of the SIP after propagation, with the quantum state's path from the center to a side of the packet as well displayed on a Bloch sphere. (d) Corresponding scalogram.

cone, and the appearance of interferences patterns as the packet overlaps with itself. In order to analyse the SIP and its peculiar dynamics, we recourse to the wavelet transform, unraveling the counter propagating flows (see the corresponding scalogram in Fig. 1(d)). The status of such objects, sitting between self-accelerating beams and solitons, is discussed.

[1] A. Kavokin, J. J. Baumberg, G. Malpuech, and F. P. Laussy, *Microcavity*, Oxford University Press, (2011).

[2] G. Lerario *et al.* ArXiv : 1502.00602 (2015).

[3] V. Bargmann, *Ann. Math.* **59**, 1 (1954).

[4] L. Dominici *et al.* *Phys. Rev. Lett.* **113**, 226401 (2014).

[5] S.S. Demirchyan *et al.* *Phys. Rev. Lett.* **112**, 196403 (2014).

[6] D. Colas *et al.* ArXiv : 1412.4758 (2014).

Ultrafast manipulation of a double quantum-dot system based on Lyapunov technology

S. Cong¹, M.-Y. Gao¹ and G.-P. Guo²

¹School of Information Science and Technology,

University of Science and Technology of China, Hefei, 230027, China

²Key Laboratory of Quantum Information, University of Science and Technology of China,

Chinese Academy of Sciences, Hefei, 230026, China,

e-mail: scong@ustc.edu.cn

The Lyapunov control technology was used in the manipulation of a single qubit in the two-level double quantum-dot (DQD) system in order to obtain better control performance. The control process is composed of three parts: firstly, a slope pulse takes the system from a positive detuning adiabatically to the anti-crossing point, which corresponds to the resonance state of the system; then, a Lyapunov-based control pulse drives the charge qubit transfer non-adiabatically; finally, another slope pulse takes the system away from the anti-crossing point to keep the system stable. The charge state probability $P_{|L\rangle}$ and the curve of Lyapunov-based control pulse were studied under different control parameters. Simulation results showed that: the designed Lyapunov-based control pulse has a rise time $\sim 100\text{ps}$, which is in the scope of the Aglient 81134A pulse generator for implement. The maximum charge qubit probability $P_{|L\rangle}$ can reach $\sim 96\%$, and the stable probability can be $\sim 86\%$ for transition from the initial charge state $|R\rangle$ to the desired target charge state $|L\rangle$. The whole control scheme for the DQD system should be made up by the control fields:

$$f_z(t) = \begin{cases} f_{z1} = -vt & 0 \leq t < t_o \\ f_{z2} = k\lambda(t) = \varepsilon_0 & t_o \leq t < t_o + \tau \\ f_{z3} = -\varepsilon_0 + v(t - t_o - \tau) & t_o + \tau \leq t < 2t_o + \tau \end{cases}$$

where, v is the rise velocity of the ramp pulse, τ is the duration of the control field via Lyapunov-based control, and it can be obtained by the $\lambda(t) = 2\Delta(\rho_{11} - \rho_{22}) + i\hbar(\rho_{21} - \rho_{12})/dt$, when $t \in [0, t_o]$, there is $\lambda > 0$; when $t \in [t_o, t_o + \tau]$, the control field f_{z2} drives the qubit transfer, as soon as

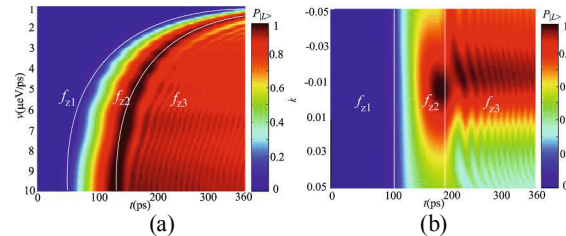


Figure 1: The varying pattern of $P_{|L\rangle}$ under v and k ; (a) for the fixed $k = 0$. (b) For the fixed $v = 4 \mu\text{eV} / \text{ps}$.

$\lambda(t_o + \tau) \leq 0$, f_{z2} finishes; the duration time from $\lambda(t) > 0$ to $\lambda(t) \leq 0$ should be $(t_o + \tau) - t_o = \tau$.

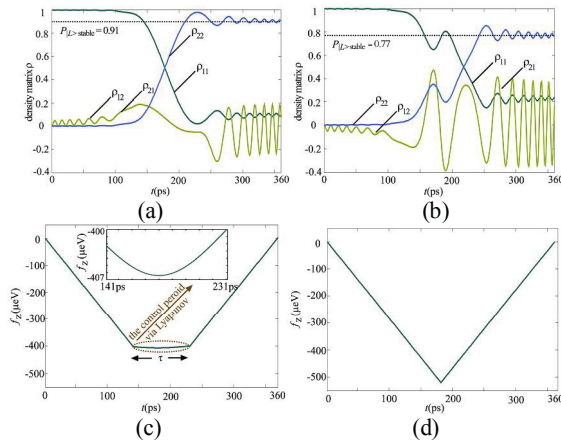


Figure 2: The charge qubit transfer properties and the curves of the control fields under two control schemes with $k = -0.01$, $v = 2.89 \mu\text{eV} / \text{ps}$; (a) and (c): The density matrix and control field under the control scheme via Lyapunov-based control. (b) and (d): The density matrix and control field under the control scheme via LZSM interference.

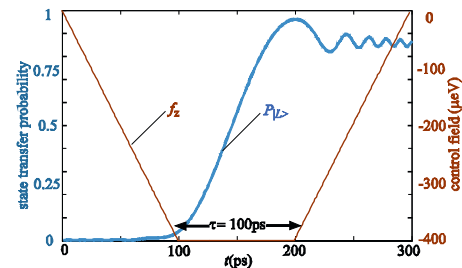


Figure 3: Illustration of the qubit transfer property and the control curve under $k = 0$ and $v = 4 \mu\text{eV} / \text{ps}$.

- [1] G. Cao, H. Li, T. Tu, L. Wang, C. Zhou, M. Xiao, G.-C. Guo, H. Jiang and G.-P. Guo, Nature Commun., 4, 1401 (2013).
- [2] J. Berezovsky, M.-H. Mikkelsen, N.-G. Stoltz, L.-A. Coldren and D.-D. Awschalom, Science, 320, 349-352 (2008).
- [3] D. Press, T.-D. Ladd, B. Zhang and Y. Yamamoto. Nature, 456, 218-221 (2008).

Spontaneous, collective coherence in driven, dissipative cavity arrays

E. del Valle¹, J. Ruiz-Rivas², C. Gies³, P. Gartner⁴ and M. J. Hartmann⁵

¹*Física Teórica de la Materia Condensada, Universidad Autónoma de Madrid, 28049 Madrid, Spain*

²*Departament d' Optica, Universitat de Valencia, Dr. Moliner 50, 46100 Burjassot, Spain*

³*Institute for Theoretical Physics, University of Bremen, 28334 Bremen, Germany*

⁴*Institute of Physics and Technology of Materials, P.O. Box MG-7, Bucharest-Magurele, Romania*

⁵*Institute of Photonics and Quantum Sciences, Heriot-Watt University, Edinburgh, EH14 4AS, U.K.*

e-mail: elena.delvalle.reboul@gmail.com

Arrays of optical or microwave cavities, each interacting strongly with a quantum emitter and mutually coupled via the exchange of photons, have been introduced as prototype setups for the study of quantum many-body physics of light. They can be experimentally realised in superconducting circuit, photonic crystal, micropillar and waveguide coupled cavities.

In this work [1], we address the question of whether a non-equilibrium superfluid phase can develop in these structures, despite dissipation, and under an incoherent pumping mechanism (see Fig. 1). In the lasing regime, we indeed find correlations between the light fields of distant cavities. Such correlations decay exponentially with distance in any dimension, with finite correlation length for any non-vanishing cavity decay rate. We also characterize the spontaneous build-up of collective coherence in the array through a series of observable features, such as the formation of an extended Mollow triplet in the PL spectrum [2].

[1] *Spontaneous, collective coherence in driven, dissipative cavity arrays*. J. Ruiz-Rivas, E. del Valle, C. Gies, P. Gartner and M. J. Hartmann, Phys. Rev. A 90, 033808 (2014).

[2] *Mollow Triplet under Incoherent Pumping*. E. del Valle and F. P. Laussy. Phys. Rev. Lett. 105, 233601 (2010).

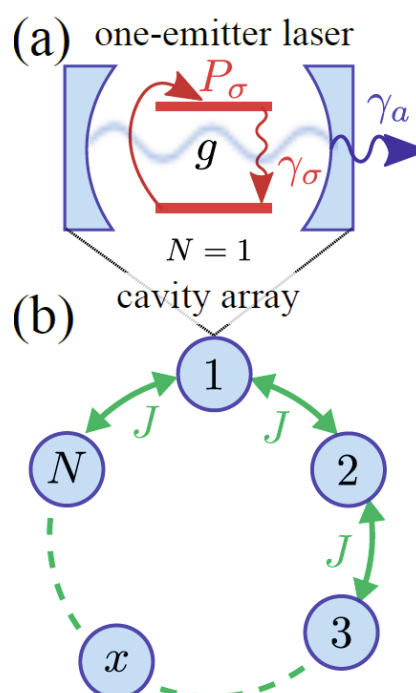


Figure 1: The system under study is an array of coupled cavities (b), each of them containing a two-level emitter (a). Both the cavity and emitter undergo dissipation. The emitter is incoherently and continuously driven.

Analytical theory of moving solitons in a fermionic superfluid

Dmitry K. Efimkin, Victor Galitski

Joint Quantum Institute and Condensed Matter Theory Center, Department of Physics, University of Maryland, College Park, Maryland, 20742-4111, USA

A fully analytical theory of a traveling soliton in a one-dimensional fermionic superfluid is developed within the framework of time-dependent self-consistent Bogoliubov-de Gennes equations, which are solved exactly in the Andreev approximation. The soliton manifests itself in a kink-like profile of the superconducting order parameter and hosts a pair of Andreev bound states in its core. They adjust to soliton's motion and play an important role in its stabilization. A phase jump across the soliton and its energy decrease with soliton's velocity and vanish at the critical velocity, corresponding to the Landau criterion, where the soliton becomes unstable. The "inertial" and "gravitational" masses of the soliton are calculated and the former is shown to be orders of magnitude larger than the latter. This results in a slow motion of the soliton in a harmonic trap, reminiscent to the observed behavior of a soliton-like texture in related experiments in cold fermion gases [1]. Furthermore, we calculate the full non-linear dispersion relation of the soliton and solve the classical equations of motion in a trap. The strong non-linearity at high velocities gives rise to anharmonic oscillatory motion of the soliton. A careful analysis of this anharmonicity may provide a means to experimentally measure the non-linear soliton spectrum in superfluids.

- [1] T. Yefsah, A. T. Sommer, M. J. H. Ku, L. W. Cheuk, W. Ji, W. Bakr, and M. W. Zwierlein, *Nature* 499, 426 (2013).
- [2] D.K. Efimkin, V. Galitski, *Phys. Rev. A* 91, 023616 (2015).



Limitations for Quantum hacking Superconducting Single-Photon Detector

M. Elezov¹, O. Ozhegov¹, Y. Kurochkin², V. Makarov³ and G. Goltsman¹

¹Moscow State Pedagogical University, 29 M.Pirogovskaya, Moscow 119435, Russia

²Russian Quantum Center, 100 Novaya St., Skolkovo, Moscow 143025, Russia

³Institute for Quantum Computing, University of Waterloo, Waterloo, Ontario N2L 3G1, Canada

e-mail: elezovms@rplab.ru

Using high-sensitivity single-photon detectors in optical telecommunication systems enables one to register signals without employment of expensive optical amplifiers, which is important for long-distance transcontinental fiber-optic communication lines. The development of single-photon detectors is the rapidly expanding interest in application of quantum optics information. Many scientists and engineers around the world have been developing and quantum-cryptographic systems. One of these features of quantum cryptography is the transmission of quantum key distribution, which, in principle, allows transmitting information being transmitted from point A (Alice) to point B (Bob) with absolute security, i.e. with the third party E (Eve) being unable to steal the information being transmitted. That can be achieved by using single photons. Their behavior is described by quantum mechanical laws. Nowadays, there are several commercial quantum-cryptographic systems with single-photon avalanche photodiodes or superconducting single-photon detectors (SSPDs). However, real systems always have shortcomings, which can be used by the third party. One of these shortcomings is bright-light control of the detector (the blinding attack) [1].

We explore bright-light control of Superconducting Single-Photon Detectors (SSPDs) with an autoreset system. In our experiment we simulate an illumination pattern the SSPDs would receive in a typical quantum-cryptographic systems under hacking attack.

In our work we use the system for registration single photons in the visible and near IR ranges. It consists of a compact low-power cold head SRDK-101D, an optimized cryostat with SSPD, compressor and control unit with the autoreset system. The operating temperature of the registration system is 2.5 K.

The SSPD with sensitive an area of $7 \times 7 \mu\text{m}^2$ has a level of dark counts of less than 10 cps, with a quantum efficiency of 14 % at 1550 nm (see Fig. 1).

In [2] was shown that it effectively blinds and controls the SSPDs.

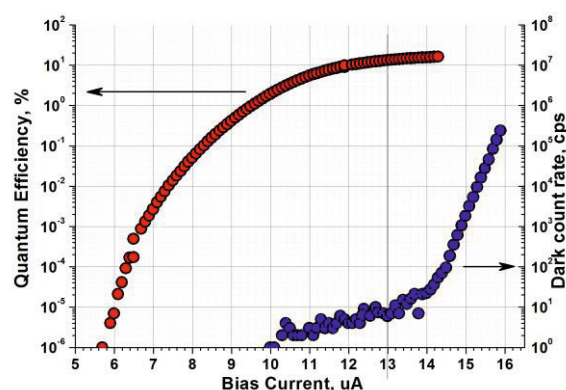


Figure 1: Quantum efficiency (red symbols) and dark count rate (blue symbols) of the SSPD at 1550 nm.

When illuminated with a bright ‘blinding’ pulse of light, the detector becomes resistive over a larger area than the single hotspot generated by single photon absorption. The mechanism of the single-photon absorption is given in [3].

We can produce several deterministic fake clicks during definite time. But if a bright “blinding” pulse serial of light is very power or very long then the detector can latch into the normal state and stops working. In order to the detector worked again, the readout should have the autoreset system. The autoreset system returns the SSPD in superconducting state. Therefore using of the autoreset system imposes limitations on the blinding attack.

Analyzing the features of the autoreset system and limitations for the blinding attack we can propose recommendations for protection a typical quantum-cryptographic systems from such an attacks.

- [1] G. Gol'tsman et al, Appl.Phys.Lett., **79**, 705 (2001).
- [2] M. Tanner, V. Makarov, R. Hadfield, Optic Express, **22**, 6 (2014).
- [3] A. Semenov, G. Gol'tsman, A. Korneev, Physica C: Superconductivity, **351**, 4 (2001).

Measurements of non-locality and phase coherence in Bose-Einstein condensates

M. Fadel¹, B. Allard¹, R. Schmied¹, J.-D. Bancal², N. Sangouard¹ and P. Treutlein¹

¹*Department of Physics, University of Basel, Klingelbergstrasse 82, Basel CH-5046, Switzerland*

²*Center for Quantum Technologies, National University of Singapore, 3 Science Drive 2, Singapore 117543*

e-mail: matteo.fadel@unibas.ch

Atomic Bose-Einstein condensates (BECs) are highly controllable isolated quantum systems with long coherence times, and offer applications in metrology and quantum information processing. We experimentally prepare two-component Rubidium-87 BECs, consisting of a few hundred atoms, on an atom-chip [1]. Using state-selective potentials to tune the collisional interactions (one-axis twisting dynamics), we prepare many-particle non-classical states [2] that we analyze by quantum state tomography.

By observing non-locality, it is possible to demonstrate that a system cannot be described by a local (classical) theory, even if the underlying local variables are hidden [3]. As a consequence, provably secure randomness can be extracted from any non-local system. We present a robust experimental technique for detecting non-locality in a two-mode BEC, and the most recent experimental results.

In finite-temperature BECs, interactions with the non-condensed fraction are predicted to limit the phase coherence [4]. We experimentally study the decoherence dynamics and its fundamental limits by performing Ramsey spectroscopy with BECs of different temperatures and densities, which are prepared by controlled shaking of the trap.

- [1] P. Böhi, et al., *Nature Physics* **5**, 592 (2009).
- [2] M.F. Riedel, et al., *Nature* **464**, 1170 (2010).
- [3] N. Brunner et al., *Rev. Mod. Phys.* **86**, 419 (2014).
- [4] A. Sinatra, Y. Castin, and E. Witkowska, *Phys. Rev. A* **80**, 033614 (2009).

Quantum key distribution protocol with floating bases and decoy states

Yu.V. Kurochkin, A.K. Fedorov, and V.L. Kurochkin

Russian Quantum Center, 100 Novaya St., Skolkovo, Moscow 143025, Russia

e-mail: yk@rqc.ru; akf@rqc.ru

Among all promising areas of quantum technologies such as high-efficient information processing and ultra-sensitive metrology, exclusively quantum key distribution (QKD) systems reach a stage of device implementation and commercialization.

Due to the fact of breaking of public-key encryption algorithms using quantum computing, QKD systems have attracted a great deal of interest. The foundation of security of public-key encryption algorithms is the complexity of several mathematical problems, *e.g.*, computing discrete logarithms (Diffie–Hellman–Merkle cryptosystem) and integer factorization (RSA cryptosystem). However, using the Shor’s algorithm, these problems are solvable in polynomial time.

Providing of a useful method for key distribution between two legal users, QKD systems change the paradigm of cryptography and restore the idea of the one-time-pad encryption. Security of a quantum key is guaranteed not by limitations of computational and technological resources of an eavesdropper, but fundamental laws: according to the no-cloning theorem, it is impossible to create an exact copy of a quantum object, and an eavesdropper cannot distinguish orthogonal states without their perturbations. Thus, QKD systems are not unbreakable, but they always allow to detect Eve.

Security of QKD systems is limited by the quantum bit error rate (QBER) and attacks on the channel. In turn, they are caused by imperfections of practical QKD systems. In practical QKD setups, weak coherent states $|\mu \exp(i\theta)\rangle$ with the mean number $\mu = 0.1-0.5$ of photons per pulse are used instead of true single photons. Since there is no reference phase, Bob and Eve have no information on the phase θ . According to the Poisson statistics, a non-negligible fraction of pulses contains more than one photon. This fact provides certain constrains for length of communication channels for QKD, which is limited by the photon number splitting (PNS) attack.

A promising approach is the decoy state protocol, in which Alice randomly sends some of laser pulses with a lower average photon number. These decoy states are used in the protocol to detect a PNS attack, because Eve has no way to verify is a pulse is signal and decoy.

Recently, a new QKD protocol with floating bases has been proposed [1]. In this approach, Alice and Bob use a previously shared auxiliary key k_0 to generate secret additional rotations $\Delta\varphi$ of BB84 bases. In

other words, for i th signal state, Alice uses k_0 and a random function to generate rotation to BB84 bases as follows:

$$\Delta\varphi_i = \chi(i, k_0) \pmod{2\pi}. \quad (1)$$

It is important that function (1) with auxiliary key k_0 generates the uniform distribution over the circle.

Thus, the crucial feature of this protocol is that it allows move away from fixed set of bases:

$$\begin{aligned} \hat{\sigma}_{y+\Delta\varphi} &\equiv \{|\uparrow + \Delta\varphi\rangle, |\rightarrow + \Delta\varphi\rangle\}, \\ \hat{\sigma}_{x+\Delta\varphi} &\equiv \{|\nearrow + \Delta\varphi\rangle, |\searrow + \Delta\varphi\rangle\} \end{aligned} \quad (2)$$

In other words, this basis can float at any position on the circle. However, for floating bases QKD protocol problems related with the PNS-attack are still a challenge.

We present an extension of the QKD protocol with floating bases [1] by combining this approach with the basic version of the decoy states protocol [2]. We suppose that Alice has, first, previously shared with Bob an initial key k_0 , which gives the uniform distribution over the circle, and, second, a random sequence k_d for choosing type of transmitted state: vacuum state with the mean number of photons μ_0 , decoy state with the mean number μ_d , and signal state the mean number μ_s ,

We provide the security analysis of the suggested protocol and discuss its realization using current experimental tools.

- [1] Y.V. Kurochkin, SPIE Proc. **5833**, 213 (2005).
- [2] W.-Y. Hwang, Phys. Rev. Lett., **91**, 057901 (2003).

Roton-maxon spectrum and local density waves in two-dimensional Bose gas of dipoles

A.K. Fedorov¹, I.L. Kurbakov², and Yu.E. Lozovik²

¹Russian Quantum Center, 100 Novaya St., Skolkovo, Moscow 143025, Russia

²Institute for Spectroscopy RAS, Fizicheskaya str., 5, Moscow Region, Troitsk 142190, Russia

Many-body systems with dipole-dipole interaction provide an interface between physics of strongly and weakly correlated quantum matter. The anisotropy and the region of attraction of the dipole-dipole interaction potential provide a set of interesting many-body phenomena. In the limit of strongly correlated system of in-plane dipoles, the ground state of the system has the chain structure; the 3D system of parallel dipoles has the chain structure as well.

Being typical for strongly correlated systems, local minimum in a non-monotonic excitation spectrum — roton-maxon character — originally observed in liquid helium appears in a weakly interacting gas. [1].

This facts itself opens fascinating prospectives for revealing of non-conventional structural properties of dipolar condensates close to the threshold of an instability. Several important achievements in exploring of phonon collapse, superfluidity, density waves, as well as supersolid phase of dipolar BEC have been reported. However, interesting phases such as supersolid state are unattainable due to the divergence of the condensate depletion at the threshold for dipoles with dipole moments polarized orthogonally to a wide layer. In this case, condensate disappears before the roton gap in the spectrum becomes zero.

In this contribution, we discuss two realizations for dipolar bosonic systems: dipolar excitons in semiconductor layers of heterostructures and tilted dipolar particles in a homogeneous quantum layer.

We predict the formation of the roton-maxon excitation spectrum and the roton instability effect for a *weakly* correlated Bose gas of dipolar excitons. According to numerical estimations, the threshold of the roton instability for Bose-Einstein condensed exciton gas with roton-maxon spectrum is achievable experimentally in GaAs semiconductor layers.

For a two-dimensional weakly interacting gas of tilted dipoles in a single homogeneous thin layer, we predict the effect of the roton instability. It is important that in contrast to a system of normal to wide layer dipoles, breaking of the rotational symmetry for a system of tilted dipoles leads to the convergence of the condensate depletion even up to the threshold of the instability, with mean-field approach being valid.

Convergence of the condensate depletion allows us to investigate local density waves at mesoscopic scales in a dilute Bose gas of tilted dipoles in a homogeneous thin layer. Local density waves manifest themselves in diagonal short-range order in one-body and

two-body density matrices and exist in the system together with Bose-Einstein condensation and superfluidity. The effect of local density waves at mesoscopic scales is sizably gained at non-zero temperature.

We discuss observation of the roton instability phenomena and local density waves in experiments with ultracold atoms and polar molecules with large dipole moment using time-of-flight imaging techniques.

- [1] L. Santos, G.V. Shlyapnikov, and M. Lewenstein, Phys. Rev. Lett. **90** 250403 (2003).
- [2] A.K. Fedorov, I.L. Kurbakov and Yu.E. Lozovik, Phys. Rev. B **90** 165430 (2014).
- [3] A.K. Fedorov, I.L. Kurbakov, Y.E. Shchadilova and Yu.E. Lozovik, Phys. Rev. A **90** 043616 (2014).

Quantum synchronization in superconducting metamaterials

M.V. Fistul^{1,2}

¹Theoretische Physik III, Ruhr-Universität Bochum, D-44801 Bochum, Germany

²National University of Science and Technology "MISIS", 119049, Moscow, Russia

e-mail: fistul@tp3.rub.de

I report a theoretical study of coherent collective quantum dynamic effects in superconducting metamaterials, i.e. an array of N qubits (two-level systems) incorporated into a low-dissipation resonant cavity (Fig. 1) [1,2]. Individual qubits are characterized by energy level differences Δ_i and a spread of Δ_i is taken into account. Non-interacting qubits display coherent quantum beatings with N different frequencies. Virtual emission and absorption of cavity photons provides a long-range interaction between qubits. Moreover, the capacitive or inductive coupling between individual qubits and a resonator determines the sign (positive or negative) of the interaction.

In the presence of such interaction we analyze quantum correlation functions of individual qubits $C_i(t)$. We show that $C_i(t)$ is determined by randomly distributed in imaginary time τ instantons and anti-instantons minimizing the effective action $S_{\text{eff}}\{\varphi_i(\tau)\}$. The quantum correlation functions display oscillations of the frequencies that, in turn, are proportional to the probability of the excitation of such instantons. If the (anti)instantons are strongly localized on single qubits, the N different frequency are obtained in the correlation functions [2]. The spread of instantons across the qubits indicates the *quantum synchronization*, i.e. the coherent quantum beatings of a few qubits on a single frequency, and determines a number of qubits showing the synchronized quantum beatings. Notice here, that the quantum synchronization in a superconducting metamaterial has been observed recently in Ref. [3].

The quantum correlation function and, therefore, the quantum synchronization effects can be directly observed, e.g. by measurements of frequency dependent transmission coefficient $D(\omega)$ of electromagnetic field propagating in a transmission line coupled to the system (Fig. 2) [2,3].

I acknowledge the financial support of the Ministry of Education and Science of the Russian Federation in

the framework of Increase Competitiveness Program of NUST "MISIS"(K2-2014-015).

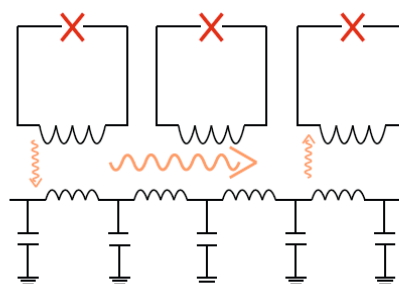


Fig.1 The schematic of an array of RF SQUIDs incorporated into a resonator. An interaction through emission (absorption) of virtual photons is shown.

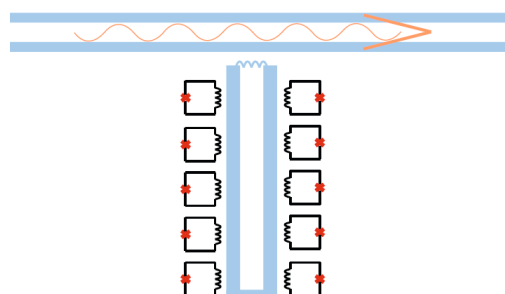


Fig.2 A schematic of the experimental setup: a low-dissipative transmission line (TL) is inductively coupled to the investigated system, i.e. array of qubits incorporated in a resonator.

[1] S. I. Mukhin and M. V. Fistul, *Supercond. Sci. Technol.*, **26**, 084003 (2013). (Focus on Superconducting Metamaterials)

[2] P. A. Volkov, and M. V. Fistul, *Phys. Rev. B*, **89**, 054507 (2014).

[3] P. Macha, G. Oelsner, J.-M. Reiner, M. Marthaler, St. André, G. Schön, U. Hübner, H.-G. Meyer, E. Il'ichev and A. V. Ustinov, *Nature Communications*, **5**, 5146 (2014).

Discrete time quantum walks on dynamically changing graphs

F. Elster¹, S. Barkhofen¹, T. Nitsche¹, J. Novotný², A. Gábris^{2,3}, I. Jex², and Ch. Silberhorn¹

¹*Applied Physics, University of Paderborn, Warburger Straße 100, 33098 Paderborn, Germany*

²*Department of Physics, Faculty of Nuclear Sciences and Physical Engineering, Czech Technical University in Prague, Břehová 7, 11519 Prague, Czech Republic*

³*Department of Theoretical Physics, University of Szeged, Tisza Lajos körút 84, 6720 Szeged, Hungary*
e-mail: gabris.aurel@fjfi.cvut.cz

Quantum simulators are advanced quantum systems that can be used to answer challenging questions about complex systems. Discrete time quantum walks are a proven and universal model [1–3] and are regarded as a promising platform for building quantum simulators[4], including localisation effects [5], topological phases [6, 7], energy transport in photosynthesis [8, 9]. Inspired by the random walk, the discrete time quantum walk (DTQW) is a particular quantum mechanical process consisting of iterative applications of a unitary operator factorising as $\hat{U} = \hat{S}\hat{C}$. The *coin operator* \hat{C} modifies the walker's internal coin state and is crucial for the non-trivial quantum dynamics, while the *shift operator* \hat{S} implements transitions across the links of the graph in dependence of the internal state.

Quantum walks on percolation structures constitute an attractive platform for studying the open system dynamics generated by random media. The percolation quantum walk [10] (PQW) model is defined on a finite set of vertices, with each step having a probabilistically chosen edge configuration κ from all possible configurations \mathcal{K} . For each graph with edge configuration κ the dynamics is defined in analogy to the DTQW with the shift operator \hat{S} modified by inserting reflection operators at the gaps, resulting in the operator \hat{S}_κ . The probabilistic choice of the configuration κ yields an open system dynamics described by the random unitary map (RUM)

$$\hat{\rho}(n) = \sum_{\kappa \in \mathcal{K}} p(\kappa, \mathbf{p}) \left(\hat{S}_\kappa \hat{C} \right) \hat{\rho}(n-1) \left(\hat{S}_\kappa \hat{C} \right)^\dagger, \quad (1)$$

of the state of the walker during one step, with $p(\kappa, \mathbf{p})$ being the probability of the configuration κ .

On our poster, we present an optical time-multiplexed implementation of percolation quantum walks on a device differing from earlier experiments by the ability of dynamical control of the underlying graph structure. Our simulator is based on the time-multiplexing technique [11]. Thus, it inherits advantageous features such as remarkable resource efficiency, excellent access to all degrees of freedom throughout the entire time evolution, and stability sustained over many consecutive measurements providing sufficient statistical ensembles. The walker is implemented by an attenuated laser pulse, and its polarization, expressed in the horizontal and vertical

basis states $|H\rangle$ and $|V\rangle$, is used as the internal coin state. Standard linear elements are used to perform various operations on the coin state. Different fibre lengths in the loop setup introduce a well defined time delay between the polarisation components, allowing the mapping of the position states to discrete time bins. To attain repeated action, similarly to the 2D quantum walk [12], we have completed the apparatus with a loop geometry that consists of two paths, albeit each used alternatively. In one of the return paths we placed a half-wave plate (HWP) to serve as the operator \hat{C} in Eq. (1), while to allow us to change the underlying graph structure in the other one we included a fast electro-optic modulator (EOM). Two round trips in the setup thus implement the unitary $\hat{U}_\kappa = \hat{S}_\kappa \hat{C}$, with $\hat{S}_\kappa = \hat{S} \hat{G}_\kappa \hat{S}$. The *graph operation* \hat{G}_κ is defined by the signal delivered to the EOM yielding full control over the structure of the graph.

We demonstrate the evolution of the percolation quantum walk on a three-site graph for six steps, revealing the intricate interplay between the internal and external degrees of freedom. Our work is a proof-of-principle experiment of a quantum walk on a dynamical percolation graph, marking a way towards complex simulation of quantum transport in random media.

- [1] D. A. Meyer, *J. Stat. Phys.*, **85**, 551 (1996)
- [2] J. Kempe, *Contemp. Phys.*, **44**, 307 (2003)
- [3] K. Manouchehri and J. Wang, *Physical Implementation of Quantum Walks*. Springer, 2014
- [4] A. M. Childs, *Commun. Math. Phys.*, **294** 581 (2009)
- [5] N. Inui, Y. Konishi, and N. Konno, *Phys. Rev. A*, **69**, 052323 (2004)
- [6] T. Kitagawa, M. Rudner, E. Berg, and E. Demler. *Phys. Rev. A*, **82**, (2010)
- [7] J. K. Asbóth, *Phys. Rev. B*, **86**, 195414 (2012)
- [8] M. Mohseni, et al., *J. Chem. Phys.*, **129**, 174106 (2008)
- [9] M. B. Plenio and S. F. Huelga, *New J. Phys.*, **10**, 113019 (2008)
- [10] B. Kollár, T. Kiss, J. Novotný, and I. Jex, *Phys. Rev. Lett.*, **108**, 230505 (2012)
- [11] A. Schreiber *et al.*, *Phys. Rev. Lett.*, **104**, 050502 (2010)
- [12] A. Schreiber *et al.*, *Science*, **336**, 55 (2012)

Raman amplification and trapping of radiation in an inhomogeneous and disordered system of cold atoms

L. Gerasimov¹, D. Kupriyanov¹, and M. D. Havey²

¹Department of Theoretical Physics, St-Petersburg State Polytechnic University, 195251, St.-Petersburg, Russia

²Department of Physics, Old Dominion University, Norfolk, VA 23529
e-mail: lndgrsmv@gmail.com

The phenomenon of the so-called random laser was predicted originally by V. Letokhov in 1968. As was shown in his seminal paper [1], if an amplifying active medium is distributed throughout another elastically scattering medium, and if the sample geometry fulfills certain threshold conditions, there is an instability point in the amplification process. The role of randomly distributed elastic scatterers in this process consists of sufficient trapping of the amplified radiation such that they serve as an effective cavity in a conventional laser scheme.

We consider a mechanism of light trapping and amplifying utilizing transitions among the hyperfine manifold of the ⁸⁵Rb D_2 -line. The atomic gas serves in a two-fold capacity, both a scattering and gain medium. We perform Monte-Carlo simulations for the combined processes. It has been proposed that this effect could be observed in a system of ultracold alkali-metal atoms prepared in a MOT; recent experimental results showing that the threshold conditions can be overcome in a system of ultracold atoms have been reported in [2].

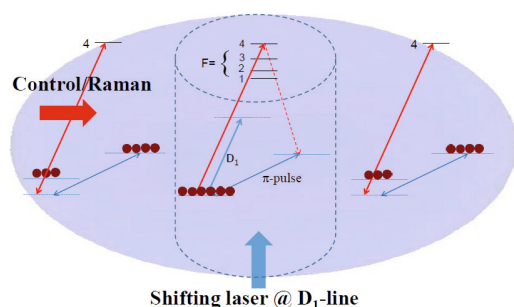


Figure 1: Excitation geometry, energy structure and transition diagram for the spatially inhomogeneous atomic system.

In Fig. 1 we show one possible experimental architecture, which implies preparation of a spatially inhomogeneous energy structure and population distribution of the hyperfine sublevels in the atomic ensemble. This can be performed via controllable light shift of only one hyperfine energy level for the atoms located in a spatially selected volume of cylindrical symmetry inside the atomic cloud. If we assumed the level $F_0 = 2$ as light shifted and organized the population inversion for all the atoms in the selected volume onto this level (for example, with a π -type microwave

pulse) then these atoms could form an active medium for photon emission. The control mode would create the photon emission on the $F = 4 \rightarrow F_0 = 3$ transition only for the atoms inside the selected volume and the interaction would be off-resonant with the control field for the other atoms of the ensemble. Then the atoms outside the active volume have the capability to trap the emitted light and play the role of a soft cavity redirecting the light into the quasi-one-dimensional propagation channel. That could lead to an instability if each spontaneously emitted photon would have a diffusion path long enough for stimulation of extra photon emission while it propagates through the channel. In such a spatially inhomogeneous configuration (when the amplification and trapping areas are spatially separated) the problem with the extra losses, related to the control mode nonlinearity, can be solved, as was indicated in [3].

Fig. 2 illustrates an experimental realization of a quasi one dimensional configuration by optical manipulation of a micron-scale optical dipole trap (FORT) containing ⁸⁷Rb atoms.

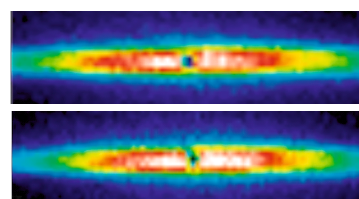


Figure 2: The upper panel illustrates absorption of a tightly focused probe beam on the $F_0 = 2 \rightarrow F = 3$ transition of ⁸⁷Rb, as measured in forward scattering. The lower panel shows the influence of a light shift laser on the process; the noticeably smaller dark spot, which shows the modified attenuation of the probe beam, is several microns in diameter.

This work was supported by RFBR Grants 15-02-01060 and 13-02-00944, by the Foundation "Dynasty" and by the External Fellowship Program of RQC.

- [1] V.S. Letokhov, Sov. Phys. JETP **26**, 1246 (1968).
- [2] Q. Baudouin *et al.*, Nature Phys. **9** 357 (2013).
- [3] L.V. Gerasimov *et al.*, Phys. Rev. A **90** 013814 (2014).

Prospects of observing the non-classicality with optical-terahertz biphoton pairs

S.A. Germanskiy, V.V. Kornienko, A.N. Tuchak, G.Kh. Kitaeva, A.N. Penin

Faculty of Physics, Lomonosov Moscow State University, 1 Leninskiye Gory, Moscow 119991, Russia

e-mail: semen.germansky@gmail.com

The spontaneous parametric down-conversion (SPDC) process is a well-known source of quantum states of light [1]. In the strongly non-degenerate regime the idler wave frequency may hit the terahertz range (0.3–10 THz). In this case the nonlinear crystal becomes a source of correlated optical-terahertz biphoton pairs. These states of light may be of considerable interest due to various problems of quantum processing and quantum communications [2,3]. These include a design of a terahertz single-photon source and generation of the optical-terahertz twin beams. The corresponding experiments for the degenerate regime of parametric conversion are well-known and are described, for example, in [4].

The study of non-classical states in the terahertz range is hampered by high terahertz absorption in the nonlinear crystals and by a considerable noise at room temperatures due to the thermal radiation [5]. However, the growth of interest may be expected to the applicability of the quantum optical methods to the terahertz wave radiation due to the design of sources with greater spectral brightness than before, such as in [6].

The possibility for observing the non-classicality in the case of optical-terahertz biphotons depends on the ratio between numbers of SPDC-generated terahertz photons and background thermal ones. The latter are distributed in accordance with the Bose-Einstein statistics at fixed temperature of thermostat. In the case of conventional quantum optics when both signal and idler wave frequencies hit optical or infrared range, the number of thermal photons is extremely small and can thus be neglected. However, in the terahertz frequency range the number of thermal photons is an important factor ($N_T \approx 6$ at $f = 1$ THz). These additional thermal photons result in the background lighting in the idler wave output channel.

Two values have been calculated as degrees of non-classicality: a normalized second-order correlation function ($g^{(2)}$) and a noise reduction factor (NRF). Due to non-zero contribution of thermal radiation, the usual equation for $g^{(2)}$ is changed. According to our results, the normalized second-order correlation function in case of strongly non-degenerate parametric converter takes the following form:

$$g^{(2)} = 1 + \frac{1}{1 + F(T)/g^{\text{PDC}}} + \frac{1}{g^{\text{PDC}} + F(T)} \quad (1)$$

Here, $g^{\text{PDC}} = |U_{11}|^2 - 1$ is the brightness of the SPDC signal radiation not taking into account the thermal fluctuations. The spectral brightness is expressed in terms of number of photons per radiation mode via the elements of the transformation matrix of the parametric process [1]. The dependence of $F(T)$ function on temperature is shown on Fig. 1. The correlation function and the noise reduction factor have been calculated for the SPDC-generated optical-terahertz biphoton fields. The prospects of experimental investigation of these states are discussed.

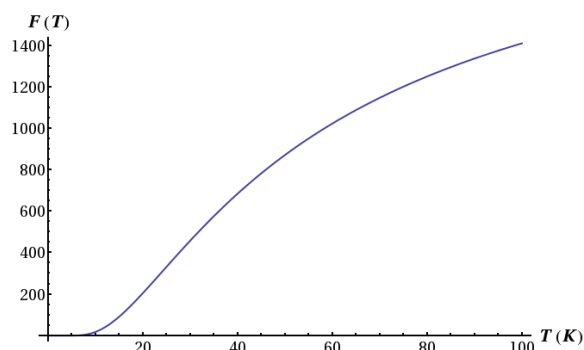


Figure 1: $F(T)$ function behavior.

- [1] D.N. Klyshko, *Photons and Nonlinear Optics* // New York: Gordon and Breach Science, 1988.
- [2] Z.-S. Yuan, X.-H. Bao, C.-Y. Lu, J. Zhang, C.-Z. Peng, J.-W. Pan, *Physics Reports* **497** (1), 1 (2010).
- [3] E. Knill, R. Laamme, G.J. Milburn, *Nature* **409**, 46–52, (2001).
- [4] M. Stobińska, F. Töppel, P. Sekatski, M.V. Chekhova, *Phys. Rev. A* **86**, 022323 (2012).
- [5] G.Kh. Kitaeva, P.V. Yakunin, V.V. Kornienko, A.N. Penin, *Appl. Phys. B* **116** (4), 929 (2014).
- [6] E.A. Cheshev, G.N. Goltsman, G.Kh. Kitaeva, A.P. Shkurinov, V.G. Tunkin et al., *Laser Phys. Lett.* **11**, 015004 (2014).

Si vertical nanowires for photonics applications

L. S. Golobokova¹, Yu. V. Nastaushev¹, N.V. Kryzhanovskaya²,

E.I. Moiseev², V.A. Seyfi¹, F.N. Dultsev¹, A.V. Latyshev¹

¹Rzhanov Institute of Semiconductor Physics Siberian Branch of Russian Academy of Sciences, 13 pr. Lavrentieva, Novosibirsk 630090, Russia

²St. Petersburg Academic University—Nanotechnology Research and Education Centre of Russian Academy of Sciences, 8 Khlopina str., Saint Petersburg 194021, Russia
e-mail: GolobokovaLS@isp.nsc.ru

Recently, semiconductor nanowires have attracted increasing attention due to their unique optical and electrical characteristics. Previously, the new mechanism to generate structural color through the silicon nanowires has been demonstrated [1, 2]. Nanowires show the vivid color generation that vary with nanowire diameter.

In this work, the optical properties of ordered arrays of silicon nanowires (Si NW) were investigated. We used Electron Beam Lithography (EBL) and dry etching to create arrays of Si NW. Si NWs with diameters ranging from 60 nm to 340 nm with heights from 200 nm to 700 nm were fabricated. The passivation of Si NWs was performed too. Si NWs were treated in boiling nitric acid. Then, Si NWs were chemically and electrically passivated through the deposition of TiON_x nanolayer at 8 nm thickness. It is worth noting that Si NW arrays (after nitric acid) exhibit similar color but lower intensity.

Scanning Electron Microscope (SEM) and Atomic Force Microscopy (AFM) were used to characterize the Si NWs. Silicon NW arrays viewed under the bright-field illumination can demonstrate the vivid color generation (Figure 1). Reflectance spectra from arrays of Si NW were measured at wavelengths ranging from 500 nm to 1150 nm. Spectra were normalized with the spectrum taken from a gold wafer. The measured reflectance spectra consist of different characteristic dip, the position of the dip varies with the diameter of NW (Figure 2). It was found visible shift in the longer wavelength region of the spectrum with increasing diameter of NW.

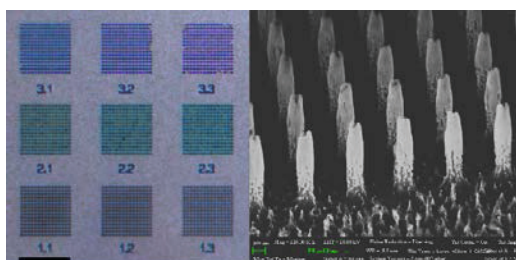


Figure 1: The bright-field (a) and SEM image (b) of NW arrays with pitch 600 nm, diameter from 250 nm (№1.1) to 150 nm (№3.3), and height 600 nm. The scale bar is 10 μ m and 100 nm.

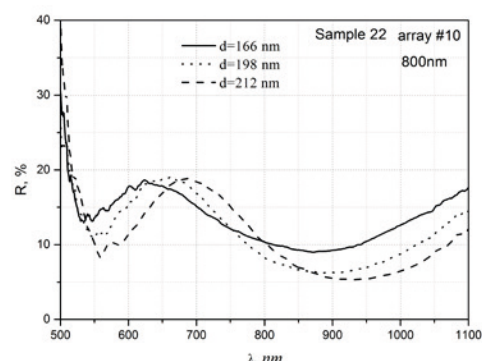


Figure 2: The reflection spectra of SiNW arrays for different diameters (800 nm pitch).

Spectral characteristics of arrays of Si vertical nanowires are simulated. The Ansoft HFSS system is used to calculate the reflectance and the absorptance of the array. The presence of an additional resonance peak in the reflectance spectrum of the Si NW was observed, and its dependence on the diameter of the NW with allowance for the substrate influence was studied.

The work was partly supported by RFBR under Project No. 13-02-01216.

- [1] Hyunsung Park, Yaping Dan, Kwanyong Seo, Young J. Yu, Peter K. Duane, Munib Wober, Kenneth B. Crozier, *Nano Lett*, **14** 1804 (2014)
- [2] Yichen Shen, Veronika Rinnerbaue, Imbert Wang, Veronika Stelmakh, John D. Joannopoulos, Marin Soljacić, *ACS Photonics*, **2** 27 (2015)
- [3] Sheng-Chieh Yang, Karola Richter and Wolf-Joachim Fischer, *Appl. Phys. Lett*, **106** 081112 (2015)
- [4] L.S. Golobokova, Yu.V. Nastaushev, F.N. Dultsev, D.V. Gulyaev, A.B. Talochkin, A.V. Latyshev, *J. Phys.: Conf. Ser.*, **541** 012074 (2014)

First investigation of the potentially clock transition in ultracold thulium atoms

A.Golovizin^{1,2,3}, E.Kalganova^{1,2,3}, D.Sukachev^{1,3}, G.Vishnyakova^{1,2,3}, D.Tregubov^{1,2,3}, S.Fedorov^{1,2,3}, A.Akimov^{1,3}, N.Kolachevsky^{1,2,3}, K.Khabarova^{1,3}, V.Sorokin^{1,3}

¹*P.N.Lebedev Physical Institute of the Russian Academy of Sciences 53, Leninskiy Prospekt, Moscow, Russia*

²*Moscow Institute of Physics and Technology, 9 Institutskiy per., Dolgoprudny, 141700, Russia*

³*Russian Quantum Center, 100 Novaya St., Skolkovo, Moscow 143025, Russia*

e-mail: artem.golovizin@gmail.com

Today the precision measurement of time and frequency is of a great importance not only for fundamental science but also for technologies that used for telecommunication networks and navigation systems. The SI second is currently realized by the microwave transition in Cs atoms with fractional uncertainty of 10^{-15} . Thanks to the frequency comb technique which established the direct link between optical and microwave frequencies, the optical clocks have attracted the interest as a future atomic clock of a superior precision. To date the optical clocks based on single ions have achieved the lowest systematic uncertainty of any frequency standard [1]. In the same time the many-atom lattice clocks have shown advantages in measurement precision even over trapped-ion clocks. The many-atom Sr clock that achieves an accuracy of 6.4×10^{-18} has been demonstrated in JILA, which is not only better than a single-ion-based clock, but also reduces the required measurement time by two orders of magnitude [2].

The fine structure of the thulium ground state $4f^{13}6s^2$ is optically coupled to a narrow (the spectral linewidth of 1.2 Hz) magnetic dipole transition at 1.14 μm . This transition is a good candidate for the optical clock realization because of two reasons. First, 4f electron is shielded by outer closed 5s and 6s shells that makes it much less sensitive to external disturbances. Second, as both levels are two components of the fine structure of ground level, they have very similar polarisabilities that should significantly cancel AC-Stark shift in optical lattice and the BBR shift.

Since 2009 our group is focused on developing of the optical lattice clock based on ultracold Tm atoms. For optical cooling the strong transition $4f^{13}(^2F_0)6s^2 - 4f^{12}(^3H_5)5d_{3/2}6s^2$ at 410.6 nm with natural linewidth $\gamma = 10$ MHz has been chosen and first magneto optical trap of thulium atoms was realised [3]. To improve MOT lifetime and reach lower temperatures needed for optical lattice loading ($\sim 1\mu\text{K}$) second stage optical cooling was implemented [4] on transition $4f^{13}(^2F_0)6s^2 - 4f^{12}(^3H_6)5d_{5/2}6s^2$ at 530.7 nm with 360 kHz linewidth.

Recently about 30% of atoms were loaded from the secondary MOT to 1D optical lattice and di-

rect optical excitation of 1.14 nm clock transition in thulium atoms has been observed by registration of atom losses in the trap vs frequency detuning of the clock laser (fig. 1). The clock laser was stabilised to

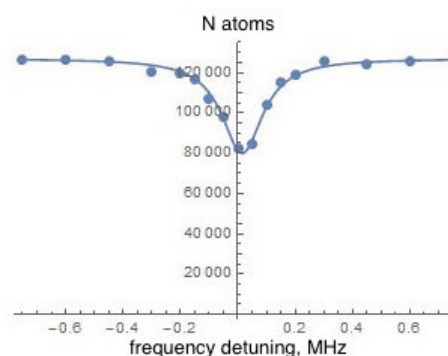


Figure 1: Number of atoms in the ground state in the optical lattice vs. frequency detuning of the clock 1.14 μm laser from the resonance.

rect optical excitation of 1.14 nm clock transition in thulium atoms has been observed by registration of atom losses in the trap vs frequency detuning of the clock laser (fig. 1). The clock laser was stabilised to the ULE cavity. The resonant frequency of the laser was measured using Angstrom WS-5 wavemeter and equals to 262.955 GHz with uncertainty 3GHz (due to the wavemeter calibration precision). The linewidth of the transition is now limited to the power and Zeeman broadening and in the order of 100 kHz.

- [1] Huntemann, N. et al. High-accuracy optical clock based on the octupole transition in $^{171}\text{Yb}^+$, Phys. Rev. Lett. 108, 090801 (2012)
- [2] B. J. Bloom, et.al. An optical lattice clock with accuracy and stability at the 10⁻¹⁸ level Nature 506, 7175 (2014)
- [3] Sukachev, D., et al. "Magneto-optical trap for thulium atoms." Physical Review A 82.1 (2010) 011405
- [4] Sukachev, Denis Dmitrievich, et al. "Secondary laser cooling and capturing of thulium atoms in traps." Quantum Electronics 44.6 (2014): 515

Laser cooling on the weak transition and optical trapping of thulium atoms

E. Kalganova^{1,2,3}, G. Vishnyakova^{1,2,3}, A. Golovisin^{1,2,3}, D. Tregubov^{1,2,3}, D. Sukachev^{1,3}, S. Fedorov^{1,2,3}, K. Khabarova^{1,3}, A. Akimov^{1,2,3}, N. Kolachevsky^{1,2,3}, , and V. Sorokin^{1,3}

¹*P. N. Lebedev Physical Institute of the Russian Academy of Sciences, 53 Leninsky prosp., Moscow 119991, Russia*

²*Moscow Institute of Physics and Technology, 9 Institutsky per., Dolgoprudny, Moscow region, 141700, Russia*

³*Russian Quantum Center, 100 Novaya St., Skolkovo, Moscow 143025, Russia*
e-mail: *kalganova.elena@gmail.com*

In recent years laser cooling of rare-earth elements has attracted close interest. This is partly because of high ground state magnetic moments of lanthanoids with the hollow inner $4f$ shell that make them attractive for study atom-atom interactions and for quantum simulation. Also, some of lanthanoids, for example, Er, Yb and Tm, are proposed to be used for optical clock applications.

Our group deals with an investigation of collisional properties of ultracold thulium atoms. Thulium magnetic moment in a ground state is $4\mu_B$ therefore it is a promising object for study dipole-dipole interaction. Furthermore, a lot of low-field Fano-Feshbach resonances are expected in an ultracold thulium gas.

The first step towards research of cold collision is a laser cooling and trapping of thulium atoms. For this purpose we use a magneto-optical trap (MOT) in a standard configuration [1]. A loading of MOT is fulfilled from an atomic beam decelerated by Zeeman slower. To obtain low temperature, a two-stage cooling process is performed.

For the first stage cooling and Zeeman slowing a strong transition at wavelength 410.6 nm is used. Its natural linewidth is 10 MHz and a corresponding Doppler limit is $T_D = 240 \mu\text{K}$. It is worth to note that Lande g -factors of lower and the upper states for this transition are very close to each other, so Sub-Doppler cooling mechanism at this transition works effectively directly in MOT. This feature allows to obtain a temperature about $25 \mu\text{K}$ during the first stage cooling by working with large detuning of cooling light [2]. However, the number of atoms in this case significantly decreases.

To achieve lower temperature without reduction of number of atoms the second-stage cooling at weak closed transition is used. A wavelength of second-stage cooling transition is 530.7 nm, a natural linewidth is 350 kHz and Doppler limit is $T_D = 9 \mu\text{K}$. A Sub-Doppler cooling mechanism also works in MOT for this transition. The dependence of an atomic cloud temperature after second-stage cooling on a detuning is shown on the figure 1.

After cooling and trapping in MOT, thulium atoms are recaptured in an optical lattice. Its confinement

potential is formed by a laser beam at wavelength 532 nm with a power up to 4 W focused into the atomic cloud. An estimated depth of the optical trap is $100 \mu\text{K}$. A temperature of atoms in MOT is much lower than the depth of an optical lattice so an efficiency of recapture is determined by spatial overlapping of MOT and optical lattice.

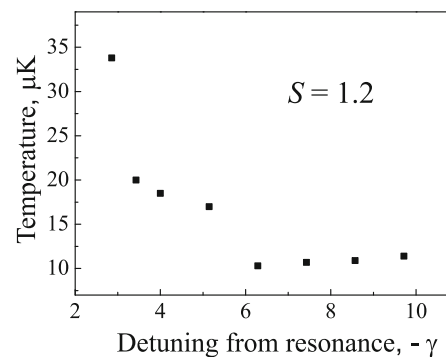


Figure 1: Temperature of atoms versus the detuning of laser beams at a value of the saturation parameter $S = 1.2$.

Thus, we obtained a cloud of thulium atoms in an optical lattice with a temperature about $10 \mu\text{K}$ and number of particles 10^5 . Now we are working on optimization of the cooling process to increase the number of atoms and to decrease the temperature of the atomic ensemble for enhancement of signal to noise ratio in a further study of thulium cold collision properties.

- [1] D. Sukachev, A. Sokolov, K. Chebakov, A. Akimov, S. Kanorsky, N. Kolachevsky and V. Sorokin, *Phys. Rev. A* **82**, 011405 (2010).
- [2] D. Sukachev, A. Sokolov, K. Chebakov, A. Akimov, N. Kolachevsky, and V. Sorokin, *JETP Letters* **92** (10), 703 (2010).

Polarisation reversal in spin-dependent polariton condensates

K. Kalinin^{1,2} and N. Berloff¹

¹Skolkovo Institute of Science and Technology, Moscow, Russia

²Moscow Institute of Physics and Technology, Moscow, Russia

e-mail: kirill.kalinin@skolkovotech.ru

My work is devoted to theoretical investigation of polariton condensates. Spin-dependent properties of multicomponent exciton-polariton condensates have been probed in a number of recent experiments where optically trapped polariton condensates were created using non-resonant excitation in a microcavity. Polariton trap was formed either with the 4 spot potential or with the ring pump by using a spatial light modulator. Since the initial short-continuous radiation was linearly polarized, the equal distributions of populations of excitons with spin-up and down in the reservoirs created, and therefore it would be reasonable to expect that the resulting polariton condensate in the trap will have a stochastic linear polarization. However, experiments carried out in the universities of Cambridge and Southampton showed the presence of a strong circular polarization of condensate – it accidentally took a left or a right circular polarization in each new realization of the experiment. My work is dedicated to theoretical substantiation of these experiments.

The theoretical model consists of a system of the coupled complex Gross-Pitaevskii equations, written in the basis of left- and right-circular polarized polariton wavefunctions (spin-up and spin-down), denoted by ψ_{\pm} (the two possible polarizations of polaritons), and the rate equation for the reservoir that represents the evolution of the exciton density:

$$i\hbar \frac{\partial \psi_{\pm}}{\partial t} = \left\{ -\frac{\hbar^2}{2m} \nabla^2 + U_0 |\psi_{\pm}|^2 + (U_0 - 2U_1) |\psi_{\mp}|^2 + \hbar g_R n_{\pm} + \frac{i\hbar}{2} (R_R n_{\pm} - \gamma_C) \right\} \psi_{\pm} + \Omega_{\parallel} \psi_{\mp}. \quad (1)$$

$$\frac{\partial n_{\pm}}{\partial t} = -(\gamma_R + \beta_1 |\psi_{\pm}|^2 + \beta_2 |\psi_{\mp}|^2) n_{\pm}(\mathbf{r}, t) + P_{\pm}(\mathbf{r}, t) \quad (2)$$

The relaxation of the density of reservoir n_{\pm} is much faster than the relaxation of the condensate, therefore we can neglect the dynamics of the reservoir and assume that it takes a stationary value. We non-dimensionalize (1), neglect the spatial variation of all parameters, and used a convenient reparametrisation:

$$\begin{cases} \psi_{\pm} = \sqrt{\rho_{\pm}} \cdot e^{i(\phi_{\pm} \pm \frac{\theta}{2})} \\ \rho = \frac{\rho_+ + \rho_-}{2} \\ z = \frac{\rho_+ - \rho_-}{2} \end{cases} \quad (3)$$

where ρ_{\pm} is the density of polaritons with spin-up and spin-down, ϕ is the global phase which doesn't

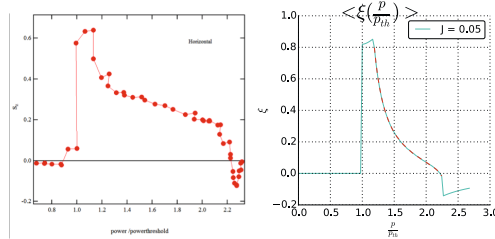


Figure 1: On the left side – experimental graph, on the right side – the result of our theoretical modelling.

have an influence on our solution due to non-resonant incoherent pump, θ is the phase difference between the polaritons of different species, ρ is the averaged density, $\xi = z/\rho$ is the polarization degree. Separating real and imaginary parts in and simplifying we are getting coupled equations for θ , ρ , and z as follows:

$$\begin{cases} \dot{\theta} = -U_{\alpha} z - \frac{g}{2}(n_+ - n_-) + \frac{Jz \cos \theta}{\sqrt{\rho - z^2}} \\ \dot{z} = \frac{R}{4}(n_+(\rho + z) - n_-(\rho - z)) - J\sqrt{\rho - z^2} \sin \theta - \frac{z}{2} \\ \dot{\rho} = \frac{R}{4}(n_+(\rho + z) + n_-(\rho - z)) - \frac{\rho}{2} \end{cases} \quad (4)$$

where

$$n_{\pm} = \frac{p_{\pm}}{\gamma + b_1(\rho \pm z) + b_2(\rho \mp z)}. \quad (5)$$

This system (4) have been further analyzed numerically and lead us to a number of interesting results. On the Figure (1) you can see that our theoretical calculations in a good agreement with experimental data. The bifurcation diagram of our model is showed below – the linear splitting J as a function of the pumping intensity p when the pumping spin discrepancy is 10% ($\eta = p_+/p_- = 1.1$).

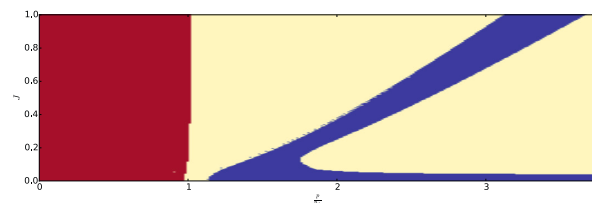


Figure 2: Bifurcation Diagram: red color is a threshold below which $R \leq 10^{-4}$; yellow color represents fixed point solutions ξ ; blue color stays for limit cycle solution's type.

Three-photon spontaneous parametric down-conversion in optical nanofiber resonators

A. Khamidullina¹, A. Kalachev^{1,2}

¹Kazan State University, 18 Kremlevskaya st., Kazan 420008, Russia

²Zavoisky Physical-Technical Institute of RAS, 10/7 Sibirsky Trakt st., Kazan 420029, Russia

e-mail: *mle.trickster@gmail.com*

The possibility of generation of three-photon correlated states (triphotons) by spontaneous parametric down-conversion (SPDC) in an optical nanofiber resonator is analyzed.

The development of sources of non-classical states of light is one of the most important tasks of modern quantum optics. In particular, the generation of three-photon entangled states (triphotons) is of special interest. Such entangled states can be used in experiments aimed to elucidate the foundations of quantum mechanics and are currently considered as a key resource in the field of multipartite quantum communications.

Using the resonator to observe nonlinear effects in the nanofibers will significantly increase spectral brightness of the source of one-photon or two-photon states of light, or reduce the length of the nanowires with the same brightness value. Controlled dispersion of nanofibers using the surrounding atoms resonant system allows you to control the spectral width of the one-photon and two-photon sources based on SPDC or spontaneous four-wave mixing (SFWM).

Among the results obtained in recent years and is most closely related to the topic of research are the following: experimental implementation of photon emission by quantum dots and NV-centers in diamond to nanofibers modes [1-4]; second and third generation of optical harmonics [5, 6]; implementation of a Fabry-Perot resonator based on nanofibers with Bragg mirrors [7, 8]. The theory of SPDC in the nanofibers (without a resonator) was developed in [9, 10], and the ability to generate entangled two-photon states one atom located near the nanofibers was analyzed in [11]. Generation of correlated photon pairs in the mode SFWM nanofibers (without a resonator) was observed in [12]. Thus developing sources of non-classical states of light based on nonlinear effects in optical nanofibers is a topic of active research.

In the present work we develop the theory of three-photon SPDC in a nanofiber forming a resonator for the interacting fields. We analyze the joint spectral amplitude of the generated three-photon states and estimate the rate of emission into specific resonator modes under expected experimental conditions. The enhancement of spectral brightness of such a three-photon source due to the resonator effect is discussed.

- [1] M. Fujiwara, et al. *Nano Lett.* **11**, 4362–4365 (2011)
- [2] T. Schroder, et al. *Opt. Express* **20**, 10490–10497 (2012)
- [3] R. Yalla, et al. *Phys. Rev. Lett.* **109**, 063602 (2012)
- [4] L. Liebermeister, et al. *Appl. Phys. Lett.* **104**, 031101 (2014)
- [5] S. Richard. *J. Opt. Soc. Am. B* **27**, 1504–1512 (2010)
- [6] A. Couillet, Ph. Grelu *Opt. Commun.* **285**, 3493–3497 (2012)
- [7] C. Wuuttke, et al. *Opt. Lett.* **37**, 1949 (2012)
- [8] F. Le Kien, et al. *J. Mod. Opt.* **59**, 274 (2012)
- [9] M. Corona, K. Garay-Palmett, A. U'Ren. *Phys. Rev. A* **84**, 033823 (2011)
- [10] M. Corona, K. Garay-Palmett, A. U'Ren. *Opt. Lett.* **36** 190 (2011)
- [11] F. Le Kien, K. Hakuta. *Phys. Rev. A* **84**, 053801 (2011)
- [12] L. Cui, et al. *Optics Lett.* **38**, 5063 (2013)

Multi-element superconducting single-photon detector

E. Khan¹, A. Divochiy², V. Seleznev², Yu. Vakhomin^{1,2}, K. Smirnov^{1,2}

¹ Moscow State Pedagogical University, 1 Malaya Pirogovskaya St., 119435, Moscow, Russian Federation

² CJSC "Superconducting nanotechnology" (Scontel), 5/22-1 Rossolimo St., 119021, Moscow, Russian Federation

e-mail: scontel@scontel.ru

Presently, the performance requirements for the characteristics of the highly sensitive near-infrared single photon detectors increase, so need to build detectors with fundamentally new properties. One of the most successful implementation of the single-photon detectors today are the superconducting single-photon detectors (SSPD) based on thin superconducting NbN film [1], that have record characteristics: maximum counting rate - $2 \times 10^9 \text{ s}^{-1}$, quantum efficiency (QE) in near IR - up to 45%, dark counts rate - 0,0001 counts/s, time resolution - 25 ps. The principle of operation of SSPD consists in suppression of superconductivity by the absorption of a photon in a NbN thin film nanostrip, that biased with transports current, which is close to the critical current (I_c). The main fields of SSPD application are various areas of spectroscopy, astronomy, biomedical researches, non-invasive diagnosis and testing of integrated circuit, quantum cryptography etc.

The scientific publications of the last years reveal that the separation of the sensitive area of SSPD into several independent areas, i.e. the creation of multi-element detectors, is a promising task, as it allows simultaneously and significantly improve several basic characteristics of SSPD - counting rate, quantum efficiency, time resolution, and to implement the detectors with the ability to resolve the number of photons in a optical pulse of radiation and the spatial position of photon absorption by the superconductor [2]. The usage of multi-element single-photon detectors, undoubtedly, is promising for infrared spectroscopy, optical communications (especially in case of extremely low photon flux) and others [3].

This paper represents the first results of the development and characterization of SSPD, that composed of 7 independent SSPD elements. We have designed two types of multi-element SSPD allowing to locate the sensitive areas of each SSPD elements most tightly, developed a technological route for multi-element SSPD, produced the first samples of multi-element SSPD. These two types of multi-element SSPD differ from each other in layout of sensitive areas that makes possible different implementations of the optical coupling. A multimode fiber can be used with the first type detectors (fig. 1 a), whose sensitive area fills the place with a diameter ~ 20 microns. The sensitive area of the second type detectors (fig. 2 b) fills the place with a diameter ~ 8 microns, that allows

the use of single-mode fiber. The sensitive area of each detector elements was made in the form of narrow ($\sim 100 \text{ nm}$) and thin ($\sim 4 \text{ nm}$) NbN strip that looks like a meander with filling factor $\sim 0,5$ (fig. 1 c, d). The square of the first type SSPD's meander is 7×7 microns², of the second type SSPD's meander is $2,5 \times 2,5$ microns². The results of measurements of critical temperature (T_c) and critical current density (j_c) showed, that all detectors in our multi-element SSPD have very similar T_c and j_c ($T_c = 10.5 - 10.8 \text{ K}$; $j_c = 2.5 - 3,4 \cdot 10^6 \text{ A/cm}^2$ at $T = 4.2 \text{ K}$). In our first measurements the QE of each detector comes to 3 % at $\lambda = 1.55 \mu\text{m}$. The slightly deviation of these values from its mean value indicates that one of the main problems in the creation of multi-element superconducting single-photon detectors - the problem of its high identity, has been successfully solved.

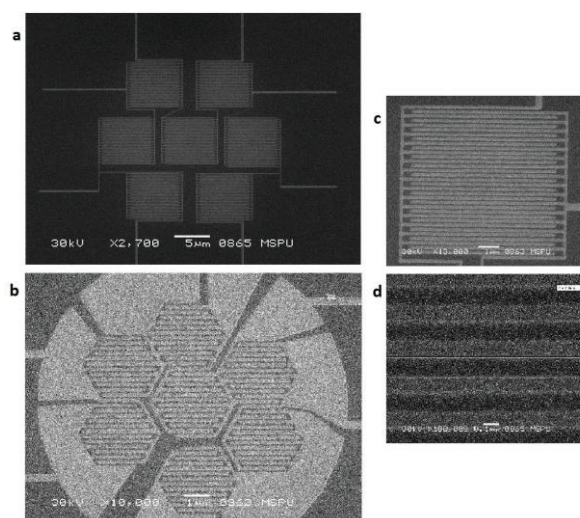


Figure 1: SEM images of (a) the first type multi-element SSPD, (b) the second type multi-element SSPD, (c), (d) sensitive area of one element of detector. Dark areas are a superconducting film, light area is area where the superconducting film was removed.

- [1] Gol'tsman G., Okunev O., Chulkova G. [et al.], *App. Phys. Lett.* **79**, 705 – 707 (2001).
- [2] Miki S., Yamashita T., Terai H. [et al.], *Physics Procedia* **36**, 77 – 81 (2012).
- [3] Verma V.B., Horansky R., Marsili F. [et al.], *App. Phys. Lett.* **104**(5), 051115 (2014).

Aharonov-Bohm effect induced by circularly polarized photons

H. Sigurdsson^{1,2}, O.V. Kibis^{3,1} and I.A. Shelykh^{1,2}

¹Division of Physics and Applied Physics, Nanyang Technological University 637371, Singapore

²Science Institute, University of Iceland, Dunhagi-3, IS-107, Reykjavik, Iceland

³Department of Applied and Theoretical Physics, Novosibirsk State Technical University, Karl Marx Avenue 20, Novosibirsk 630073, Russia

e-mail: oleg.kibis@nstu.ru

Progress in modern nanotechnologies has resulted in rapid developments in the fabrication of various mesoscopic objects, including such nanostructures as quantum rings. The fundamental interest attracted by these systems is caused by a wide variety of purely quantum-mechanical effects which can be observed in ring-like mesoscopic structures. The most notable phenomenon amongst them is the Aharonov-Bohm (AB) effect arisen from the direct influence of a vector potential on the electron phase [1]. In the ballistic regime, this effect results in magnetic-flux-dependent oscillations of the conductance in ring-like structures with a period equal to the fundamental magnetic flux quantum $\Phi_0 = h/|e|$. In the diffusive regime, a second type of conductance oscillations with the period $\Phi_0/2$ can be observed. They are known as the Altshuler-Aronov-Spivak (AAS) oscillations and are associated with the weak localization of electrons [2].

From a fundamental viewpoint, the AB-AAS oscillations arise from the broken time-reversal symmetry in the electron system (conducting mesoscopic ring) subjected to a magnetic flux through the ring. Namely, the flux breaks the equivalence of clockwise and counterclockwise electron rotations inside the ring, which results in the flux-controlled interference of electron waves corresponding to these rotations. However, the time-reversal symmetry can be broken not only by a magnetic flux but also by a circularly polarized electromagnetic field [3]. Indeed, the field breaks the symmetry since time reversal turns clockwise polarized photons into counterclockwise polarized ones and vice versa. Therefore, phenomena similar to the AB-AAS effects can take place in ring-like electronic systems strongly interacting with a circularly polarized electromagnetic field. Recently, we shown that the conductance of these electron-photon systems can exhibit oscillations which are formally equivalent to the AB-AAS oscillations induced by a magnetic flux (see Fig. 1). Periods of the optically-induced oscillations in the ballistic regime and the diffusive regime differ from each other by a factor of 2 in the same manner as periods of the oscillations induced by a magnetic flux. The discussed

phenomenon can be described in terms of an artificial $U(1)$ gauge field generated by the strong coupling between electrons and circularly polarized photons. The theory of such an optically-induced AB effect, which lies at the border between condensed-matter physics and quantum optics, will be presented in the given talk.

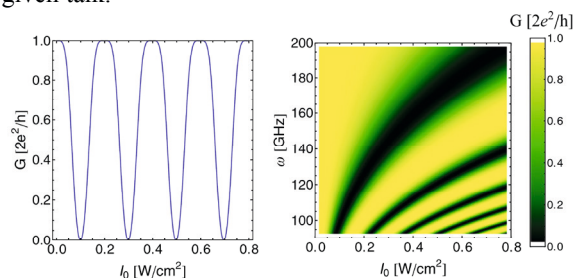


Figure 1: Conductance of a mesoscopic ring, G , under a circularly polarized electromagnetic wave as a function of wave intensity I_0 and wave frequency ω [4].

The work was partially supported by FP7 IRSES projects POLATER, POLAPHEN and QOCaN, FP7 ITN project NOTEDEV, Tier 1 project ‘‘Polaritons for novel device applications’’, RFBR projects 13-02-90600 and 15-52-05002, and the Russian Ministry of Education and Science.

- [1] Y. Aharonov and D. Bohm, *Phys. Rev.* **115**, 485 (1959).
- [2] B. L. Altshuler, A. G. Aronov, and B. Z. Spivak, *JETP Lett.* **33**, 94 (1981).
- [3] O. V. Kibis, *Phys. Rev. Lett.* **107**, 106802 (2011).
- [4] H. Sigurdsson, O. V. Kibis, I. A. Shelykh, *Phys. Rev. B* **90**, 235413 (2014).

Operating with five-level superconducting circuit as a two-qubit system

E.O. Kiktenko^{1,2}, A.K. Fedorov^{2,3}, and V.I. Man'ko⁴

¹ Geoelectromagnetic Research Center of Schmidt Institute of Physics of the Earth, Russian Academy of Sciences, Troitsk, Moscow Region 142190, Russia

² Bauman Moscow State Technical University, Moscow 105005, Russia

³ Russian Quantum Center, 100 Novaya St., Skolkovo, Moscow 143025, Russia

⁴ P. N. Lebedev Physical Institute, Russian Academy of Sciences, Moscow 119991, Russia

e-mail: evgeniy.kiktenko@gmail.com

The main building blocks for quantum computers — qubits — are usually thought to be physically independent objects such as two-level atoms, photons with polarization degree of freedom, and many others. This new generation of computational devices demonstrates a potential to outperform their classical counterparts greatly, *e.g.*, discrete logarithm, integer factorization, and in searching an unsorted database.

We report about investigation of two-qubit systems realized by noncomposite five-level anharmonic oscillator (see Fig. 1a), motivated by great experimental progress in manipulation with multilevel artificial atoms realized via superconducting circuits [1].

To encode two-qubit 4×4 density matrices, we use the following isomorphic correspondence between energy levels:

$$\begin{aligned} |0\rangle &\leftrightarrow |0\rangle_A \otimes |1\rangle_B & |1\rangle &\leftrightarrow |0\rangle_A \otimes |1\rangle_B \\ |2\rangle &\leftrightarrow |1\rangle_A \otimes |0\rangle_B & |3\rangle &\leftrightarrow |1\rangle_A \otimes |1\rangle_B \end{aligned}$$

We assume that the population of the fifth ancillary level is negligibly small.

As a tool for operating with the system we consider applying θ -pulses of rotation around x -axis of Bloch sphere related to particular pair of energy levels. It is possible due to anharmonicity of the potential, which opens a direct way to address desired transition between two levels.

We introduce a scheme for preparation of two-qubit entangled states with identical reduced density matrices as well as states with equal level of purity. We demonstrate how these states can be used for verification of entropic inequalities, related with the quantity $\log N$ with N being the dimensionality of the Hilbert space, for noncomposite systems [2].

Being unitary operators with unit determinant, sequences of θ -pulses applied only to the first four levels of the circuit allow to implement operators belonging to the $SU(4)$ group, *e.g.*, Hadamard and NOT gates, acting on particular qubits of two-qubit system.

We show that the additional fifth level in the systems allows to apply operators from $SU(5)$ group that can effectively realize two-qubit gates with matrix beyond $SU(4)$ group. Thus, the fifth level makes it possible to construct the universal set of two-qubit gates consisting of Hadamard, $\pi/8$ and CNOT gates.

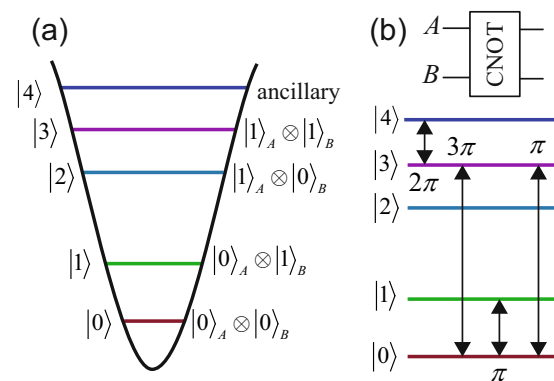


Figure 1: Quantum information processing with noncomposite quantum systems. In (a) correspondence between five level anharmonic potential and two-qubit system. In (b) implementation of CNOT gate by applying pulses of various duration to different transitions of the multi-level system

Using this universal set, we provide a blueprint for realization of the seminal two-qubit algorithm — *e.g.* Deutsch—Jozsa algorithm [3].

Such highly controllable and easily implementable setup as superconducting circuit is promising framework for implementation of many-qubit systems and investigation of computational speed-up from single qubit realization of oracle-based algorithms [4].

We thank Olga V. Man'ko and Alexey A. Strakhov for helpful comments.

- [1] J. Braumüller, J. Cramer, S. Schlör, H. Rotzinger, L. Radtke, A. Lukashenko, P. Yang, M. Marthaler, L. Guo, A.V. Ustinov, and M. Weides, *Phys. Rev. B* **91**, 054523 (2015)
- [2] E.O. Kiktenko, A.K. Fedorov, O.V. Man'ko, and V.I. Man'ko, arXiv:1411.0157.
- [3] E.O. Kiktenko, A.K. Fedorov, A.A. Strakhov, and V.I. Man'ko, arXiv:1503.01583.
- [4] Z. Gedik, arXiv:1403.5861.

Quantum walks with strong trapping

B. Kollár¹, T. Kiss¹, and I. Jex²

¹*Institute for Solid State Physics and Optics, Wigner Research Centre for Physics, Hungarian Academy of Sciences, P.O. Box 49, H-1525 Budapest, Hungary*

²*Department of Physics, Faculty of Nuclear Sciences and Physical Engineering, Czech Technical University in Prague, Břehová 7, 115 19 Praha 1 - Staré Město, Czech Republic*
e-mail: kollar.balint@wigner.mta.hu

Discrete time quantum walks (DTQWs) are non-trivial extensions of classical random walks, gaining considerable attention since their introduction [1]. The fundamental behavior of DTQWs is governed by the choice of the unitary operator acting on the internal structure of the particle — the so-called coin operator. Similarly to random walks, DTQWs can be classified based on their spreading properties. In two-dimensional DTQWs a rather interesting class of walks can be found, namely that exhibiting the effect of trapping (localization) [2]. In this class the probability of finding the particle at its initial location throughout the whole time of the evolution is non-vanishing. We post the question: Which coins exhibit trapping?

We present a large class of trapping coins, and point out some important physical consequences for the corresponding DTQWs. We investigate two-dimensional quantum walks on an infinite square lattice. The Hilbert space of the system is composite: $\mathcal{H} = \mathcal{H}_P \otimes \mathcal{H}_C$, where \mathcal{H}_P is the position space spanned by state vectors corresponding to the lattice sites, and \mathcal{H}_C is the coin space correspond to nearest neighbour step directions $|L\rangle, |D\rangle, |U\rangle, |R\rangle$. In the momentum picture a single step of the DTQW is generated by the following unitary propagator: $\tilde{U}(k, l) = \text{Diag}(e^{-ik}, e^{-il}, e^{il}, e^{ik}) \cdot C$, where C is the unitary coin operator.

The trapping effect in quantum walks appears when the quasi-energy spectrum of the walk contains flat bands. Equivalently, $\tilde{U}(k, l)$ must have at least a single constant (k, l independent) eigenvalue. We found the following broad class of coins having this trapping property:

$$C = P(\varphi)(C_1 \otimes C_2)P(-\varphi)W, \quad (1)$$

where $W = |L\rangle\langle L| + |D\rangle\langle U| + |U\rangle\langle D| + |R\rangle\langle R|$ is the swap operation, $P(\varphi) = \text{Diag}(1, 1, 1, e^{i\varphi})$ is the controlled phase gate and $C_{1(2)} \in SU(2)$. This coin class depends on 7 real parameters. Although it is possibly not the most general class, but it contains all previously known (one-parameter) cases of the trapping coins.

The DTQWs driven by the C coin class exhibit novel effects which we briefly summarize in the following. First, for a certain parameter range, the walker suffers strong trapping [3], *i.e.* all localized initial

states are trapped. This effect was not reported before. Next, the proposed coin class exhibits topological effects. With numerical methods, we found that DTQWs with two contacted bulk regions using certain pairs of C coins lead to the appearance of robust, topologically protected edge states. One can also see, that the non flat band spectrum of the walk can be matched with the spectrum of the so-called split step (alternate step) quantum walks.

Lastly, we comment on the applicability of the C -coins for the quantum walk based search. The original search algorithm [4] was defined on $M \times M$ tori and used a flip-flop Grover coin. However, this arrangement for general $N \times M$ tori turns out to be suboptimal. Our numerical tests show, that the C class of coins can achieve higher success rates on general tori in comparison with the original algorithm. In conclusion, one can possibly optimize the quantum walk based search algorithm for general tori through the C coin class.

Summarizing, the proposed C class of coins is potentially very useful: It exhibits a novel phenomena called “strong trapping”, topological effects and might be employed for the optimization of the two-dimensional quantum walk based search algorithm. The analytically given concise form of the class allows for further theoretical studies.

We acknowledge support by the Hungarian Scientific Research Fund (OTKA) under Contract Nos. K83858, NN109651 and the Hungarian Academy of Sciences (Lendület Program, LP2011-016). B. K. acknowledges the support of the Wigner conference travelling 2015/I. grant of the Director General of the Wigner Research Centre for Physics.

- [1] Y. Aharonov, L. Davidovich, N. Zagury, *Phys. Rev. A* **48**, 1687 (1993); D. A. Meyer, *J. Stat. Phys.* **85**, 551 (1996)
- [2] T. D. Mackay et al., *J. Phys. A: Math. Gen.* **35**, 2745 (2002); N. Inui, Y. Konishi, N. Konno, *Phys. Rev. A* **69**, 052323 (2004); K. Watabe et al., *Phys. Rev. A* **77**, 062331 (2008)
- [3] B. Kollár, T. Kiss and I. Jex, *Phys. Rev. A* **91**, 022308 (2015)
- [4] N. Shenvi, J. Kempe, K. B. Whaley, *Phys. Rev. A* **67**, 052307 (2003)

Waveguide integrated superconducting nanowire single-photon detector for on-chip quantum applications

V. Kovalyuk¹, O. Khal², S. Ferrari², A. Korneev^{1,3}, E. Zubkova¹, K. Teplyakova¹, G. Goltsman^{1,4},
and W. H. P. Pernice^{1,2}

¹Department of Physics, Moscow State Pedagogical University, Moscow 119992, Russia

²Institute of Nanotechnology, Karlsruhe Institute of Technology, Eggenstein-Leopoldshafen 76344, Germany

³Moscow Institute of Physics and Technology (State University), Moscow 141700, Russia

⁴National Research University Higher School of Economics, 20 Myasnitskaya str., Moscow 101000, Russia
e-mail: conference@icqt.org

Nanophotonic circuits allow for realizing complex optical functionality on a chip and enable the assembly of functional devices with many optical components in a scalable fashion. One of the main components of such circuits is a fast and efficient single-photon detector. Here we continue our study a new approach of integrating superconducting nanowire single-photon detector (SSPD) with a nanophotonic circuit [1,2]. The main idea of this approach is to increase the effective interaction length due to evanescent mode coupling of a SSPD with optical radiation inside waveguide.

We use silicon nitride (Si_3N_4) as a waveguide material. Such waveguides provide low optical absorption in the infrared and visible wavelength region, good mechanical properties as well as compatibility with a superconducting niobium nitride film deposition process. Furthermore, silicon nitride offers both high nonlinearity of the third order (Kerr effect), and the second order nonlinearity (nonlinear effect of the surface), which can be used to create single-photon sources.

The ultrathin 4 nm NbN film was deposited on a substrate with several functional layers: $\text{Si}/\text{SiO}_2/\text{Si}_3\text{N}_4$ ($350\mu\text{m}/2.6\mu\text{m}/0.45\mu\text{m}$) by reactive magnetron sputtering in an argon and nitrogen atmosphere. For fabrication of Au-contact pads, W-shaped nanowire and a rib nanophotonic waveguide we used three steps of electron beam lithography.

In Fig. 1. shown SEM image of a fabricated nanophotonic structure with NbN nanowire atop. For input/output light in/out nanophotonic device we use focusing grating couplers with coupling efficiency up to 20% at telecommunication wavelength 1550nm. We use the AttoCube system for precision alignment such couplers with an fiber array at liquid-helium temperatures.

In Fig. 2. shown measured dependence of the on-chip detection efficiency (OCDE) (blue) and dark counts rate (black) vs normalized bias current for fabricated W-shaped NbN nanowire at 1.75K. Also we found jitter of a fabricated device less than 50 ps.

Such devices are promising for use in both classical and quantum optical technologies, including characterization of quantum emitters, optical time

domain reflectometry, quantum key distribution and other tasks, where several key requirements have to be met simultaneously: compact design, high quantum efficiency, broad spectral range, low dark counts rate and high timing resolution.

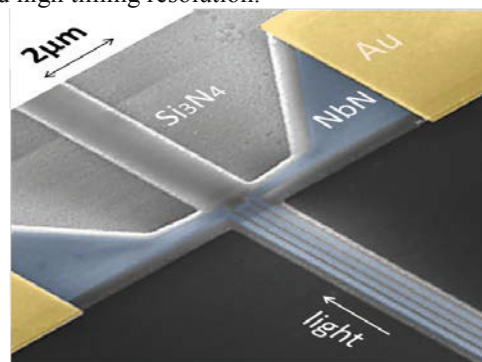


Figure 1: SEM image of a U-shaped NbN nanowire atop of a Si_3N_4 nanophotonic waveguide in false colors.

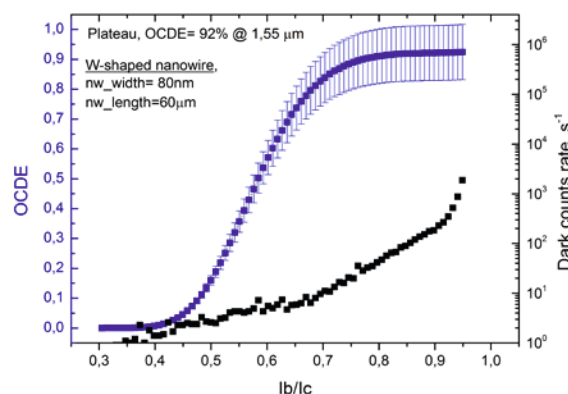


Figure 2: Measured dependence of on-chip detection efficiency (OCDE) (blue) and dark counts rate (black) vs normalized bias current.

- W. Pernice, C. Schuck, O. Minaeva, M. Li, G. N. Goltsman, A. V. Sergienko, H. X. Tang, Nature Comm. **3**, 1325 (2012).
- V. Kovalyuk, W. Hartmann, O. Kahl, N. Kaurova, A. Korneev, G. Goltsman, W. H. P. Pernice, Opt.Express **21**(19), 22683-22692 (2013)

Ion-Beam Implanted Erbium Spin-Ensemble in Y_2SiO_5

Nadezhda Kukharchyk¹, Sebastian Probst², Shovon Pal¹, Kangwei Xia³, Roman Kolesov³,

Arne Ludwig¹, Alexey V. Ustinov², Pavel Bushev⁴ and Andreas D. Wieck¹

¹Angewandte Festkörperphysik, Ruhr-Universität Bochum, 44780 Bochum, Germany

²Physikalisches Institut, Karlsruhe Institute of Technology, 76128 Karlsruhe, Germany

³Physikalisches Institut, Universität Stuttgart, 70569 Stuttgart, Germany

⁴Experimentalphysik, Universität des Saarlandes, 66123 Saarbrücken, Germany

e-mail: nadezhda.kukharchyk@ruhr-uni-bochum.de

Rare earth doped solids are attractive due to long optical and spin coherence times of the 4f-electrons. In particular, Erbium doped Yttrium Orthosilicate (Y_2SiO_5 , YSO) is interesting due to paramagnetic properties, low symmetry oxygen-rich structure and low nuclear spin-bath environment of the substrate, which allows a prospective reversible and coherent quantum media-conversion between optical C-band at $1.54 \mu\text{m}$ and microwave frequencies.

Recently, we demonstrated first experiments on luminescence [1] and magnetic coupling [2] of selectively implanted Erbium ions in YSO. In this work, we show the influence of implantation and post-implantation treatment parameters on the resulting optical properties of the implanted ions. Measured parameters are compared to those of a doped as-grown crystal.

Erbium ions are implanted (fig. 1 (a)) in a focused ion beam machine with an energy of 300 keV under high-vacuum conditions with varied substrate temperature during the implantation (300 K and 600 K) and annealed in different atmospheres.

Micro-photoluminescence (micro-PL) picture of four implanted patterns is demonstrated in fig. 1 (b). Spectra of the implanted samples are similar independently on the implanted fluence. Thus, the observed consistency in the optical spectra proves high reproducibility of the procedure, which however includes small differences in ion-phonon interaction strength and local ion surrounding as compared to the doped as-grown sample.

At room temperature, all emission lines follow the Lorentzian shape - which is a result of phonon broadening. At low temperature of 4 K, shorter wavelength lines have pure Gaussian shape, which for the longer wavelength lines broadens and is dominated by the Lorentzian. At 4 K, only eight transition lines are observed in the $^4S_{3/2} \rightarrow ^4I_{15/2}$ multiplet. The extracted linewidths of these lines are plotted on the wavelength in fig. 1 (c). Interestingly, linewidths in the spectra of the implanted sample (filled symbols) are smaller than in the doped as-grown (hollow symbols). This is possible mainly due to smaller isotopic broadening as only ^{166}Er isotope with zero nuclear spin is implanted.

PL intensity per ion is found to decrease with increase of the fluence. Similar behaviour was observed

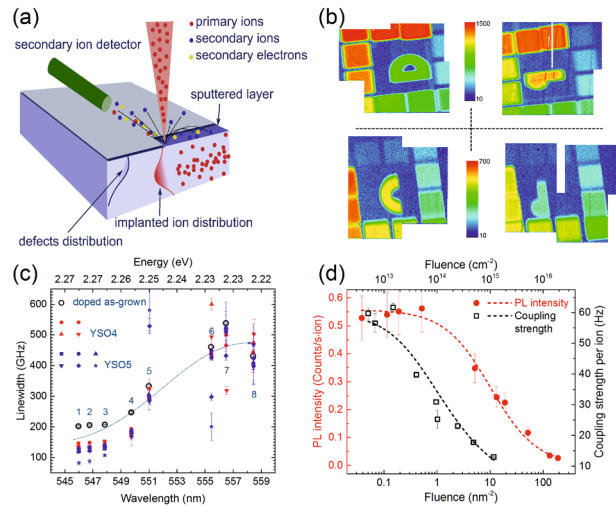


Figure 1: (a) Illustration of the implantation process. (b) Micro-PL picture of the implanted patterns with markers in the middle. (c) Dependence of the linewidth of $^4S_{3/2} \rightarrow ^4I_{15/2}$ transitions on the wavelength at 4 K. (d) Intensity and coupling strength as function of the fluence, fit with RET-expected dependence.

in the coupling strength [2]. This is believed due to non-radiative resonance energy transfer (RET) between the Erbium ions. The RET influence can be described with the dependence

$$I = \frac{I_0}{1 + C_I \times F} \quad \text{and} \quad g = \frac{g_0}{\sqrt{1 + C_g \times F}}, \quad (1)$$

where C in the RET constant and F is the fluence. Results of the fit are demonstrated in fig. 1 (d). Both equations nicely describe experimental data. Thus we may conclude, RET has a strong impact on the properties of the ion responses at the fluence above 10^{14} cm^{-2} , which is also true for the doped as-grown crystals. With this, our work paves the way towards the local integration of Erbium spins in superconducting quantum circuits.

[1] N. Kukharchyk et al., Phys. Status Solidi RRL **8**, 880 (2014).

[2] S. Probst et al., Appl. Phys. Lett. **105**, 162404 (2014).

Control of polar molecules by Rydberg atoms

E.Kuznetsova^{1,2}, **S.T.Rittenhouse**³, **H.R. Sadeghpour**⁴, **S.F. Yelin**^{4,5,6}

¹*Institute of Applied Physics, 46 Ulyanov Street, Nizhny Novgorod, 603950, Russia*

²*Russian Quantum Center, 100 Novaya St., Skolkovo, Moscow 143025, Russia*

³*Western Washington University, 516 High Street, Bellingham, WA 9822, USA*

⁴*ITAMP, Harvard-Smithsonian Center for Astrophysics, 60 Garden Street, Cambridge, MA 02138, USA*

⁵*Department of Physics, Harvard University, Cambridge, MA 02138, USA*

⁶*Department of Physics, University of Connecticut, Storrs, CT 06269, USA*

e-mail: lena.kuznetsova@gmail.com

Ultracold polar molecules became an active research topic in recent years, promising applications in quantum computation and quantum simulation, ultracold chemistry and precision measurements [1]. Exciting new directions can be explored with ultracold molecules placed in optical lattices such as simulation of quantum magnetism phenomena [2]. Many of these applications require reading out molecular rotational states, which usually cannot be done using resonant fluorescence similar to atoms due to the lack of closed (cycling) molecular transitions. The readout of rotational states is currently realized via destructive resonance enhanced multiphoton ionization (REMPI) or in the case of alkali dimers by converting the molecule back into a pair of atoms followed by readout of atomic states. We propose and analyze a non-destructive method to read out populations of rotational states using molecule's interaction with a neutral atom in a highly excited Rydberg state. An atom and a polar molecule interact via a charge-dipole interaction $V_{ch-dip} = \vec{d}(\vec{R} - \vec{r}) / |\vec{R} - \vec{r}|^3$, where \vec{d} is the molecular permanent dipole moment, \vec{R} is the distance between the atomic core and the molecule, and \vec{r} is the distance between the Rydberg electron and the core. The charge-dipole interaction shifts the energies of states of a combined atom-molecule system, and the shift depends on the rotational state of the molecule. In this way it is possible to read out molecular populations by exciting the nearby atom to the Rydberg state and measuring its shift [3]. As an example, the shift of the 90s state of Rb interacting with a RbCs molecule is shown in Fig.1a for two rotational states $|J=0, m=0\rangle$ and $|J=1, m=0\rangle$ as a function of the atom-molecule distance. This technique can also be applied to read out collective molecular rotational states. In studies of strongly interacting many-body quantum systems using polar molecules in optical lattices they are transferred into a superposition of ground and first excited rotational states $\alpha|J=0\rangle + \beta|J=1\rangle$, and interact via dipole-dipole interaction producing at the end a collective entangled state

$$\sum_{J_1, J_2, \dots, J_N=0,1} \alpha_{J_1, J_2, \dots, J_N} |J_1, J_2, \dots, J_N\rangle. \quad \text{Readout of}$$

populations $|\alpha_{J_1, J_2, \dots, J_N}|^2$ of the collective rotational states can be realized using the charge-dipole interaction of the molecular array with a single Rydberg atom, as shown in Fig.1b. If the wavefunction of the Rydberg electron overlaps with the whole molecular array the shifts of the states $|\psi_{Rydb}\rangle |J_1, J_2, \dots, J_N\rangle$ of the combined atom-molecule system will be in general different, allowing to read out the populations of the collective states by exciting the atom to the Rydberg state.

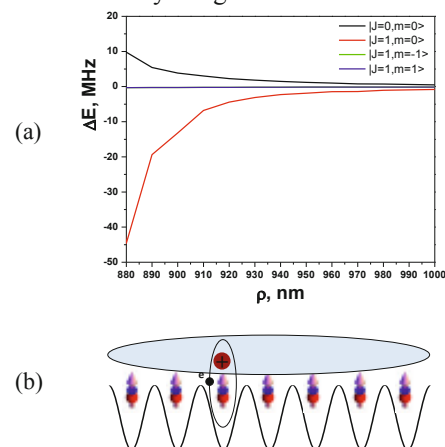


Figure 1: (a) Shifts of the atom-molecule states $|ns\rangle |J, m\rangle$ for Rb $n=90$ and RbCs with $J=0, m_j=0$ and $J=1, m_j=0, \pm 1$; (b) Schematic of the setup, which allows to readout populations of collective molecular rotational states by exciting the atom to a Rydberg state.

- [1] G. Quemener, P.S. Julienne, Chem. Rev. **112**, 4949 (2012).
- [2] M.L. Wall, K.R.A. Hazzard, A.M. Rey, arxiv:1406.4758.
- [3] S.T. Rittenhouse, H.R. Sadeghpour, Phys. Rev. Lett. **104**, 243002 (2010); E. Kuznetsova, S.T. Rittenhouse, H.R. Sadeghpour, S.F. Yelin, Phys. Chem. Chem. Phys. **13**, 17115 (2011).

Generation and detection of robust entanglement between two different mechanical resonators in cavity optomechanics

Jie Li¹, I. Moaddel Haghghi¹, N. Malossi¹, S. Zippilli¹, and D. Vitali¹

¹*School of Science and Technology, Physics Division, University of Camerino, via Madonna delle Carceri, 9, I-62032 Camerino (MC), Italy*

e-mail: jieli6677@hotmail.com; li.jie@unicam.it

We investigate a scheme for generating a continuous variable entangled state of two mechanical resonators with different frequencies. We employ an optomechanical system in which an optical cavity mode driven by a suitably chosen two-tone field is coupled to the two resonators. The scheme is robust with respect to temperature, and for a specific set of parameters it is equivalent to an optomechanical version of the Sørensen-Mølmer scheme for entangling trapped ions.

[6] P. Marian, T. A. Marian, and H. Scutaru, *Phys. Rev. A* 68, 062309 (2003).

[7] J. Eisert, Ph.D. thesis, University of Potsdam, (2001); M.B. Plenio, *Phys. Rev. Lett.* 95, 090503 (2005).

[8] G. J. Milburn, arXiv:quant-ph/9908037.

[9] A. Sørensen and K. Mølmer, *Phys. Rev. A* 62, 022311 (2000).

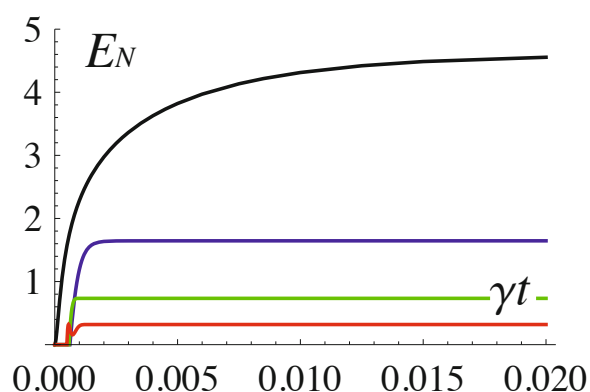


Figure 1: Time evolution of the logarithmic negativity EN starting from an initial uncorrelated state with the optical mode fluctuations in the vacuum state and each MR in its thermal state with mean phonon number: i) $n_1 = n_2 = 0$, $G_1 = 0.995 G_2$ (black line); ii) $n_1 = 100$, $n_2 = 200$, $G_1 = 0.918 G_2$ (blue line); iii) $n_1 = 500$, $n_2 = 1000$, $G_1 = 0.82 G_2$ (green line); $n_1 = 1000$, $n_2 = 2000$, $G_1 = 0.75 G_2$ (red line); the other parameters are $\gamma = 10 \text{ s}^{-1}$, $k = 105 \text{ s}^{-1}$, $G_2 = 105 \text{ s}^{-1}$, $\Delta = 103 \text{ s}^{-1}$.

References:

- [1] Y-D. Wang and A. A. Clerk, *Phys. Rev. Lett.* 108, 153603 (2012).
 [2] M. C. Kuzyk, S. J. van Enk, and H. Wang, *Phys. Rev. A* 88 062341 (2013).
 [3] L. Tian, *Phys. Rev. Lett.* 108, 153604 (2012).
 [4] H. Tan, G. Li, and P. Meystre, *Phys. Rev. A* 87, 033829 (2013).
 [5] M. J. Woolley and A. A. Clerk, *Phys. Rev. A* 89, 063805 (2014).

A new spectroscopic technique with quantum light

C. López Carreño,¹ C. Sánchez Muñoz,¹ E. del Valle¹ and F.P Laussy.^{1,2}

¹*Departamento de Física Teórica de la Materia Condensada and Condensed Matter Physics Center (IFIMAC), Universidad Autónoma de Madrid, E-28049, Spain*

²*Russian Quantum Center, Novaya 100, 143025 Skolkovo, Moscow Region, Russia*
e-mail: *fabrice.laussy@gmail.com*

We introduce “*Mollow spectroscopy*”, a theoretical concept for a new spectroscopic technique that consists in scanning the output of resonance fluorescence onto an optical target to be characterized.

The Mollow triplet [1, 2] is the emission of a two-level system (atom, quantum dot, etc.) when strongly driven by a laser. Dressing of the $|ground\rangle$ and $|excited\rangle$ states of the emitter by the N photons from the laser, results in a splitting $|+\rangle_N$ and $|-\rangle_N$. Transitions by spontaneous emission between these new states from a manifold to that below ($\nu = 1$) result in a triplet with a ratio 1:2 as two transitions of the four combinations are almost degenerate:

$$|+\rangle_N \rightarrow |+\rangle_{N-\nu} \quad (1)$$

$$|+\rangle_N \rightarrow |-\rangle_{N-\nu} \quad (2)$$

$$|-\rangle_N \rightarrow |+\rangle_{N-\nu} \quad (3)$$

$$|-\rangle_N \rightarrow |-\rangle_{N-\nu} \quad (4)$$

The correlations of the photons from these peaks but also from any spectral window of the spectrum are rich and span from strong antibunching to extremely bunched, even though the emitter itself is a single-photon source. Indeed, transitions between every other manifold by “leapfrog processes” jumping over an intermediate manifold, result in a *two-photon Mollow triplet*, with $\nu = 2$ in Eqs. (1–4) [3]. Frequencies of such photons are spread all over the spectrum and embed strong quantum correlations [4, 5]. Such a two-photon correlation spectrum has been recently comprehensively mapped experimentally [6].

Our technique relies thus on the variety of different quantum light straightforwardly available in the output of the Mollow triplet, that can be scanned over the target to probe its response to all types of input, from single-photon light to super-bunched, strongly-correlated photon pairs. Even weak nonlinearities damped in strongly radiative respond strongly to at least some of this quantum input. Indeed, the spectral window that provides with high probability two-photon simultaneously, optimizes the nonlinearity, rather than taking chances with Poisson fluctuations from a coherent source. The effect can furthermore be measured absolutely thanks to the symmetric lineshape of the Mollow triplet that probes interacting polaritons with the same statistics but different energies. Making the pairwise difference of these cases, very small nonlinearities, otherwise hiding in the radiative broadening, can then be observed and quan-

tified:

$$\Delta(\omega) = g^{(2)}(\omega) - g^{(2)}(-\omega) \quad (5)$$

While quantum effects become weaker when increasing the classical drive [7], our effect becomes stronger when increasing the laser intensity, which is a “healthy” and sound property for experimental applications.

We illustrate our technique to the case of microcavity polaritons [8], with a proposal to measure the α_1 and α_2 constants [9] of particles with the same/opposite sign of spin. Further applications are discussed.

- [1] Mollow, B. R. Power spectrum of light scattered by two-level systems. *Phys. Rev.* **188**, 1969 (1969).
- [2] del Valle, E. & Laussy, F. P. Mollow triplet under incoherent pumping. *Phys. Rev. Lett.* **105**, 233601 (2010).
- [3] del Valle, E., Gonzalez-Tudela, A., Laussy, F. P., Tejedor, C. & Hartmann, M. J. Theory of frequency-filtered and time-resolved n -photon correlations. *Phys. Rev. Lett.* **109**, 183601 (2012).
- [4] Sanchez Muñoz, C., del Valle, E., Tejedor, C. & Laussy, F. Violation of classical inequalities by photon frequency filtering. *Phys. Rev. A* **90**, 052111 (2014).
- [5] Sánchez Muñoz, C., González-Tudela, A., del Valle, E., Tejedor, C. & Laussy, F. Photon bundles: a new type of light. Poster contribution to this conference.
- [6] Peiris, M. *et al.* Two-color photon correlations of the light scattered by a quantum dot. *arXiv:1501.00898* (2015).
- [7] Verger, A., Ciuti, C. & Carusotto, I. Polariton quantum blockade in a photonic dot. *Phys. Rev. B* **73**, 193306 (2006).
- [8] Kavokin, A., Baumberg, J. J., Malpuech, G. & Laussy, F. P. *Microcavities* (Oxford University Press, 2011), 2 edn.
- [9] Kavokin, K. *et al.* Linear polarisation inversion: A signature of Coulomb scattering of cavity polaritons with opposite spins. *Phys. Stat. Sol. C* **2**, 763 (2005).

Exciton-plasmon interaction in hybrid metal-semiconductor structures with proximal InAs/AlGaAs QDs and bowtie antennas

A.A. Lyamkina^{1,2}, K. Schraml³, S.P. Moshchenko¹, A.I. Toropov¹, J.J. Finley³, M. Kaniber³

¹A.V. Rzhanov Institute of Semiconductor Physics SB RAS, Lavrentieva, 13, Novosibirsk 630090, Russia

²Russian Quantum Center, 100 Novaya St., Skolkovo, Moscow 143025, Russia

³Walter Schottky Institut and Physik Department, Technische Universität München, Am Coulombwall 4, Garching 85748, Germany

e-mail: lyamkina@isp.nsc.ru

Interaction between plasmon modes in metal nanoparticles and quantum emitters like quantum dots (QDs) is of great interest for nanophotonics and quantum optics due to local field enhancement that may lead to shortening of the life-time and increasing the emitter efficiency. Exciton-plasmon interaction is especially important for solid-state QD systems that can be used for next generation optical devices.

In this work structures with proximal InAs/AlGaAs QDs (distance to surface of 8 nm) grown in Stranski-Krastanov mode were studied. On the structure surface a periodical array of gold bowtie antennas was formed by electron lithography. Bowtie parameters were chosen to provide a spectral overlap of plasmon resonance and QD emission band [1]. Bowtie triangle size of 100 nm and the gap of 5 nm were verified by scanning electron microscopy (SEM) measurements. Microphotoluminescence (micro-PL) measurements were conducted with the excitation laser wavelength of 850 nm. As self-assembled QDs are randomly distributed, the part of QDs that strongly interact with antennas is low. On the map of integral intensity of micro-PL of $15 \times 15 \mu\text{m}$ three QDs with an optical signal that exceeds average by an order of magnitude were observed. Laser reflection scan demonstrates a periodic structure with parameters corresponding to SEM image of antennas. The correlation of positions of high intensity QDs with maximums of laser reflection indicates that QDs are located directly under nanoantennas. Detection of mutual position of a QD and an antenna provides a new insight into the investigation of exciton-plasmon interaction that was obtained for proximal QDs and self-assembled indium clusters [2].

Micro-PL spectra were measured for different polarizations in the detection channel relative to bowtie main axis. In Fig. 1 spectra of a QD with high intensity are shown that were measured in co-polarization and cross-polarization that are parallel and perpendicular to the bowtie axis respectively. It can be seen that the maximum PL intensity for these polarizations differs by a factor of 5. The inset shows detailed polarization dependences of integral PL intensity for the QD in Fig. 1 and a reference QD that is located

out of the bowtie field. The proximity to a bowtie antenna dramatically changes the QD emission pattern from an isotropic one to a dipole pattern with the degree of polarization of 70%.

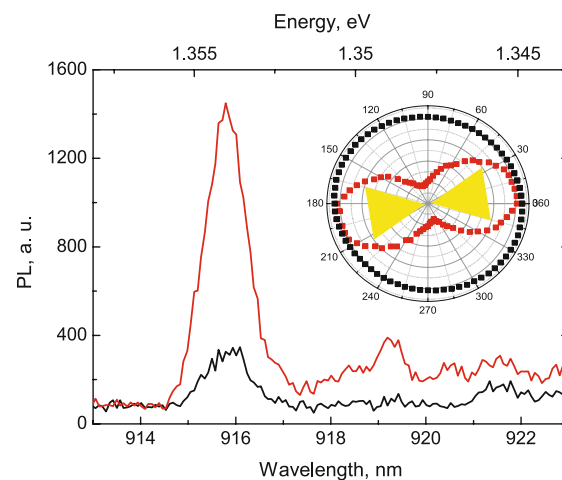


Figure 1: Micro-PL spectra for a QD with high signal measured in co-polarization (red) and cross-polarization (black). The inset shows polarization dependence for the interacting QD (red) and a reference QD (black).

The micro-PL dynamics reveals a decrease of the exciton life-time for the QDs interacting with antennas by a factor of 3 that was limited by the setup resolution. Therefore the increase of micro-PL intensity, strong polarization dependence and the decrease of the life-time confirm that there is strong exciton-plasmon interaction between proximal QDs and nanoantennas. The obtained results open the door to the control over emitter properties in hybrid metal-semiconductor nanostructures.

The work was supported by RFBR via grant 13-02-00959. AAL acknowledges the financial support via RF president scholarship (SP-805.2013.3).

- [1] K. Schraml, M. Spiegl, M. Kammerlocher, G. Bracher, J. Bartl, T. Campbell, J. J. Finley, and M. Kaniber, *Phys. Rev. B* **90**, 035435 (2014)
- [2] A.A. Lyamkina, S.P. Moshchenko, D.V. Dmitriev, A.I. Toropov, T.S. Shamirzaev, *JETP Letters*, **99(4)**, 219 (2014).

Large spatial superpositions of nanoparticles immersed in superfluid helium

O. Lychkovskiy¹

¹*Russian Quantum Center, 100 Novaya St., Skolkovo, Moscow 143025, Russia*
e-mail: o.lychkovskiy@rqc.ru

There is an ongoing activity in performing interference experiments with massive nanoscale objects [1]. The goal of this activity is to test superposition principle which lies in the heart of quantum theory but resists incorporating it in a fundamental theory of gravity. An interference of molecules with the mass of 10^4 amu on an optical grating with the period of 266 nm has been demonstrated [2]. The next goal is to push the mass of interfering objects by one or two orders of magnitude [1].

To observe interference of large massive objects one needs to diminish parasitical decoherence due to interaction with the environment. A conventional way do manage this is to perform experiments in sufficiently high vacuum. For example, in the record-breaking experiments [2] the pressure was less than 10^{-8} mbar. Increasing the mass (and, hence, the size) of the interfering particles will require progressively better vacuum.

The goal of this presentation is to demonstrate that vacuum is not the only low-decoherence medium: Superfluid helium can be a viable alternative. Indeed, as long as an object immersed in a pure superfluid at zero temperature moves with a velocity less than the critical one, it does not create, absorb or scatter any excitations of the superfluid. Consequently, in this idealized situations the decoherence is absent, despite the fact that the object is surrounded by dense medium. In reality the decoherence emerges due to scattering on the ^3He atoms which inevitably contaminate the superfluid ^4He , as well as due to interactions with thermal excitations of the superfluid. We estimate the contributions of various sources of decoherence and find that the collisional decoherence due to ^3He is the dominant source in the experimentally relevant conditions.

Consider e.g. a nanosphere of radius 10 nm and mass 10^6 immersed in superfluid ^4He at temperature 1 mK. We estimate a decoherence rate for a superposition with spatial separation of 100 nm (this is usually determined by grating period). A method to purify ^4He up to a relative concentration better than $5 \cdot 10^{-13}$ is well established, the latter figure reflecting the lack of technique to measure small concentration of ^3He rather than the ultimate concentration [3]. Assuming a concentration of 10^{-13} , we find the rate of decoherence due to scattering on the ^3He impurities to be $\lesssim 1\text{s}^{-1}$. This is enough to perform an interference experiment. Decoherence rate due to interaction

with thermal excitations of the superfluid is several orders of magnitude lower.

While the robustness of large spatial superpositions of objects surrounded by dense medium is remarkable in its own right, performing matter-wave interferometry in superfluid helium can provide some advantages compared to conventional schemes relying on high vacuum. First, cooling a nanoparticle to mK temperatures necessary for producing an interference pattern can require sophisticated techniques in vacuum but is seamless in superfluid helium. Second, almost complete compensation of gravity force is often desirable in interference experiments, which can be accomplished in superfluid helium with the use of buoyancy force.

- [1] M. Arndt and K. Hornberger, *Nature Physics* **10**, 271 (2014).
- [2] S. Gerlich, S. Eibenberger, M. Tomandl, S. Nimmrichter, K. Hornberger, P. J. Fagan, J. Tuxen, M. Mayor, and M. Arndt, *Nature Communications* **2**, 263 (2011).
- [3] P. Hendry and P. V. McClintock, *Cryogenics* **27**, 131 (1987).

Coherent controlization using superconducting qubits

Nicolai Friis¹, Alexey A. Melnikov¹, Gerhard Kirchmair^{2,3}, and Hans J. Briegel¹

¹*Institute for Theoretical Physics, University of Innsbruck, Technikerstraße 21a, 6020 Innsbruck, Austria*

²*Institute for Quantum Optics and Quantum Information,*

Austrian Academy of Sciences, Technikerstraße 21a, 6020 Innsbruck, Austria

³*Institute for Experimental Physics, University of Innsbruck, Technikerstraße 25, 6020 Innsbruck, Austria*

e-mail: alexey.melnikov@uibk.ac.at

Extended Abstract. Coherent controlization is a process by which a priori unspecified (or “unknown”) operations on subsystems are coherently conditioned on the state of a control qubit [1]. This is of great significance for black box subroutines in quantum computation [2]. In addition, such processes play a pivotal role in the flexible construction of the quantum-enhanced deliberation of learning agents [3] in the context of the projective simulation model for artificial intelligence [4, 5].

The practical realization of coherent controlization requires access to an auxiliary system in addition to the control and target qubits. However, the details of the implementation depend on the nature of the ancilla system and the type of qubit used. Here, the system under consideration is a register of superconducting transmon qubits coupled to an auxiliary microwave resonator, similar to the setups in [6, 7]. For this setup, we propose a method that allows coherent controlization by using unconditional displacements of the cavity mode and qubit operations conditioned on the resonator state. We present explicit protocols for 2 and 3-qubits and we discuss the scalability of our proposal. In particular, the performance of the protocol under the influence of the cavity self-Kerr effect is analyzed. This effect arises from the coupling of the qubits and the resonator. For one qubit, the system is described by the Hamiltonian

$$H/\hbar = \omega_r a^\dagger a + \omega_q b^\dagger b - \chi_{qr}/2 (a^\dagger a b^\dagger b) - \chi_{rr}/2 (a^\dagger a)^2 - \chi_{qq}/2 (b^\dagger b)^2, \quad (1)$$

where a and b are the dressed mode operators of the resonator and the qubit, respectively, ω_r and ω_q are their frequencies, χ_{qr} is the coupling between them and χ_{rr} , χ_{qq} are the anharmonicities. The cavity is used for applying the entangling gates between two superconducting qubits. In order to apply an arbitrary unspecified 2-qubit operation, as illustrated in Fig. 1(a), we use unconditional single-qubit rotations (blue box in Fig. 1), unconditional cavity displacements (white rectangles in Fig. 1(b)) and single-qubit operations conditioned on the state of the cavity (green and orange boxes in Fig. 1). The waiting times Δt in Fig. 1(b) specify the times between the applied operations. The dynamics of the quantum state during these periods is governed by the free evolution under the Hamiltonian in Eq. (1).

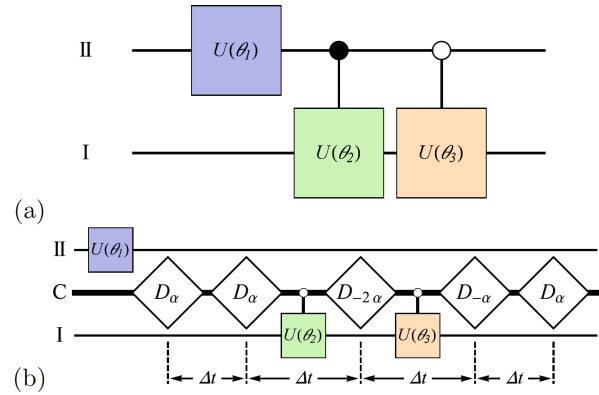


Figure 1: Two-qubit probability unitaries implementation.

The 2-qubit scheme can be extended to more qubits via a nesting procedure [3], as we show in detail for the case of three qubits.

- [1] N. Friis, V. Dunjko, W. Dür, and H. J. Briegel, *Phys. Rev. A*, **89**(3), 030303 (2014).
- [2] M. Araújo, A. Feix, F. Costa, and Č. Brukner, *New J. Phys.* **16**, 093026 (2014).
- [3] V. Dunjko, N. Friis, and H. J. Briegel, *New J. Phys.*, **17**, 023006 (2015).
- [4] H. J. Briegel and G. De las Cuevas, *Scientific reports* **2** (2012).
- [5] G. D. Paparo, V. Dunjko, A. Makmal, M. A. Martin-Delgado and H. J. Briegel, *Phys. Rev. X* **4**, 031002 (2014).
- [6] Z. Leghtas, G. Kirchmair, B. Vlastakis, M. H. Devoret, R. J. Schoelkopf and M. Mirrahimi, *Phys. Rev. A* **87**(4), 042315 (2013).
- [7] B. Vlastakis, G. Kirchmair, Z. Leghtas, S. E. Nigg, L. Frunzio, S. M. Girvin, M. Mirrahimi, M. H. Devoret and R. J. Schoelkopf, *Science* **342**, 6158 (2013).

Polarization orientation influence on filamentation in non-axis-symmetrical focusing

A.A Ionin¹, D.V. Mokrousova^{1,2}, L.V. Seleznev¹, D.V. Sinityn¹, E.S. Sunchugasheva^{1,2}, N.P. Fokina^{1,2}

¹*P.N. Lebedev Physical Institute of RAS, 53 Leninsky prospekt, Moscow 119991, Russia*

²*Moscow Institute of Physics and Technology, 9 Institutsky per., Dolgoprudny, Moscow region 141700, Russia*

e-mail: daria.mokrousova@yandex.ru

Propagation of a femtosecond laser pulse with overcritical power through transparent medium results in beam self-focusing and plasma channels formation – process of filamentation [1]. The distinction in self-focusing and filamentation of linear-polarized and circular-polarized pulses were investigated both theoretically and experimentally [2-5]. Nevertheless in the most of the papers axis-symmetrical optical schemes were used. The aim of this research is to experimentally find out the influence of polarization orientation of linear-polarized femtosecond laser pulse on the filamentation and plasma channel formation with non-axis-symmetrical focusing (different NA in horizontal and vertical planes).

Experiment was carried out by using a Ti-sapphire laser system. Laser pulses of 100 fs pulse duration (FWHM) at the wavelength of 744 nm were used. The beam was focused to the gap between cylindrical electrodes. When the laser pulse went through the electrodes gap, its capacity was changed by arising laser plasma and voltage corresponding to the capacitor recharge current was measured by an oscilloscope. Thereby this voltage is proportional to the linear density of the plasma channel.

In the first experiment strong astigmatism (incidence angle 22.5°) was introduced by a concave mirror with 50 cm focal length. The polarization plane was horizontal or vertical. Pulse energy was 1.2mJ. The results (fig. 1) show strong dependence of the polarization orientation in the foci on plasma density.

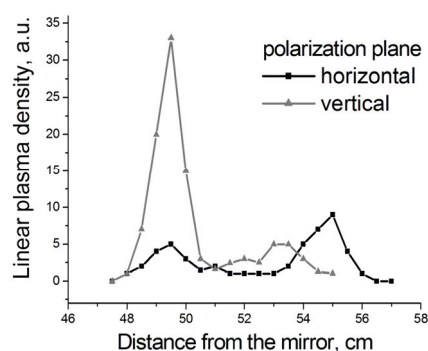


Figure 1: Plasma distribution with wavefront astigmatism

In the second experiment the beam (diameter 6 mm) passed through the slit (width 1.5 mm) was focused by lens with 50 cm focal length. The slit was parallel or perpendicular to the polarization plane of the laser pulse. The pulse energy measured right after the slit was 0.6mJ. The results are shown on figure 2. The peak linear plasma density changed almost twice with turn the slit orientation.

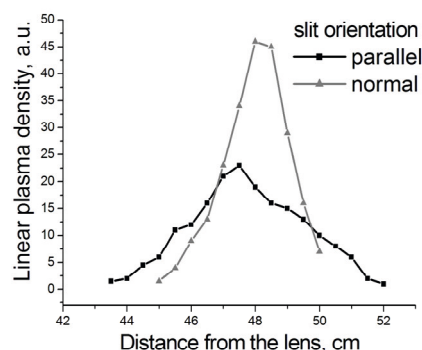


Figure 2: Plasma distribution with the slit

Thus the strong influence of polarization orientation on the filamentation and plasma channel formation in two different non-axis-symmetrical optical schemes was showed experimentally.

- [1] V.P. Kandidov, S.A. Shlenov, O.G. Kosareva. *Quantum Electronics* **39**, 205 (2009)
- [2] D.H. Close, C.R. Giuliano, R.W. Hellwarth, L.D. Hess, F.J. McClung, W.G. Wagner. *IEEE Journal of Quantum Electronics*, **2**(9), 553 (1966)
- [3] C.C. Wang. *Physical Review* **152**, 149 (1966)
- [4] S. Petit, A. Talebpour, A. Proulx, S.L. Chin. *Optics Communications*, **175**(4-6), 323 (2000)
- [5] N.A. Panov, O.G. Kosareva, A.B. Savel'ev-Trofimov, D.S. Urupina, I.A. Perezgogin, V.A. Makarov. *Quantum Electronics* **41**(2), 160 (2011)

Radiative dynamics in spatially resolved two-atom cavity QED

A. Neuzner¹, M. Körber¹, O. Morin¹, S. Ritter¹ and G. Rempe¹

¹Max Planck Institut für Quantenoptik, Hans-Kopfermann-Strasse 1, 85748 Garching, Germany
e-mail: andreas.neuzner@mpq.mpg.de

Surrounding optical emitters with an optical resonator has become a well-established technique to study the interaction of matter with a single mode of the lightfield well protected against the environment. Resonant enhancement of the electric field by the cavity strengthens light-matter interaction and ultimately, in the so-called strong-coupling regime, the field generated by a single photon suffices to saturate a single atom. Experimentally, the strong-coupling regime has been reached for a single atom $N = 1$ embedded in an optical resonator by several groups[1]. A variety of effects when exciting the system with $n \leq 1$ and nonlinear effects with $n > 1$ photons were demonstrated. Experiments with more than a single atom typically work in a regime of large ensembles $N \gg 1$ and weak excitation $n \ll 1$. Here fluctuations in the atom number are tolerable as the relevant dynamics depends only weakly on the actual number of atoms and the weakly excited ensemble in many cases can be regarded as a single superatom with \sqrt{N} collectively enhanced coupling strength.

The intermediate regime of mesoscopic ensembles that combines the high degree of control over individual emitters with interactions mediated by the common cavity mode remains an experimentally largely unexplored territory. Here the dynamics depend on the exact number of atoms and their positions. Applications of such a system range from the investigation of fundamental quantum optical effects[2] to the implementation of quantum information protocols that use the shared cavity mode to generate effective interactions between the atomic qubits[3].

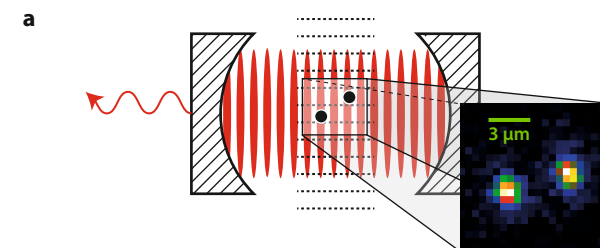


Figure 1: Sketch of the experimental apparatus together with an example picture of a trapped atom pair.

Here, we report on the preparation of a well-known number of ^{87}Rb atoms pinned with a deep two-dimensional optical lattice within an optical cavity. During optical cooling close to the mechanical groundstate of the lattice, emitted fluorescence light is collected via a high numerical aperture objective and used to image the atoms. The achieved optical resolution is sufficient for single-site detection of the atoms. The system is applied to study several aspects of the dynamics of light-matter interaction in the resonator as a function of the spatial arrangement of the atoms, which is deduced from the images.

- [1] A. Reiserer and G. Rempe, arXiv:1412.2889
- [2] S. Fernández-Vidal, S. Zippilli, G. Morigi, PRA **76**, 053829 (2007)
- [3] M. Kastoryano, F. Reiter, A. Sørensen, PRL **106**, 090502 (2011)

Enhanced thermoelectric coupling near electronic phase transition: The rôle of fluctuation Cooper pairs

H. Ouerdane^{1,2}, A. A. Varlamov^{1,3}, A. V. Kavokin^{1,3}, C. Goupil¹, and C. B. Vining⁴

¹Russian Quantum Center, 100 Novaya Street, Skolkovo, Moscow Region 143025, Russia

²Laboratoire Interdisciplinaire des Energies de Demain (LIED) UMR 8236 Université Paris Diderot
CNRS, 4 Rue Elsa Morante, 75013 Paris France

³CNR-SPIN, Viale del Politecnico 1, I-00133, Rome, Italy

⁴ZT Services 1685 H Street, #872, Blaine, WA USA 98230

e-mail: h.ouerdane@rqc.ru

Research in thermoelectricity is widely recognised as a strategic activity in view of the critical problems related to electrical power production and storage, considering that thermoelectric devices may be designed for specific purposes involving powers over a range spanning ten orders of magnitude: typically from microwatts to several kilowatts. Potential applications are varied and include, e.g., biomedical devices, generators, coolers in microelectronics, and wireless sensors. However, as of yet, due to low conversion efficiency, thermoelectric systems mostly find applications as generators and heat pumps in contexts where reliability and sustainability are more important than cost. Colossal efforts are devoted to the breaking of the glass ceiling over performance, but the low thermoelectric conversion efficiency still precludes wide-scale applications, and in terms of performance of actual devices, we are still in the range of what became standard 30 years ago.

The objective of our work is to identify areas where genuine and significant progress is yet to be made, and to stimulate experimental research in the proposed direction. We meet this objective thanks to a rigorous theoretical analysis of the very essence of thermoelectric systems: their electronic working fluid. The corner stone of our approach is the observation that: *i/* heat engines are particularly efficient when their operation involves a phase transition of their working fluid; *ii/* thermoelectric transport is essentially a convective process and convection may be enhanced in the vicinity of a phase transition. The key point is thus to see how to characterize the thermoelastic properties of the electronic working fluid and its capacity for enhanced convective transport.

This we did with the introduction and computation of specific thermoelastic coefficients of various charged systems, including Bose and Fermi gases, and fluctuation Cooper pairs [1]. Combination of these coefficients yields the definition of the thermodynamic figure of merit, the divergence of which at finite temperature (see Fig. 1) indicates that conditions are fulfilled for the best possible use of the thermoelectric working fluid. The meaning of the thermodynamic figure of merit is physically transparent: it is related to the compressibility of the considered

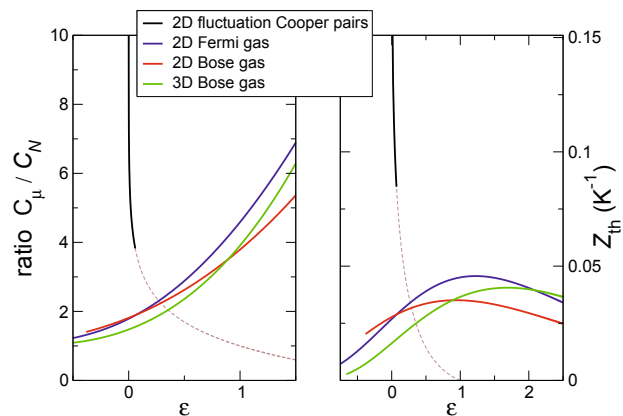


Figure 1: Thermoelectric heat capacity ratio C_μ/C_N and thermodynamic figure of merit Z_{th} as functions of $\epsilon = \ln T/T_c$ for various systems.

fluid and to the Prandtl number. As a matter of fact, this latter characteristic number in fluid dynamics provides a direct link between the thermodynamic properties of the fluid and its capacity for convective transport. Our analysis [2] shows that fluctuation Cooper pairs are particularly suited as a working fluid, while the other illustrative cases of charged Bose and Fermi gases boast no drastically enhanced thermoelectric coupling. In our work we also considered quatron-polaritons [3], which would be a promising novel system as the coupling of electric charges to light could yield a strong enhancement of the thermoelectric coupling above the low temperature range.

- [1] A. Larkin and A. Varlamov, *Theory of Fluctuations in Superconductors*, revised edition, (Oxford Science publications, 2009).
- [2] H. Ouerdane, A. A. Varlamov, A. V. Kavokin, C. Goupil, and C. B. Vining, *Enhanced thermoelectric coupling near electronic phase transition: the rôle of fluctuation Cooper pairs*, arXiv:1412.8641.
- [3] A. Kavokin, D. Solnyshkov, and G. Malpuech, *Quatron-polaritons: charged quasi-particles having the bosonic statistics*. J. Phys. Condens. Matter. **19**, 295212 (2007).

Quasiprobability distributions in the stochastic wavefunction methods

Evgeny A. Polyakov¹, Pavel N. Vorontsov-Velyaminov¹

¹*Faculty of Physics, St. Petersburg State University, St. Petersburg 198504, Russia*

e-mail: *e.a.polyakov@gmail.com*

In our recently published work [1], we investigate the quasiprobability distributions which emerge in the stochastic wavefunction method of Carusotto *et al* [2]. We show that there are actually two types of quasiprobabilities. The first one, the ‘diagonal Hartree-Fock state projection’ representation, is useful in representing the initial conditions for stochastic simulation in the most compact form. It defines antinormally ordered expansion of the density operator and normally ordered mapping of the observables to be averaged. We completely characterize the equivalence classes of this phase space representation. The second quasiprobability distribution, the ‘non-diagonal Hartree-Fock state projection’ representation, extends the first one in order to achieve stochastic representation of the quantum dynamics. We demonstrate how the differential identities of the stochastic ansatz generate the automorphisms of this phase space representation. These automorphisms turn the stochastic representation into a gauge theory. We describe the general form of the gauge transformations and rederive all the stochastic methods which are based on the single orbital Hartree-Fock dyadic ansatz [3, 4].

This work is supported by the Russian Foundation for Basic Research (Grant No. 14-02-31109) and by the program of grants for postdocs of Saint Petersburg State University (Grant No. 11.50.1573.2013).

- [1] Evgeny A. Polyakov and Pavel N. Vorontsov-Velyaminov, Phys. Rev. A **91**, 042107 (2015).
- [2] I. Carusotto, Y. Castin, and J. Dalibard, Phys. Rev. Lett. **63**, 023606 (2001).
- [3] D. Lacroix, Ann. Phys. **322**, 2055 (2007).
- [4] D. Lacroix and S. Ayik, Eur. Phys. J. A **50**, 95 (2014).



Thulium as new atom for quantum simulators

S. Pyatchenkov¹, S. Snigirev^{1,2}, I. Kozhokaru¹, A. Horoshilov¹, D. Sukachev^{1,2}, A. Akimov^{1,2}.

¹*Russian Quantum Center, Skolkovo, Moscow Region, Novaya, 100*

²*P.N. Lebedev Institute*

e-mail: pjatchenkov@gmail.com

Quantum simulators permit the study of quantum systems that are difficult to study in the laboratory or analyze theoretically. In this instance, simulators are special purpose devices, which are designed to provide insight about specific physics problems. Most often, the basis of quantum simulators is ensemble of cold atoms loaded in optical lattice. The choice of cold atoms is due to unique combination flexibility and controllability. Optical potentials are relatively easy to form, interactions between atoms could be tuned both on side and with neighbor, artificial field could be created [1]. One of the examples of such control is control of atomic interactions via Feshbach resonances, which enabled observation of BCS-BEC crossover [2,3].

We are suggesting new species as a platform for quantum simulation. Thulium atom have several benefits that make it a good candidate for applications in ultracold physics. As a lanthanide it has a vacancy on the f shell providing large orbital moment in the ground state, which is expected to led to large number of Feshbach resonance even at low magnetic field, similar to other lanthanides [4] but providing better control due to simpler level structure. More over, Tm provides relatively large magnetic momentum in the ground state enabling substantial dipole - dipole interactions even in optical lattice. Moreover, as Tm atom has a full S shell, its ground state is shielded leading to narrow "clock" transition that makes it promising for metrology.

In this talk I would present our experimental results towards achieving BEC of Tm atom studding its collisional properties as a first step toward future quantum simulations.

References:

- [1] M. Georgescu, S. Ashhab, Franco Nori: Quantum simulation, Reviews of modern physics, volume 86, January 2014.
- [2] Wolfgang Ketterle, Nobel Lecture: When atoms behave as waves: Bose-Einstein Condensation and the atom laser. December 8, 2001.
- [3] Regal, C. A., M. Greiner, and D. S. Jin, Phys. Rev. Lett. 92, 040403, 2004.
- [4] Frisch, M. Mark, K. Aikawa, F. Ferlaino, J. L. Bohn, C. Makrides, A. Petrov, S. Kotochigova Quantum Chaos in Ultracold Collisions of Erbium, Nature 507 475 (2014-03-27)

Photon bundles: a new type of light

C. Sánchez Muñoz¹, A. González-Tudela², E. del Valle¹, C. Tejedor¹ and F.P. Laussy^{1,3}

¹Departamento de Física Teórica de la Materia Condensada and Condensed Matter Physics Center (IFIMAC), Universidad Autónoma de Madrid, E-28049, Spain

²Max-Planck-Institut für Quantenoptik, Hans-Kopfermann-Strasse 1, 85748 Garching, Germany,

³Russian Quantum Center, Novaya 100, 143025 Skolkovo, Moscow Region, Russia

e-mail: carlossmwolf@uam.es

Recent theoretical works [1, 2] have evidenced how a family of physical processes giving rise to strong correlations is revealed by retaining the energy degree of freedom in the usual second-order correlation function. The resulting maps of frequency-frequency correlation –the *two-photon spectra* (2PS)–display rich landscapes of correlations that are washed out when disregarding the energies and are not featured in the normal, single-photon spectrum.

One of the most fundamental systems in quantum optics is represented by a two level system (2LS) under coherent driving. In this configuration, the correlations emerging in the frequency-frequency domain have been demonstrated to violate both Cauchy-Schwarz and Bell inequalities [3], and very recently these predictions have been experimentally demonstrated with outstanding agreement [4]. This experiment confirms our theoretically predicted [2, 3] two-photon *leapfrog* emission processes, including their properties in terms of energy, statistics and quantum correlation (degree of violation of classical inequalities). These processes are featured as three antidiagonal lines in the 2PS (see Fig. 1)

In this contribution we show how these correlations can be harvested in a cavity QED device providing a source that releases all of its energy exclusively in groups, or *bundles*, of N -photons [5]. The underlying principle relies on the Purcell enhancement of strongly correlated photons belonging to a leapfrog process. The fundamental relationship between energy E and frequency ν is then given by an effectively renormalized Planck's constant $E = N\hbar\nu$, which has momentous medical applications, allowing to penetrate tissues with increased depth and accuracy with no harm to the body. The replacement of the photon by a “bundle” leads to the emergence of a new physics that requires its own set of tools and concepts. Photon statistics, which is at the heart of quantum optics, needs to be redefined, as one has to consider now bundle statistics to recover fundamental concepts such as coherence and behaviours such as antibunching.

- [1] E. del Valle, A. Gonzalez-Tudela, F. P. Laussy, C. Tejedor, M. J. Hartmann, *Phys. Rev. Lett.* **109**, 183601, (2012).
- [2] A. Gonzalez-Tudela, F. P. Laussy, C. Tejedor, M. J Hartmann, E. del Valle, *New J. Phys.* **15**, 033036, (2013)
- [3] C. Sánchez Muñoz, E. del Valle, C. Tejedor, F. P. Laussy, *Phys. Rev. A* **90**, 052111 (2014)

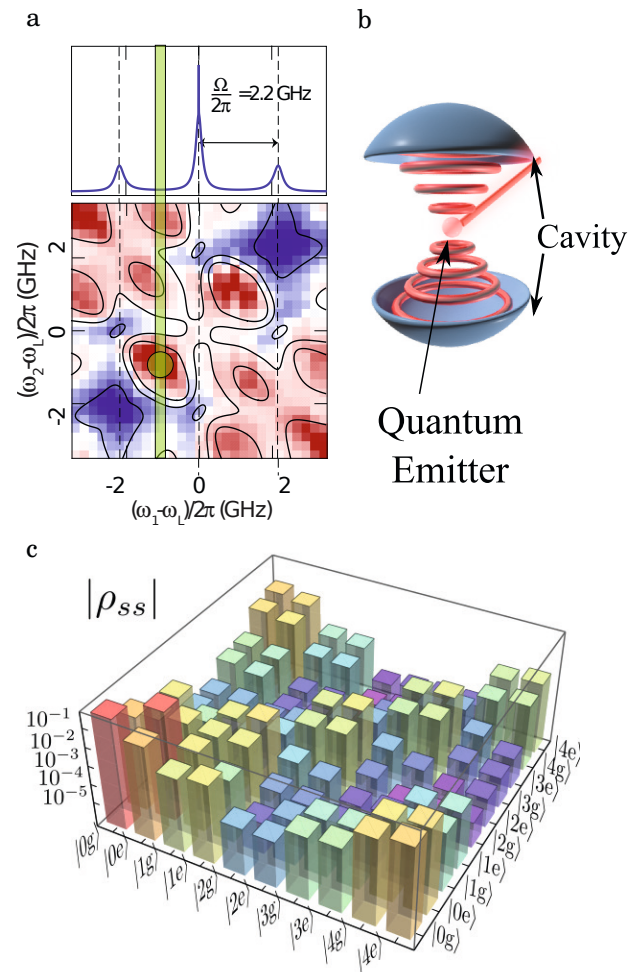


Figure 1: a. Experimentally measured two-photon spectrum (2PS) of the light emitted by a resonantly driven two level system (2LS) [4]. Despite not being apparent in the normal spectrum, photons emitted at an energy between a sideband and the central peak are strongly correlated. b. This correlations can be harvested in a cavity QED setup, and the principle is extensible to N -photon emission. c. Density matrix of the cavity-2LS system for four-photon emission, showing strong coherences between the states of 0 and 4 photons, and the radiative cascade of the 4-photon bundles.

- [4] M. Peiris, B. Petrak, K. Konthasinghe, Y. Yu, Z. C. Niu, A. Muller, [arXiv:1501.00898v1](https://arxiv.org/abs/1501.00898v1)
- [5] C. Sanchez Muñoz, E. del Valle, A. González Tudela, K. Müller, S. Lichtmannecker, M. Kaniber, C. Tejedor, J.J. Finley, F.P. Laussy, *Nature Photonics*, **8**, 550 (2014).

Nanomechanical membranes as transducers for classical and quantum signals

A. Schliesser¹, C. Møller, W. Nielsen¹, A. Simonsen¹, Y. Tsaturyan¹, and E. S. Polzik¹

¹Niels Bohr Institute, Blegdamsvej 17, 2100 Copenhagen, Denmark

e-mail: albert.schliesser@nbi.dk

A first generation of micro- and nanomechanical systems can now be coupled to modes of an electromagnetic field in a quantum-coherent manner [1,2,3], enabling, e. g., entanglement and interconversion between photons and phonons, and the preparation of mechanical devices in low-entropy quantum states. Using mechanical devices as a coherent transducer between different quantum systems—through appropriate functionalization—has thus become an intriguing, but realistic possibility. In the simplest case, these quantum systems can be different electromagnetic field modes, including microwave and optical fields [4].

Proof of principle transducers operating in a classical regime have recently been realized [5,6,7]. Our first approach [6] has been based on a high-Q silicon nitride membrane resonator, which is simultaneously coupled to a degenerate radio-frequency resonance circuit, and an optical readout mode. By detecting the phase fluctuations imprinted by the membrane on the optical mode with a quantum-noise limited imprecision, we can optically measure sub-nV signals induced in the RF circuit. The device resides in the strong coupling regime with electromechanical cooperativities exceeding 6000, enabling suppression of thermomechanical noise in the transduction cascade by the same factor. We are developing an integrated version of such a device, which may find applications as a sensitive transducer also for classical fields, e.g. in NMR.

Future work with more complex hybrid systems—involving several electromagnetic modes [4,8,9] or spin ensembles [10,11]—will require the weakest possible coupling of the mechanical mode to its relatively hot thermal bath (since $f_m < 10$ MHz). We have therefore developed [12] nanomechanical membranes embedded in a phononic bandgap shield that suppresses mechanical decoherence by radiation loss (or “phonon tunneling” [13]). These membranes—an example is shown in Figure 1—achieve $Q_m > 10^7$ and $f_m Q_m > 10^{13}$ Hz, sufficient to realize the required quantum-coherent coupling [3] at modest cryogenic temperatures (~ 10 K).

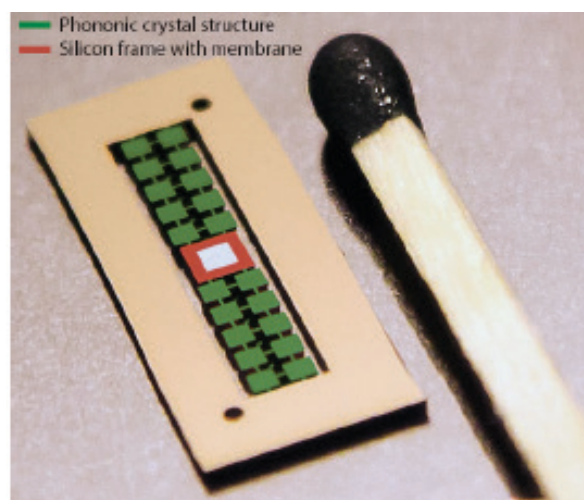


Figure 1: False-color photograph of a SiN membrane (white) stretched on a silicon frame (red), which is suspended in the center of a phononic crystal structure (green). The latter exhibits a full band-gap around the frequencies of the membranes’ mechanical modes of interest and thus prevents phonons from tunneling on and off the membrane.

- [1] J. D. Teufel *et al.*, *Nature* **471**, 204 (2011).
- [2] J. Chan *et al.*, *Nature* **478**, 89 (2011).
- [3] E. Verhagen *et al.*, *Nature* **482**, 63 (2012).
- [4] L. Tian, *Ann. der Physik* **527**, 1 (2015).
- [5] J. Bochmann *et al.*, *Nature Physics* **9**, 712 (2013).
- [6] T. Bagci *et al.*, *Nature* **107**, 81 (2014).
- [7] R. Andrews *et al.*, *Nature Physics* **10**, 321 (2014).
- [8] Sh. Barzanjeh *et al.*, *PRL* **109**, 130503 (2012).
- [9] A. Nunnenkamp *et al.*, *PRL* **113**, 023604 (2014).
- [10] K. Hammerer *et al.*, *PRL* **102**, 020501 (2009).
- [11] E. Polzik *et al.*, *Ann. der Physik* **527**, A15 (2015).
- [12] Y. Tsaturyan *et al.*, *Optics Express* **22**, 203879 (2014).
- [13] I. Wilson-Rae, *PRB* **77**, 245418 (2008).

Stochastic conversion processes in bosonic condensate of exciton-polaritons

A.S. Sheremet¹, Y.G. Rubo², I.A. Shelykh³ and A.V. Kavokin^{1,4}

¹Russian Quantum Center, 100 Novaya St., Skolkovo, Moscow 143025, Russia

²Instituto de Energías Renovables, Universidad Nacional Autónoma de México, Temixco, 62580, Mexico

³Science Institute, University of Iceland, Dunhagi-3, IS-107, Reykjavik, Iceland

⁴School of Physics and Astronomy, University of Southampton, SO17 1NJ Southampton, United Kingdom
e-mail: sheremet.alexandra@gmail.com

We present here a theory of stochastic exciton-photon transitions in bosonic condensates of exciton polaritons. In 1957 V.M. Agronovich proposed to consider each individual polariton as a chain of transmission acts between exciton and photon states. This idea implies that an exciton polariton spends some time as an exciton and some time as a photon. Based on this assumption, a hidden variable $1/\tau_{xc}$ can be introduced as a characteristic of the rate of stochastic exciton-photon and photon-exciton conversions.

We describe the system of exciton polaritons by the density matrix $\hat{\rho}$, which evolves according to the Liouville equation:

$$\begin{aligned} \frac{d\hat{\rho}(t)}{dt} &= -\frac{i}{\hbar} [\hat{H}_0, \hat{\rho}] \\ &- \frac{1}{2} \sum_j \frac{1}{\tau_j} \left(\hat{A}_j^\dagger \hat{A}_j \hat{\rho} + \hat{\rho} \hat{A}_j^\dagger \hat{A}_j - 2\hat{A}_j \hat{\rho} \hat{A}_j^\dagger \right) \end{aligned} \quad (1)$$

Here we assume that the coherent exciton-photon coupling is described by a non-perturbative Hamiltonian $\hat{H}_0 = \Omega(\hat{a}^\dagger \hat{b} + \hat{b}^\dagger \hat{a})$, where Ω is a Rabi frequency, and \hat{a} (\hat{a}^\dagger) and \hat{b} (\hat{b}^\dagger) are annihilation (creation) operators for excitons and photons, respectively. All decay processes evolve at $t > 0$ and can be described by four Lindblad terms with $j = x, c, xc, cx$, where $\hat{A}_x = \hat{a}$ and $\hat{A}_c = \hat{b}$ describe the escape of exciton and photon with life-times τ_x and τ_c , respectively. Two conversion processes: exciton to photon and photon to exciton are characterized by operators $\hat{A}_{xc} = \hat{b}^\dagger \hat{a}$ and $\hat{A}_{cx} = \hat{a}^\dagger \hat{b}$ and the characteristic conversion time τ_{xc} .

The role of stochastic conversions can be understood in terms of the generalized exciton-photon correlator:

$$G_{xc}(t) = \frac{\langle n_a(t)n_b(t) \rangle^2}{\langle n_a(t) \rangle^2 - n_a(t) \langle n_b(t) \rangle^2 - n_b(t)} \quad (2)$$

where $\langle n_a(t) \rangle$ and $\langle n_b(t) \rangle$ are average numbers of excitons and photons respectively, that can be obtained from the diagonal elements of the density matrix $P(n_a, n_b, t)$ defined in Eq. (1). In Figure 1 we demonstrate the time evolution of several diagonal elements $P(n_a, n_b, t)$ of the density matrix for the initial coherent state. In the panel (a) the stochastic conversion time is finite while in the panel (b)

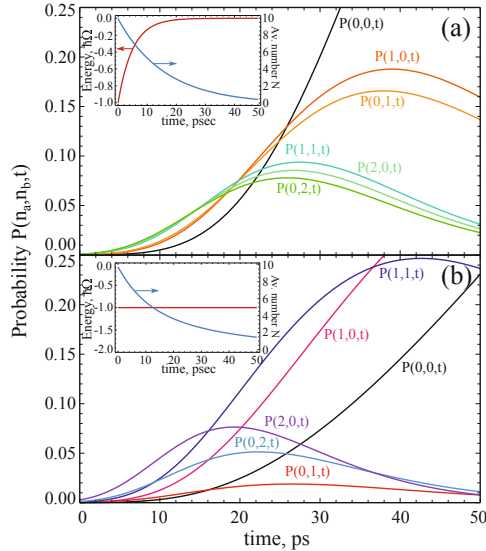


Figure 1: Evolution of diagonal elements $P(n_a, n_b, t)$ and the average number of particles N as well as the energy per particle on insets. The panel (a) corresponds to the finite time of the exciton-photon conversion $\tau_{xc} = 5$ ps, while the behavior in the absence of stochastic conversion is shown in the panel (b). The polariton condensate is initially in the coherent state with $N = 10$. The life-times of excitons and photons are $\tau_x = 40$ ps and $\tau_c = 10$ ps.

the stochastic process is neglected. Here the fingerprint of the exciton-photon conversion is evident in the similar behaviour of the density matrix elements $P(n_a, n_b, t) \approx P(n_b, n_a, t)$ if $t > \tau_{xc}$ in the panel (a), while the behaviour of the density matrix elements for $\tau_{xc} \rightarrow \infty$ is randomised due to the different lifetimes of excitons and photons, as the panel (b) shows. In addition, we analyze time evolutions of the average number of particles and the energy, which have different behaviours in the presence or absence of the stochastic exciton-photon conversion processes. These evolutions are presented in inserts of Figure 1.

We discuss several possible experimental configurations which would allow for measurement on the generalized correlator (2), including the photocurrent-photoluminescence and Kerr rotation-photoluminescence correlations.

Raman sideband cooling of Mg^+ ions

T. Shpakovsky,^{a, c} K. Khabarova,^{a, b, c} V. Sorokin,^{a, c} I. Zalivako,^a N. Kolachevsky^{a, b}

^a *P.N. Lebedev Physical Institute, 119991 Moscow, Leninsky prospekt 53, Russia*

^b *VSUE VNIIFTRI, Mendeleevo, Moscow Region, Russia*

^c *Russian Quantum Center, ul. Novaya 100, Skolkovo, Moscow region, Russia*

Today one of the most precise frequency sources is an optical $^{27}Al^+$ single-ion clock based on the $^1S_0 \rightarrow ^3P_0$ clock transition with a natural line width of 8 mHz. Extremely low sensitivity of this transition to BBR shift allowed to demonstrate frequency instability of 8.3×10^{-18} [1] thus opening new perspectives for precision metrology, tests of fundamental theories and gravimetry.

To achieve ultimate characteristics of an optical standard one should reach deep laser cooling of ions. Though, the laser cooling transition at 165 nm in Al^+ is not accessible by existing narrow line cw lasers. For deep ground state cooling of an Al^+ ion, an additional laser cooled Mg^+ ion is used (method of sympathetic cooling). Cooling transition $^3S_{1/2} \rightarrow ^3P_{3/2}$ in Mg^+ has a wavelength of 279.6 nm, which is easily accessible by the fourth harmonic of a semiconductor laser [2]. According to [3] a Mg^+ is also used for reading quantum information about excitation of the clock transition (the method of quantum logic).

In frames of cooperation between National Russian Metrology Institute (VNIIFTRI) and P.N. Lebedev institute we started a project aimed for study of clock transition in single Al^+ ion. Current progress in development of the linear quadrupole ion trap (fig. 1), and laser sources for cooling and interrogation of the ions is presented in this report.

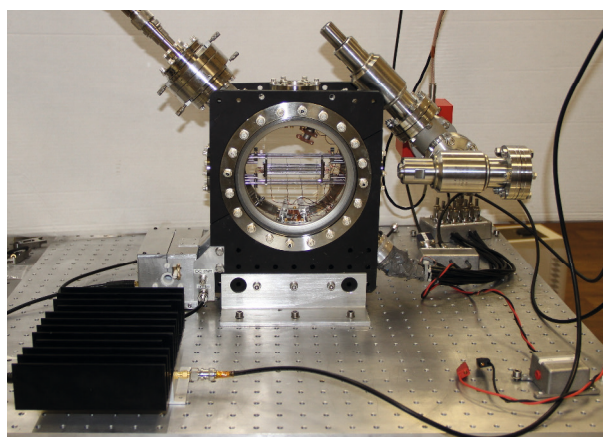


Figure 1: Linear quadrupole Paul trap for simultaneous confinement of aluminum and magnesium ions

[1] C. W. Chou, D. B. Hume, et al., Phys. Rev. Lett., 104, 070802 (2010).

[2] M. Herrmann, V. Batteiger, S. Knunz, et al., Phys. Rev. Lett., 102, 013006 (2009).

[3] P. O. Schmidt, T. Rosenband, C. Langer, et al., Science 309, 749 (2005).

False vacuum decay in ultracold atoms

A. I. Sidorov¹, O. Fialko², B. Opanchuk¹, P. D. Drummond¹ and J. Brand²

¹ CQOS, Swinburne University of Technology, Melbourne, Victoria 3122, Australia

² Massey University, Auckland 0745, New Zealand

e-mail: asidorov@swin.edu.au

Universal relations can be found in different areas of modern physics, e. g., in condensed matter, cosmology and ultracold quantum gases. A quantum field in a metastable state (the false vacuum) can decay by a tunneling process forming bubbles of true vacuum that grow with the speed of light [1]. We propose [2] to use dynamical evolution of the relative phase of a two-component Bose-Einstein condensate for simulating the decay of a metastable quantum field [1] which has a close analogy to the cosmological theory of the inflationary universe [3].

The quantum field decay can be simulated in the relative phase domain of two spin components which are coupled by a radiofrequency field [4,5]. Fast modulation of the coupling allows to create the potential with a local minimum at the phase of π (Fig 1). Using the variational method and the action functional we obtain the equation of motion for the relative phase [2] which is analogous to the equation of motion for the relativistic scalar field in inflationary universe [3]. We simulate the dynamical evolution of the coupled Bose fields using stochastic numerical simulations and the truncated Wigner approximation.

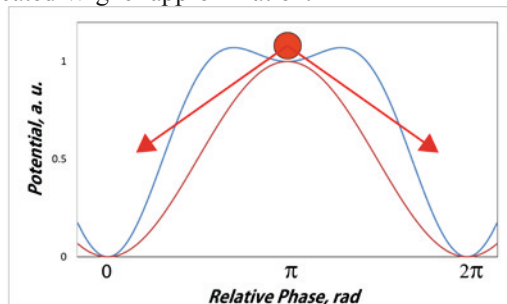


Figure 1: Decay of a vacuum field from the metastable state of the effective (blue) potential.

Quantum fluctuations initiate tunneling of the scalar field into the global minima (0 or 2π) leading to the nucleation of bubbles in the 2D spatial distribution of the relative phase (Fig 2a). The bubbles randomly appear in different locations and grow in size with the speed of sound (the quantum fluid analogue of the speed of light in cosmology) until they collide (Fig 2b). The outcome of bubble collisions depends on which global minimum they occupy. If the relative phase is the same, the bubbles will merge. If two bubbles have the 2π difference, domain walls will form separating the bubbles [2].

Our proposal requires repulsive intra-component interactions (a_{11} and a_{22}) to dominate over inter-component interactions (a_{12}). For implementing an analogue quantum simulator of the false vacuum decay we propose to use a two-component condensate of ^{41}K atoms prepared in two Zeeman states $|1\rangle = |F=1, m_F=1\rangle$ and $|2\rangle = |F=1, m_F=0\rangle$ which have an inter-state Feshbach resonance with the zero crossing at 675.3 G. At this magnetic field two states are separated by 61.93 MHz and are coupled via the magnetic dipole transition. The stretched state $|1\rangle$ will be condensed in an optical dipole trap and a pulsed RF field will prepare the 50:50 superposition of two states $|1\rangle$ and $|2\rangle$. Read-out of the relative phase values will be carried out using Ramsey interferometry with spatially resolved imaging of atomic densities of two components [4,5].

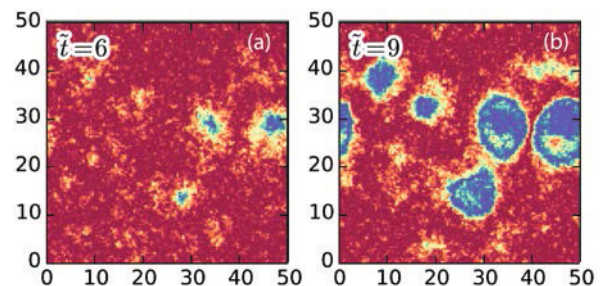


Figure 2: Decay of the false vacuum in the form of the bubble nucleation and growth in the 2D spatial distribution of the relative phase of two condensates at different evolution times [2].

Demonstrating the false vacuum decay in Bose-Einstein condensates will offer a pathway to analog quantum simulations of a cosmological process in a millimeter-size sample of ultracold atoms.

- [1] S. Coleman, *Phys. Rev. D* **15**, 2929 (1977).
- [2] O. Fialko, B. Opanchuk, A.I. Sidorov, P.D. Drummond and J. Brand, *arXiv*: 1408.1163 (2014).
- [3] A.H. Guth, *The Inflationary Universe* (Perseus Books, Reading, 1997).
- [4] M. Egorov, R. Anderson, V. Ivannikov, B. Opanchuk, P. Drummond, B. Hall and A.I. Sidorov, *Phys. Rev A* **84**, 021605(R) (2011).
- [5] M. Egorov, B. Opanchuk, P. Drummond, B. Hall, P. Hannaford and A.I. Sidorov, *Phys. Rev A* **87**, 053614 (2013).

Ultra-high time resolution SSPD coupled to single-mode fiber

M. Sidorova¹, A. Divochiy², Yu. Vakhtomin^{1,2} and K. Smirnow^{1,2,3}

¹Moscow State Pedagogical University, 1 Malaya Pirogovskaya str., Moscow 119992, Russia

²CJSC "Superconducting nanotechnology" (Scontel), 5/22 Rossolimo str., Moscow 119991, Russia

³National Research University Higher School of Economics, 20 Myasnitskaya str., 101000, Moscow, Russia

e-mail: sidorova.m.89@gmail.com

Quantum key distribution, optical quantum computing, research of single-photon emission from atoms, quantum dots and molecules require efficient and ultrafast single-photon detectors with low dark counts, low jitter and high sensitivity in visible and infrared range. At present the performances of the Superconducting Single-Photon Detectors (SSPDs) make it suitable for many applications [1] since the first presentation more than decade ago [2].

The operation mechanism of SSPDs is based on suppression of superconductivity after a photon absorption in current biased superconducting nanowire (thickness ~ 4 nm, width ~ 120 nm) which leads to output voltage pulse that after amplifying allows indicating a detection event. The device operates at liquid helium temperature 2 – 4.2 K. The detector active area (typical $10 \times 10 \mu\text{m}^2$) is a long nanowire (typical 0.5 mm) shaped in meander form for maximal effective optical coupling. Such long strip defines detector kinetic inductance (L_k) and consequently limits characteristic times ($\tau \sim L_k$) [3]. Thus improving timing performances of SSPD is required reducing device active area for this end we fabricated the new SSPD with smaller active area size $3 \times 3 \mu\text{m}^2$ which is smaller in comparison with typical SSPD.

Here we present *new ultra-high time resolution NbN SSPD* with record performances. Our detector in contrast to conventional SSPD has record timing jitter < 25 ps (Fig.1), ultra-short recovery time < 2 ns, extremely low dark count rate < 10 Hz and high system detection efficiency (SDE) over a wide spectral range (from UV to near-IR). These record performances were obtained thanks to employing new technique of coupling between smaller active area ($3 \times 3 \mu\text{m}^2$) of SSPD and special lensed single-mode fiber with optical spot diameter $3 \mu\text{m}$. To couple detector to lensed fiber we used precise alignment method based on sub-micron placement set up. To guarantee coupling stability after several thermocycles the coupled detector and optical fiber were mechanically fixed together in the holder. Thus this technique allowed us to improve timing performances of new SSPD and safe its high system detection efficiency (Table 1).

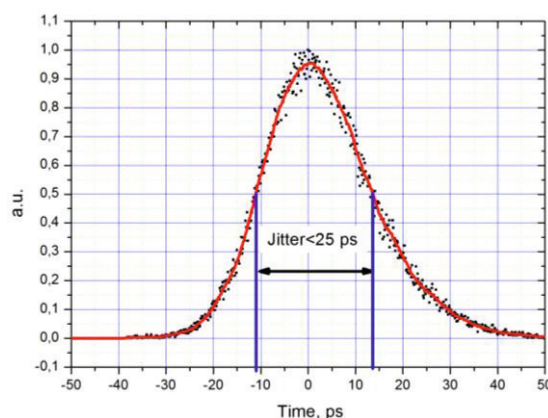


Figure 1: The timing jitter histogram of the ultrafast SSPD system (Axis Y – normalized counts).

Table 1: Comparison of performances several types of SSPDs at $\lambda = 1550$ nm.

	SSPD	Ultra-high time resolution SSPD
SDE, %		~ 25
Dark counts, Hz		< 10
Dead time, ns	< 10	< 2
FWHM, ns	< 5	< 1
Timing jitter, ps	< 50	< 25

- [1] C. M. Natarajan, et al., Supercond. Sci. Technol. 25, 063001 (2012).
- [2] G. N. Gol'tsman, et al., Appl. Phys. Lett. 79, 705, (2001).
- [3] Kerman A. J., et al., Appl. Phys. Lett. 88, 111116 (2006).

Measuring photon correlations simultaneously in time and frequency

B. Silva^{1,2}, A. González-Tudela³, C. Sánchez², D. Ballarini¹, M. de Giorgi¹, E. del Valle², D. Sanvitto¹ and F.P. Laussy^{2,4}

¹NNL, Istituto Nanoscienze-CNR, Via Arnesano, 73100 Lecce, Italy

²Departamento de Física Teórica de la Materia Condensada and Condensed Matter Physics Center (IFIMAC), Universidad Autónoma de Madrid, E-28049, Spain

³Max-Planck Institut für Quantenoptik, 85748 Garching, Germany

⁴Russian Quantum Center, Novaya 100, 143025 Skolkovo, Moscow Region, Russia

e-mail: blanca.silva@uam.es

Photon correlations are at the focus of research in quantum optics due to their ability to characterize the nature of a source from the relationship between emitted photons. With their seminal experiment, Hanbury Brown and Twiss provided for the first time the evidence of the inherent correlation existing between photons due to their bosonic nature. These correlations are described by the second order correlation function $g^{(2)}$.

In this work we report a technical and conceptual advance by measuring simultaneously photon correlations both in time and frequency. By using a streak camera, we are able to measure the *two-photon spectrum* (2PS)[1, 2], a full map of photon correlations in time-frequency space, for a condensate of exciton-polaritons. Unlike in the usual approach using beam splitters and avalanche photodiodes, our procedure allows us to obtain both the energy and temporal information in only one measurement (see Fig.1).

The resulting landscape of correlations shows an excellent agreement with the theoretical prediction, calculated by novel methods for the computation of frequency correlations[3, 4]. This new theoretical approach has recently revealed the potential of the 2PS to unravel rich dynamics of quantum emission in a variety of systems which are otherwise washed out when there is no energy discrimination.

The resulting 2PS displays bunching in the diagonal ($\omega_1 = \omega_2$) and color-antibunching in the antidiagonal ($\omega_1 = -\omega_2$), providing the first observation of anticorrelations at the single particle level in a condensate of exciton-polaritons. We demonstrate for the first time that the observed tendency of photons to cluster when they are equal and repel when they are different is not a specific feature of the system under consideration, but a general property of photon themselves due to its bosonic nature that can be described by a general *bosonic form factor*. This fundamental observation deepens our understanding of the nature of the intrinsic correlations between bosons, extending Glauber's conventional theory of photon correlations.

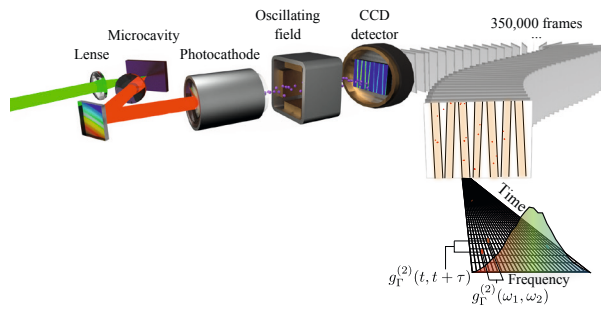


Figure 1: Setup of the experiment. The microcavity is excited with a CW. The photons emitted are opened into energies in a grating. This new beam enters in the streak camera, in which the photons are converted to photoelectrons (photocathode) and by means of an oscillating field they are deflected to a different position of the CCD detector depending on the time of arrival. These detection events are correlated. Depending on the horizontal position on the beam, the energy will be determined, and on the vertical position the time of arrival. Taking into account these two components on the CCD the $g^{(2)}(\omega_1, t; \omega_2, t + \tau)$ can be obtained.

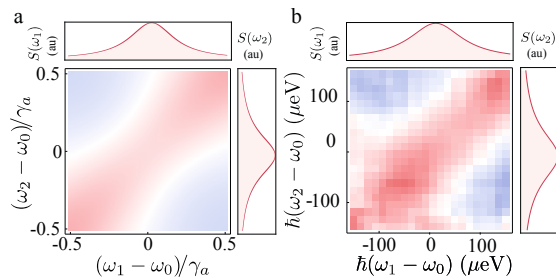


Figure 2: Theoretical (a) and experimental (b) 2PS for a condensate of exciton-polaritons.

- [1] E. del Valle, A. Gonzalez-Tudela, F. P. Laussy, C. Tejedor and M. J. Hartmann, Phys. Rev. Lett. **109**, 183601 (2012).
- [2] A. Gonzalez-Tudela, F. P. Laussy, C. Tejedor, M. J Hartmann and E. del Valle, New Journal of Physics **15**, 033036 (2013).
- [3] C. Sanchez Muñoz, E. del Valle, C. Tejedor and F.P. Laussy, Phys. Rev. A **90**, 052111 (2014).
- [4] C. Sanchez Muñoz, E. del Valle, A. González Tudela, K. Müller, S. Lichtmannecker, M. Kaniber, C. Tejedor, J.J. Finley and F.P. Laussy, Nat. Phot. **8**, 550 (2014).

Coherent Quantum Phase Slips in AlO_x Nanowires

S. T. Skacel¹, M. Pfirrmann¹, J. N. Voss¹, J. Münzberg¹, S. Probst¹, M. Weides¹, H. Rotzinger¹, J. E. Mooij^{1,2}, and A. V. Ustinov^{1,3}

¹Physikalisches Institut, Karlsruhe Institute of Technology, Wolfgang-Gaede-Str. 1, D-76131 Karlsruhe, Germany

²Kavli Institute of Nanoscience, Delft University of Technology, 2628 CJ Delft, The Netherlands

³Russian Quantum Center, 100 Novaya St., Skolkovo, Moscow 143025, Russia

e-mail: sebastian.skacel@kit.edu

Superconducting nanowires in the quantum phase slip (QPS) regime allow to study the charge and phase dynamics in duality to Josephson junction systems. However, due to the vanishing self-capacitance of the nanowires, their microwave response significantly differs. We experimentally study the QPS effects in superconducting AlO_x nanowires, which are embedded in a resonant circuit at GHz frequencies.

The AlO_x nanowires, with a sheet resistance in the $\text{k}\Omega$ range, are fabricated by sputter deposition of aluminium in a controlled oxygen atmosphere [1]. The wires are subsequently defined by conventional electron beam lithography and reactive ion etching to a width in the range of 15-30 nm (see Fig. 1 Right).

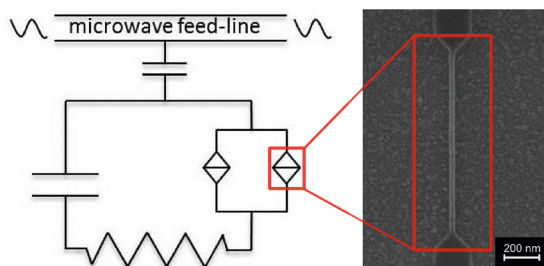


Figure 1: *Left*: Schematic of a microwave lumped element resonator with an embedded loop with two nanowires. The resonator is capacitively coupled to a microwave feed-line. *Right*: SEM picture of a typical AlO_x nanowire.

We present the fabrication of the nanowire arrays and measurements of an array of two parallel nanowires galvanically coupled to a superconducting lumped element microwave resonator (see Fig. 1 *Left*). Resonator and wires are fabricated from the same AlO_x layer, allowing for a compact design and high resonator impedance.

The resonator is probed using dispersive readout technique by measuring the microwave reflection to a feed-line, common to several frequency detuned AlO_x resonators. By applying a magnetic field perpendicular to the substrate, the anti-crossing shown in Fig. 2 is observed at a magnetic flux through the QPS loop close to $\Phi_0/2$, where Φ_0 is the magnetic flux quantum. We present measurement results, indicating the behaviour similar to other QPS systems where coherent properties have been observed [2].

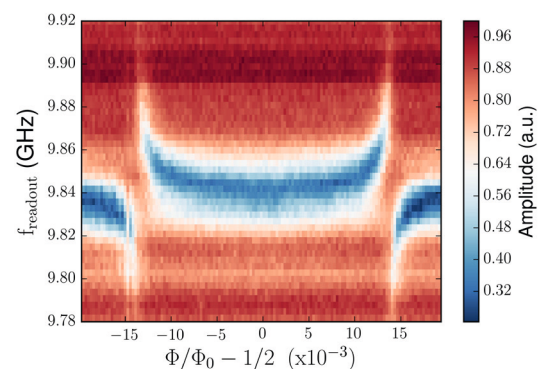


Figure 2: Anti-crossing of the resonator with QPS at $\Phi_0/2$.

- [1] H. Rotzinger, S. T. Skacel, M. Pfirrmann, J. N. Voss, J. Münzberg, S. Probst, P. Bushev, M. P. Weides, A. V. Ustinov, J. E. Mooij, *Sputter deposited aluminium-oxide for superconducting high kinetic inductance circuits*, arXiv:1408.4347 (2014)
- [2] O. V. Astafiev, L. B. Ioffe, S. Kafanov, Y. A. Pashkin, K. Y. Arutyunov, D. Shahar, O. Cohen, J. S. Tsai, *Coherent quantum phase slip*, *Nature*, **484**, 355–358 (2012)

High-fidelity cluster state generation using orbital degrees of freedom of ultracold atoms in an optical lattice

Yuuki Tokunaga

NTT Secure Platform Laboratories, 3-9-11, Midoricho, Musashinoshi, Tokyo 180-8585, Japan

e-mail: tokunaga.yuuki@lab.ntt.co.jp

We propose a method for generating high-fidelity multipartite spin entanglement of ultracold atoms in an optical lattice in a short operation time with a scalable manner, which is suitable for measurement-based quantum computation [1]. To perform the desired operations based on the perturbative spin-spin interactions, we propose to actively utilize the extra degrees of freedom (DOFs) usually neglected in the perturbative treatment but included in the Hubbard Hamiltonian of atoms, such as, (pseudo-)charge and orbital DOFs. Our method simultaneously achieves high fidelity, short operation time, and scalability by overcoming the following fundamental problem: enhancing the interaction strength for shortening the operation time breaks the perturbative condition of the interaction and inevitably induces unwanted correlations among the spin and extra DOFs. See ref. [1] for more details.

[1] K. Inaba, Y. Tokunaga, K. Tamaki, K. Igeta, and M. Yamashita, *Phys. Rev. Lett.*, **112**, 110501 (2014), arXiv:1202.6446.



Measurement of the 5D Level Polarizability in Laser Cooled Rb Atoms

S. Snigirev^{1,2}, A. Golovizin^{1,2,3}, D. Tregubov^{1,2,3}, S. Pyatchenkov^{1,2}, D. Sukachev^{1,2}, A. Akimov^{1,2}, V. Sorokin^{1,2}, and N. Kolachevsky^{1,2,3}

¹*P.N. Lebedev Physical Institute, Leninsky Prospekt 53, 119991 Moscow, Russia*

²*Russian Quantum Center, 100 Novaya St., Skolkovo, Moscow 143025, Russia*

³*Moscow Institute of Physics and Technology, 141704 Dolgoprudny, Moscow region, Russia*

e-mail: *treg.dim@gmail.com*

Study of atomic and molecular polarizabilities remains an important task in atomic physics. The atomic polarizability

$$\alpha_\gamma = \sum_{\gamma'} \frac{|\langle \psi_\gamma | e\mathbf{r} | \psi_{\gamma'} \rangle|^2}{E_\gamma - E_{\gamma'}} \quad (1)$$

depends on electric dipole matrix elements $\langle \psi_\gamma | e\mathbf{r} | \psi_{\gamma'} \rangle$ [1], which also describe transition strengths, state lifetimes, van der Waals interactions, and scattering cross sections. Here $e\mathbf{r}$ denotes an electric dipole operator, E_γ the level energy with quantum number γ , and ψ_γ its wave functions. Accurate measurements of polarizability facilitate progress in sophisticated atomic structure calculations and the theory of heavy atoms, which results in more precise predictions for other important atomic parameters (see, e.g., [2]). Measurements of polarizabilities become even more crucial in applications for modern optical atomic clocks. Predictions of the magic wavelength in optical lattice clocks [3] and accurate estimation of the blackbody radiation shift require precise knowledge of static and dynamic polarizabilities [4].

Polarizabilities of ground and highly excited states of alkali atoms are known quite accurately. In case of Rb, the polarizabilities of 5S and 5P levels have been measured long ago with high precision while being in agreement with theory [5]. However, considering intermediate states there are some difficulties both theoretically and experimentally. For example, 5D level in Rb. There are several theoretical predictions which differ up to 20% [6, 7].

We report on accurate measurements of the scalar α_S and tensor α_T polarizabilities of the 5D fine structure levels $5D_{3/2}$ and $5D_{5/2}$ in Rb-87 [8]. α_S and α_T describe the dependance of α on total angular momentum F and its projection m_F :

$$\alpha = \alpha_S + \alpha_T P(F, m_F) \quad (2)$$

Rb atoms were laser cooled in a regular six-beam magneto-optical trap, forming a cloud at the center of a plane capacitor. Excitation to 5D level was performed in a cascade mode, the population was measured by spontaneous emission.

Optical pumping of atoms to a specific magnetic sublevel allowed us to measure the tensor polariz-

ability component with relatively high precision. In order to perform optical pumping we applied a circularly σ^+ -polarized pump pulse to transfer atoms to the $5P_{3/2}(F = 3, m_F = +3)$ magnetic sublevel. Using the probe $5P \rightarrow 5D$ pulse with certain polarization (σ^+ or σ^-) we defined both scalar and tensor polarizabilities.

The measured values (in atomic units) $\alpha_S(5D_{3/2}) = 18400(75)$, $\alpha_T(5D_{3/2}) = 750(30)$, $\alpha_S(5D_{5/2}) = 18600(76)$ and $\alpha_T(5D_{5/2}) = 1440(60)$ show reasonable correspondence to previously published theoretical predictions, but are more accurate. We demonstrated a relative uncertainty of 4% for the tensor polarizability and 0.4% for the scalar polarizability, which is comparable to accurate measurements in ground-state alkali atoms. Our result is close to the theoretical prediction [6].

- [1] L. D. Landau and E. M. Lifshitz, Quantum Mechanics.
- [2] J. Mitroy, M. S. Safronova, and Charles W. Clark, J. Phys. B **43**, 202001 (2010).
- [3] H. Katori, M. Takamoto, V. G. Palchikov, and V. D. Ovsianikov, Phys. Rev. Lett. **91**, 173005 (2003).
- [4] K. Beloy, U. I. Safronova, and A. Derevianko, Phys. Rev. Lett. **97**, 040801 (2006).
- [5] Daniel A. Steck, Rubidium 87 D Line Data.
- [6] A.A. Kamenski and V.D. Ovsianikov, J.Phys. B: At. Mol. Opt.Phys., **39**, 2247 (2006).
- [7] D.A. Kondrat'ev, I.L. Beigman, and L.A. Vainshtein, Bull. Lebedev Phys. Inst. **35**, 355 (2008).
- [8] S. Snigirev, A. Golovizin, D. Tregubov, S. Pyatchenkov, D. Sukachev, A. Akimov, V. Sorokin and N. Kolachevsky, Measurement of the 5D-level polarizability in laser-cooled Rb atoms, Phys. Rev. A **89**, 01251 (2014).

Parallel quantum memory applications in quantum information

A.N. Vetlugin and I.V. Sokolov

St. Petersburg State University, Faculty of Physics, ul. Ul'yanovskaya 3, St. Petersburg, 198504, Russia
e-mail: conference@icqt.org

We investigate theoretically addressable spatially multimode (parallel) quantum memory applications in quantum information. Quantum information protocols (in our case in continuous variables) such as quantum computation, quantum networks, quantum repeaters etc., are based on using of squeezed and entangled states and on write-in, store and read-out possibility of these states. Quantum memory tuning allows one to use both squeezed and entangled states generation and quantum fields write-in/read-out regimes.

The scheme proposed is shown on Figure 1. To increase the effective light-matter interaction an atomic ensemble (placed in constant magnetic field) and a high-Q optical cavity are used. We do not use the bad-cavity limit. The use of the atomic ensemble also allows one to solve one of the most important problems – to increase the capacity due to using multimode write-in/read-out and non-classical states generation protocols. We assume that atomic ensemble

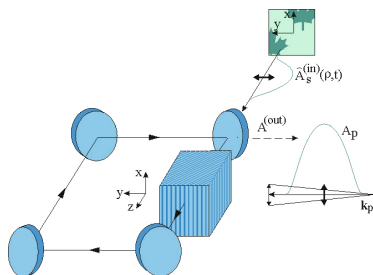


Figure 1: The parallel quantum memory scheme based on atomic ensemble in cavity.

consists of atoms with spin 1/2 both in the ground and in the excited states. This levels scheme allows one to use quantum memory as write-in/read-out device (Figure 2 (a)) or entangled states generator (Figure 2 (b)) because these processes are developed on different frequencies for the atomic ensemble in the constant magnetic field. So, by changing the cavity frequency and pump wave frequency or the magnetic field direction to opposite we can support one of these processes (for which frequency is close to cavity frequency) and suppress the other one.

For write-in/read-out regime we achieve the decrease of the output field and as it should be the increase of the write-in efficiency due to the matching of reflected and leakage fields, i.e. making the conditions of the destructive interference on the input mirror. With a view to reach this type of interference we research time-reversal and impedance-

matching approaches. The figure of merit for these approaches is the number of the stored modes with efficiency higher than 50%. Current research shows that the time-reversal approach gives the best results for short (from one to ten lifetimes of the cavity field) pulses of the signal field, at the same time long pulses (more than ten lifetimes of the cavity field) are equally good stored in both approaches. The advantage of the impedance-matching approach is its ability to store pulses of the arbitrary smooth temporal shapes and as consequence the ability to organize the memory-cells communication. For the read-out process we examine the addressability, i.e. the ability to read-out the desired spatial mode in required direction and/or the desired pulse from the sequence in required order.

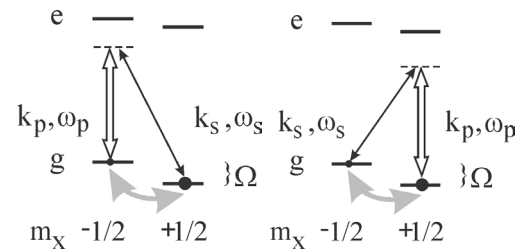


Figure 2: (a) The memory levels scheme and (b) the entanglement levels scheme.

For non-classical states generation regime we investigate input and output fields profiles, so that corresponding amplitudes undergo the squeezing and entanglement transformations. The spin coherence mode with transverse momentum \vec{q} is entangled, like in parametric down conversion, with the field mode with transverse momentum $-\vec{q}$. By changing the temporal shape of the pump field pulse we can create the entangled states of spin coherence with the output field pulse of the desired temporal shape. We research the squeeze rate and the squeeze ellipses orientation in dependence on the pump pulse duration and the transverse momentum. The diffraction effect is considered and the entangled modes number is calculated. We use the spatio-temporal approach to find eigenmodes of the effective squeezing and entanglement.

References

- [1] A.N. Vetlugin and I.V. Sokolov. Eur. Phys. J. D **68**, 269 (2014)

Nonlinear exciton-photon oscillations in a polariton condensate

N. Voronova¹, A. Elistratov², and Yu. Lozovik³

¹National Research Nuclear University MEPHI, Moscow 115409, Russia

²Institute for Nanotechnology in Microelectronics, Russian Academy of Sciences, Moscow 119991, Russia

³Institute for Spectroscopy, Russian Academy of Sciences, Troitsk 142190, Russia

e-mail: nsvoronova@mephi.ru

We theoretically investigate internal dynamics of a uniform two-component condensate of exciton-polaritons. Whereas for an equilibrium condensate with zero energy detuning between the photon and exciton dispersions Rabi oscillations are but density oscillations between the photon and exciton fractions of the polariton system with no change of the relative phase, we show that in a more general case various different regimes of internal oscillations are possible. For the conservative system, the parameter which controls the regime of the dynamics is photon-exciton detuning [1]. For an open system with gain and dissipation, crucial role is being played by the gain-saturation rate of the system.

Within the mean-field approach, the system is described by a set of two generalized complex Ginzburg-Landau equations for macroscopic wave functions of photons ψ_C and excitons ψ_X , where non-resonant pumping is described by the generalized model of the so-called saturable gain introduced by Berloff *et al.* in [2]:

$$i\hbar\partial_t\psi_C = \left[E_C^0 - \frac{\hbar^2\nabla^2}{2m_C} - i\kappa_C \right] \psi_C + \frac{\hbar\Omega_R}{2} \psi_X, \quad (1)$$

$$i\hbar\partial_t\psi_X = \left[E_X^0 - \frac{\hbar^2\nabla^2}{2m_X} + g_X|\psi_X|^2 + i(\gamma_X - \kappa_X - \Gamma_X|\psi_X|^2) \right] \psi_X + \frac{\hbar\Omega_R}{2} \psi_C. \quad (2)$$

Here $E_{C,X}^0$ are the bottoms of the photon and exciton dispersions, $m_{C,X}$ the cavity photon and exciton effective masses, $g_X > 0$ the constant of exciton-exciton repulsive interaction. The particle transfer from one subsystem to the other is described by the Josephson-like coupling term $\hbar\Omega_R/2$, where $\hbar\Omega_R$ is vacuum Rabi splitting energy. The imaginary terms in the right-hand side of the Eqs. (1) and (2) account for the dynamics of particle gain and loss in the system.

For an idealized conservative system without pump and losses, we obtain fully analytical solution of the above equations. Different regimes of dynamics of the relative quantum phase and population imbalance between the two subsystems of the polariton condensate are shown in Fig. 1. For a fixed value of the effective detuning e , depending on the initial state of the system, the relative phase of the two components can

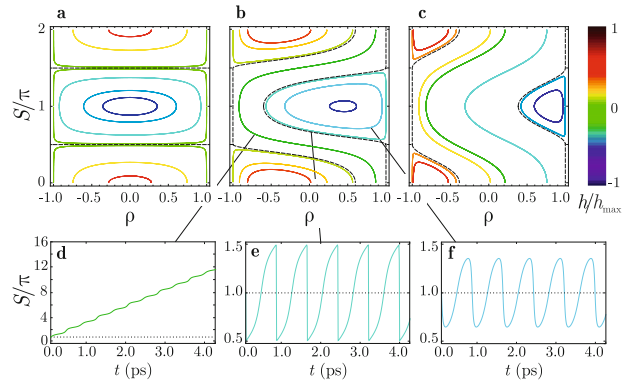


Figure 1. Top: Phase-plane portraits of the conjugate variables $\rho = n_C - n_X$ and $S = S_C - S_X$ for different effective detunings. Colors of the trajectories correspond to the value of total energy h according to the scale given on the right. (a) $e = 0$, (b) $e = -0.5$, (c) $e = -1.5$ (all energies are in the units of $\hbar\Omega_R$). Bottom: Relative phase S against time, for the trajectories of the phase-plane portrait at $e = -0.5$ given in (b) as marked.

exhibit harmonic or anharmonic oscillations ('modified Rabi' regime — see Fig. 1(f)), become sawtooth-like (Fig. 1(e)), or boundlessly grow in time as shown in Fig. 1(d) (this regime corresponds to the so-called internal Josephson effect).

When pump and losses are taken into account, the polariton condensate undergoes transient oscillations followed by the establishment of the dynamical equilibrium. Temporal evolution of the system becomes strongly dependent on the total population of the condensate. We analyze the averaged dynamics of the system and find equilibrium points corresponding to the lower and upper polariton condensates. For the unaveraged evolution, in the limit of small-amplitude oscillations, we solve the equations analytically and then define the conditions for γ , κ and Γ at which our analytical results are in accordance with the numerical simulations. We predict that at a certain value of gain and saturation rates ratio, the two-component condensate of lower polaritons becomes unstable and may show the transition to the upper polariton state.

[1] N. S. Voronova and Yu. E. Lozovik, <http://arxiv.org/abs/1411.2346> (2014).

[2] J. Keeling and N. G. Berloff, Phys. Rev. Lett. **100**, 250401 (2008).

Photon-assisted tunnelling with nonclassical microwaves in hybrid circuit QED systems

J.-R. Souquet^{1,2}, M. J. Woolley³, J. Gabelli², P. Simon², and A. A. Clerk¹

¹ Department of Physics, McGill University, Montréal, Québec H3A 2T8, Canada

² Laboratoire de Physique des Solides, Université Paris-Sud, Orsay 91405, France

³ School of Engineering and Information Technology, University of New South Wales, ADFA, Canberra, Australian Capital Territory 2600, Australia

e-mail: m.woolley@unsw.edu.au

Among the most exciting recent advances in the field of superconducting quantum circuits is the ability to coherently couple microwave photons in low-loss cavities to quantum electronic conductors (e.g. semiconductor quantum dots or carbon nanotubes). These hybrid quantum systems hold great promise for quantum information processing applications; even more strikingly, they enable exploration of completely new physical regimes. Here we study theoretically the new physics emerging when a quantum electronic conductor is exposed to non-classical microwaves (e.g. squeezed states, Fock states) [1]. We study this interplay in the experimentally-relevant situation where a superconducting microwave cavity is coupled to a conductor in the tunneling regime, depicted schematically in Fig. 1.

The physics of a tunnel junction illuminated by a purely classical microwave field has been understood since the 1960s with the classic work of Tien and Gordon [2]. This situation is equivalent to simply having an ac bias voltage across the conductor, and the resulting modification of the current is known as photon-assisted tunnelling; it has been measured in countless experiments [3]. Despite the word ‘photon’ in the effect’s name, in this standard formulation there is nothing quantum in the treatment of the applied microwave field. To study a more truly quantum version of photon-assisted-tunnelling, one could consider driving a tunnel junction with a quantum microwave field produced in a cavity. Such cavity-plus-conductor set-ups have been realised experimentally [4]. If the cavity is not driven, the set-up realises another well-studied quantum transport problem: dynamical Coulomb blockade [5].

Here we develop a comprehensive theory describing how *non-equilibrium, driven* states of a microwave cavity influence electronic transport in a coupled tunnel junction, with a particular focus on cavities which are maintained in truly nonclassical states. Generalising both standard photon-assisted tunnelling theory and dynamical Coulomb blockade theory, we show that the emission and absorption of photons by the conductor is naturally characterised by a quasi-probability distribution, which can fail to be positive. The resulting negative quasi-probabilities can have a direct influence on both the conductance and finite-

frequency current noise of the tunnel junction. We also show that this new quasi-probability distribution has a direct connection to the well-known Glauber-Sudarshan P -function of quantum optics. We present results for parameter regimes relevant to state-of-the-art experiments, and show that for sufficiently large tunnel resistances, the tunnel junction acts as a non-trivial and nonlinear probe of the cavity state.

Our results suggest the general potential of using quantum conductors as a powerful tool to characterise, and perhaps control, quantum microwave states in hybrid systems incorporating superconducting microwave cavities and semiconductor electronic devices.

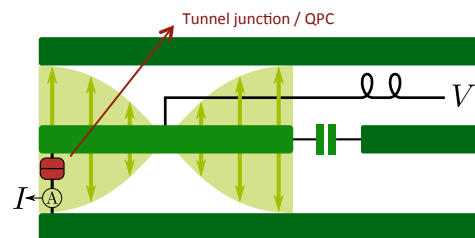


Figure 1: Schematic showing a resonant mode of a half-wavelength coplanar waveguide resonator with a quantum conductor. The state of the resonant mode provides a quantum ac voltage across the junction; we are interested in how this influences the dc junction current I .

- [1] J.-R. Souquet, M. J. Woolley, J. Gabelli, P. Simon, and A. A. Clerk, *Nat. Commun.* **5**, 5562 (2014).
- [2] P. K. Tien and J. P. Gordon, *Phys. Rev.* **129**, 647 (1963).
- [3] J. R. Tucker and M. J. Feldman, *Rev. Mod. Phys.* **57**, 1055 (1985).
- [4] T. Frey *et al.*, *Phys. Rev. Lett.* **108**, 046807 (2012).
- [5] G.-L. Ingold and Y. Nazarov, *Single Charge Tunneling* Vol 7 (Eds. Grabert, H and Devoret, M. H.), 935, Plenum, 1992.

Controlling the interactions of a few cold Rb Rydberg atoms by radio-frequency-assisted Förster resonances

D. B. Tretyakov¹, V. M. Entin¹, E. A. Yakshina^{1,2,3}, I. I. Beterov^{1,2}, C. Andreeva^{4,5}, and I. I. Ryabtsev^{1,2,3}

¹Rzhanov Institute of Semiconductor Physics SB RAS, Novosibirsk 630090, Russia

²Novosibirsk State University, Novosibirsk 630090, Russia

³Russian Quantum Center, 100 Novaya St., Skolkovo, Moscow 143025, Russia

⁴University of Latvia, LV-1002 Riga, Latvia

⁵Institute of Electronics, Bulgarian Academy of Sciences, Sofia 1784, Bulgaria

ryabtsev@isp.nsc.ru

Long-range interactions between highly-excited Rydberg atoms are being investigated for several important applications like neutral-atom quantum computing, quantum simulations, phase transitions in cold Rydberg gases, or nonlinear optics with single photons. Depending on the particular Rydberg states, these are van der Waals (vdW) or dipole-dipole (DD) interactions with different dependences on interatomic distance R (R^{-6} and R^{-3} , correspondingly).

Atoms in an identical nL Rydberg state generally interact via vdW, which is much weaker than DD at long distances. To make atoms interact via DD, the Rydberg state should be tuned exactly midway between two other Rydberg states of the opposite parity to induce a Förster resonance. It can be tuned using the Stark effect in a dc electric field. This method, however, works only for a limited number of Rydberg states.

We demonstrate another method when rf electric fields can be used to induce “inaccessible” Förster resonances which cannot be tuned by a dc electric field. In this case one or several microwave photons compensate for the energy defect and induce the transitions between nearly degenerate collective states of the quasi-molecule formed by the interacting Rydberg atoms.

Experiments were performed with cold 85Rb atoms in a magneto-optical trap. The excitation to the $nP_{3/2}(|M_J|=1/2)$ Rydberg state is realized via three-photon transition $5S_{1/2} \rightarrow 5P_{3/2} \rightarrow 6S_{1/2} \rightarrow nP_{3/2}$ by means of three cw lasers modulated to form 2 μ s exciting pulses at a repetition rate of 5 kHz. The small Rydberg excitation volume of 30-40 μ m size is formed using crossed-beam geometry. Our experiment provides atom-number-resolved measurement of the signals obtained from $N = 1-5$ of the detected Rydberg atoms with a detection efficiency of 65%.

In the first experiment we observed the spectra S_N of the Förster resonance $Rb(37P_{3/2})+Rb(37P_{3/2}) \rightarrow Rb(37S_{1/2})+Rb(38S_{1/2})$ in a 15 MHz rf-field of various amplitudes recorded for $N=2-5$ detected Rydberg atoms as a function of the dc electric field. One of these spectra is presented on the figure 1(b) at 100 mV rf-field. The frequency interval between the peaks in corresponds exactly to 15 MHz.

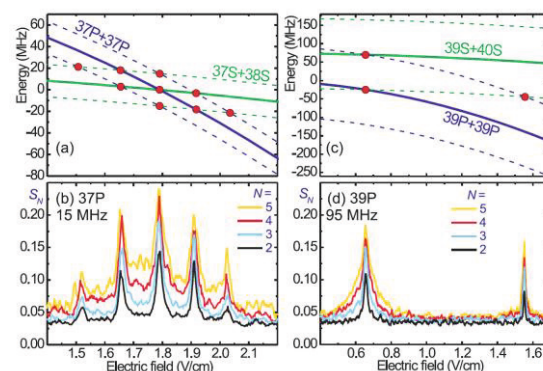


Figure 1: (a) Energy levels of the initial $37P+37P$ and final $37S+38S$ collective states of two Rydberg atoms in the electric field in the presence of the first Floquet sidebands at ± 15 MHz. The red (gray) circles indicate the intersections of the Floquet sidebands corresponding to rf-assisted Förster resonances. (b) Experimental record of the rf-assisted Förster resonances at a 100 mV rf-amplitude for $N=2-5$ detected Rydberg atoms. (c)-(d) The same for the “inaccessible” Förster resonances on the $39P$ state at 95 MHz and 100 mV. The first- and second-order resonances are observed.

In the second experiment we turned to the “inaccessible” Förster resonances, which cannot be tuned by dc electric field. Figures 1(d) present the experimental records of the Förster resonance $Rb(39P_{3/2}) + Rb(39P_{3/2}) \rightarrow Rb(39S_{1/2}) + Rb(40S_{1/2})$ in the 100 mV rf-field at frequency 95 MHz. The rf-induced Förster resonance is clearly seen. This spectrum evidences the possibility to tune vdW to DD interaction with high efficiency using the rf-field, which is resonant to a quasi-molecular transition instead of atomic transition.

The physical interpretation of the rf-assisted Förster resonances can be given in terms of the Floquet sidebands of the Rydberg energy levels by the periodic perturbation of the Rydberg energy levels by the rf electric field due to the Stark effect (figure 1(a,c)).

Thus we have shown that the van der Waals interaction of almost arbitrary high Rydberg states can thus be efficiently tuned to a resonant dipole-dipole interaction using the rf-field with frequencies below 1 GHz. This enhances the interaction strength and distance and can give rise to a much stronger dipole blockade effect.

D.B. Tretyakov, V.M. Entin, E.A. Yakshina, I.I. Beterov, C. Andreeva, and I.I. Ryabtsev, Phys. Rev. A 90, 041403(R).

Rogue Waves in Optical Lattices

C. Yuce

Department of Physics, Anadolu University, Turkey

e-mail: cyuce@anadolu.edu.tr

Abstract: We predict the existence of linear discrete rogue waves. We discuss that Josephson effect is the underlying reason for the formation of such waves. We study linear rogue waves in continuous system and present an exact analytical rogue wave solution of the Schrodinger-like equation.

Rogue waves, sometimes known as freak waves or extreme waves, are waves that appear on a finite background as a result of modulational instability. The height of rogue waves is defined as at least two times higher than the average surrounding background. Rogue waves were observed long time ago in oceans. The well-known one-dimensional nonlinear Schrodinger equation (NLS) with attractive nonlinear interaction is a model equation to investigate rogue waves theoretically. In 1983, Peregrine found an analytic solution of the nonlinear Schrodinger equation [1].

The Peregrine soliton, limiting case of Kuznetsov and Ma soliton [2, 3] and Akhmediev breather [4], explains how rogue waves appear from nowhere and disappear without a trace. The Peregrine soliton is formed from slightly modulated uniform background and grows until it reaches its maximum value at a specific time. Then the amplitude of the soliton decreases while the width increases and finally it vanishes. That is why the Peregrine soliton is known as doubly localized wave (localized both in space and time). It is well known that some physical systems such as optics, plasma and ultracold atoms are also described by the nonlinear Schrodinger equation. Therefore, the existence of the Peregrine soliton, or more generally rogue wave, is not restricted to oceans [5, 6, 7]. The experimental realization of Peregrine soliton was first made in an optical system in 2010 [8] and then in a water wave tank in 2011 [9]. These experimental realizations show good agreement between theory and the experiments. The Peregrine soliton is the first order rational solution of the NLS and the second order rational solution was studied in [10] and observed experimentally in [11]. The ratio of maximum amplitude of the rogue wave to the background amplitude is 3 for the first order rational solution while it is 5 for the second order one. Rogue wave solution of the NLS in the presence of disorder is also investigated in [12]. The originating mechanism of rogue waves is still a matter of debate. The modulational instability is the most popular one but is restricted to nonlinear systems. The

interpretation of rogue waves in terms of the two Akhmediev breather collisions was also made for the rogue waves can occur even in the absence of nonlinear interaction.

Motivated by the investigations of rogue waves in linear systems and by the question of underlying mechanism for the appearance of large amplitude waves, we inquire whether rogue waves occur in a linear optical lattice.

Initially, we take $\Psi = \text{Exp}[i a n + i b n^2]$ and we numerically find the time evolution for the discrete nonlinear Schrodinger equation. Below are the results. In the original paper [13], we discuss that the reason for the appearance of linear rogue waves can be explained using Josephson effect.

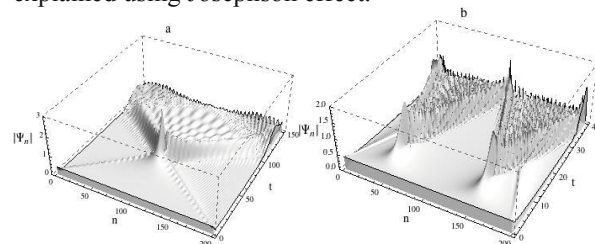


Figure 1: The absolute of the wave function in the non-interacting limit. The system has a single peak when $a=0$, $b=0.005$ (a) W-shaped structure when $a=0$, $b=0.03$ (b)

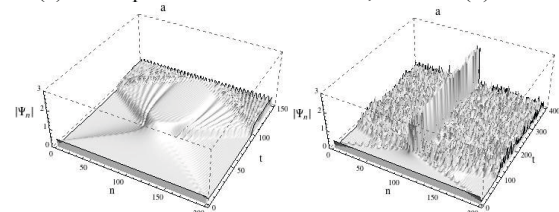


Figure 2: The same parameters as in the Fig.1.a but $g=-1$ (a) and $g=1$ (b) are used. Rogue wave is destroyed in (a) while long-living one is generated in (b).

- [1] D. H. Peregrine, J. Austral. Math. Soc. B 25 16 (1983).
- [2] E. A. Kuznetsov, Sov. Phys. Dokl. 22 507 (1977).
- [3] Ya. C. Ma, Stud. Appl. Math. 60 43 (1979).
- [4] N. N. Akhmediev, V. M. Eleonskii, N. E. Kulagin, Theor. Math. Phys. 72 809 (1987).
- [5] N. Akhmediev, et. al., J. Opt. 15 060201 (2013).
- [6] Yu. V. Bludov, et. All., Phys. Rev. A 80 033610 (2009).
- [7] D. R. Solli et. all. Nature 45 01054 (2007).
- [8] B. Kibler et. all, Nature Physics 6 790 (2010).
- [9] A. Chabchoub, et. all., Phys. Rev. Lett. 106 204502 (2011).
- [10] N. Akhmediev et. all., Phys. Lett. A 373 675 (2009).
- [11] A. Chabchoub, et. all. Phys. Rev. X 2 011015 (2011).
- [12] N. Akhmediev, et. all., Phys. Lett. A 373 2137 (2009).
- [13] C. Yuce, submitted to Phys. Rev. E (2015)

Identifications of S and D Rydberg states in ultracold lithium-7 atoms

B.B. Zelener^{1,2}, V.A. Sautenkov^{1,3}, S.A. Saakyan¹, B.V. Zelener¹, V.E. Fortov¹

¹Joint Institute for High Temperatures of Russian Academy of Sciences, 13 Bd.2 Izhorskaya St., Moscow 125412, Russia

²National Research Nuclear University, "MEPhI", 31 Kashirskoye Chaussee, Moscow 115409, Russia

³P. N. Lebedev Physical Institute of Russian Academy of Sciences, 53 Leninskii Prospect, Moscow 119991, Russia

e-mail: bobozel@mail.ru

In this work we describe our approach for preparation and study of an ultracold gas of Rydberg atoms. Our goals are creation of a Rydberg matter [1] and applications for quantum computers. A magneto-optical trap for ⁷Li atoms was assembled. We trapped 10⁹ ultracold ⁷Li atoms. By using ultraviolet laser (350 nm) a cw two-step excitation of the ground state atoms to highly-excited states is performed. For the identification of highly-excited Rydberg states S and D with n from 41 to 160 we recorded the resonance fluorescence of ultracold atoms in the trap. In Fig. 1 the resonances which correspond to the transitions 2P_{3/2} - 114S_{1/2}, 2P_{3/2} - 114D_{3/2} and 2P_{3/2} - 114D_{5/2} are presented.

- [1] E. A. Manykin, B. B. Zelener, B. V. Zelener, JETP Lett. **92**, 630 (2010).
- [2] M. A. Butlitsky, B. B. Zelener, B. V. Zelener, Journal of Chemical Physics **14**, 141 (2014).
- [3] B. B. Zelener, S. A. Saakyan, V. A. Sautenkov, E. A. Manykin, B. V. Zelener, V. E. Fortov, JETP Lett. **100**, 366 (2014).

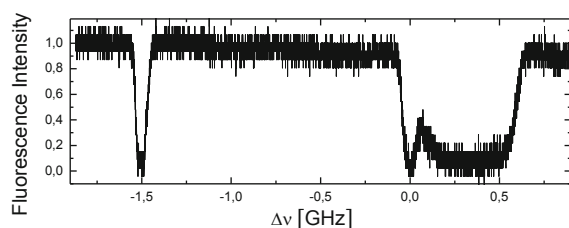


Figure 1: Resonance fluorescence of the trapped ⁷Li atoms on transitions 2P_{3/2} - 114S and 2P_{3/2} - 114D.

The isolated resonance, which corresponds to the transition 2P_{3/2} - 114S, shows a minimal spectral width of 0.1 GHz. The S-states (l = 0) are less sensitive to external perturbations to compare with the D-states (l = 2). The components of 114D-state are not completely resolved due to a large spectral broadening. The measured average frequencies of transitions 2P_{3/2} - 114S_{1/2} and 2P_{3/2} - 114D_{3/2} are 856647.1(3) GHz and 856648.6(3) GHz. We plan to improve the spectral resolution.

Our recent theoretical [2] and experimental [3] results will be discussed.

The work was supported by the Russian Science Foundation, project no. 14-50-00124.

Practical Squeezed-State Measurement-Device-Independent Quantum Cryptography

Yi-Chen Zhang¹, Zhengyu Li², Song Yu¹, Hong Guo^{1,2}

¹ State Key Laboratory of Information Photonics and Optical Communications, Beijing University of Posts and Telecommunications, Beijing 100876, China

² State Key Laboratory of Advanced Optical Communication Systems and Networks, School of Electronics Engineering and Computer Science and Center for Quantum Information Technology, Peking University, Beijing 100871, China
e-mail: zhangyc@bupt.edu.cn

Quantum key distribution (QKD) [1] is one of the most practical applications in the field of quantum information and it enables two distant legitimate parties, Alice and Bob, to establish a secret key through insecure quantum and classical channels. Continuous-variable quantum key distribution (CV-QKD) [2] has attracted much attention in the past few years [1, 2] mainly because it does not need single photon detectors.

Continuous-variable measurement-device-independent QKD (CV-MDI QKD) using coherent or squeezed states [3, 4] have been proposed to defend all attacks against detectors, where squeezed-state based protocol has a better performance than coherent-state based protocol, in terms of secret key rates and the most tolerable excess noise [4]. Comparing to the generation of a coherent state, generating a squeezed state is much more difficult, which becomes the most difficult part of implementing the CV-MDI QKD protocol using squeezed states. Recent researches show that the largest achievable two-mode squeezing in a stable optical configuration has already reached about 10dB [5], where 10dB corresponds to an Einstein-Podolsky-Rosen (EPR) variance of 5.04.

Here we propose a CV-MDI QKD protocol using practical squeezed states, where the variance of the EPR source is only 5.04 [5]. Such practical squeezed-state protocol keeps the advantages of using squeezed

states in CV-MDI QKD protocol, attaining higher secret key rates and transmits longer distance than coherent-state based protocol, and such protocol with a small variance allows one to directly use the EPR state as the source in a practical experiment. If Alice and Bob do use EPR sources, they could completely outplay side-channel attacks in their private spaces which make the CV-MDI QKD protocol more secure.

- [1] V. Scarani, H. Bechmann-Pasquinucci, N. J. Cerf, M. Dusek, N. Lütkenhaus, and M. Peev, “The security of practical quantum key distribution”, *Rev. Mod. Phys.* 81, 1301-1350 (2009).
- [2] C. Weedbrook, S. Pirandola, R. García-Patrón, N. J. Cerf, T. C. Ralph, J. H. Shapiro, S. Lloyd, “Gaussian quantum information”, *Rev. Mod. Phys.* 84, 621-669 (2012).
- [3] Z. Li, Y.-C. Zhang, F. Xu, X. Peng, and H. Guo, “Continuous-variable measurement-device-independent quantum key distribution”, *Phys. Rev. A* 89, 052301 (2014).
- [4] Y.-C. Zhang, Z. Li, S. Yu, W. Gu, X. Peng, and H. Guo, “Continuous-variable measurement-device-independent quantum key distribution using squeezed states”, *Phys. Rev. A* 90, 052325 (2014).
- [5] T. Eberle, V. Händchen, and R. Schnabel, “Stable control of 10 dB two-mode squeezed vacuum states of light”, *Opt. Expr.* 21 11546 (2013).

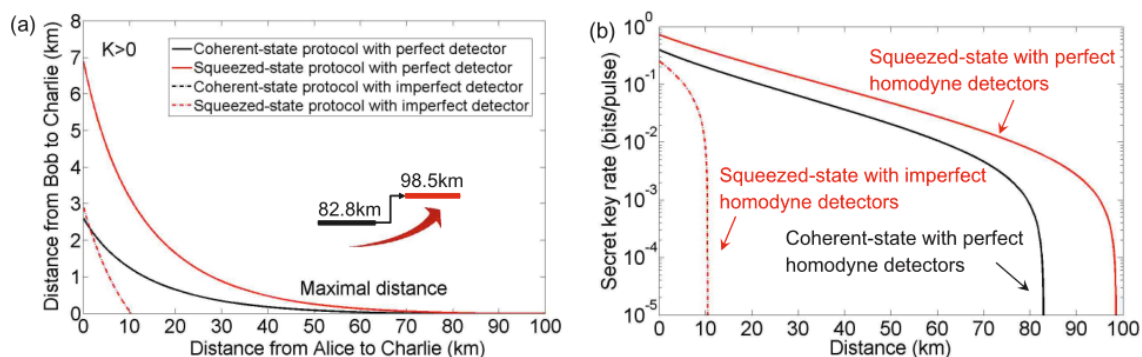


Figure 1: (a) A comparison among the maximal transmission distance for the coherent-state, squeezed-state CV-MDI QKD protocol with perfect and imperfect homodyne detectors, within which the key rate K is positive. (b) Secret key rates of the coherent-state (black), squeezed-state (red) CV-MDI QKD protocol in the most asymmetric case ($L_{BC} = 0\text{ km}$) with perfect and imperfect homodyne detectors. The dot-dash line and solid line represent the situation of using perfect and imperfect detectors, respectively. Here we use the realistic parameters: $V_A = V_B = 5.04$, $\varepsilon = 0.002$, ($\eta = 1$, $v_{el} = 0$) and ($\eta = 0.9$, $v_{el} = 0.015$) representing for the perfect and imperfect homodyne detectors.

Capability investigation of superconductive single-photon detectors optimized for 800 – 1200 nm spectrum range

P. Zolotov^{1,2}, A. Divochiy², Yu. Korneeva¹, Yu. Vakhtomin^{1,2}, V. Seleznev² and K. Smirnov^{1,2}

¹ Moscow State Pedagogical University, 1/1 M. Pirogovskaya Str, Moscow 119991, Russia

² CJSC "Superconducting nanotechnology", 5/22-1 Rossolimo Str, Moscow 119021, Russia

e-mail: zolotovphilipp@gmail.com

We report on our recent studies of the main characteristics of superconductive single-photon detectors (SSPD), modified for micron wavelength, which draw more and more attention due to the modern studies of quantum dots, carbon nanotubes [1] and development of the units for quantum systems. For this work, we have fabricated a number of devices with refined layer design. The easiest way to increase efficiency of SSPD is to add isolator layer $\lambda/4$ thick [2]. In this case, it allowed us to raise detection efficiency up to 30% mark. To reach this number, we have decreased SiO₂ layer thickness under the value of 200 nm thick.

The main aim that we pursued was making a strong opponent for APDs (Avalanche Photo Diode) which have spread worldwide thanks to their ease of use and high efficiency. However, one of the major disadvantages of this type of detectors is sensitivity drop, related to energy gaps in the superconductors they are based on. When we compare spectrum sensitivities of Si- and GaAs-based APDs, we find cavity-formed drop, which on practice can't be completely resolved by neither type of APD. Figure 1 presents comparison of spectrum sensitivity for two forenamed types of APD and SSPD with optimized layer design. As we can see on the figure, SSPD gives efficiency advantage over two types of APD on the range of 950-1200 nm.

It is worth mentioning that cryogenic detectors have a number of advantages related to their work temperatures. Thus, besides high efficiency, SSPD show excellent counting rate without afterpulsing and using gated-mode, low jitter and dark counts rate.

Our paper shows advantages of using SSPD over APD by demonstrating the main characteristics of detectors. Numbers obtained in this work justify popularity growth of SSPD and have straightened the position of SSPD on the market of high efficient single-photon detectors.

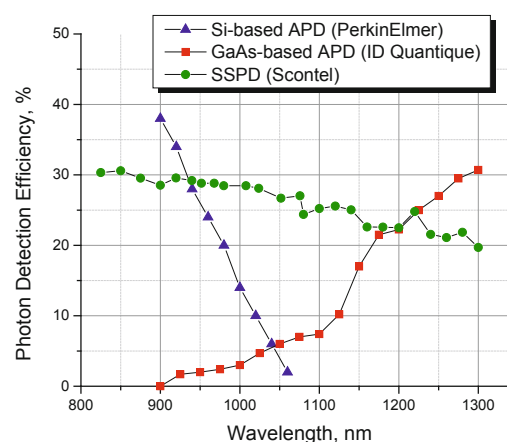


Figure 1: Wavelength dependence of detection efficiency for two types of APD and SSPD with modified isolator layer

[1] Khasminskaya, Svetlana, Feliks Pyatkov, Benjamin S. Flavel, Wolfram H. Pernice, and Ralph Krupke. "Waveguide-Integrated Light-Emitting Carbon Nanotubes." *Advanced Materials* 26, no. 21 (2014): 3465-3472

[2] Korneev, A., Korneeva, Y., Manova, N., Larionov, P., Divochiy, A., Semenov, A., ... & Goltsman, G. (2013). Recent nanowire superconducting single-photon detector optimization for practical applications. *IEEE transactions on applied superconductivity*, 23(3).

Quantum vampire: a new type of action at a distance

I. A. Fedorov^{1,2}, A. E. Ulanov¹, Y. V. Kurochkin¹ and A. I. Lvovsky^{1,2,4}

¹Russian Quantum Center, 100 Novaya St., Skolkovo, Moscow 143025, Russia

²P. N. Lebedev Physics Institute, Leninskiy prospect 53, Moscow 119991, Russia

³Moscow Institute of Physics and Technology, 141700 Dolgoprudny, Russia

⁴Institute for Quantum Science and Technology, University of Calgary, Calgary, Canada T2N 1N4
e-mail: LVOV@ucalgary.ca

We study a situation in which a single photon is with certainty removed from a part of a mode in which a certain optical state has been prepared. Contrary to the "macroscopic" intuition, such intervention will not create any shadow in the beam. The energy will be drawn out of the whole mode, leaving its spatial and temporal structure undisturbed, regardless of the mode to which the annihilation operator is applied. In the experiment, we demonstrate this effect in application to the 1- and 2-photon Fock states of an optical field, distributed over the two arms of the Mach-Zehnder interferometer. Photon annihilation, realized in one of its arms, affects the quantum state in the other arm – so that the recombined state at the output of the interferometer is a pure 0- or 1-photon Fock state, respectively. We verify this experimentally via homodyne tomography.

of the quantum state, as it is in case of the projective measurement.

We expect the quantum vampire effect to find applications in quantum information technology. For example, it enables non-local manipulation of quantum states without precise knowledge of their modes, such as in protocols for distillation of continuous-variable entanglement by photon annihilation. The ability to "steal" a photon without casting a shadow may prove useful for eavesdropping in quantum key distribution as well as developing quantum cloaking devices. We also believe the effect to be of fundamental interest, as quantum action at a distance that is not associated with a local state collapse has not yet been studied.

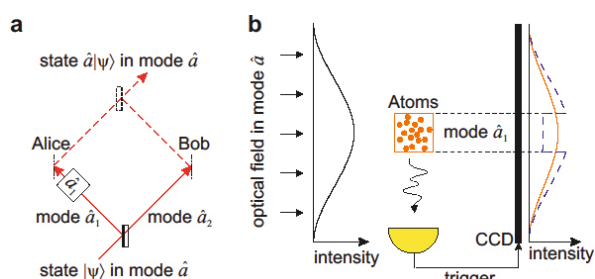


Figure 1: The quantum vampire effect. a) When state $|\psi\rangle$ in the mode defined by annihilation operator a is split between two remote parties, the application of the photon annihilation operator a_1 by one of these parties affects state $|\psi\rangle$ globally. This can be verified by recombining modes a_1 and a_2 on another beamsplitter and analyzing the state in the output. b) Implementation with a cloud of absorptive atoms. Detection of a re-emitted photon heralds a photon annihilation event and triggers recording of image on a CCD camera. Photon subtraction will not cast a shadow on the resulting quantum state, so its intensity distribution (solid orange line) does not change. This contrasts with regular linear absorption, which would cause a local shadow to appear in the intensity distribution (dashed blue line).

Our results show that the photon annihilation operation realizes a new type of a quantum action at a distance, since it is not the projection measurement, which is the only quantum operator whose nonlocal action has been tested to date. One remarkable feature of this action is that it is not associated with collapse

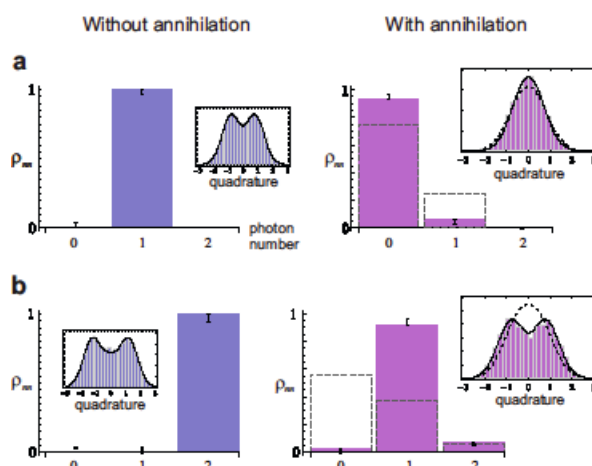


Figure 2: Experimental results for the initial state of mode a being the one-photon (a) and two-photon (b) Fock states. In each panel, the experimentally observed quadrature distributions and reconstructed diagonal elements of the density matrix are displayed together with those theoretically expected.

[1] I. A. Fedorov, A. E. Ulanov, Y. V. Kurochkin and A. I. Lvovsky, *Optica* **2**, 112 (2015).

Symmetry breaking in quantum dot coupled to ultracold bosons

Dmitry Chichinadze^{1,2}, Pedro Ribeiro¹, Yulia Shchadilova¹, and Alexey Rubtsov^{1,2}

¹Russian Quantum Center, 100 Novaya St., Skolkovo, Moscow 143025, Russia

²Department of Physics, Lomonosov Moscow State University, 119991 Moscow, Russia

e-mail: dchichinadze@gmail.com

The physics of a single impurity interacting with its environment remains a cornerstone for the understanding of condensed matter systems. The Kondo [1], impurity-Anderson [2] and Caldeira and Leggett [3] models as well as Fermi and Bose polarons [4] are some of the many remarkable examples exhibiting rich physics on the core of our understanding of many physical phenomena.

Besides their direct experimental relevance, single impurity models constitutes an important basis for advanced computational approaches, such as dynamical mean field theory [5].

Recent experimental progress made it possible to prepare an arbitrary landscape potential for gases of ultracold atoms, including creation of the local defects in the lattices, e.g. quantum dots. These defects behaves similarly to impurities in solid state materials. Depending on the statistics of the particles on the optical lattice these impurities can be of bosonic or fermionic nature. While the former are quite well studied, only recently bosonic impurities started to receive more attention [6, 7].

We deal with such a bosonic impurity model - the Bose-Anderson model - describing the coupling of quantum dot with local on-site interaction with gas of non-interacting bosons on the lattice is described. The Hamiltonian reads

$$H = \varepsilon_0 \hat{a}_0^\dagger \hat{a}_0 + \frac{1}{2} U \hat{a}_0^\dagger \hat{a}_0^\dagger \hat{a}_0 \hat{a}_0 - V (\hat{b}_0^\dagger \hat{a}_0 + \hat{a}_0^\dagger \hat{b}_0) - t \sum_{\langle ij \rangle} (\hat{b}_i^\dagger \hat{b}_j + \hat{b}_j^\dagger \hat{b}_i), \quad (1)$$

where operators \hat{a}_0 and \hat{b}_i correspond to the impurity site and the lattice sites respectively.

Despite the fact that only local interactions present in the model, it exhibits a continuous symmetry breaking on the impurity site and phase transition from Mott to superfluid state takes place [6, 7].

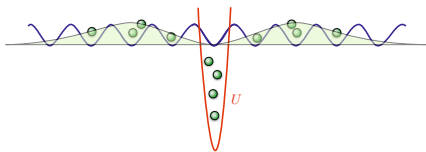


Figure 1: Sketch of the lattice with non-interacting bosons coupled to single impurity (red) with on-site interaction U . In the state with $\langle \hat{a}_0 \rangle = 0$ the density of bosons on the lattice vanishes near the impurity site.

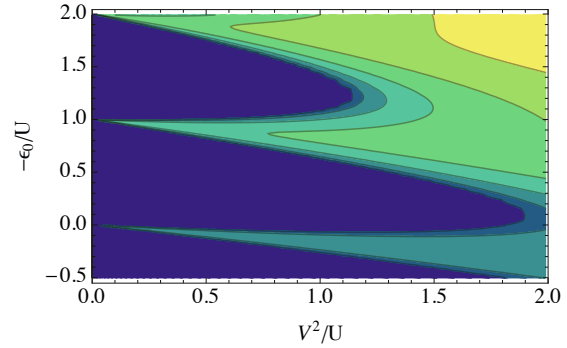


Figure 2: Phase diagram of the single impurity Bose-Anderson model (1) on the cubic lattice with $U = 1$. Dark regions of the phase diagram correspond to the states with $\langle \hat{a}_0 \rangle = 0$, other regions correspond to the symmetry is broken phase with $\langle \hat{a}_0 \rangle \neq 0$.

We develop an approach that is able to capture the essential features of phase transition in the Bose-Anderson model. In particular, it is capable to reproduce an equilibrium phase diagram of the model (Fig. 2). Our method is based on the factorization of the wave-function in the form of tensor product $|\Psi\rangle = |\Psi_{\text{cluster}}\rangle \otimes |\Psi_{\text{bath}}\rangle$, where $|\Psi_{\text{cluster}}\rangle$ describes the impurity and several neighboring sites and treated exactly, while the other part is treated on the mean-field level. Using this factorization it is possible to build up variational scheme to find the ground state of the system in this class of trial wave-functions. A key advantage of our method is its extension to describe dynamics of the system. We study the evolution of the the order parameter $\langle \hat{a}_0 \rangle$ as the system is quenched to the Mott phase.

The authors acknowledge the support from the Dynasty foundation and the RFBR 14-02-01219.

- [1] J. Kondo *Progr. Theor. Phys.* **32**(1), 37 (1964).
- [2] P.W. Anderson *Phys. Rev.* **124**(1), 41 (1961).
- [3] A.O. Caldeira, et al. *Annals of Physics* **149**(2), 374 (1983).
- [4] L.D. Landau *Phys. Z. Sowjet.* **3**, 664 (1933).
- [5] A. Georges, et al. *Rev. Mod. Phys.* **68**(1), 13 (1996).
- [6] H.-J. Lee, et al. *Phys. Rev. B* **82**, 054516 (2010).
- [7] J. Warnes, et al. *Eur. Phys. J. B* **85**, 341 (2012).

Coherence, absorption and heating in a molecule interferometer

J. P. Cotter¹, S. Eibenberger¹, L. Mairhofer¹, X. Cheng¹, P. Asenbaum¹, M. Arndt¹
K. Walter², S. Nimmrichter² and K. Hornberger²

¹University of Vienna, Faculty of Physics, VCQ & QuNaBioS, Boltzmannngasse 5, A-1090 Vienna, Austria

²University of Duisburg-Essen, Faculty of Physics, Lotharstrae 1-21, 47048 Duisburg

e-mail: joseph.cotter@univie.ac.at

Matter-wave interferometry can be used to make precise measurements of particle properties and fundamental constants and help probe the foundations of quantum physics.

At the core of all interferometers is a beam splitter capable of dividing and recombining the wave function whilst maintaining a well defined phase difference. Optical phase gratings are used as beam splitters for a wide variety of large, complex molecules in both far-field diffraction [1] and in near-field Kapitza-Dirac-Talbot-Lau interferometry [2] (KDTLI). Recently, this has enabled quantum interference with particles consisting of more than 800 atoms and with a combined mass exceeding 10^4 amu to be observed [3].

The inherently rich internal structure of molecules makes their interaction with an optical grating more complex. Although the dominant beam splitting mechanism in the KDTLI interferometer occurs at a phase grating, photon absorption can still occur and play an important role in the diffraction process. If the absorbing molecule has a sufficiently complex internal structure then the energy of any absorbed photon can rapidly be redistributed across many internal degrees of freedom. By transferring the photon energy into vibrational excitation no which-path information is revealed, enabling spatial coherence to be maintained. The complex internal structure can also been exploited to achieve photo-depletion beam splitters using single-photon ionisation [4] and fragmentation [5].

Here, we describe some recent experiments in the KDTLI interferometer. Using a pseudo-random time-of-flight technique we have improved our velocity resolution by an order of magnitude over our previous experiments. This has enabled us to study a three component beam splitting mechanism which occurs for complex molecules in a standing light wave. We observe matter-wave phase modulation induced by the electric dipole interaction between a polarisable molecule and the laser field. In addition, the absorption of photons induces a matterwave amplitude modulation which increases the internal temperature of the molecule. Each absorption event also splits the molecular wave function into a coherent superposition of momentum states which arise from the indistinguishability of the photon propagation directions in the standing light wave. We find that center-

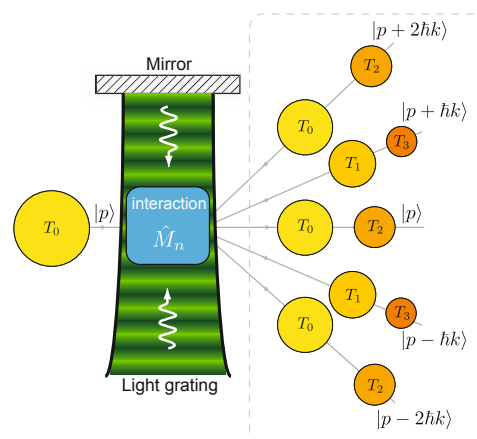


Figure 1: An ensemble of molecules with temperature T_0 diffracts at a standing light wave. The periodic dipole potential they experience distributes the ensemble into different orders separated by even multiples of the photon momentum, $2m\hbar k$. The absorption of n photons increases the temperature of the molecule, $T_n = T_0 + n\delta T$. Those molecules which absorb populate different orders, namely those with odd integer multiples of the photon momentum, $m\hbar k$. This results in a series of overlapping, position synchronous interference patterns.

of-mass coherence can be maintained even when the internal energy and entropy of the interfering particle are substantially increased by the absorption of photons. This may lead to the realisation of temperature labelling interferometers for particles that neither ionise, fragment nor reradiate upon absorption.

- [1] O. Nairz *et. al.*, Phys. Rev. Lett., **87**, 160401 (2001).
- [2] S. Gerlich *et. al.*, Nat. Phys., **3** 711-715 (2007).
- [3] S. Eibenberger *et. al.*, Phys. Chem. Chem. Phys., **15**, 14696-14700 (2013).
- [4] P. Haslinger *et. al.*, Nat. Phys., **9**, 144 - 148 (2013).
- [5] N. Dörre *et. al.*, Phys. Rev. Lett., **113**, 233001 (2014).

Optical Coherence in Closed-Loop Double-V Configuration

D. Eger, S. Smartsev, O. Firstenberg and N. Davidson

Department of the Physics of Complex Systems, Weizmann Institute of Science, Rehovot 76100, Israel

email: david.eger@weizmann.ac.il

Coherent interactions of light with atomic ensembles have been extensively studied in various electronic level configurations, such as Λ , ladder, V, double- Λ and N [1]. Recently it has been suggested [2] that a double-V configuration may provide robust quantum superposition states in closed-loop multilevel system which results in several quantum interference phenomena.

In this presentation we demonstrate an experimental realization of a closed double-V configuration using D1 transition in ^{87}Rb vapor (see Fig. 1). We investigate four-wave-mixing (FWM) in this system and show that as predicted we can get a whole scale of atomic phenomena including electromagnetically-induced-transparency (EIT), electromagnetically-induced -absorption (EIA), parametric generation, and huge enhancement of refractive index accompanied with negligible absorption. Furthermore we show that the transition between the different processes can be controlled by selecting the frequency detuning from the atomic resonance.

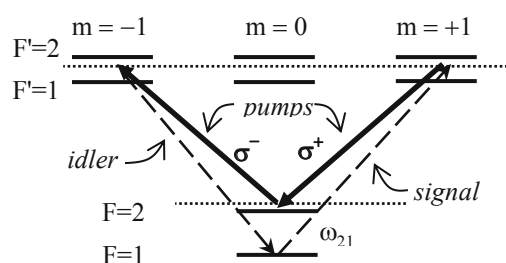


Figure 2: Closed Double-V electronic level configuration for D1 transition in ^{87}Rb .

A ^{87}Rb cell heated to 50°C with 10 torr of N_2 buffer-gas is used in the experiment. We direct a strong ‘pump’ beam collinearly with a weak ‘signal’ with identical circular polarization, as well as an additional strong ‘pump’ with the orthogonal polarization. A small angular deflection in the range of 1.5 to 20 mrad is introduced between the two pump beams. The signal frequency is $\omega_{21} = 6.834$ GHz higher than the pumps’ frequency. The signal and the ‘generated idler’ (along the direction of the second pump beam) are detected at the cell output after removing the pumps. Spectra of intensity versus the two-photon detuning were recorded by scanning the frequency of the signal using an acousto-optic modulator. Results of spectra taken for different one-photon detuning values are shown in Fig. 2. As seen in the figure, the signal spectra changes from EIT to dispersive and EIA as the frequency is detuned from one photon resonance, while the idler

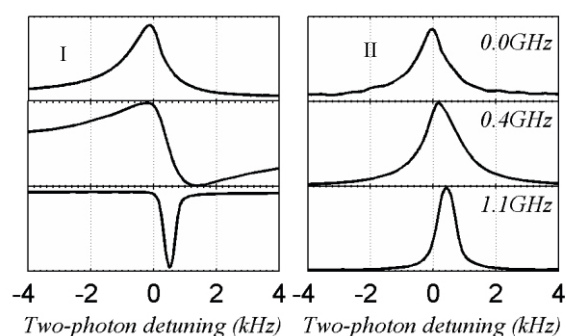


Figure 1 Experimental lineshapes for different one-photon detunings (written on the right). (I) signal and (II) idler

spectra keep its Lorentzian shape. In Fig. 3 we show an example of pulse delay measurements in the two channels.

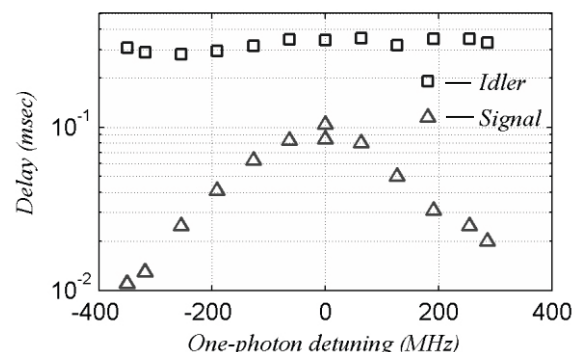


Figure 3: Delay of signal and idler pulses with respect to the incoming signal pulse as a function of one-photon detuning.

As seen, the delay of the idler pulse is constant while that of the signal drops sharply with the one photon detuning. By reducing the pumps power we were able to increase the idler’s delay to up to 2 ms, corresponding to a group velocity of 37 m/s. At the same conditions, the delay of the signal pulse was only 0.05 ms.

In conclusion, the closed double-V configuration system investigated here presents a variety of quantum interference effects that may be applied for different low power and quantum optical processes.

- [1] M. D. Lukin, P.R. Hemmer and M.O. Scully, *Advances in Atomic, Molecular And Optical Physics*, **42**,347 (2000)
- [2] A. Kani and H. Wanare, *Opt. Exp.*, **22**, 15305 (2014)

Defining the properties of the electromagnetic field in photonic crystals by method of plane waves expansion

A. Garifullin¹, M. Khamadeev¹ and R. Gainutdinov¹

¹*Department of Physics, Kazan Federal University, 18 Kremlevskaya St., Kazan 420008, Russia*

e-mail: *adelgarifullin2012@gmail.com*

Photonic crystals (PCs) are periodic structures, whose period is comparable to the wavelength of light of the optical range [1-2]. PCs are very interesting due to the broad field of perspective applications. Possible application of photonic crystals is their use in fiber optics, in the creation of light sources with high efficiency, electro-optical and completely optical integrated circuits, low-threshold lasers, etc.. Such a wide range of applications of photonic crystals is possible due to the presence of so-called photonic band gap. It is spectral range within which propagation of light in a photonic crystal is suppressed in all or in some chosen directions. However, despite on interest to PCs with the practical point of view, it is interesting for studying of important properties such as the ability to control the frequency of the spontaneous emission and the rate of emission, and even to control the electron mass [3]. To study these quantum electrodynamic phenomena requires knowledge of field structure. In this paper, this problem is studied with the help of Maxwell's equations and periodic boundary conditions. Starting with the analysis of one-dimensional case, was obtained a graphical representation of changes in the components of the Bloch functions depending on the wave vector, and the corresponding band diagrams. Using these results allow to monitor the distribution of the photon energies for the various components for the various states that may be necessary for the theoretical calculations.

- [1] V. N. Astratov, V. N. Bogomolov, A. A. Kaplyanskii, A. V. Prokofiev, L. A. Samoilovich, S. M. Samoilovich, Yu. A. Vlasov, *Nuovo Cimento D* **17**, 1349 (1995).
- [2] S. John, *Phys. Rev. Lett* **58**, 2486 (1987).
- [3] R. Kh. Gainutdinov, M. A. Khamadeev, M. Kh. Salakhov, *Phys. Rev. A* **85**, 053836(1-7) (2012).



Manifestations of nematic degrees of freedom in the Raman response function of iron pnictides

U. Karahasanovic¹ and J. Schmalian¹

¹*Institut für Theorie der Kondensierten Materie, Karlsruher Institut für Technologie, DE-76131 Karlsruhe, Germany*

e-mail: una.karahasanovic@kit.edu

The electronic nematic phase in pnictides, characterized by the broken C_4 symmetry, is believed to be generated by the presence of magnetic fluctuations associated with the striped phase [1], and occurs as a thin sliver in the phase diagram, above the magnetic transition temperature.

Detecting the presence of nematic degrees of freedom in iron-based superconductors is a difficult task, since it involves measuring four spin correlation functions. We show that the nematic degrees of freedom manifest themselves in the experimentally measurable Raman response function, which is a density-density correlation weighted by an appropriate form factor [2, 3]. We calculate the Raman response function in the large N limit by considering Aslamazov-Larkin type of diagrams that contain series of inserted boxed-like diagrams that resemble the nematic coupling constant of the theory. These diagrams effectively account for collisions between spin fluctuations. We demonstrate that the Raman response function diverges at the structural phase transition.

- [1] R. Fernandes and J. Schmalian, *Supercond. Sci. Technol.* **25**, 084005 (2012).
- [2] Y. Gallais et al, *Phys. Rev. Lett.* **111**, 267001 (2013).
- [3] S. Caprara et al, *Phys. Rev. Lett.* **95**, 117004 (2005).

Electron-phonon interaction time in disordered TiN films

A.I. Kardakova¹, P.C.J.J. Coumou², M.I. Finkel¹, G.N. Goltsman¹, and T.M. Klapwijk^{1,2}

¹Physics Department, Moscow State Pedagogical University, Moscow, 119435, Russian Federation

²Kavli Institute of the Nanoscience, Delft University of Technology, 2628 CJ Delft, The Netherlands

e-mail: kardakova@rplab.ru

Thin titanium nitride films have recently demonstrated advantageous properties for superconducting quantum computing and astrophysics applications. The high quality factors of TiN coplanar resonators, on the order of 10^7 [1], result in long lifetimes for quantum information storage circuits [1, 2], and microwave kinetic inductance detectors (MKID) [3, 4] that have potential for single photon sensitivity at low temperatures. Furthermore, the high kinetic inductance of TiN films have been used in microwave parametric amplifiers [5] and show potential for use in coherent quantum phase slip qubits [6]. In all these applications, the essential characteristics of the devices such as noise in detectors and decoherence time in qubits are strongly dependent on the energy relaxation process in the material. An accurate knowledge of the relaxation rate is needed for the successful development of the devices.

However, in materials like TiN the increase of the normal state resistivity leads gradually to a transition from the superconducting state to some form of an insulating state [7]. It has been shown that the superconducting state becomes spatially inhomogeneous for increasing disorder. Moreover, a systematic study of the electrodynamic response of the microwave resonators showed that the behavior of TiN films deviates from conventional Mattis-Bardeen theory and from the behavior of conventional superconductors such as aluminum [8]. A proposed conjecture is that the anomalous response occurring in materials like TiN is due to their inhomogeneous superconducting properties.

Our focus in this work is a study of the electron-phonon interaction rate for the case of strongly disordered TiN films in order to identify a possible dependence of the relaxation time on the level of disorder.

In the superconducting state, the relaxation process occurs initially by a redistribution of the non-equilibrium quasiparticles over energy and is followed by a recombination into Cooper pairs. The recombination time increases exponentially with decreasing temperature reflecting the reduced availability of quasiparticles [9], therefore one prefers to work far below T_c . In addition the scale for the recombination time is set by the electron-phonon interaction time.

To determine the electron-phonon time we used the strong temperature dependence of resistance at the

superconducting transition. A film carrying a small dc current I is exposed to an amplitude-modulated signal from a submillimeter source. The modulation frequency is ω_m . The absorbed radiation power causes an increase of the electron temperature T_e , which leads to an increase of the film resistance δR followed by a voltage signal proportional to the bias current $\delta V = I\delta R$. To extract the energy relaxation time we use the frequency dependence of the amplitude of the output voltage $\delta V(\omega_m)$, and the 3-dB roll-off provides the characteristic time.

We have measured the energy relaxation times from the electron-bath to phonon-bath in strongly disordered TiN films, grown by atomic layer deposition. The measured values of τ_{eph} vary from 12 ns to 91 ns. Over a temperature range from 3.4 to 1.7 K they follow T^{-3} temperature dependence, consistent with values of τ_{eph} reported before for sputtered TiN films [10]. For the most disordered film, with an effective elastic mean free path of 0.35 nm, we find a faster relaxation and a stronger temperature dependence, which may be an additional indication of the influence of strong disorder on a superconductor.

- [1] M. R. Vissers, et al, Appl. Phys. Lett., 97, 232509, (2010).
- [2] J. B. Chang, et al, Appl. Phys. Lett., 103, 012602, (2013).
- [3] H. G. Leduc, et al, Appl. Phys. Lett., 97, 102509, (2010).
- [4] J. Gao, et al, Appl. Phys. Lett., 101, 142602, (2012).
- [5] B. H. Eom, et al, Nature Phys., 8, 623, (2012).
- [6] O. V. Astafiev, et al, Nature, 484, 355, (2012).
- [7] B. Sacepe, et al, Phys. Rev. Lett., 101, 157006, (2008).
- [8] E.F.C. Driessen, et al, Phys. Rev. Lett., 109, 107003, (2012).
- [9] S.B. Kaplan, et al, Phys. Rev. B., 14, 4854, (1976).
- [10] A. Kardakova, et al, Appl. Phys. Lett., 103, 252602, (2013).

Probing radially- and azimuthally polarized light with photo-induced azobenzene polymers

A.V. Kharitonov and S.S. Kharintsev

Department of Optics and Nanophotonics, Institute of Physics, Kazan Federal University, Kremlevskaya, 16, Kazan, 420008, Russian Federation
e-mail: antonkharitonov91@gmail.com

Over the last few years, together with the development of three dimensional optical material engineering [1], the designing and manipulation of the spatial structure of optical fields became a topical research area in photonics [2]. In general, an electromagnetic wave structure is characterized by distribution of polarization, amplitude and phase. Until recently, the diversity of polarizations was limited to three types: linear, circular and elliptical. The transformation between these polarizations, as well as their identification is easily accomplished by standard optical instruments such as polarizers, quarter- and half-wave plates. The generation of unprecedented polarization states becomes possible due to the development of polarization converters based on multi-element wave-plates [3], metamaterials [4, 5] and plasmonic metasurfaces [6].

This work focuses on investigation of radially and azimuthally polarized laser beams. According to analytical calculations [7], when focusing the radial/azimuthal mode with a high numerical aperture lens ($NA > 1$), a strong longitudinal (towards the wave vector) electric/magnetic field (up to 5 times higher compared to transverse one) arises in the focal region. On the other hand, conventionally polarized light mainly remains the transverse nature provided that light is tightly focused [7]. This unique feature of radial and azimuthal beams make them very attractive for applications, ranging from single molecule spectroscopy [8, 9, 10] and high resolution near-field optical microscopy [11] to optical data storage [12] and plasmonic nanoparticle-assisted photothermal therapy [13]. In practice, radial and azimuthal modes can be generated through transformation of linearly polarized light by means of special polarization converter. In this Letter we examine two kinds of radial/azimuthal mode converters: polarizer, consisting of four oriented half-wave plates [3], and “s-waveplate” based on metamaterial [4]. Strong focusing the radial and azimuthal modes is probed with photoinduced surface deformations in azopolymer thin films [14, 15]. In order to distinguish the longitudinal and transverse electric field components in the total intensity we apply an optical-field gradient force model [16].

- [1] W. Cai and V. Shalaev, *Optical Metamaterials: Fundamentals and applications* (Springer, New York, 2009).
- [2] J.B. Pendry, D. Schurig and D.R. Smith, *Science* **311**, 1780 (2006).
- [3] R. Dorn, S. Quabis and G. Leuchs, *Phys. Rev. Lett.* **91**, 1 (2003).
- [4] M. Beresna, M. Gecevicius and P.G. Kazansky, *Opt. Mat. Express* **1**, 783 (2011).
- [5] M. Gecevicius et al., *Appl. Phys. Lett.* **104**, 1 (2014).
- [6] N. Yu, et al., *Science* **334** (2011) 333.
- [7] L. Novotny and B. Hecht, *Principles of Nanooptics* (Cambridge University Press, Cambridge, 2006).
- [8] X.S. Xie and J.K. Trautman, *Annu. Rev. Phys. Chem.* **49**, 441 (1998).
- [9] B. Sick, B. Hecht and L. Novotny, *Phys. Rev. Lett.* **85**, 4482 (2000).
- [10] L. Novotny et al., *Phys. Rev. Lett.* **86**, 5251 (2001).
- [11] L. Novotny, E.J. Sanchez and X.S. Xie, *Ultramicroscopy* **71**, 21 (1998).
- [12] P. Rochon, J. Gosselin and S. Xie, *Appl. Phys. Lett.* **60**, 4 (1992).
- [13] H. Kang et al., *Appl. Phys. Lett.* **96**, 063702-1 (2010).
- [14] Y. Gilbert et al., *Opt. Lett.* **31**, 613 (2006).
- [15] S.S. Kharintsev et al., *ACS Photonics* **1**, 1025 (2014).
- [16] S. Bian et al., *J. Appl. Phys.* **8**, 4497 (1999).

Complete characterization of multimode quantum process

Ilya A. Fedorov, Aleksey K. Fedorov, and Yury V. Kurochkin

Russian Quantum Center, 100 Novaya St., Skolkovo, Moscow 143025, Russia

e-mail: yk@rqc.ru

Alexander I. Lvovsky

Russian Quantum Center, 100 Novaya St., Skolkovo, Moscow 143025, Russia and Institute for Quantum Science and Technology, University of Calgary, Calgary, Canada T2N 1N4

In order to develop complex quantum circuits, we need a technique to characterize each element of the circuit. This task is addressed by quantum process tomography, in which the element (quantum process) is tested by a spanning set of density matrices over the relevant Hilbert space. Measurement result allows one to predict the result of the process on an arbitrary density matrix. Previous results of complete tomography are related to single-mode processes. In this work we broaden coherent-state quantum process tomography [1] combined with the maximum likelihood method [2], to the multimode case. To demonstrate the capability of our method, we demonstrate complete characterization of the beamsplitter – the most common two-mode process. For Fock states up to $N = 2$, this process is characterized by a rank-8 tensor which has $\sim 10^3$ non-zero, generally complex elements (Fig. 1). The beautiful property of our method is that it allows predicting the quantum properties of the process like the Hong-Ou-Mandel effect (Fig 2.) while using only coherent states for process probing.

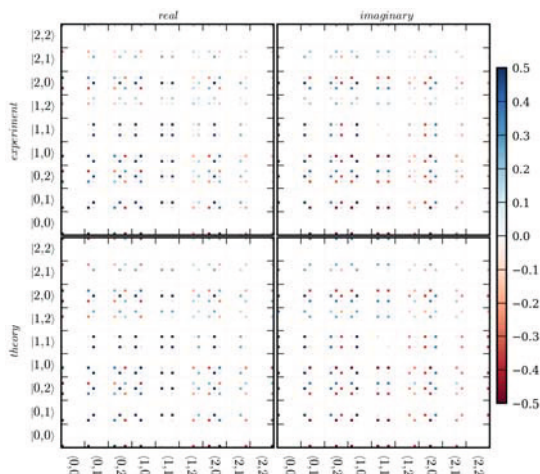


Figure 1: Reconstructed (top) and theoretically expected (bottom) process tensor in the Fock space up to maximum photon number equal two.

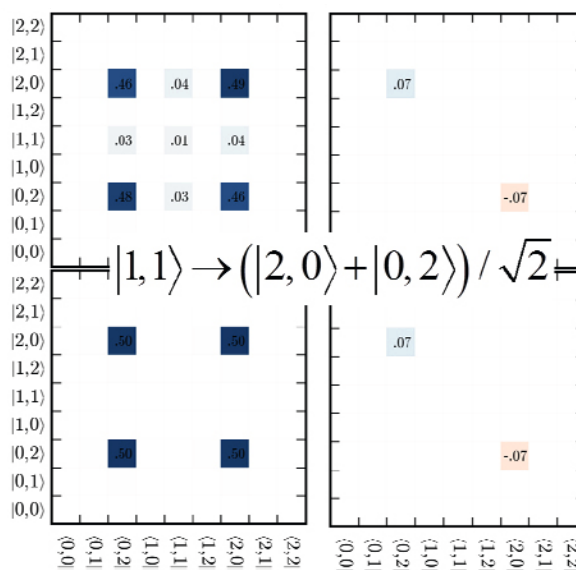


Figure 2: Reconstructed (top) and theoretically expected (bottom) part of the tensor, corresponding to the Hong-Ou-Mandel effect.

[1] M. Lobino et al., Science 322, 563 (2008).
 [2] A. Anis and A. I. Lvovsky, New Journal of Physics 14, 105021 (2012).



Frequency combs and platicons in optical microresonators with normal GVD

V.E. Lobanov¹, G. Lihachev^{1,2}, T. J. Kippenberg³ and M.L. Gorodetsky^{1,2}

¹Russian Quantum Center, 100 Novaya St., Skolkovo, Moscow 143025, Russia

²Faculty of Physics, M. V. Lomonosov Moscow State University, Moscow 119991, Russia

³Ecole Polytechnique Federale de Lausanne, CH 1015, Lausanne, Switzerland

e-mail: mg@rqc.ru

High-quality factor nonlinear optical whispering gallery mode and ring-type microresonators are attracting attention as a platform for optical frequency-comb generation [1]. When a microresonator with anomalous group velocity dispersion (GVD) is pumped by a c.w. laser, a frequency comb of equidistant optical lines in spectral domain can appear due to cascaded four-wave mixing. The spacing between the lines corresponds to the free spectral range (FSR, typically several gigahertz up to terahertz) of the fundamental azimuthal modes. Unlike conventional mode-locked laser-based frequency combs, microresonator based combs generally do not correspond to stable ultrashort pulses in time domain because of arbitrary phase relations between the comb lines obtained in the process of formation. This obstacle is possible to overcome using soliton regime, when a c.w. laser beam is converted into a train of femtosecond bright soliton pulses, corresponding to a low-noise smooth spectral envelope frequency comb in spectral domain [2].

Obtaining anomalous GVD in broad band for arbitrary centered wavelength is challenging in microresonators since material GVD in the visible and near IR is mostly normal. Mode spectra in real microresonators may significantly deviate from theoretical ones due to mode coupling between different families of modes. Individual resonant normal frequencies of coupled modes are therefore shifted due to avoided mode crossing. We show that if just the pump mode eigenfrequency is shifted due to the mode coupling, it is possible to generate in microresonators with normal GVD stable ultrashort flat-top pulses, which we call platicons [3]. We reveal that if this shift is large enough, platicons may be generated spontaneously when the laser frequency is tuned through the effective zero detuning point of a high-Q resonance. Figure 1 shows that in this solitonic regime the width of the frequency comb may be tuned varying pump detuning. We also show that platicon generation is possible even in the absence of pump mode shift under the condition of bichromatic or amplitude-modulated pump. Such approach is efficient if pump modulation frequency or frequency difference between two pump waves is close to FSR. Proposed approach is experimentally feasible since comb generation from a bichromatic pump has been already studied experi-

mentally.

We found that generation of wide platicons in normal GVD microresonators is significantly more effective in terms of transformation of c.w. power into power of pulse train than generation of bright solitons in microresonators with the same absolute value anomalous GVD.

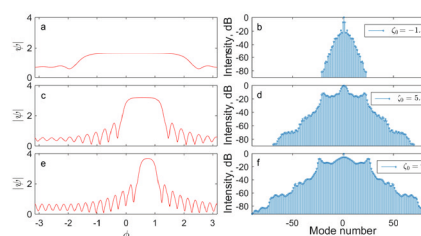


Figure 1: Left: Numerically simulated shapes Ψ of optical platicons in normal GVD microresonators for different values of laser detunings ζ_0 . Right: Corresponding optical spectra.

- [1] T. J. Kippenberg, R. Holzwarth, and S. A. Diddams, Microresonator-based optical frequency combs, *Science* **332**, 555–559 (2011).
- [2] T. Herr, V. Brasch, J. D. Jost, C. Y. Wang, N. M. Kondratiev, M. L. Gorodetsky, and T. J. Kippenberg, Temporal solitons in optical microresonators, *Nature Photon.* **8**, 145–152 (2014).
- [3] V.E. Lobanov, G. Lihachev, T. J. Kippenberg, and M.L. Gorodetsky, Frequency combs and platicons in optical microresonators with normal GVD, *Opt. Express* **23**, 7713–7721 (2015)

A scalable method for measuring entanglement entropy of quantum many-body systems.

A. Lukin¹, P. Preiss¹, E. Tai¹, M. Rispoli¹, R. Ma¹, R. Islam¹, and M. Greiner^{1,2}

¹*Department of Physics, Harvard University, Cambridge, Massachusetts, 02138, USA*
e-mail: alukin@physics.harvard.edu

Quantum many-body systems far from equilibrium are challenging to understand due to the spreading of quantum correlations among the constituents. Measuring the entanglement growth in such a system can serve to characterize the dynamical phases. We use high precision optical potentials in a quantum gas microscope to investigate quench dynamics and entanglement of a few-body bosonic system. The entanglement entropy is directly estimated by interfering two identically prepared copies of the same dynamical state, in a many-body extension of the two particle Hong-Ou-Mandel interference of bosons. This approach provides a versatile and scalable protocol for investigating the purity and entanglement growth of our system.



One-dimensional model of chirped slab photonic crystal

M. Libman¹, **N. M. Kondratyev**², and **M. L. Gorodetsky**^{1,2}

¹Moscow State University, Leninskie Gory, Moscow 119991, Russia

²Russian Quantum Center, 100 Novaya St., Skolkovo, Moscow 143025, Russia

e-mail: limixis@gmail.com

Several photonic applications need devices with special spectral and dispersive properties. Generating optical signals of a given form such as ultra-short laser pulses or super-continuum are among those tasks [1]. Photonic crystals which spectral and dispersive properties are set by their design can be employed for that purpose [2]. A simple model of such one-dimensional photonic crystal is a Bragg mirror, consisting of alternating dielectric layers with high and low refractive indices. This simple model enables us to understand the way of engineering optical properties. It is possible to achieve required dispersion law and to extend the bandwidth of the mirror at the same time by chirping width of the layers [3]. These methods were mostly used for lasers and coatings [4, 5]. The same methods are now applied for the photonic crystal.

In our work we show that a simple one-dimensional model of a multi-layered mirror can be employed for modeling of a slab waveguide with periodically changing width. It is shown that this width change can be recalculated to the effective refraction index modulation. Using the transfer-matrix method [4, 6] of transmission properties calculation we investigate semi-analytically the properties of the system's bandgap. We derive the equation for the bandgap

$$\left(\frac{n - n_0}{n + n_0}\right)^2 \geq \left(\frac{e^{k(nl+n_0l_0)} \pm 1}{e^{knl} \pm e^{kn_0l_0}}\right)^2,$$

where $n = n_{\text{eff}}(k, d)$ and $n_0 = n_{\text{eff}}(k, d_0)$ are effective refraction indexes of layers, l and l_0 – layer lengths, d, d_0 – layer widths, and k is free-space wavenumber, and show that there are thicknesses, where the bandgap shrinks, and give simple relations for that points locations. Thus, using waveguide dispersion approximations from [8], we build an analytical approximations for bandgap borders near those special points (fig. 1).

Furthermore a one-dimensional chirped Bragg mirror model was built taking into account the waveguide dispersion. Analytical method [3] was realized in this model to calculate the chirp law for the desired dispersive characteristics. Though the obtained GVD is not exactly the desired one, the mean value of it corresponds to the required law (fig. 2). To get rid of the oscillations one can apply known optimization techniques to the mirror structure [3].

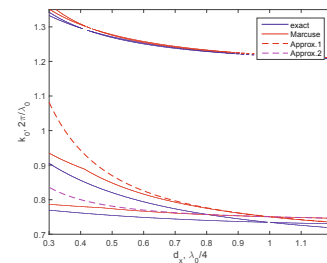


Figure 1: Band structure (gap borders) for exact dispersion [7] and for waveguide dispersion approximation [8]. The dashed lines are $d^{3/2}$ -approximations near the intersection point (d is first layer width)

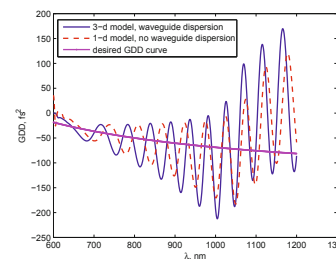


Figure 2: Desired GDD dispersion law (in magenta) and dispersions of the mirror with calculated chirp. Solid and dashed lines represent 1-D and 3-D models, respectively.

- [1] R. Szipcs, K. Ferencz, C. Spielmann, and F. Krausz, *Opt. Lett.*, **19**, 201-203, (1994).
- [2] R. Szipcs and A. Kohazi-Kis, *Appl. Phys. B*, **65**, 115-136, (1997).
- [3] N. Matuschek, Ph.D thesis, Swiss Federal Institute of Technology Zurich, 1999.
- [4] T. Makino, *Progress In Electromagnetics Research*, **10**, 271-319, (1995).
- [5] Z. Knittel, *Optics of Thin Films* (John Wiley & Sons Ltd., 1976), Sec. 2.5.
- [6] S. J. Orfanidis, *Electromagnetic Waves and Antennas*, (Rutgers University, 2008), Chap. 6.
- [7] J. Adams, *An Introduction to Optical Waveguides* (Wiley-Interscience, New York, 1981), Chap 6.
- [8] D. Marcuse, *Light Transmission Optics* (Van Nostrand Reinhold, New York, 1982), Chap.8.

Squeezing of a collective atomic motion

Oxana Mishina, Giovanna Morigi

Theoretische Physik, Universitt des Saarlandes, D-66041 Saarbrcken, Germany

e-mail: omishina@gmail.com

Experiments with the trapped particles show the ability to manipulate the motion of a single particle at the quantum level, and to drive it into an arbitrary quantum state following a generic algorithm [1]. When instead of one particle several of them would be driven into a collective quantum state of motion, the quantum correlations between the particles will emerge. Existence of such quantum correlations between the motion of different particles has been predicted for nano-mechanical objects [2], which is estimated to be a hard challenge as a prize for the observation of the quantum correlation between the motion of the macroscopic objects.

Meanwhile, an experimentally feasible system to create and observed quantum correlations between the motion of different particles is an array of atoms hold by a deep optical lattices and placed inside a high fines optical resonator. This configuration allowed to demonstrate an efficient cooling of the collective motion to its ground state [3], where the inter-atomic correlations do not yet emerge, but the uncertainty of the collective position and momentum reaches the standard quantum limit (SQL). One way to mediate the correlations between different atoms is to squeeze the quantum uncertainty beyond the SQL.

The task of this work was to design an experimentally feasible scheme to driving an atomic collective motion into such a squeezed state. The proposal is to pump the cavity by a two color light, one positively and the other negatively detuned from the cavity resonance frequency, similar to the one suggested for the squeezing of a single mechanical oscillator [4]. The right balance between the cavity mediated cooling and heating will than provide the desirable squeezing as a steady state of the evolution.

Here we present two main results of the work: (i) the maximal squeezing achievable in such a configuration and (ii) the minimal squeezing observable using the quantum swapping between the atomic motion and light as a read out. Figure 1 shows the suppression of the collective quantum noise Δx_{opt}^2 , which is stronger for higher atom number N (figure 1). We also derived the analytical expression for the noise in the limit of a fast cavity decay κ , and a large cavity cooperativity $c_r = \frac{g^2}{\kappa\gamma}$ (g - light atom coupling, γ - atomic linewidth):

$$\Delta x_{\text{an}}^2 = \sqrt{\frac{\mu}{2} \left(\frac{1}{c_r N} + \frac{\gamma^2}{4\Delta_a^2} \right)}, \quad (1)$$

where Δ_a is a detuning of the cavity resonance fre-

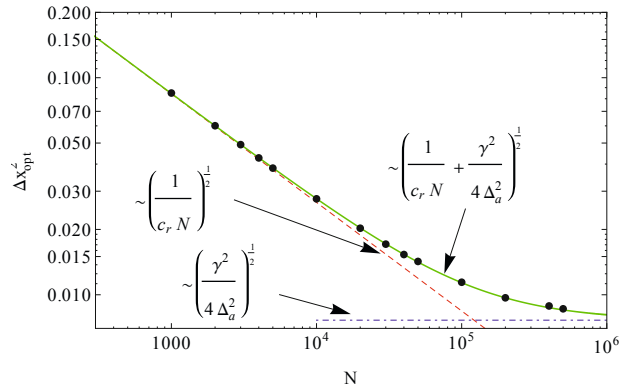


Figure 1: Noise suppression of the center of mass position. The numerical results (points) are in the agreement with the analytical estimation (solid line).

quency from the atomic transition frequency, and $\mu = \frac{7}{5}$ accounts for an atomic dipole emission pattern. This expression captures the decrease of the noise with the atom number and an additional noise caused by the atomic spontaneous emission. The validity of this expression holds for $c_r N \leq \left(\frac{2\Delta_a}{\gamma}\right)^2$, which gives the lower bound of squeezing $\Delta x_{\text{th}}^2 \geq \sqrt{\frac{\mu}{4} \frac{\gamma}{|\Delta_a|}}$. Reading the squeezing of the atomic motion with the quantum swapping technique [5], imposed an upper limit for the squeezing which is experimentally observable $\hat{x}_{\text{th}} \leq \frac{1}{2} \left(1 - c_r N \frac{\gamma^2}{4\Delta_a^2} - \frac{2\mu}{c_r N} \right)$. For the parameters currently accessible in experiment: $N = 1000$, $c_r = 5$, and $\Delta_a = 100\gamma$, the minimal observable squeezing is 1.3 dB, while the predicted squeezing is 37 dB.

Thus we have proposed a scheme to squeeze the motion of an atomic array which is not only experimentally feasible to achieve, bus is also large enough to be measured. A natural continuation towards the observation of the quantum correlation between different atoms is to design a measurement scheme revealing this property, with we plan to do in the future.

- [1] D. Leibfried et al., RMP **75**, 281 (2003).
- [2] C. Genes et al., NJP **10**, 095009 (2008).
- [3] M. Schleier-Smith et al., PRL **107**, 143005 (2011).
- [4] A. Kronwald et al., PRA **88**, 063833 (2013).
- [5] A.S. Parkins, H.J. Kimble, JOB **1**, 496 (1999).

Josephson vortex interferometer as an advanced ballistic single-shot detector for qubit readout

A.L. Pankratov^{1,2,3}, **I.I. Soloviev**^{4,5}, **N.V. Klenov**^{6,4,5}, **S.V. Bakurskiy**^{6,7}, **L.S. Revin**^{1,2,3},
E. Il'ichev⁸ and **L.S. Kuzmin**^{2,4,9}

¹*Institute for Physics of Microstructures of RAS, Nizhny Novgorod, 603950, Russia*

²*CCN, Nizhny Novgorod State Technical University n.a. R.E. Alekseev, Nizhny Novgorod, 603950, Russia*

³*Lobachevsky State University of Nizhni Novgorod, Nizhny Novgorod, 603950, Russia*

⁴*Lomonosov Moscow State University Skobeltsyn Institute of Nuclear Physics, 119991, Moscow, Russia*

⁵*Lukin Scientific Research Institute of Physical Problems, Zelenograd, 124460, Moscow, Russia*

⁶*Physics Department, Moscow State University, 119991, Moscow, Russia*

⁷*FST and MESA+, IFN, University of Twente, 7500 AE Enschede, The Netherlands*

⁸*Leibniz Institute of Photonic Technology, D-07702 Jena, Germany*

⁹*Chalmers University of Technology, SE-41296 Goteborg, Sweden*

e-mail: alp@ipmras.ru

In the present report the fluctuational propagation of solitons (magnetic fluxons) in long Josephson junctions has been studied both numerically and analytically in connection with the design of the ballistic detector for readout of qubit states. This ballistic detector is formed in an interferometer manner which operational principle relies on Josephson vortex scattering at a measurement potential. Such a detector has been originally proposed in [1] and later has been studied theoretically and experimentally in [2] and [3]. Considering homogeneous Josephson transmission lines [4], [5], we have demonstrated that operation in conditions where solitons are subjected to Lorentz contraction for a significant part of the junctions length leads to drastic suppression of thermal jitter at the output junction end. Specifically, while for large-to-critical damping and small values of bias current the physically obvious dependence of the jitter versus length $\sigma \sim \sqrt{L}$ [2] is confirmed, for small damping starting from the experimentally relevant $\alpha = 0.1$ and below, strong deviation from $\sigma \sim \sqrt{L}$ is observed, up to nearly complete independence of the jitter versus length, which is supported by the obtained theory. This allows to significantly improve the sensitivity of ballistic detectors, operating in a relativistic regime.

Later we have considered relativistic soliton dynamics governed by the sine-Gordon equation and affected by short spatial inhomogeneities of the driving force and thermal noise. Developed analytical and numerical methods for calculation of soliton scattering at the inhomogeneities allowed us to examine the scattering as a measurement tool in which the soliton scattering is utilized for quantum measurements of superconducting flux qubit. We optimized the soliton dynamics for the measurement process varying the starting and the stationary soliton velocity as well as configuration of the inhomogeneities. For experimentally relevant parameters we obtained the signal-to-noise ratio above 100 reflecting good prac-

tical usability of the measurement concept [6]. We have proposed an approach to symmetrize the detector scheme and explore arising advantages in the signal-to-noise ratio (by a factor of five improvement) and in the drastic back-action reduction in comparison with the standard scheme [6]. The structures of the ballistic detectors have been fabricated, and the results of their first tests will be reported.

This work was supported by Russian Ministry of Science (projects 3.2054.2014/K, and 14.VVV.21.0015), RFBR projects 14-02-31002-mol_a, 15-32-20362-mol_a_ved, 15-02-05869, Russian President grant MK-1841.2014.2, and Dynasty Foundation.

- [1] D. V. Averin, K. Rabenstein, and V. K. Semenov, *Phys. Rev. B* **73**, 094504 (2006).
- [2] A. Fedorov, A. Shnirman, G. Schön and A. Kidiyarova-Shevchenko, *Phys. Rev. B* **75**, 224504 (2007).
- [3] A. Herr, A. Fedorov, A. Shnirman, E. Ilchev and G. Schön, *Supercond. Sci. Technol.* **20**, S450 (2007).
- [4] A. L. Pankratov, A. V. Gordeeva, and L. S. Kuzmin, *Phys. Rev. Lett.* **109**, 087003 (2012).
- [5] I. I. Soloviev, N. V. Klenov, A. L. Pankratov, E. Il'ichev and L. S. Kuzmin, *Phys. Rev. E* **87**, 060901(R) (2013).
- [6] I. I. Soloviev, N. V. Klenov, S. V. Bakurskiy, A. L. Pankratov and L. S. Kuzmin, *Appl. Phys. Lett.* **105**, 202602 (2014).

Spectral linewidth and coherent dynamics in parallel chains of inductively coupled Josephson junctions

A.L. Pankratov^{1,2,3}, E.V. Pankratova⁴, and S.V. Shitov^{5,6}

¹Institute for Physics of Microstructures of RAS, Nizhny Novgorod, Russia

²CCN, Nizhny Novgorod State Technical University n.a. R.E.Alexeyev, Nizhny Novgorod, Russia

³Lobachevsky State University of Nizhni Novgorod, Nizhny Novgorod, Russia

⁴Volga State University, 5, Nesterov str., Nizhny Novgorod, Russia

⁵Institute of Radio-engineering and Electronics of RAS, Moscow, Russia

⁶Laboratory of Superconducting Metamaterials, NUST "MISIS", Moscow, Russia

e-mail: pankratova@vgavt-nn.ru

In this work we study the dynamics of the parallel one-dimensional array of inductively coupled Josephson junctions (JJ) with resistive-capacitive load [1] (Fig. 1) in the frame of discrete sine-Gordon equation

$$\ddot{\varphi}_j + \alpha \dot{\varphi}_j + \sin \varphi_j = i_{dc} + i_f(t) + \varepsilon(\varphi_{j-1} - 2\varphi_j + \varphi_{j+1}), \quad (1)$$

where $j = 1, \dots, n$ is the number of junction in the chain, φ_j is the phase across the j -th Josephson junction, ε is the coupling parameter, α is the dissipation coefficient, i_{dc} is normalized dc -current, $i_f(t)$ is fluctuational current modeled by white Gaussian noise: $\langle i_f(t) \rangle = 0$, $\langle i_f(t)i_f(t+\tau) \rangle = 2\alpha\gamma\delta(\tau)$, where $\gamma = I_T/I_C$ is the dimensionless noise intensity, I_T is the thermal current and I_C is the critical current of the junction. The considered number of junction is equal to $N=21$, $\alpha = 0.03$, $\varepsilon = 4$.

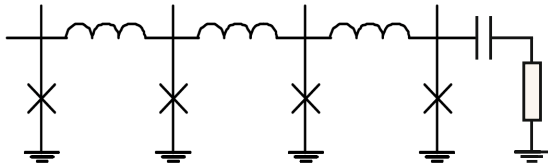


Figure 1: An example of a parallel chain with RC-load.

The current-voltage characteristic (IVC) of the system consists of a number of steep zero-field steps. In Ref. [2] it has been experimentally demonstrated that in a complex 2-D array at first steps of IVC the radiation power is rather weak, but, starting from a certain number, the radiation power grows significantly. In the present work we perform detailed numerical analysis of the system (1) and demonstrate that qualitatively similar behavior to [2] can be observed in a much simpler system, but with account of the RC-load. Namely, at different zero field steps of the IVC we examine the variation of the output power and radiation linewidth versus the injected current for unmatched and matched RC-load. While at first steps single or few running soliton regimes are observed, at higher steps various standing wave regimes are established, which demonstrate most efficient radiation regimes. Here, at the matched RC-

load, the efficiency of radiation reaches 10% of the total dc power, see Fig. 2. Also we demonstrate that the spectral linewidth at the 10-th step, where the most efficient radiation is observed, agrees well with the half of theoretical linewidth for a short Josephson junction [3] and a double of the linewidth for a shuttle fluxon oscillator [4], divided by the number of junctions in the cell.

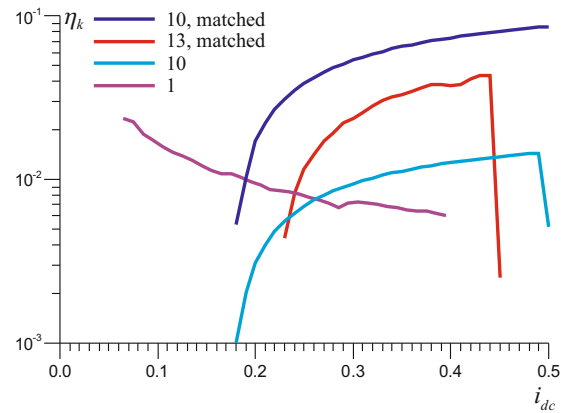


Figure 2: The radiation efficiency for well-matched and nearly unmatched cases for the n -th steps of the current-voltage characteristics.

The work was supported by RFBR (projects 14-02-31727 and 15-02-05869), and the Russian Ministry of Science (project 11.G34.31.0062).

- [1] A. L. Pankratov, A. S. Sobolev, V. P. Koshelets, and J. Mygind, Phys. Rev. B **75**, 184516 (2007).
- [2] P. Barbara, A. B. Cawthorne, S. V. Shitov and C. J. Lobb, Phys. Rev. Lett., **82**, 1963 (1999).
- [3] K.K. Likharev, *Dynamics of Josephson Junctions and Circuits*, Gordon and Breach, New York (1986) 634.
- [4] E. Joergensen, V.P. Koshelets, R. Monaco, J. Mygind, M.R. Samuelsen, and M. Salerno, Phys. Rev. Lett., **49**, 1093 (1982).

Emergence of traps for fast control of a qubit

Nikolay Il'in and Alexander Pechen

Steklov Mathematical Institute of Russian Academy of Sciences
Gubkina str., 8, Moscow 119991, Russia

e-mail: ilyn@mi.ras.ru; pechen@mi.ras.ru

Among the major requirements for successful development of quantum technologies is the ability to control atomic and molecular scale quantum systems. Generally, quantum control problem can be formulated as maximization of some objective functional $J[f]$ of the control $f(t)$ (the control can be, for example, shaped laser pulse). Analysis of the underlying control landscape, that is, graph of the map $f \rightarrow \mathcal{J}[f]$, in particular, analysis of traps (i.e., local but not global extrema of $\mathcal{J}[f]$), attracts now high attention of the researchers [1–4].

In this work we discuss the possibility for emergence of traps for fast coherent control of a qubit—basic system for quantum information and computation. For sufficiently large control duration T the control landscape of the qubit was shown to have no traps [5,6]. We show that for short T the situation is different and traps do appear for some values of the initial states, Hamiltonians, and target observables, while for other values they do not appear even for arbitrarily small T [7].

Dynamics of a two-level quantum system (qubit) under the action of coherent control $f(t)$, e.g., shaped laser pulse, is described by the Schrödinger equation

$$i\dot{U}_t^f = (H_0 + f(t)V)U_t^f, \quad U_{t=0}^f = \mathbb{I} \quad (1)$$

Here H_0 and V are 2×2 Hermitian matrices. An important for applications problem is to maximize average value of a quantum-mechanical observable of the qubit at some fixed time $T > 0$. Such problem can be formulated as maximization of the objective functional of the form

$$\mathcal{J}_A[f] = \text{Tr}(U_T \rho_0 U_T^\dagger A) \quad (2)$$

which describes the average value of the observable A at time T . Here A is Hermitian 2×2 matrix and ρ_0 is the initial density matrix. Control landscape for two-level quantum systems was studied in [5,6], where the absence of traps for sufficiently large T was proved. This finding gave the first class of quantum control problems which are free of traps at least for sufficiently large T . In [6] the following statement was proved.

Theorem 1. *If $\text{Tr}V = 0$, $T \geq T_0$, where $T_0 = \pi/\|H_0 - (1/2)\text{Tr}H_0 + f_0V\|$, $f_0 = -\text{Tr}(H_0V)/\text{Tr}(V^2)$, then all the extrema of the objective $\mathcal{J}_A[f]$ are global maxima and global minima.*

Moreover, it was proved that any control $f \neq f_0$ can not be trap for any $T > 0$. In [7] the case of

small T is studied and for sufficiently small T under certain conditions it is proved that $f = f_0$ is a trap. We consider $H_0 = \sigma_z$ and $V = v_x\sigma_x + v_y\sigma_y$ so that $f_0 = 0$. Parameter space for this control problem is defined by the final time T and three vectors $\mathbf{v} = 1/2\text{Tr}(V\boldsymbol{\sigma})$, $\mathbf{r}^0 = \text{Tr}(\rho_0\boldsymbol{\sigma})$, $\mathbf{a} = \text{Tr}(A\boldsymbol{\sigma})$. Here $|\mathbf{r}| \leq 1$ and $\boldsymbol{\sigma} = (\sigma_x, \sigma_y, \sigma_z)$ are Pauli matrices. We define four domains in the parameter space:

I domain: $[(\mathbf{v} \times \mathbf{r}^0)_z \cos 2T + (\mathbf{v} \cdot \mathbf{r}^0) \sin 2T](\mathbf{v} \times \mathbf{a})_z > 0$ and $(\mathbf{r}^0 \times \mathbf{a})_z \cos 2T < (\mathbf{r}^0 \cdot \mathbf{a}) \sin 2T$.

II domain: $[(\mathbf{v} \times \mathbf{r}^0)_z \cos 2T + (\mathbf{v} \cdot \mathbf{r}^0) \sin 2T](\mathbf{v} \times \mathbf{a})_z < 0$ and $(\mathbf{r}^0 \times \mathbf{a})_z \cos 2T > (\mathbf{r}^0 \cdot \mathbf{a}) \sin 2T$.

III domain: $[(\mathbf{v} \times \mathbf{r}^0)_z \cos 2T + (\mathbf{v} \cdot \mathbf{r}^0) \sin 2T](\mathbf{v} \times \mathbf{a})_z > 0$ and $(\mathbf{r}^0 \times \mathbf{a})_z \cos 2T > (\mathbf{r}^0 \cdot \mathbf{a}) \sin 2T$.

IV domain: $[(\mathbf{v} \times \mathbf{r}^0)_z \cos 2T + (\mathbf{v} \cdot \mathbf{r}^0) \sin 2T](\mathbf{v} \times \mathbf{a})_z < 0$ and $(\mathbf{r}^0 \times \mathbf{a})_z \cos 2T < (\mathbf{r}^0 \cdot \mathbf{a}) \sin 2T$.

The main result of [7] is the following theorem:

Theorem 2. *For the domain I, there exists $T_1 > 0$ such that for any $T \leq T_1$ the control $f(t) = 0$ is a trap for maximization of $\mathcal{J}_A[f]$. For the domain II, there exists T_1 such that for any $T \leq T_1$ the control $f(t) = 0$ is a trap for minimization of $\mathcal{J}_A[f]$. For the domains III and IV, the control $f(t) = 0$ is a saddle point for any T .*

The importance of this result is that it shows for which Hamiltonians, initial states and target observables of a qubit traps do or do not exist.

This research was supported by the Russian Science Foundation (project 14-50-00005).

- [1] H. Rabitz, H. Hsieh, and C. Rosenthal, *Science* **303**, 1998 (2004).
- [2] A. Pechen and D. Tannor, *Phys. Rev. Lett.* **108**, 198902 (2012).
- [3] K. W. Moore and H. Rabitz, *Phys. Rev. A* **108**, 012109 (2011).
- [4] P. de Fouquieres and S. G. Schirmer, *Infinite Dimensional Analysis, Quantum Probability and Related Topics*. **16(3)**, 1350021 (2013).
- [5] A. Pechen and N. Il'in, *Phys. Rev. A* **86**, 052117 (2012).
- [6] A. Pechen and N. Il'in, *Proceedings of the Steklov Institute of Mathematics*, **285**, 233–240 (2014).
- [7] A. Pechen and N. Il'in, *Proceedings of the Steklov Institute of Mathematics*, (2015). In press.

From plasmonic to cold-atomic disordered chains.

D. F. Kornovan¹, A.S. Sheremet², M. I. Petrov^{1,3,4}

¹Saint-Petersburg Academic University, Khlopina str. 8/3, Saint-Petersburg, 194021, Russia

²Russian Quantum Center, 100 Novaya St., Skolkovo, Moscow 143025, Russia

³ITMO University, Metamaterials Laboratory, Birzhevaya line 14, Saint-Petersburg, 199034, Russia

⁴University of Eastern Finland, Yliopistokatu 7, Joensuu, 80101, Finland

e-mail: trisha.petrov@gmail.com

Plasmonic nanoparticle and cold atomic chains play an important role in modern photonics. While nanoparticle chains allows subwavelength guiding of light, the chains of cold atoms are prospective for implementation in optical memory storage and novel atomic optical components such as atomic Bragg mirrors. For these application the introduction of disorder is crucial and, usually, leads to destruction of interference and smearing the optical effects. We, on the contrary, report on *disorder-induced* fine optical structure that can be observed in one-dimensional resonant chains.

We consider the fluctuations of interaction constant related to positional (non-diagonal) disorder. In the pioneer paper [1] on oscillatory chain with random parameters it was shown that non-diagonal disorder may lead to singularity in the density of states (DOS). We have considered a nanoparticle chain shown in Fig. 1 (a) and applied dipole-dipole interaction model to compute the DOS [2]. The results are shown in Fig. 1 (b). One can trace the evolution of the DOS function from the regular case $\Delta_x = 0$ to the case of disordered chain. Instead of smearing we predict the appearance of sharp peak in the DOS close to the resonance frequency ω_0 of individual nanoparticle. This results in Purcell enhancement in the vicinity of plasmonic chain (see Fig. 1 b) inset) that can find applications in random lasing and Raman spectroscopy. However, to observe Purcell enhancement one can achieve ultra low losses not typical for plasmonic particles.

This problem can be overcome by using the cold atomic systems. The recent progress in atomic trapping allows observing of light scattering on atomic ensembles coupled to optical fibre. To calculate the scattering cross section we have applied the T-matrix approach [3]: $\hat{T}(E) = \hat{V} + \hat{V} \left((E - \hat{H})^{-1} \right) \hat{V}$, where \hat{H} is full Hamiltonian, and \hat{V} is the interaction operator, and the scattering cross section $\sigma \sim |T|^2$. One can see that with the increase of disorder the high frequency peak related to super radiance effects is damped. At the same time, the peak close to the individual atom resonance becomes more pronounced. We need to emphasize that the reported calculations neglected the interaction with optical fiber, but accounting on that will give us stronger interaction between the atoms and, consequently, stronger effects

related to interaction constant fluctuations.

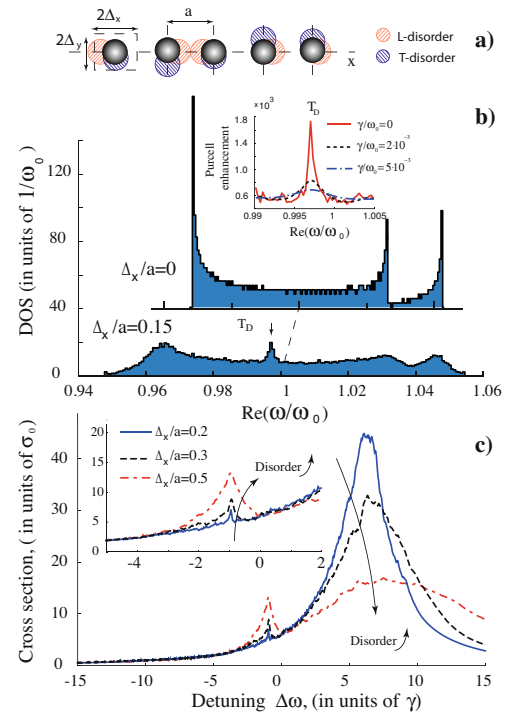


Figure 1: a) The positional disorder in a chain: transversal (T) and longitudinal disorder (L). b) The density of resonant states computed for regular $\Delta_x = 0$ and T-disordered plasmonic chain. The inset: the disorder-induced Purcell enhancement and the damping induced by ohmic losses γ . c) The scattering cross section of a cold atomic chain. Cross section is given in units of individual atom resonant cross section σ_0 , and the detuning in units of damping constant γ .

Finally, concluding we predict the disorder-induced fine structure in plasmonic and cold atomic chains related to positional fluctuations. The performed calculations allow one designing the proper experiment and, if such will be established, it would be the first direct observation of fundamental effect predicted by F.J. Dyson more than 60 years ago.

- [1] F. Dyson, Phys. Rev., **92** (6), 1331 (1953).
- [2] M. Petrov, Phys. Rev. A, **91** (2), 023821 (2015).
- [3] A. S. Sheremet, A. D. Manukhova, N. V. Lari-onov, and D. V. Kupriyanov, Phys. Rev. A, **86** (4), 043414 (2012).

Pattern formation in non-equilibrium correlated electronic systems

Pedro Ribeiro¹, Andrey Antipov², and Alexey Rubtsov^{1,3}

¹*Russian Quantum Center, 100 Novaya St., Skolkovo, Moscow 143025, Russia*

²*Department of Physics University of Michigan, Randall Laboratory, 450 Church Street, Ann Arbor, MI 48109-1040*

³*Department of Physics, Lomonosov Moscow State University, 119991 Moscow, Russia*
e-mail: pribeiro@pks.mpg.de

Strong non-equilibrium conditions eventually drive a system away from its linear response regime, deeply affecting the properties of the underlying equilibrium phase. A well known example is the Rayleigh-Bernard convection arising for classical fluids that develop convection rolls of a specific wave-length. A seminal experiment, revealing pattern formation in strongly correlated systems [1] reported a current-induced pattern formation in a quasi-one dimensional organic charge-transfer complex, on the verge of Mott breakdown. Recently, experimental results for spinor Bose-Einstein condensates [2] also reported patterned phases. Considerable theoretical efforts have been done in the field of non-equilibrium correlated quantum systems (see [3] for a recent review).

We report on recent results regarding effects of large bias voltages applied across a half-filled Hubbard chain. At equilibrium this system shows a charge gap and strong antiferromagnetic correlations. We show that out of equilibrium the wave-vector maximizing the spin-susceptibility shifts from its equilibrium antiferromagnetic value $q=$ as a function of the applied voltage and temperature. We describe a rich set of phases induced by the interplay between electron-electron interactions and non-equilibrium conditions. Some of phases found are examples of non-equilibrium-induced spacial pattern formation. We comment on the properties and stability of these phases.

Finally we argue that, although no symmetry breaking arises in the 1D system, these results suggest that a spatially modulated charge gap may be observed experimentally by STM in engineered atomic chains and nano-wires.

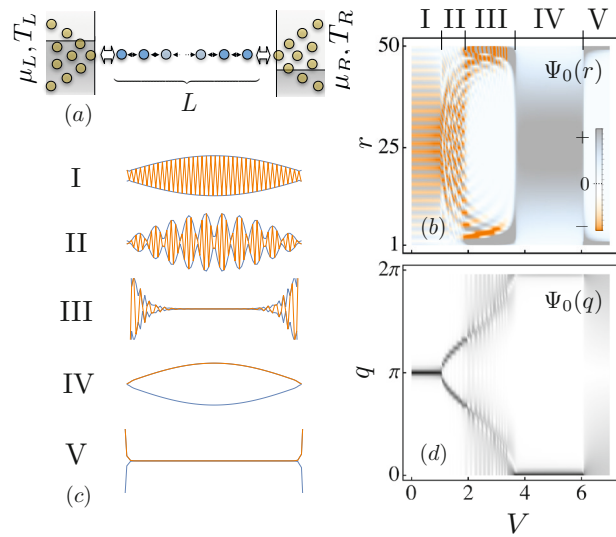


Figure 1: (left-top) Schematic view of the physical setup. (right-top) Density plot of the most unstable mode $\Psi_0(r)$ plotted as a function of the bias V for $\Gamma = 0.25$, $T = 0.25$ and $L = 50$. The phase labels I,...,V point to qualitatively different behavior of $\Psi_0(r)$. (left-bottom) Typical spatial dependence of $\Psi_0(r)$ in each phase (orange line), plotted for $L = 80$. The blue line depicts the envelope function. (right-bottom) Density plot of the Fourier transform $\Psi_0(q)$ of $\Psi_0(r)$ as a function of q computed for $L = 50$.

References

- [1] R. Kumai, Science 284, 1645 (1999).
- [2] J. Kronjager, C. Becker, P. Soltan-Panahi, K. Bongs, and K. Sengstock, Physical Review Letters 105, 090402 (2010).
- [3] H. Aoki, N. Tsuji, M. Eckstein, M. Kollar, T. Oka, and P. Werner, Reviews of Modern Physics 86, 779 (2014).

Self-focusing and wave-guiding of optical beam in rubidium atomic vapor

V. A. Sautenkov^{1,2}, M. N. Shneider³, S. A. Saakyan¹, E. V. Vilshanskaya^{1,4}, D. A. Murashkin^{1,5},
B. V. Zelener¹, B. B. Zelener^{1,5}

¹Joint Institute for High Temperatures of RAS, 13 bld. 2, Izhorskaya St., Moscow 125412, Russia

²P. N. Lebedev Physical Institute of RAS, 53 Leninskii Prospect, Moscow 119991, Russia

³MAE Department, Princeton University, Princeton, New Jersey 08544, USA

⁴National Research University, "MPEI", 14 Krasnokazarmennaya St., Moscow 111250, Russia

⁵National Research Nuclear University, "MEPhI", 31 Kashirskoye Chaussee, Moscow 115409, Russia

e-mail: vsautenkov@gmail.com

The self-focusing and self-trapping of optical beams in a nonlinear medium were predicted and explained around fifty years ago [1, 2]. One can find a short review of these effects in [3]. Recently research interest to self-focusing and wave-guiding is regained [4, 5]. We would like to investigate propagation of several optical beams through optically induced waveguide in atomic vapor. Nonlinear properties of atomic vapor are enhanced near resonance transitions. Strong nonlinear interactions will help to generate new optical fields with correlated quantum fluctuations. The expected results may be useful for different applications in quantum optics.

The first step is study of propagation of a single optical beam in rubidium atomic vapor. Diode cw laser was used. The laser frequency was tuned to the blue wing of D₂ line (780 nm). A typical profile of the laser beam after nonlinear propagation in rubidium vapor cell (cell length L = 10 cm, temperature T = 400 K) is shown in Figure 1.

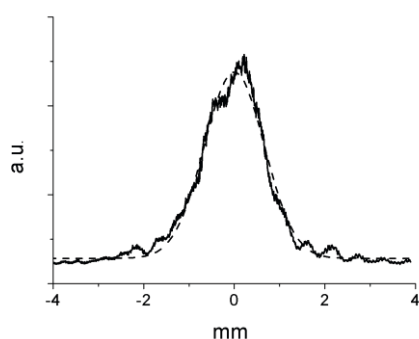


Figure 1: Solid curve presents experiment results. Dashed curve is result of fitting by Gaussian function.

The profile was recorded at distance 28 cm from the back cell window. Laser beam with diameter 0.1 cm and power 14 mW was focused at the front cell window by lens ($f = 6$ cm). The diameter of the input laser beam at interface glass/vapor was less than a size of established nonlinear waveguide in the rubidium vapor.

We define a threshold input power at the level, when a single waveguide mode is established. The size of the optically induced nonlinear waveguide depends on atomic density N . The input beam diameter can be made less or more than the size of the stable nonlinear waveguide by using different focusing lenses. When input beam diameter is increased, the threshold optical power decreases, reaches minimum and then the threshold slowly grows up. Our observations are in agreement with results of theoretical work [5].

The work is supported by Research Center FAIR (FAIR, Russia), MK-4092.2014.2, NS-6614.2014.2, the RFBR 14-02-00828, the Presidium of the RAS (Basic Research Program "Investigation of Matter in Extreme States" headed by V. E. Fortov).

- [1] G. A. Askaryan, Sov. Phys. JETP **15**, 1088 (1962).
- [2] R. Chiao, E. Garmire, C. H. Townes, Phys. Rev. Lett. **13**, 479 (1964).
- [3] R. W. Boyd, Nonlinear Optics, Chapter 7, Academic Press, 2003.
- [4] A. M. Zheltikov, Phys. Rev. A **88**, 063847 (2013).
- [5] V. V. Semak and M. N. Shneider, J. Phys. D **46**, 185502 (2013).

Underdamped Josephson junction as a switching current detector

G. Oelsner¹, **L.S. Revin**^{2,3,4}, E. Il'ichev^{1,5}, A.L. Pankratov^{2,3,4,*}, H.-G. Meyer¹, L. Gronberg⁶,

J. Hassel⁶, and L. S. Kuzmin^{3,7}

¹Institute of Photonic Technology IPHT, D-07702 Jena, Germany

²Institute for Physics of Microstructures of RAS, GSP-105, Nizhny Novgorod 603950, Russia

³Center of Cryogenic Nanoelectronics, Nizhny Novgorod State Technical University, Russia

⁴Institute for Physics of Microstructures of RAS, GSP-105, Nizhny Novgorod 603950, Russia

⁵Novosibirsk State Technical University, 20 Karl Marx Avenue, 630092 Novosibirsk, Russia

⁶VTT Technical Research Center of Finland, P.O. Box 1000, FI-02044 VTT, Finland

⁷Chalmers University of Technology, SE-41296 Gothenburg, Sweden

e-mail: alp@ipmras.ru

We demonstrate the narrow switching distribution of an underdamped Josephson junction from the zero to the finite voltage state at millikelvin temperatures. We argue that such junctions can be used as ultrasensitive detectors of the single photons in the GHz range, operating close to the quantum limit: a given initial (zero voltage) state can be driven by an incoming signal to the finite voltage state. The width of the switching distribution at a nominal temperature of about $T = 10$ mK was 4.5 nA, which corresponds to an effective noise temperature of the device below 60 mK.

The current-biased Josephson junction (CBJJ) is a device in which the Josephson phase variable is trapped in a washboard potential. Modulation of the potential tilt or a radiation field can lead to an escape of the "particle" from the well, which corresponds to a voltage drop over the CBJJ [1]. This switching can also occur due to thermal activation (TA) [2] and due to macroscopic quantum tunneling (MQT) [3].

The sample, a current-biased Josephson junction, was fabricated using the 30 A/cm² process at VTT, Finland [4]. A small current density was chosen to reduce the heating power connected to switching of the junction into the voltage state and therewith heating of the sample. The sample was thermally anchored to the base of a dilution refrigerator, providing a minimal temperature below 10 mK.

The switching current distributions of the sample were measured at bath temperatures T between 10 mK and 1000 mK. The current was ramped up by the following law: it is set in steps of $\Delta I = 0.1$ nA/ms during 10ms with a waiting time of 10 ms between steps.

In Fig. 1 the temperature dependence of the mean $\langle I_{sw} \rangle$ and the standard deviation σ of the switching current (symbols), together with the results calculated from the TA and MQT theories (curves) are shown. In the temperature range between 1 K and approximately 56 mK σ decreases with T indicating that TA is the dominant escape mechanism. In this temperature range

the critical current I_c can be determined by fitting of current probability distribution $W(I)$ using the TA theory. In our case the I_c has a value of 2.2 μ A. One can see that below the crossover temperature, σ demonstrates saturation at the level ~ 4.5 nA, meaning that the quantum tunneling through the barrier is the main mechanism of escape in this case. Taking the $W(I)$ peak position in the MQT regime, we find that the crossover temperature calculated from these parameters is roughly $T_{cr} \approx 56$ mK.

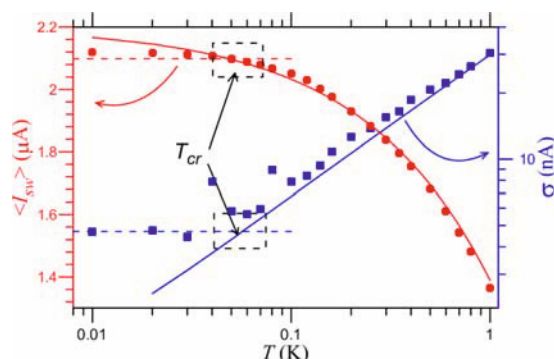


Figure 1: The standard deviation σ (rectangular symbols) and the mean value $\langle I_{sw} \rangle$ (circular symbols) of the $W(I)$ distribution vs. the nominal temperature T . The solid curves - TA theory. Dashed lines — MQT theory. The crossover temperature T_{cr} around 56 mK is indicated.

- [1] A. Wallraff, A. Lukashenko, C. Coqui, A. Kemp, T. Duty, and A. V. Ustinov, *Rev. Sci. Instrum.* **74**, 3740 (2003).
- [2] J.M. Martinis and R.L. Kautz, *Phys. Rev. Lett.* **63**, 1507 (1989).
- [3] F.V. Richard and A.W. Richard, *Phys. Rev. Lett.* **47**, 265 (1981).
- [4] M.G. Castellano, L. Gronberg, P. Carelli, F. Chiarello, C. Cosmelli, R. Leoni, S. Poletto, G. Torrioli, J. Hassel, and P. Heliö, *Supercond. Sci. Technol.* **19**, 860 (2006).

Quantum statistical ensemble for emissive correlated systems

A. Shakirov^{1,2}, Y. Shchadilova¹, and A. Rubtsov^{1,2}

¹Russian Quantum Center, 143025 Skolkovo, Moscow region, Russia

²Lomonosov Moscow State University, 119991 Moscow, Russia

e-mail: a.shakirov@rqc.ru

Relaxation dynamics of strongly correlated quantum systems brought out of equilibrium reveal invaluable information on their fundamental properties. These systems are characterized by a non-linear coupling between degrees of freedom and undergo a complex redistribution of energy before reaching the steady state. In many cases stationary values of local observables in the steady state can be predicted by using a proper statistical ensemble. Quantum statistical mechanics offers a range of ensembles which can be overall viewed as generalizations of the canonical Gibbs ensemble. In this contribution we consider relaxation of a correlated quantum system brought into contact with a vacuum bath (we refer to such a system as emissive). We study the stationary probability distribution for energy of the system and show that a special statistical ensemble should be used to describe the steady state.

An open many-body system coupled to a vacuum bath generally loses energy and particles and relaxes to the vacuum state. In the presence of an evaporation threshold some of its populated eigenstates become stable and can also appear in the steady state. In this case the stationary probability distribution of the system for an arbitrary initial state is a priori not known. We study this distribution for an emissive system of hard-core bosons on a two-dimensional lattice and show that it has a regular dependence on energy in each N -particle sector which is of Boltzmann form (see Figure 1). The steady state is however not

the Gibbs state since temperature characterizing the distribution is not the same in different sectors. We characterize this steady state by a special quantum statistical ensemble and discuss its application to calculating expectation values of observables.

The stationary probability distribution of an open system is determined by statistics of transitions induced by coupling to the bath. We show that transition rates between eigenstates of the system under study depend smoothly on the transition energy. By this behaviour of transition rates we explain the emergence of the Boltzmann distribution in the system. We connect this behaviour with statistical properties of off-diagonal matrix elements of local annihilation operators which appear in expressions for transition rates.

We are grateful to A. E. Antipov, P. V. Elyutin, P. Grišins and P. Ribeiro for fruitful discussions. The authors acknowledge a financial support from the RFBR grant 14-02-01219 and the Dynasty foundation.

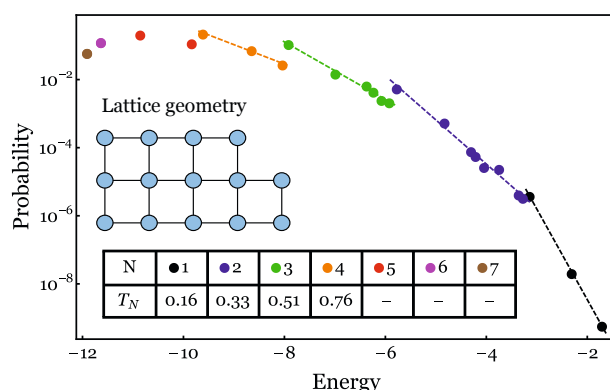


Figure 1: Probability distribution of an emissive system of hard-core bosons on a 14-site lattice (shown in the inset) in the steady state. The initial state of the system is the pure state with maximal occupation of the lattice. Temperatures T_N characterizing the Boltzmann distribution in N -particle sectors are presented in the table.

Quantum dynamics of an impurity in ultracold Bose gas

Y.E. Shchadilova^{1,2}, F. Grusdt^{1,3,4}, A.N. Rubtsov^{1,5}, and E. Demler²

¹Russian Quantum Center, 100A Novaya Street, Skolkovo, Moscow Region 143025, Russia

²Department of Physics, Harvard University, Cambridge, MA 02138, USA

³Department of Physics and Research Center OPTIMAS, University of Kaiserslautern, Kaiserslautern 67663, Germany

⁴Graduate School Materials Science in Mainz, Kaiserslautern 67663, Germany

⁵Department of Physics, Moscow State University, Moscow 119991, Russia

e-mail: yes@rqc.ru

A system of an impurity immersed in a Bose-Einstein condensate (BEC) exhibits the polaronic effect, which is a ubiquitous phenomenon in a wide range of physical systems including semiconductors, doped Mott insulators, and high- T_c superconductors. This polaronic effect can be described by means of Fröhlich model [1] in a wide range of experimentally relevant parameters. Though this model was introduced more than 80 years ago [2], its properties in the regime of the intermediate coupling remain poorly understood. Moreover, recent analysis of the BEC-polaron problem showed that existing analytical approaches [3, 4, 5] do not provide reliable results in the experimentally relevant range of parameters when tested against Monte Carlo simulations [6].

In this contribution we demonstrate that the description of Fröhlich polarons at finite momentum can be done by employing an analytical class of wavefunctions based on the correlated Gaussian ansatz (CGWs) [7]. We show that CGWs are in excellent agreement with existing diagrammatic Monte Carlo results [6] for the polaron binding energy for the wide range of interactions (see Fig. 1). This ansatz allows us to investigate properties of the polaronic cloud at finite momentum, such as polaronic mass, as well as impurity induced correlations between host atoms.

Employing the time-dependent variational principle we extended the approach of correlated Gaussian wavefunctions to describe quantum dynamics of the impurity in the ultracold Bose gas. This allows us to calculate the onset of correlations between host atoms after a sudden immersion of impurity as well as radio-frequency absorption spectra.

The authors acknowledge support from the NSF grant DMR-1308435, Harvard-MIT CUA, AFOSR New Quantum Phases of Matter MURI, the ARO-MURI on Atomtronics, ARO MURI Quism program. Y.E.S. and A.N.R. thank the Dynasty foundation and the RRBR grant 14-02-01219 for financial support. F.G. is a recipient of a fellowship through the Excellence Initiative (DFG/GSC 266) and is grateful for financial support from the Marion Köser Stiftung.

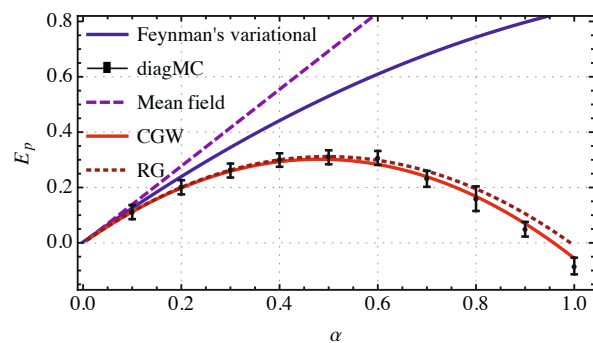


Figure 1: The polaron binding energy is computed using different approaches as a function of the dimensionless interaction parameter $\alpha = a_{BB}^2/(a_{IB}\xi)$, where a_{BB} and a_{IB} are boson-boson and impurity-boson scattering lengths, ξ is the healing length of the condensate. Our result (CGWs) [7] is compared with Feynman's variational method [3, 4], mean-field [5], Renormalization Group [8], and diagrammatic Monte-Carlo approach [6]. We used parameters corresponding to ${}^6\text{Li}$ impurities in ${}^{23}\text{Na}$ BEC for comparison with Refs. [3, 6].

- [1] J. T. Devreese and A. S. Alexandrov, Reports Prog. Phys. **72**, 066501 (2009).
- [2] L.D. Landau Phys. Z. Sowjet. **3**, 664 (1933).
- [3] J. Tempere, W. Casteels, M. Oberthaler, S. Knoop, E. Timmermans, and J. Devreese, Phys. Rev. B **80**, 184504 (2009).
- [4] W. Casteels, J. Tempere, and J. T. Devreese, Phys. Rev. A **86**,043614 (2012).
- [5] A. Shashi, F. Grusdt, D. A. Abanin, E. Demler, Phys. Rev. A **89**, 053617 (2014).
- [6] J. Vlietinck, W. Casteels, K. Van Houcke, J. Tempere, J. Ryckebusch, J. T. Devreese, arXiv:1406.6506 (2014).
- [7] Y.E. Shchadilova, F. Grusdt, A.N. Rubtsov, E. Demler, arXiv:1410.5691 (2014).
- [8] F. Grusdt, Y.E. Shchadilova, A.N. Rubtsov, E. Demler, arXiv:1410.2203 (2014).

Fractional stable statistics for cold atoms in optical lattices

R.T. Sibatov¹

¹*Ulyanovsk State University, 42 Leo Tolstoy str., Ulyanovsk 432017, Russia*
e-mail: *conference@icqt.org*

Marksteiner et al. [1] studied numerically spatial diffusion of two-level atoms in one- and two-dimensional optical molasses. Using quantum Monte Carlo calculations they predicted distributions with power law tails for trapping times and path lengths. The diffusion of cold atoms in optical lattices is described by the Lévy flight model. Recently, employing the Sisyphus cooling scheme, Sagi et al. [2] observed anomalous superdiffusion of ultra-cold ⁸⁷Rb atoms in a one-dimensional lattice. The atomic cloud is characterized by the Lévy-type distribution function obeying nonlocal diffusion equation with fractional Laplacian [2, 3].

The authors [1] obtained that distributions of flight distances and waiting times have power law tails with the exponents ν and μ , respectively, which are defined by the relations

$$\begin{aligned}\nu &= \frac{\alpha}{3D_1} + \frac{1}{3} = \frac{10}{369} \frac{U_0}{E_R} + \frac{1}{3}, \\ \mu &= \frac{\alpha}{2D_1} - \frac{3}{2} = \frac{5}{123} \frac{U_0}{E_R} - \frac{3}{2}.\end{aligned}\quad (1)$$

Here U_0 and E_R are the potential depth and the recoil energy, respectively, α and D_1 are the constants in the following relations, for the force

$$F(p) = -\frac{\alpha p}{1 + (p/p_c)^2},$$

and the momentum diffusion coefficient

$$D(p) = D_1 + \frac{D_2}{1 + (p/p_c)^2},$$

which are presented in the standard Klein-Kramers equation for p.d.f. $W(z, p, t)$ of the atom position in phase space at time t [1].

As one can see from Eq. (1) the exponents $\mu > 0$ and ν are connected by the relation $\nu = 2\mu/3 + 4/3$. It means that $\nu > 4/3$ and the first moment of random distances is always finite. In this case asymptotic solutions of Lévy walks coincide with distributions for Lévy flights accurate within scale constants. We show that asymptotic p.d.f. of the atom position can be expressed through symmetrical fractionally stable densities (FSD)

$$p(z, t) = (Ct^\mu)^{-1/\nu} q\left((Ct^\mu)^{-1/\nu} z; \nu, \mu, 0\right),$$

where $C(U_0, E_R)$ is the scale constant. This class of distributions appeared in [4] was partially investigated in work [5]. M. Kotulski obtained the expression for FSD when he considered the Montroll-Weiss

problem and FSD's appeared as limit ones for continuous time random walks (CTRW) [4]. They are expressed via the Lévy stable densities,

$$q(x; \alpha, \beta, \theta) = \int_0^\infty g(xy^{\beta/\alpha}; \alpha, \theta) g_+(y; \beta) y^{\beta/\alpha} dy, \quad (2)$$

where $g(x; \alpha, \theta)$ can be determined via its characteristic function

$$\tilde{g}(k; \alpha, \theta) = \exp(-|k|^\alpha \exp\{-i\alpha\theta(\pi/2)\text{sign}k\}).$$

Here α is the exponent of stable distribution, θ is its skewness parameter (we consider standard strictly stable laws when the scale parameter is 1 and the shift parameter is 0); $g_+(y; \beta)$ is the one-sided stable density ($\theta = 1$).

Lutz[6] derived that the stationary solution $V_0(p)$ of the Rayleigh equation (corresponding to the Klein-Kramers equation mentioned above), is given by the Tsallis distribution,

$$V_0(p) = Z_q^{-1} [1 - \beta(1 - q)p^2]^{1/(1-q)}.$$

Here Z_q is a normalizing factor, $\beta(\alpha, D_1, D_2)$ and $q(\alpha, D_1, p_c)$ are constants. This distribution was experimentally confirmed by Douglas et al. [7].

Using the combined statistics we analyze phase space dynamics of cold atoms and study three regimes predicted in [3], i.e. Gaussian diffusion, Lévy flights and Richardson-Obukhov scaling. Also, we discuss the possibility of implementation of quantum Lévy walks in optical lattices.

This work is supported by the Russian Foundation for Basic Research (project 15-01-99674-a).

- [1] S. Marksteiner et al. *Phys. Rev. A* **53**, 3409 (1996).
- [2] Y. Sagi et al. *Phys. Rev. Lett.* **108**, 093002 (2011).
- [3] D.A. Kessler, E. Barkai E. *Phys. Rev. Lett.* **108**, 230602 (2012).
- [4] M. Kotulski, *J. Stat. Phys.* **81**, 777 (1995).
- [5] V. Kolokoltsov et al. *J. Math. Sciences* **105**, 2569 (2001).
- [6] E. Lutz, *Phys. Rev. A* **67**, 051402 (2003).
- [7] P. Douglas et al., *Phys. Rev. Lett.* **96**, 110601 (2006).

Partial suppression of the bleaching effect in AlGaAs/GaAs quantum well by lowering Al concentration in barriers

I. Solovev, V. Davydov, Yu. Kapitonov, P. Shapochkin, Yu. Efimov, V. Lovtsus, S. Eliseev, V. Petrov, V. Ovsyankin

St. Petersburg state university, 3 Ulyanovskaya St., St. Petersburg 198504, Russia
e-mail: solivan2007@yandex.ru

Semiconductor Heterostructures A3B5 with quantum wells (QW) are very attractive for research because of theoretical possibility to create an all-optical logic element[1]. We showed that the molecular beam epitaxy technique (MBE) allows us produce high-quality samples (inhomogeneous broadening is comparable to homogeneous broadening) with both $\text{In}_{0.02}\text{GaAs}_{0.98}/\text{GaAs}$ [2] and $\text{Al}_{0.3}\text{Ga}_{0.7}\text{As}/\text{GaAs}$ QW[3]. There are limitations of using these structures in optical information processing due to the bleaching effect manifested as broadening of exciton spectral lines. The effect is resonant with excitons and has characteristic time longer than 1s. In this work we have shown, that the bleaching effect can be reduced through lowering Al concentration in barriers from 30% to 3% when spectral quality of sample remains the same.

The sample T670 grown by MBE techniques contains 14 nm GaAs QW with $\text{Al}_{0.03}\text{Ga}_{0.97}\text{As}$ barriers. We carried out the experiment in Brewster geometry [2,3]. In this case spectral shape is quite described by the Lorentz curve:

$$K_R(\omega) = \frac{\Gamma_R^2}{(\omega - \omega_0)^2 + (\Gamma_R + \Gamma_{NR})^2}, \quad (1)$$

Where ω_0 frequency of e1-hh resonance, Γ_R radiative width, Γ_{NR} - nonradiative broadening. We work in line arrange of reflection from probe fs light pulse, temperature of the sample is about 8 K.

We use an additional monochromatic pump light

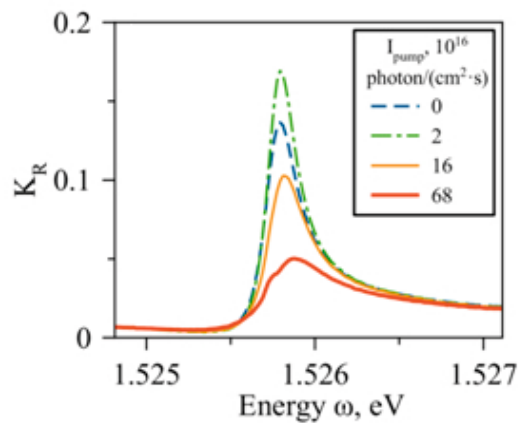


Figure 1: RR spectra with different I_{pump}

which is set to e1-hh exciton resonant. Fig.1 illus-

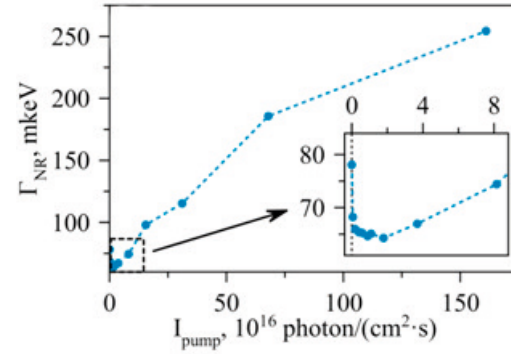


Figure 2: Dependence Γ_{NR} on I_{pump}

trates dependence of resonant reflection (RR) spectra on pump intensity. It should be noted that there is no dramatic shift of spectral line so thermal broadening is negligible. Approximation of spectral lines by (1) taking into account weak nonresonant background lets us obtain Γ_R and Γ_{NR} .

It has been experimentally established that Γ_R remains constant in wide range of pump intensity and equals $363 \mu\text{eV}$ so that this structure is as good as e296 sample which was investigated previously [2]. Observing in linear mode ($I_{pump} = 0$) for both T670 and E296 $\frac{\Gamma_{NR}}{\Gamma_R} = 0.46$ ratio also shows high quality of the sample. However significant nonradiative broadening appears when I_{pump} is more than 10^{18} photon/cm²s which is higher by 2 orders of magnitude than in the e296 sample (Fig.2). It can be connected with low-level charge effect. Absence of trion line in spectra proves this indirectly. Nevertheless, to negligible charging effects is not worth because insignificant decrease Γ_{NR} is observed (Fig.2 inset), which may be caused by compensation of level of free carries in QW.

The reported study was partially supported by RFBR, research project 15-52-12013 nnio.a. This work was carried out on the equipment of the SPbU Resource Center Nanophotonics (photon.spbu.ru)

- [1] I.Ya. Gerlovin et al., Nanot. 11 (2000) 383-386
- [2] S.V. Poltavtsev et al., Solid State Communications 199 (2014), 47-51
- [3] S. V. Poltavtsev and B. V. Stroganov, Phys. of the Sol. St., 2010, Vol. 52, No. 9, pp. 1899-1905

Plasmon effect on single-electron spectrum near Mott transition

E.A. Stepanov¹, E.G.C.P. van Loon¹, A.I. Lichtenstein², A.N. Rubtsov³, M.I. Katsnelson¹

¹Radboud University, Institute for Molecules and Materials, 6525AJ Nijmegen, The Netherlands

²Institute of Theoretical Physics, University of Hamburg, 20355 Hamburg, Germany

³Department of Physics, M.V. Lomonosov Moscow State University, 119991 Moscow, Russia

e-mail: e.stepanov@science.ru.nl

Strong correlated electron systems remain one of the interesting subjects in modern condensed matter physics. It is hard to treat such systems analytically due to the large local and *nonlocal* electron–electron interaction. Nonlocal correlations are very important for studying charge–ordering and Wigner–Mott transitions, plasmon and magnon modes [1, 2, 3, 4, 5] and other interesting features of such systems. As an example of such models can be considered the systems of adatoms on semiconducting surfaces, such as $Si(111) : X$ with $X = Sn, C, Si, Pb$ [1, 2, 3], system of cold atoms [6] and graphene [4]. Nowadays the dynamical mean–field theory (DMFT) [7] stays as the standard approximation for strongly correlated fermionic systems. In this model all the correlations are treated in impurity level, i.e. one site electron interacts with effective local electronic bath formed by other electrons. DMFT successfully describes atomic environment at the level of one–electron processes, nevertheless, bosonic hybridization associated with the collective modes should be taken into account too. There were many attempts to go beyond DMFT and extend this model to take into account collective modes, however, all of them were not good enough to describe them correctly. Plasmons have strong nonlocal nature, thus approaches such as extension dynamical mean–field theory (EDMFT) [8] are not suitable for these systems. For this reason, (E)DMFT+GW extension [2, 3] was recently developed, but the main drawback of this method is that conservation laws are not fulfilled within this approach. Here, we introduce Dual Boson (DB) approach for strongly correlated systems that gives correct results for both strong and weak interaction limits, whereas conservation laws are fulfilled [5, 9, 10, 11]. Dual Boson method is a diagrammatic extension of EDMFT that can be applied to correlated lattice fermion models with local and nonlocal interaction. This allows us to include spatial correlations beyond EDMFT introducing new dual variables. In DB approach the lattice problem is reduced to impurity model by introducing hybridization functions Δ_ν and Λ_ω for fermionic and bosonic variables, respectively. Then, the obtained impurity model serves as a starting point for perturbation expansion. Importantly, hybridization functions should be determined self–consistently. The use of diagrammatic expansion for dual variables and new self–consistency condition allows us to account local

bosonic fluctuations with good accuracy. Figure 1 shows the local fermionic Green function dependence on Matsubara frequencies for EDMFT and DB case. One can see that accounting the spatial correlations makes the system more insulating, as was expected.

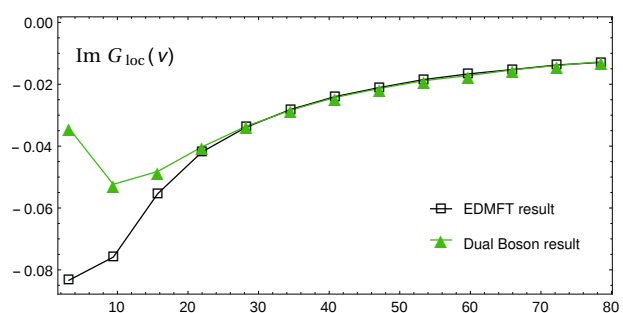


Figure 1: EDMFT and Dual Boson local Green function result for large $U=12$ and small $V=0.03$ case; $\beta = 1$, $t=1$.

- [1] Tosatti, E., Anderson, P.W., *Jpn. J. Appl. Phys.* **13**, 381, (1974);
- [2] Hansmann, P., Ayrat, T., Vaugier, L. *et al.*, *Phys. Rev. Lett.* **110**, 166401 (2013);
- [3] Huang, L., Ayrat, T., Biermann, S., Werner, P., *Phys. Rev.* **B 90**, 195114 (2014);
- [4] Wehling, T.O., Şaşıoğlu, E., Friedrich, C. *et al.*, *Phys. Rev. Lett.* **106**, 236805 (2011);
- [5] Hafermann, H., Van Loon, E.G.C.P., Katsnelson, M.I. *et al.*, *Phys. Rev.* **B 90**, 235105, (2014);
- [6] Lewenstein, M., Sanpera, A., Ahufinger, V., Oxford University Press (2012);
- [7] Georges, A., Kotliar, G., Krauth, W., Rozenberg, M.J., *Rev. Mod. Phys.* **68**, 13 (1996);
- [8] Si, Q., Smith, J.L., *Phys. Rev. Lett.* **77**, 3391 (1996);
- [9] Rubtsov, A.N., Katsnelson, M.I., Lichtenstein, A.I., *Ann. of Phys.* **327**, 1320 (2012);
- [10] Van Loon, E.G.C.P., Lichtenstein, A.I., Katsnelson, M.I. *et al.*, *Phys. Rev.* **B 90**, 235135, (2014);
- [11] Van Loon, E.G.C.P., Hafermann, H., Lichtenstein, A.I. *et al.*, *Phys. Rev. Lett.* **113**, 246407 (2014);

Measurement-assisted Landau-Zener transitions

A. N. Pechen¹ and A. S. Trushechkin^{1,2}

¹*Steklov Mathematical Institute of Russian Academy of Sciences, 8 Gubkina St., Moscow 119991, Russia*

²*National Research Nuclear University "MEPhI", 31 Kashirskoe shosse, Moscow 115409, Russia*

e-mail: trushechkin@mi.ras.ru

Among the major requirements for successful development of quantum technologies is the ability to control atomic and molecular scale quantum systems. Significant efforts are directed towards development of efficient methods for finding optimal controls for quantum systems. In this work, we approach this problem for optimal acceleration of the Landau-Zener (LZ) transitions [1] by non-selective quantum measurements, i.e., measurements without reading the results, which are nowadays often exploited as a resource for manipulating quantum systems [2, 3].

The LZ model considers a two-level quantum system with the time-dependent Hamiltonian

$$H(t) = \begin{pmatrix} -t/2 & \sqrt{\gamma} \\ \sqrt{\gamma} & t/2 \end{pmatrix}, \quad (1)$$

where $\gamma > 0$. This is a simple model of nonadiabatic transition caused by avoided energy level crossing with a wide range of applications in physics, chemistry, and biochemistry.

Let ρ be density matrix of the LZ system. Nonselective measurement of the population of the diabatic state $|0\rangle\langle 0|$ instantaneously changes the density matrix into

$$\rho' = |0\rangle\langle 0|\rho|0\rangle\langle 0| + |1\rangle\langle 1|\rho|1\rangle\langle 1|. \quad (2)$$

That is, the measurement causes a change of the quantum state even if the result of the measurement is not read.

Optimal acceleration of the LZ transitions by non-selective measurements can be formulated as the following problem: given natural N , find instants of measurements $t_1 \leq t_2 \leq \dots \leq t_N$ such that the adiabatic transition probability $\langle 0|\rho(+\infty)|0\rangle$ is maximal for the initial condition $\rho(-\infty) = |0\rangle\langle 0|$. The system evolves according to the unitary evolution given by the Hamiltonian (1) between measurements and with jumps according to formula (2) at the instants of measurements.

The difficulty for the analysis is that the transition probability as function of time instants has a huge number of local maxima. We resolve this problem both analytically by asymptotic analysis and numerically by development of efficient algorithms mainly based on the dynamic programming.

The results are presented on Fig. 1. Note a surprising effect of non-monotonic dependence of the maximal transition probability on γ for large number of measurements. As $N \rightarrow \infty$, the maximal transition

probability tends to one in agreement with the quantum Zeno effect. Thus, this problem can also be considered as a problem of optimal approximation of the quantum Zeno effect by N measurements. We have found that the convergence of the maximal transition probability to one for large N can be very slow for the LZ system, especially for values of γ in the intermediate range 0.2–2.

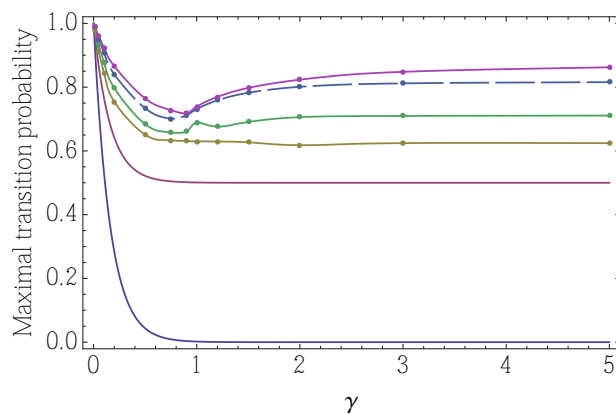


Figure 1: Maximal transition probability vs γ for a fixed number of measurements; from bottom to top $N = 0, 1, 3, 5, 10, 15$.

To solve this problem, we developed a set of analytical and numerical methods which can be applied, besides this problem, to a wide class of measurement-based quantum optimal control problems.

The results published in [4]. This work was supported by the Russian Science Foundation (project 14-11-00687).

- [1] L. Landau, Phys. Z. Sowjetunion **2**, 43 (1932); C. Zener, Proc. R. Soc. London A **137**, 696 (1932); E. C. G. Stückelberg, Helv. Phys. Acta **5**, 369 (1932); E. Majorana, Nuovo Cim. **9**, 43 (1932).
- [2] A. Pechen, N. Ilin, F. Shuang, and H. Rabitz, Phys. Rev. A **74**, 052102 (2006); F. Shuang, A. Pechen, T.-S. Ho, and H. Rabitz, J. Chem. Phys. **126**, 134303 (2007).
- [3] M. S. Blok, C. Bonato, M. L. Markham, D. J. Twitchen, V. V. Dobrovitski, and R. Hanson, Nature Physics **104**, 189 (2014).
- [4] A. Pechen and A. Trushechkin, Phys. Rev. A **91**, 052316 (2015).

Distillation of Continuous Variable Entanglement via Quantum Catalysis.

Alexander E. Ulanov^{1,2}, Ilya A. Fedorov^{1,3}, Anastasia A. Pushkina^{1,2}, Yury V. Kurochkin¹, Timothy C. Ralph⁴ and A. I. Lvovsky^{1,3,5,*}

¹Russian Quantum Center, 100 Novaya St., Skolkovo, Moscow 143025, Russia

²Moscow Institute of Physics and Technology, 141700 Dolgoprudny, Russia

³P. N. Lebedev Physics Institute, Leninskiy prospect 53, Moscow 119991, Russia

⁴School of Mathematics and Physics, University of Queensland, Brisbane, Queensland 4072, Australia

⁵Institute for Quantum Science and Technology, University of Calgary, Calgary AB T2N 1N4, Canada
e-mail: LVOV@ucalgary.ca

Entanglement distillation (ED) allows to establish strong levels of entanglement between remote nodes when it has been degraded by losses and noise. The main entanglement resource in the continuous-variable (CV) domain is the two-mode squeezed vacuum (TMSV) state, an approximation of the Einstein-Podolsky-Rosen state [1]. TMSV is a basis for many quantum technologies, such as continuous-variable teleportation [2] or quantum repeaters [3]. In this paper we present experimental realization of CV ED protocol by means of noiseless amplification [4]. Our protocol is based on the technique known as quantum catalysis [5] and, in contrast to previous implementations of CV ED [6], entanglement amplification achievable by our technique is not limited by factor two, so it can be used in practical CV quantum repeaters.

In the case of weak squeezing, the initial TMSV state can be written as:

$$|TMSV\rangle \approx |0,0\rangle - \gamma|1,1\rangle, \quad (1)$$

where $\gamma \ll 1$. This state propagates through a lossy channel with amplitude transmissivity τ . Then, to distill the entanglement, we bring it into interference on a low-reflectivity beam splitter with an ancillary single photon [7]. The distillation event is heralded by detecting a single photon in one of the outputs of the beam splitter. As a result, the state becomes in the first order of r , λ and τ

$$r|0,0\rangle - \gamma\tau|1,1\rangle. \quad (2)$$

We see that, although the single-photon component is degraded by the loss, this is compensated by the reduction of the vacuum part due to noiseless amplification. Thus, the final entanglement depends only on the ratio $\gamma\tau/r$ and at gain level $g = (\gamma\tau)^{-1}$ the distilled state reaches initial level of entanglement.

In the experiment, we start with a TMSV with the difference position quadrature variance of $\langle\langle(X_1 - X_2)^2\rangle\rangle = 0.86 \pm 0.01$. Then we introduce a one-sided 95% loss. After the amplification, the difference quadrature variance returns to the initial level: $\langle\langle(X'_1 - X'_2)^2\rangle\rangle = 0.87 \pm 0.01$ [Fig. 1(a)]. This result

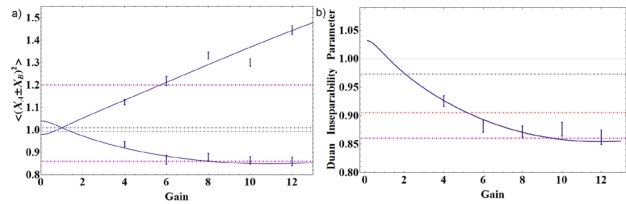


Figure 1: Experimental results. a) Two-mode squeezing as a function of the NLA gain. The vertical axis is scaled in the units of shot noise. The upper set of points correspond to the position quadrature sum (antisqueezed), lower to the difference (squeezed). The purple lines correspond to the initial state squeezing and antisqueezing; gray line to the state after one-sided 95% loss, where the squeezed and antisqueezed variances are degraded to 0.993 and 1.010, respectively. b) Duan inseparability parameter. The horizontal lines are as in (a); the red line corresponds to the inseparability parameter for a perfect EPR state that has experienced a one-sided 95% loss (total Duan variance equals 0.905).

corresponds to the amplification by factor 10 and that is much more than previously obtained results [6]. In Fig. 1(b) we calculate the Duan [8] inseparability criterion for CV systems and show that the amount of the recovered entanglement is greater than that even a perfect EPR state would exhibit after a one-sided 95% loss.

- [1] A. Einstein, B. Podolsky, and N. Rosen, Phys. Rev. 47, 777 (1935).
- [2] A. Furusawa, et al., Science 282, 706 (1998).
- [3] N. Sangouard, et al., Rev. Mod. Phys. 83, 33 (2011).
- [4] Xiang, G., et al., Nat. Photonics 4, 316 (2010).
- [5] A. I. Lvovsky and J. Mlynek, Phys.Rev.Lett. 88, 250401 (2002).
- [6] Y. Kurochkin, et al., Phys. Rev. Lett. 112, 070402 (2014).
- [7] A. I. Lvovsky, et al., Phys. Rev. Lett. 87, 050402 (2001).
- [8] L. M. Duan, et al., Phys. Rev. Lett. 84, 2722 (2000).

Temperature behavior of the reflection and diffraction spectra of resonant grating based on the InGaAs/GaAs quantum wells

L.Yu. Beliaev, Yu.V. Kapitonov, Yu.P. Efimov, Yu.K. Dolgikh, S.A. Eliseev, V.V. Petrov,

V.V. Ovsyankin

St.Petersburg State University, St.Petersburg, Russia

e-mail: lenyabelyae@mail.ru

We present the investigation of spectral properties of diffraction grating based on the GaAs/InGaAs quantum well structure with spatial periodic modulation of QW inhomogeneous broadening. It was found that the diffraction peak is narrower than corresponding reflection peak. It is shown that diffraction efficiency decreases much faster than reflectance with temperature growth, while spectral positions of peaks have same positions.

GaAs/InGaAs quantum wells can be used to build optical logic elements. These heterostructures are grown by molecular-beam epitaxy (MBE). This method allows to produce crystal samples with minimal inhomogeneous broadening of resonance [1]. Of special interest is lateral modulation of such structures.

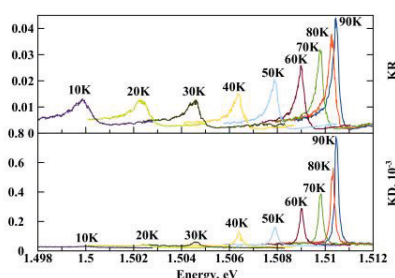


Figure 1. Temperature dependency of KR(E) and KD(E).

The sample P602 contains a quantum well whose optical properties are changed by periodic local implantation of ions (35keV He⁺, dose 1 ■ 10¹¹ cm⁻²). Spatial parameters of exposure were as follows: period 800 nm, length of the stripes 150 μm, the number of stripes 375, stripe width 400 nm. On the vicinity of the exciton resonance this quantum well can be represented as the diffraction amplitude-phase grating. The stripes of this grating may vary according to different parameters (radiation width, inhomogeneous broadening, the position of the resonance). Selected implantation dose was too small to make a significant change in morphology, but enough the formation of defects, so the contrast is defined only by the difference in inhomogeneous broadening [2]. These modulation has led to the appearance of diffraction peaks in the angular distribution of the resonant Rayleigh scattering. In addition, these peaks can be

observed only near the exciton resonance. Similar results for different structures were obtained in [3].

Sample characteristics are investigated by directing monochromatic laser beam to the sample surface at the Brewster angle in P-polarization. The reflectance spectra (KR(E)) and diffraction efficiency (KD(E)) were recorded for the temperature range between 10 and 90 K (Fig. 1).

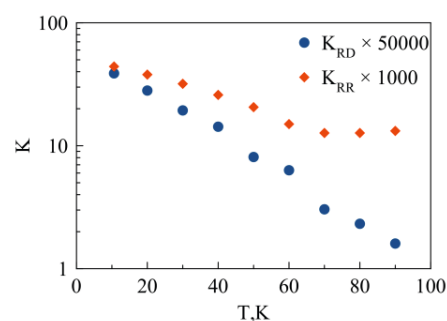


Figure 2. Temperature dependency of KR(E) and KD(E).

Reflection and diffraction peaks spectral positions coincide for equal temperatures. Increase in temperature causes band gap variation leading to quadratic red shift of the peaks. The diffraction peak is narrower than corresponding reflection peak. Moreover, the ratio of these values remains the same for different temperatures. Resonant diffraction efficiency KRD decreases with temperature much faster than resonant reflection coefficient KRR (Fig. 2).

It has been shown that the diffraction efficiency decreases with the temperature much faster than reflection coefficient in accordance with theory. It was found that the spectral width of the diffraction peak is smaller than reflection peak width and the spectral peak positions for diffracted and reflected light match each other.

The reported study was partially supported by RFBR, research project No. 14-0231617 mol-a. This work was carried out on the equipment of the SPbU Resource Center "Nanophotonics" (photon.spbu.ru).

[1] S.V. Poltavtsev et al. 2014 Solid State Communications 199 47

[2] Yu.V. Kapitonov et al. 2013 Phys. Status Solidi . B250 2180

[3] Yu.V. Kapitonov et al. 2014 arXiv-1412.7051

Sideband transitions in circuit QED based on flux qubits

J.-L. Smirr¹, I. N. Khrapach^{1,2}, V. O. Shkolnikov¹, M. Jerger⁴, V. V. Ryazanov^{1,2,3} and A. V. Ustinov^{1,4}

¹Russian Quantum Center, Skolkovo, Russia

²Moscow Institute of Physics and Technology, Dolgoprudny, Russia

³Institute of Solid State Physics, Chernogolovka, Russia

⁴Karlsruhe Institute of Technology, Germany

e-mail: jl.smirr@rqc.ru

Flux qubits are superconducting circuits forming a loop interrupted by typically three Josephson junctions of relatively high Josephson to charging energy ratio. When biased near half a flux quantum, their two lowest discrete energy levels correspond to symmetric and antisymmetric quantum superpositions of clockwise and anti-clockwise current flow and constitute a good approximation of an ideal two-level system[1].

Such qubits can be inductively coupled at a current antinode to high-quality microwave resonators in order to realize circuit QED-like control (pump) and readout (probe) experiments[2]: a transition from the ground state to the first excited state can be directly induced by a single classical microwave tone at a frequency equal the transition energy divided by h . Here we illustrate how other processes can induce such a transition, namely red- and blue-sideband, and two-photon transitions. The former processes are assisted by a resonator photon ; the latter by a second pump photon.

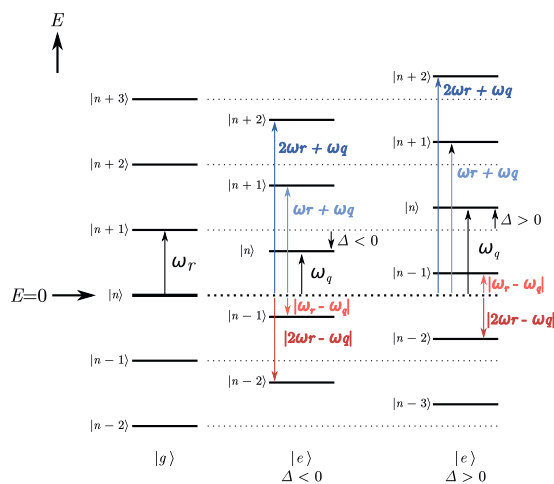


Figure 1: Example of possible sideband transitions from a qubit ground state $|g\rangle$ to excited state $|e\rangle$ assisted by photons from a cavity initially in state $|n\rangle$

We present a complete CW characterisation of the system formed by a qubit and a microwave resonator, including one- and two-tone spectroscopy, AC-Stark shift. In high probe and/or pump power two-tone spectroscopy, new features become visible in addi-

tion to the direct qubit transition that are well explained by the above-mentioned sideband and two-photon phenomena. Agreement is shown quantitatively, using only the knowledge of measured qubit characteristics like charging energy, Josephson energy and junction critical current ratio.

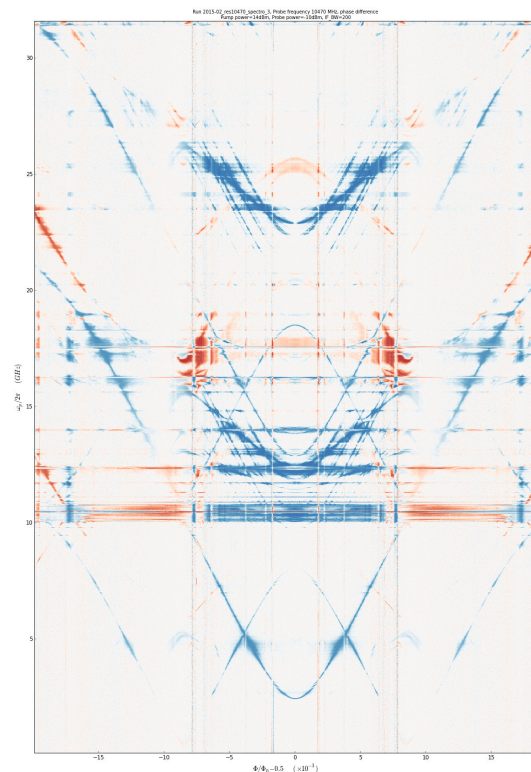


Figure 2: Two-tone spectroscopy of a flux qubit showing sideband and two-photon transitions. Background subtracted. Colour indicates the phase shift -blue: negative, red: positive)

[1] Mooij, J. E., et al. "Josephson persistent-current qubit." *Science* 285.5430 (1999): 1036-1039.
 [2] Bourassa, J., et al. "Ultrastrong coupling regime of cavity QED with phase-biased flux qubits." *Physical Review A* 80.3 (2009): 032109.



Strongly Correlated Quantum Walks in Optical Lattices

P. Preiss¹, R. Ma¹, A. Lukin¹, E. Tai¹, M. Rispoli¹, R. Islam¹, and M. Greiner¹

¹*Department of Physics, Harvard University, Cambridge, Massachusetts, 02138, USA*

e-mail: preiss@physics.harvard.edu

Microscopy techniques for ultracold quantum gases offer the opportunity to characterize complex bosonic many-body states on a single-particle level. With a novel single-site addressing scheme, we are now able to study the most elemental building blocks of such strongly correlated systems. We initialize Fock states of few bosons in an optical lattice with high fidelity and follow their dynamics in one dimension. Focusing on free quantum walks of two atoms, we directly observe the crossover from bunching to anti-bunching as the bosons fermionize due to strong repulsive interactions. We utilize our control over the initial state to prepare repulsively bound pairs and study their coherent Bloch oscillations in the presence of an externally applied gradient. Our work gives access to interaction effects in the simplest possible setting and allows the assembly of many-body states one particle at a time.

A-G INDEX BY SPEAKER NAME

Ablayev Farid	Kazan Federal University, Russia	62
Adams Charles	Durham University, UK	37
Akimov Illia	Dortmund University, Germany	52
Aksu Serhan	Mimar Sinan Fine Arts University, Turkey	63
Ali KhanMurtaza	University of Florence/ Karlsruhe Institute, Italy /Germany.	64
Alodjants Alexander	Vladimr State University, Russia	65
Altshuler Boris	Columbia University, USA.	40
Arkhipov Rostislav	Weierstrass Institute, Germany	66
Arroyo-Camejo Silvia Bettina	Max Planck Institute for Biophysical Chemistry, Germany.	67
Baranov Misha	Institute for Quantum Optics and Quantum Information, Austria	25
Basalaev Maksim	Novosibirsk State University, Russia.	68
Beliaev Leonid	Saint-Petersburg State University, Russia.	156
Belotelov Vladimir	Russian Quantum Center, Russia	30
Berloff Natalia	Skolkovo Institute of Science and Technology, Russia	43
Beyer Axel	Max Planck Insitute of Quantum Optics, Germany.	69
Bilmes Alexander	Karlsruhe Institute of Technology, Germany	70
Borovkova Olga	Russian Quantum Center, Russia	71
Braumüller Jochen	Karlsruhe Institute of Technology, Germany	72
Brazhnikov Denis	Institute of Laser Physics SB RAS, Russia.	73, 74
Bukharin Mikhail	Moscow Institute of Physics and Technology, Russia	75
Calarco Tommaso	University of Ulm, Germany	38
Chichinadze Dmitry	Russian Quantum Center, Russia	130
Cirac Ignacio	Max Planck Insitute of Quantum Optics, Germany.	39
Colas David	Universidad Autonoma de Madrid, Spain	76
Cong Shuang	University of Science and Technology of China.	77
Cotter Joseph	University of Vienna, Austria	131
del Valle Elena	Universidad Autonoma de Madrid, Spain	78
Demler Eugene	Harvard University, USA.	41
Demokritov Sergej	Münster University, Germany.	54
Efimkin Dmitry	University of Maryland, US	79
Eger David	Weizmann Institute of Science, Israel	132
Elezov Mikhail	Moscow State Pedagogical Univercity, Russia	80
Fadel Matteo	University of Basel, Switzerland	81
Fedorov Alex	Russian Quantum Center, Russia	83
Fedorov Ilya	Russian Quantum Center, Russia	129
Ferlaino Francesca	Institute for Quantum Optics and Quantum Information, Austria	24
Fistul Mikhail	Ruhr University Bochum/ National University of Science and Technology “MISIS”, Germany/Russia.	84
Gábris Aurél	Czech Technical University in Prague	85
Garifullin Adel	Kazan Federal University, Russia.	133

INDEX BY SPEAKER NAME **G-L**

Gerasimov Leonid	Peter the Great Saint-Petersburg Polytechnic University, Russia . . .	86
Germanskiy Semen	Moscow State University, Russia	87
Giessen Harald	University of Stuttgart, Germany	31
Golobokova Lyudmila	Rzhanov Institute of Semiconductor Physics SB RAS, Russia	88
Golovizin Artem	Lebedev Physical Institute of RAS, Russian Quantum Center	89
Gorodetsky Michael	Russian Quantum Center, Russia	36
Grangier Philippe	Institute d'Optique, France	26
Gross Rudolf	Walther-Meissner-Institut, TU Munich, Germany	47
Gustavsson Simon	Massachusetts Institute of Technology, USA	46
Hoefling Sven	University of St Andrews, UK.	49
Il'in Nikolay	Steklov Mathematical Institute of RAS, Russia	144
Ivanov Mikhail	Imperial Colledge, UK	45
Kalganova Elena	Lebedev Physical Institute of RAS, Russia.	90
Kalinin Kirill	Skolkovo Institute of Science and Technology, Russia	91
Karahasanovic Una	Karlsruhe Institute of Technology, Germany	134
Kardakova Anna	Moscow State Pedagogical Univercity, Russia	135
Kavokin Alexey	Russian Quantum Center, Russia	51
Keldysh Leonid	Moscow State University, Russia.	33
Khamidullina Aliya	Kazan Federal University, Russia.	92
Khan Emiliya	Moscow State Pedagogical Univercity, Russia	93
Kharitonov Anton	Kazan Federal University, Russia.	136
Kibis Oleg	Novosibirsk State Technical University, Russia	94
Kiktenko Evgeniy	Bauman Moscow State Technical University, Russia.	95
Kippenberg Tobias	Ecole polytechnique fédérale de Lausanne, Switzerland	35
Kocharovskaya Olga	Texas A&M University, US	28
Kollar Balint	Wigner Research Centre for Physics, SZFI, HAS, Hungary.	96
Kondratiev Nikita	Russian Quantum Center, Russia	140
Kovalyuk Vadim	Moscow State Pedagogical Univercity, Russia	97
Kukharchyk Nadezhda	Ruhr University Bochum, Germany	98
Kupriyanov Dmitriy	Peter the Great Saint-Petersburg Polytechnic University, Russia . .	99
Kurochkin Yury	Russian Quantum Center, Russia	82, 137
Kuznetsova Elena	Institute of Applied Physics/Russian Quantum Center, Russia . .	100
Lagoudakis Pavlos	University of Southampton, UK	50
Leuchs Gerd	Max Planck Institute for the Science of Light, Germany.	29
Li Jie	University of Camerino, Italy	101
Libman Mikhail	Russian Quantum Center, Russia	140
Likhachev Grigory	Russian Quantum Center, Russia	138
Lopez Carreno Juan	Universidad Autonoma de Madrid, Spain	102
Lukin Mikhail	Harvard University, USA.	27
Lukin Alexander	Harvard University, USA.	139

L-S INDEX BY SPEAKER NAME

Lyamkina Anna	Russian Quantum Center, Russia	103
Lychkovskiy Oleg	Russian Quantum Center, Russia	104
Melnikov Alexey	Institute for Quantum Optics and Quantum Information / University of Innsbruck, Austria	105
Mishina Oxana	Saarland University, Germany	141
Mokrousova Daria	Lebedev Physical Institute; Moscow Institute of Physics and Technology, Russia.	106
Neuzner Andreas	Max Planck Institute of Quantum Optics, Germany.	107
Ouerdane Henni	Russian Quantum Center, Russia	108
Pankratov Andrey	Institute for Physics of Microstructures of RAS, Russia	142
Pankratova Evgeniya	Volga State University of Water Transportation, Russia	143
Petrov Mihail	University of Information Technologies, Mechanics and Optics, Russia	145
Polyakov Evgeny	Saint-Petersburg State University, Russia.	109
Polzik Eugene	Niels Bohr Institute, Denmark	34
Preiss Philipp	Harvard University, USA.	158
Pyatcenkov Sergey	Russian Quantum Center, Russia	110
Ribeiro Pedro	Russian Quantum Center, Russia	146
Rubtsov Alexey	Russian Quantum Center, Russia	55
Sanchez Muñoz Carlos	Universidad Autonoma de Madrid, Spain	111
Sautenkov Vladimir	Joint Institute for High Temperatures of RAS, Russia	147
Savvidis Pavlos	University of Crete, Greece	53
Schliesser Albert	Niels Bohr Institute, Denmark	112
Schreck Florian	University of Amsterdam, Netherlands	23
Shakirov Alexey	Russian Quantum Center, Russia	149
Shchadilova Yulia	Russian Quantum Center, Russia	150
Sheremet Alexandra	Russian Quantum Center, Russia	113
Shpakovskiy Timofey	Lebedev Physical Institute of RAS, Russia.	115
Sibatov Renat	Ulyanovsk State University, Russia	151
Sidorov Andrei	Swinburne University of Technology, Australia	115
Sidorova Mariia	Moscow State Pedagogical University, Russia	116
Siegel Michael	Karlsruhe Institute of Technology, Germany	48
Silva Blanca	Universidad Autonoma de Madrid, Spain	117
Skacel Sebastian	Physikalisches Institut; Karlsruhe Institute of Technology, Germany	118
Skolnick Maurice	University of Sheffield, UK	32
Smirnova Olga	Max Born Institute, Germany.	44
Smirr Jean-Loup	Russian Quantum Center, Russia	157
Solovev Ivan	St. Petersburg State University, Russia	152
Stepanov Evgeny	Radboud University, Netherlands	153

INDEX BY SPEAKER NAME T-Z

Tokunaga Yuuki	NTT Labs, Japan	119
Tregubov Dmitry	Lebedev Physical Institute of RAS, Russia.	120
Trushechkin Anton	Steklov Mathematical Institute of RAS, Russia	154
Ulanov Alexander	Russian Quantum Center, Russia	155
Vetlugin Anton	Saint-Petersburg State University, Russia.	121
Volovik Grigory	Aalto University/ Landau Institute, Finland/Russia	42
Voronova Nina	National Research Nuclear University MEPhI, Russia	122
Vuletic Vladan	Massachusetts Institute of Technology, USA	22
Woolley Matt	University of New South Wales, Australia.	123
Yakshina Elena	Rzhanov Institute of Semiconductor Physics SB RAS, Russia	124
Yuce Cem	Anadolu University, Turkey	125
Zelener Boris	Joint Institute for High Temperatures of RAS, Russia	126
Zhang Yichen	Beijing University of Posts and Telecommunications	127
Zolotov Philipp	Moscow State Pedagogical University/ Scontel, Russia	128